Towards eradicating the tropical disease schistosomiasis – integrative mathematical and statistical modeling combining intrinsic and extrinsic parameters

Auf dem Weg zur Ausrottung der Tropenkrankheit Schistosomiasis – integrative mathematische und statistische Modellierung, die intrinsische und extrinsische Parameter kombiniert

Zadoki Tabo

(MSc. Math. Modelling)

Dissertation for the award of the degree "Doctor rerum naturalium (Dr. rer. nat.)"
at Justus Liebig University Giessen, Germany

Faculty 08-Department Animal Ecology and Systematics in conjunction with
Faculty 09-Department of Landscape Ecology and Resource Management

March 2024

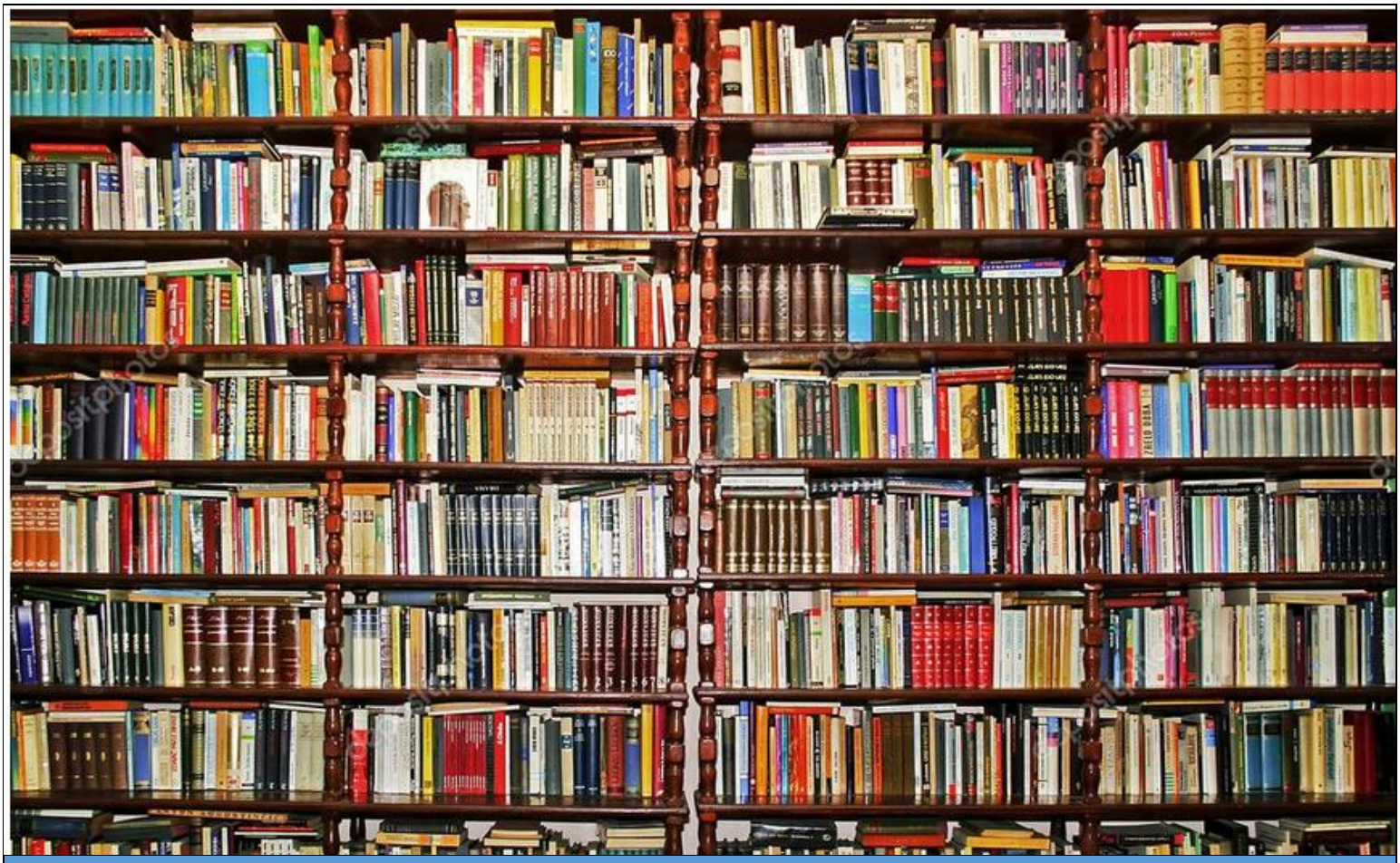

Dean: Prof. Dr. Thomas Wilke

Reviewer 1: Apl. Prof. Dr. Christian Albrecht

Reviewer 2: Prof. Dr. Lutz Breuer

Author: Zadoki Tabo

Towards eradicating the tropical disease schistosomiasis – integrative mathematical and statistical modeling combining intrinsic and extrinsic parameters

Declaration/Erklärung

I declare that I have completed this dissertation single-handedly without the unauthorized help of a second party and only with the assistance acknowledged therein. I have appropriately acknowledged and cited all text passages that are derived verbatim from or are based on the content of published work of others, and all information relating to verbal communications. I consent to the use of an anti-plagiarism software to check my thesis. I have abided by the principles of good scientific conduct laid down in the charter of the Justus Liebig University Giessen "Satzung der Justus-Liebig-Universität Gießen zur Sicherung guter wissenschaftlicher Praxis" in carrying out the investigations described in the dissertation.

Ich erkläre: Ich habe die vorgelegte Dissertation selbstständig und ohne unerlaubte fremde Hilfe und nur mit den Hilfen angefertigt, die ich in der Dissertation angegeben habe. Alle Textstellen, die wörtlich oder sinngemäß aus veröffentlichten Schriften entnommen sind, und alle Angaben, die auf mündlichen Auskünften beruhen, sind als solche kenntlich gemacht. Ich stimme einer evtl. Überprüfung meiner Dissertation durch eine Antiplagiat-Software zu. Bei den von mir durchgeführten und in der Dissertation erwähnten Untersuchungen habe ich die Grundsätze guter wissenschaftlicher Praxis, wie sie in der „Satzung der Justus-Liebig-Universität Gießen zur Sicherung guter wissenschaftlicher Praxis" niedergelegt sind, eingehalten.

Zadoki Tabo

March 2024

Giessen, Germany

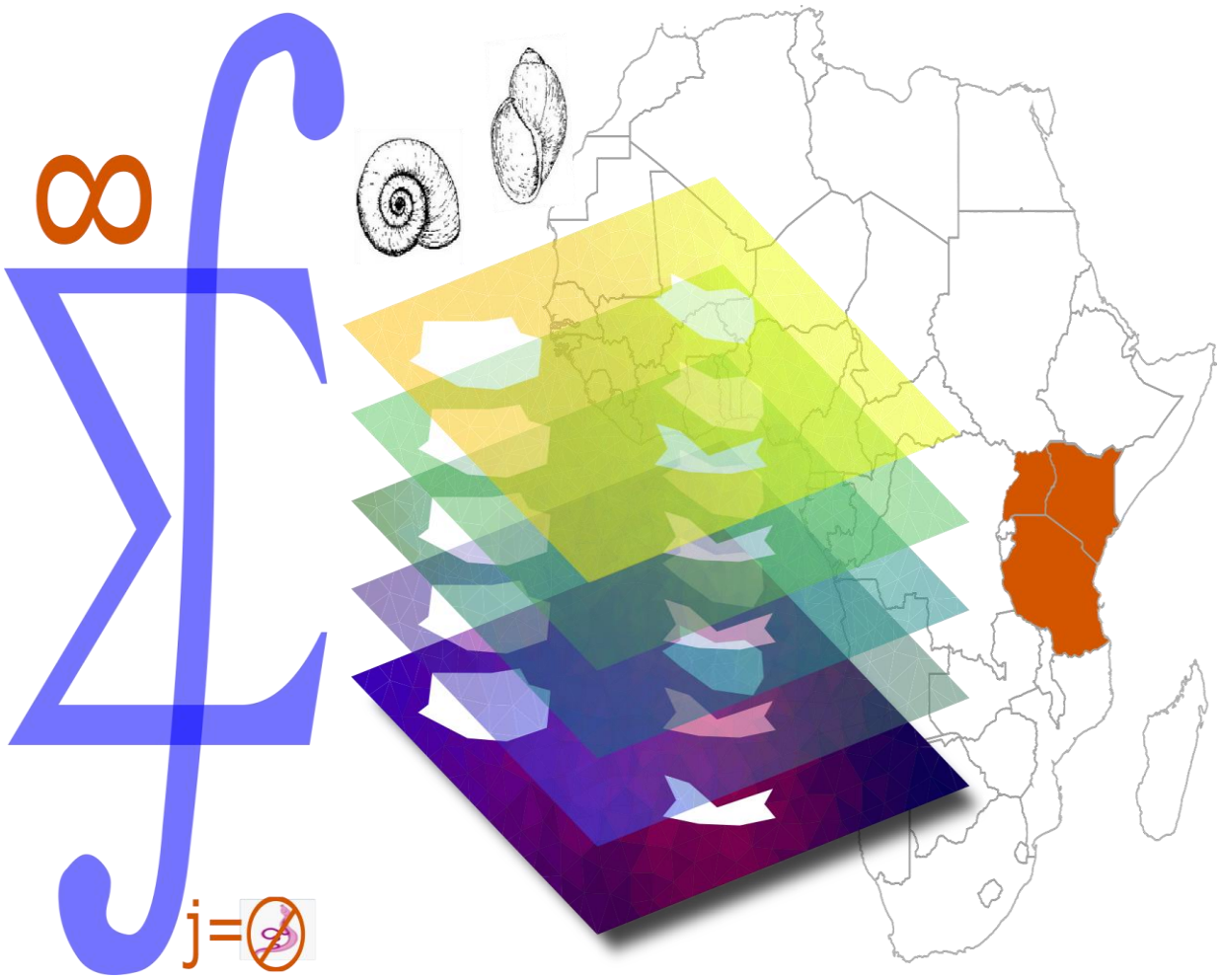
∞
j=

Printed and/or published with the assistance of the German Academic Exchange Service (DAAD)

DAAD

Deutscher Akademischer Austausch Dienst
German Academic Exchange Service

Table of Contents

I. SUMMARY

II. SYNOPSIS

1. Introduction 1

1.1. Background and Research Context 1

1.2. *Schistosoma* species diversity and transmission dynamics 1

1.3. Schistosomiasis clinical manifestations, treatment challenges, and global control efforts 3

2. Knowledge gap and research objectives 4

3. Materials and Methods 4

3.1. Factors shaping the community structure of intermediate host snails at various scales 5

3.1.1. Data at local geographical scale 5
3.1.2. Data at regional and larger geographical scales 5
3.1.3. Statistical-machine learning approach for data analysis 6

3.2. Population study of schistosomiasis transmission, prevention and management 6

3.2.1. Data for schistosomiasis population study 6
3.2.2. Mathematical modelling approach 7
3.2.3. Mathematical model analysis 7

4. Publication outlines 7

4.1. Factors controlling local distribution of intermediate host snails 7
4.2. Factors controlling regional distribution of intermediate host snails 8
4.3. Exploring the interplay between climate change and schistosomiasis transmission dynamics 8
4.4. Modeling temperature-dependent schistosomiasis dynamics in Single and co-infections 9
4.5. Selective competitive and predatory intervention of intermediate hosts 9
4.6. Adapting strategies for effective schistosomiasis prevention 10

5. Results and Discussion 11

5.1. Significant drivers of intermediate host snails across geographical scales 11

5.1.1. Geography 11
5.1.2. Climate variables 12
5.1.3. Soil content and soil composition 13
5.1.4. Habitat suitability 13
5.1.5. Associated mollusk diversity 14
5.1.6. Human activities 14
5.1.7. Non-significant parameters 14

5.2. Likelihood of genus occurrence across geographical scales 15

5.3. Climate variability and the transmission dynamics of schistosomiasis 15
5.4. Effects of non-host competitor snails and predators of intermediate host snails 17
5.5. Adapting climate based-strategies for effective schistosomiasis prevention 18

6. Conclusion and Recommendations 19

7. Reference list 20

III. PUBLICATIONS

Tabo, Z, Neubauer, T. A., Tumwebaze, I., Stelbrink, B., Breuer, L., Hammoud, C., & Albrecht, C. (**2022**). Factors Controlling the Distribution of Intermediate Host Snails of Schistosoma in Crater Lakes in Uganda: A Machine Learning Approach. *Frontiers in Environmental Science*, *341*. https://doi.org/10.3389/fenvs.2022.871735 26

Tabo Z, Breuer, L., Fabia, C., Samuel, G., & Albrecht, C. (**2024**). A machine learning approach for modeling the occurrence of the major intermediate hosts for schistosomiasis in East Africa. *Scientific Reports*, *14*(1), *4274*. https://doi.org/10.1038/s41598-024-54699-1 40

Tabo, Z, Kalinda, C., Breuer, L., & Albrecht, C. (**2024**). Exploring the interplay between climate change and schistosomiasis transmission dynamics. *Infectious Disease Modelling*, *9*(1), *158-176*. https://doi.org/10.1016/j.idm.2023.12.003 51

Tabo, Z, Kalinda, C., Breuer, L., & Albrecht, C. (**2023**). Adapting Strategies for Effective Schistosomiasis Prevention: A Mathematical Modeling Approach. *Mathematics*, *11*(12), *2609*. https://www.mdpi.com/2227-7390/11/12/2609 70

Tabo Z, Luboobi, L., Kraft, P., Breuer, L., & Albrecht, C. (**2024**). Control of schistosomiasis by the selective competitive and predatory intervention of intermediate hosts: A mathematical modeling approach. *Mathematical Biosciences*, *376, 109263*. https://doi.org/10.1016/j.mbs.2024.109263 ..89

Tabo Z, Breuer, L., & Albrecht, C. (**2024**, **revision**). Modelling temperature-dependent schistosomiasis dynamics for single and co-infections with *S. mansoni* and *S. haematobium*. (Submitted to PLOS ONE) 105

III. APPENDIX

Curriculum Vitae 132

Acknowledgement 135

(i) Summary (English)

Schistosomiasis poses a significant public health threat in Sub-Saharan Africa, particularly affecting impoverished rural communities. This disease is predominantly caused by *S. mansoni* and *S. haematobium* parasites, transmitted by freshwater snails of the *Biomphalaria* and *Bulinus* species. East Africa, characterized by densely populated rural areas, bears the highest disease burden within the region, with specific hotspots identified in Uganda, Kenya, and Tanzania. Various factors, including climatic variability, geographical features, environmental/habitat suitability, biodiversity, and anthropogenic influences, influence the distribution patterns of intermediate host (IH) snails and schistosomiasis transmission across different geographic scales. The new WHO roadmap emphasizes a One Health approach, recommending targeted snail control and alternative methods. However, limited knowledge exists about the determinants of community structure of the two genera and their role in schistosomiasis transmission, prevalence, and distribution under various scenarios, such as climatic variability in East Africa. This study reveals significant extrinsic parameters influencing the distribution of IH snails at both local (Western Uganda) and regional (East Africa) geographical scales, using Random forest, a machine learning technique. On a smaller scale, geography, diversity of the associated mollusk fauna, and climate emerged as important predictors for the presence of *Biomphalaria*, whereas mollusk diversity, water chemistry, and geography primarily controlled the occurrence of Bulinus. Mollusk diversity and geography were found to be relevant for the presence of both genera combined. On a regional scale, the results indicated geography and climate as primary factors for *Biomphalaria*, while *Bulinus* occurrence was additionally influenced by soil clay content and nitrogen concentration. These parameters signify the processes involved in meta-community assembly, encompassing factors like dispersal limitation, environmental filtering, and biotic interactions that influence the establishment of genera. Furthermore, mathematical models were formulated to quantify the dynamics of schistosomiasis transmission, focusing on the role of IH and all stakeholders in transmission and management (climate variability and control strategies). Within East Africa, this study revealed varied incidence rates among countries based on temperature and rainfall patterns, characterized by seasonal schistosomiasis emergencies and re-emergences. Conditions with temperatures between 20-27°C and precipitation ranging from 5-140 mm were found to be conducive for schistosomiasis, while June and July marked a period with fewer reported cases, attributed to adverse temperatures around 26-30°C and lower precipitation levels (5.0 to 91.8 mm). Furthermore, *Biomphalaria* snails demonstrated higher population growth and susceptibility to infection than *Bulinus* snails, particularly below 25°C, with their populations declining above this temperature threshold and it is optimal for intensifying snail interventions. Expanding the scope, this study revealed that specific non-host competitor snails and predator behaviors such as attack and handling times, can directly control the population of IH snails. However, employing a singular snail competitor or predator alone did not achieve complete disease eradication, while their simultaneous application resulted in a significant decrease in the IH snail population. This reduction brought the reproductive number below unity, indicating the effectiveness of disease control measures. Moreover, model evaluating the individual and tiered impact of remaining control strategies in the current study, including chemotherapy, awareness programs, snail removal, and environmentally dependent chemical control, revealed that no single or combination of 2-3 tiered approaches could entirely eradicate schistosomiasis, except for a four-tiered strategy that integrates all assessed interventions. All work in this dissertation contributes to a better understanding of the community structure of IH snails (where and why their distribution occurs) as well as the impact of climate variability, non-host snails, and predators, as well as evaluating the effectiveness of all stakeholders. It enables the optimization of resources, adaptation of interventions, and supports evidence-based decision-making, fostering community trust.

(ii) Zusammenfassung

Schistosomiasis stellt eine bedeutende öffentliche Gesundheitsgefahr in Subsahara-Afrika dar und betrifft insbesondere arme ländliche Gemeinden. Diese Krankheit wird hauptsächlich von den Parasiten *S. mansoni* und *S. haematobium* verursacht, die von Süßwasserschnecken der Gattungen *Biomphalaria* und *Bulinus* übertragen werden. Ostafrika, das von dicht besiedelten ländlichen Gebieten geprägt ist, trägt die höchste Krankheitslast in der Region, wobei spezifische Hotspots in Uganda, Kenia und Tansania identifiziert wurden. Verschiedene Faktoren, darunter klimatische Variabilität, geografische Merkmale, Umwelt-/Lebensraumeignung, Biodiversität und anthropogene Einflüsse, beeinflussen die Verteilungsmuster der Zwischenwirtschnecken und die Übertragung der Schistosomiasis über verschiedene geografische Skalen hinweg. Der neue WHO-Aktionsplan betont einen One-Health-Ansatz und empfiehlt gezielte Schneckenbekämpfung und alternative Methoden. Unser Wissen über die Determinanten der Populationsstruktur der beiden Gattungen und ihre Rolle bei der Übertragung, Verbreitung und Prävalenz der Schistosomiasis unter verschiedenen Szenarien, wie etwa klimatischer Variabilität in Ostafrika ist begrenzt. Diese Studie zeigt bedeutende extrinsische Parameter, die die Verteilung der Zwischenwirtschnecken auf lokaler (Westuganda) und regionaler (Ostafrika) geografischer Ebene beeinflussen, unter Verwendung von Random Forest, einer Methode des maschinellen Lernens. Auf kleinerer Ebene erwiesen sich Geografie, Vielfalt der assoziierten Molluskenfauna und Klima als wichtige Prädiktoren für das Vorkommen von *Biomphalaria*, während Molluskenvielfalt, Wasserchemie und Geografie hauptsächlich das Auftreten von *Bulinus* kontrollierten. Molluskenvielfalt und Geografie waren auch für das Vorhandensein beider Gattungen zusammen relevant. Auf regionaler Ebene deuteten die Ergebnisse darauf hin, dass Geografie und Klima primäre Faktoren für *Biomphalaria* sind, während das Auftreten von *Bulinus* zusätzlich durch den Tonanteil im Boden und die Stickstoffkonzentration beeinflusst wurde. Diese Parameter spiegeln die Prozesse wider, die bei der Metagemeinschaftszusammenstellung eine Rolle spielen und umfassen Faktoren wie Dispersionsbeschränkung, Umweltfilterung und biotische Interaktionen, die die Etablierung von Gattungen beeinflussen. Darüber hinaus wurden mathematische Modelle formuliert, um die Dynamik der Übertragung der Schistosomiasis zu quantifizieren, wobei der Schwerpunkt auf der Rolle der Zwischenwirtschnecken und aller Interessengruppen bei der Übertragung und Bewältigung (klimatischer Variabilität und Kontrollstrategien) lag. Innerhalb von Ostafrika zeigte diese Studie unterschiedliche Inzidenzraten zwischen den Ländern basierend auf Temperatur- und Niederschlagsmustern, gekennzeichnet durch saisonale Schistosomiasis-fälle und -Wiederauftreten. Bedingungen mit Temperaturen zwischen 20-27°C und Niederschlägen von 5-140 mm erwiesen sich als günstig für die Schistosomiasis, während der Juni und Juli eine Phase mit weniger gemeldeten Fällen markierten, die auf ungünstige Temperaturen um 26-30°C und niedrigere Niederschlagsmengen (5,0 bis 91,8 mm) zurückzuführen waren. Darüber hinaus zeigten *Biomphalaria*-Schnecken ein höheres Wachstum der Population und eine höhere Anfälligkeit für Infektionen als *Bulinus*-Schnecken, insbesondere unter 25°C, wobei ihre Populationen über diesem Temperaturschwellenwert abnehmen und es optimal ist, um Schnecken-interventionen zu verstärken. In einem erweiterten Rahmen zeigte diese Studie, dass bestimmte nicht-wirtsspezifische Konkurrentenschnecken und Räuberverhalten wie Angriffs- und Umgangszeiten direkt die Population der Zwischenwirtschnecken kontrollieren können. Die alleinige Anwendung eines einzigen Schneckenkonkurrenten oder -Räubers führte jedoch nicht zur vollständigen Ausrottung der Krankheit, während ihre gleichzeitige Anwendung zu einer signifikanten Abnahme der Population der Zwischenwirtschnecken führte. Diese Reduzierung brachte die Reproduktionszahl unter Eins, was auf die Wirksamkeit von Krankheitsbekämpfungsmaßnahmen hinweist

II.SYNOPSIS

1. Introduction

1.1. Background and Research Context

Human schistosomiasis, a neglected tropical disease widely known as bilharzia, emerges as a substantial public health challenge due to its endemic prevalence impacting impoverished rural communities [1,2]. Ranking second only to malaria in its incapacitating impact, it is additionally recognized as the most widespread and consequential water-borne disease [2,3]. Its repercussions are particularly pronounced across tropical and sub-tropical regions, exacerbating prevailing health disparities [4,5]. The far-reaching socioeconomic consequences of the disease manifest in reduced productivity, impaired childhood development, and increased healthcare costs [6,7]. The burden is significant, with 90% of schistosomiasis cases occurring in Sub-Saharan Africa [1].

The disease occurrence is linked to rural or semi-rural settings, characterized by poverty, inadequate sanitation, and a lack of access to clean water sources [1,8,9], along with abundant unclean freshwater sources that serve as potential habitats for intermediate host (IH) snails, which serve as vectors for schistosomiasis [3,10,11,12,13]. For example, East Africa, a region within Sub-Saharan Africa, exhibits a varied presence of freshwater gastropods that demonstrate adaptability to a wide range of habitats [2,10]. These include perennial or seasonal pools, rice fields, reservoirs, lakes, wetlands, rivers, creeks, and marshlands, as well as artificial structures like dams, drainage ditches, and irrigation schemes [11,12,14,15]. Significantly, Western Uganda, situated in East Africa, features approximately 90 maar crater lakes [15]. These lakes demonstrate distinct patterns of intermediate host (IH) snail distribution [13,16] and exhibit correlations with local disease prevalence in the region [17,18,19,20].

Furthermore, the region is characterized by an array of factors that are potential drivers of the distribution patterns of IH snails and schistosomiasis transmission across varying geographic scales, encompassing climatic variability in air and water temperature, precipitation, land surface temperatures [21,22,23,24,25,26,27], geographical factors such as altitude, slope, geographical coordinates [13,16,17,18,23,28], environmental/habitat suitability such as physio-chemical properties [13, 22,28,29], ecological settings including associated biodiversity such as competitor snails and predators [8,30,31,32,33,34,35,36,37] and anthropogenic factors influence such as settlement, fishing and agriculture [23,26,38,39]. Particularly, East Africa stands out as having densely populated rural areas within Sub-Saharan Africa, exhibiting a noteworthy annual population growth rate of 2.7% [40].

Furthermore, small areas like crater lakes in Western Uganda within East Africa, are particularly remarkable for their high population density in the rural landscape, with an annual growth rate of 3.3% [41]. In these settings, frequent contact with water contaminated by schistosome eggs poses a substantial risk of infection [42,43], potentially contributing to the significant and alarming increase in schistosomiasis in East Africa [44]. The region is characterized by specific hotspots, such as those within the highlands in Eastern and Western Uganda [16,17,18], and other areas identified as schistosomiasis persistent hotspots, including those in Kenya and Tanzania [45]. Hence, the crater lakes within Western Uganda and the broader East Africa region serve as crucial model ecosystems for studying the community composition of IH snails. Additionally, they offer valuable insights into the transmission dynamics, prevalence, and management of schistosomiasis within these distinct geographic zones. Figure 1 depicts the distribution of IH snails across 56 hotspot crater lakes within the Fort Portal, Ndali-Kasenda (C), and Bunyarugura (D) crater lake fields of Western Uganda, as a small geographical model system. Additionally, it includes a broader regional geographical model covering East Africa (B), all situated within the African continent (A).

1.2. *Schistosoma* species diversity and transmission dynamics

Globally, at least five *Schistosoma* species infect humans, with a particular focus on *S. mansoni* and *S. haematobium* in this thesis, as they are major contributors to the human disease burden [46,47]. The transmission of *S. mansoni*, causing intestinal schistosomiasis, occurs through *Biomphalaria* snails, while *S. haematobium*, responsible for urogenital schistosomiasis, is transmitted by *Bulinus* snails [48]. *Biomphalaria* species universally exhibit susceptibility to *S.*

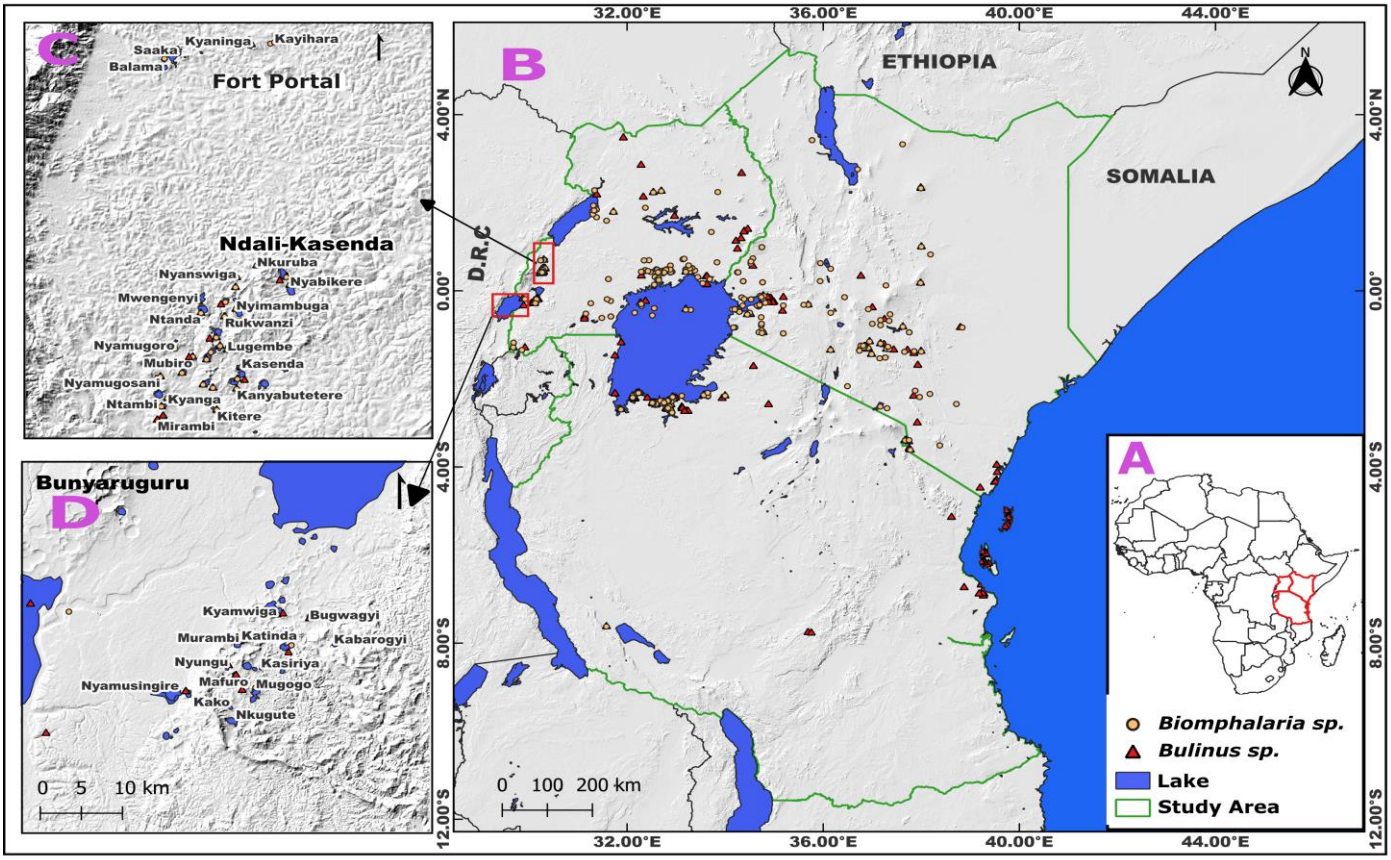

Figure 1. The map depicts the occurrence of intermediate host (IH) snails in a small geographical model system across three crater lake fields: Fort portal, Ndali-Kasenda (C) and Bunyaruguru (D) in Western Uganda, as well as a broader a regional geographical model across East Africa (B), both of which are situated within Africa (A). Symbols: a yellow circle indicate the presence of *Biomphalaria* snail, and a red triangle represents *Bulinus* snail.

mansoni infection, while *Bulinus* snails, grouped into *B. africanus, B. forskalii, B. reticulatus,* and the *Bulinus truncatus/tropicus* complex, display varying degrees of susceptibility to schistosome infection [10,49]. Beyond human health, the impact of schistosomiasis extends to veterinary implications, with several *Schistosoma* species causing schistosomiasis in livestock. These parasites find hosts among the *Bulinus* species, such as *Schistosoma bovis*, or within specific species of the genus, like *Schistosoma margrebowiei* [10,50]. Human schistosomiasis, is characterized by a complex life cycle involving two primary hosts: freshwater snails as IHs and humans as definitive hosts [2]. This intricate life history is visually represented in the simplified life cycle diagram (Figure 2).

Notably, as a waterborne disease, the environmental infective stages of the parasite, including IH snails, snail-infective miracidia, and human-infective cercariae, are confined to freshwater habitats. The life cycle of the schistosome begins with cercaria shedding from infected snails into the water. Within a few seconds of contact with the human host, they can penetrate through the skin and invade the body. The cercaria larvae enter the circulatory system and migrate through the lungs to the liver where they transform into adult schistosomes and mate inside the body. Subsequently, adult couples migrate to their final destination to reproduce. *Schistosoma mansoni* moves to the blood arteries and the portal system, where the females shed their eggs through the intestinal walls and are excreted in faeces into freshwater sources.

Conversely, *S. haematobium* migrates to the vessels of the urinary bladder, where females produce eggs that pass through the bladder wall and are excreted in the urine contaminating freshwater sources. The eggs of both schistosome species hatch into miracidia larvae in freshwater. These larvae exclusively infect respective intermediate host snails, where they undergo transformation into cercaria larvae. Subsequently, these cercariae infect humans, completing the

life cycle [46]. The simplified diagram for *Schistosoma* life cycle is depicted in Figure 2.

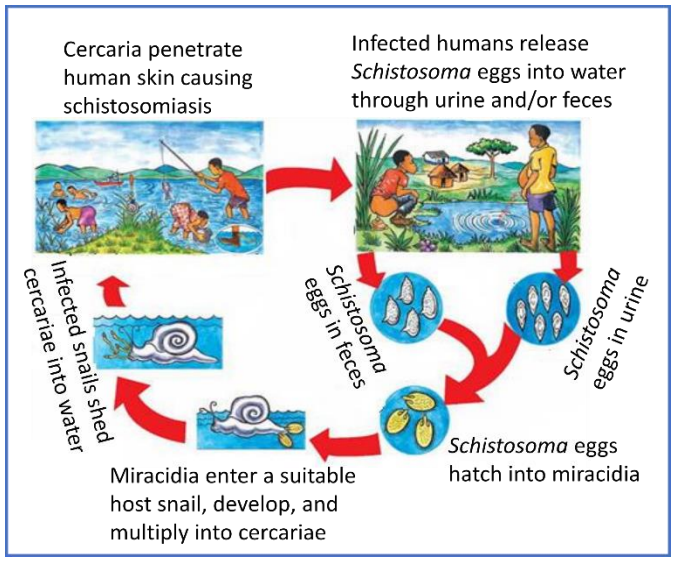

Figure 2. The *Schistosoma* life cycle for human schistosomiasis (taken from Ministry of Health, Uganda).

1.3. Schistosomiasis clinical manifestations, treatment challenges, and global control efforts

Human schistosomiasis imposes a range of debilitating symptoms upon infection. Infections caused by *S. mansoni* may lead to complications such as pulmonary hypertension and schistosomal appendicitis, among other issues [1,46,51]. In contrast, *S. haematobium* infection manifests with symptoms including hematuria, bladder cancer, anemia, and infertility, among others [1,46,52]. Additionally, co-infection with both *S. haematobium* and *S. mansoni* can result in more complex immune-mediated glomerulopathies [53]. Despite ongoing research and clinical trials, there are currently no available vaccines to protect humans against schistosomiasis infection [54, 55,56]. The primary treatment for schistosomiasis remains the anthelmintic praziquantel [8,27,45]. However, concerns have been raised about potential drug resistance and re-infections post-treatment [57, 58]. Despite the 2020 schistosomiasis elimination target failure [59], ongoing research and surveillance are crucial for refining strategies [58], to meet the renewed elimination goals by 2030 [60].

The new WHO roadmap emphasizes a One Health approach, expanding Mass Drug Administration (MDA), exploring praziquantel alternatives, improving diagnostics, and integrating WASH and animal health. Priority areas include targeted snail intervention and alternative methods [7,27,61].

Some countries like Japan and Tunisia have made significant strides in disease control, others, including Morocco, Brazil, China, Egypt, and certain Caribbean islands, have successfully reduced the burden of schistosomiasis [46,62]. Schistosomiasis elimination in Japan, predating praziquantel, involved reducing snail populations through environmental modification, complemented by health education and control of freshwater resources [62]. However, the situation in Africa, especially in East Africa, differs significantly. Mass drug administration has predominantly focused on school-aged children, overlooking vulnerable groups such as the elderly with compromised immunity and women of reproductive age [63]. Additionally, achieving nationwide treatment coverage poses a challenge, with many local areas remaining vulnerable to high transmission risks [57]. Moreover, interventions specifically targeting snails have not gained widespread acceptance.

Additionally, there is limited understanding of various aspects, including the factors influencing the community structure of IH snails and their role in the distribution and prevalence of schistosomiasis in the region. On the flip side, climate variability presents a significant global public health challenge in disease transmission [64], for example in areas like East Africa, transmission of schistosomiasis may fluctuate based on temperature and precipitation patterns across seasons and time [23,65,66,67].

In addition, climate changes have been identified as a factor influencing biodiversity including IH snails, non-host competitor snails, and snail predators [68] and the broader ecological systems, including their food webs [30,32,33,36,60,61], with a potential to influence disease transmission patterns and prevalence. Moreover, ongoing debates are fueled by persistent uncertainties surrounding the influence of climate change on diseases and their transmission [5,23,53,69,70]. This uncertainty poses a significant public health challenge, prompting the need for continued investigation and analysis. Consequently, the utilization of deterministic models becomes crucial for the study, quantification, and prediction of the population dynamics of schistosomiasis for enhancing the accuracy of predictions [71].

2. Knowledge gap and research objectives

The One Health approach, integrating interventions targeting IH snails, human treatment, and health education, effectively disrupts schistosomiasis transmission. However, the adoption of snail control methods is inconsistent in Africa. Yet, our knowledge regarding various aspects of snail hosts remains limited, with a scarcity of studies aimed at providing comprehensive prevalence data and identifying significant drivers that influence the spatial distribution of intermediate hosts, particularly at small and regional scales, especially in high-population, poverty-setting regions like East Africa. Such potential drivers include but are not limited to those illustrated in Figure 3.

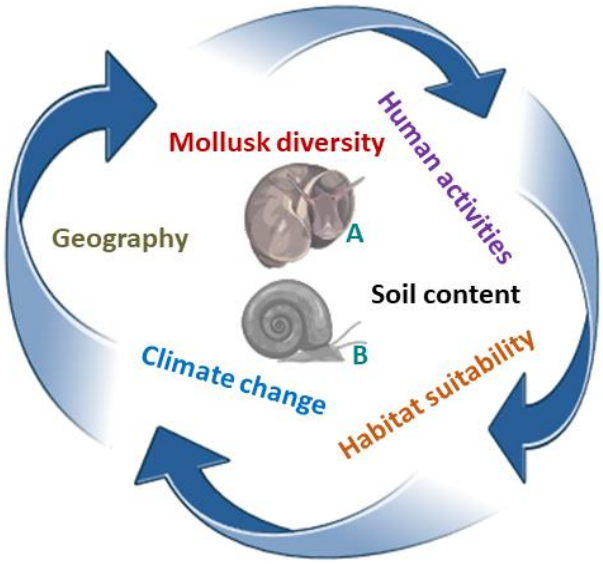

Figure 3. Potential factors influencing the distribution of (A) *Bulinus*, and (B) *Biomphalaria* intermediate snails across geographical scales.

This might pose challenges for snail-targeted prevention and control strategies, as seen in schistosomiasis hotspots in East Africa like in Western Uganda, Kenya, and Tanzania. For example, in Uganda, the general prevalence of schistosomiasis stands at 29.0%. In areas where open defecation and urination take place in surface water and the bush, the prevalence rises to 30.6% and 29.0%, respectively. Conversely, the prevalence drops to 22.3% in regions where sanitation facilities are exclusively used [72]. Therefore, there is a need to quantify the risk levels of the population due to exposure to intermediate hosts and understand their role in the transmission dynamics of the schistosome life cycle. Furthermore, climate variability's impact on vector and parasite populations, along with interactions on spatial and temporal scales, is a global public health concern, necessitating thorough research for precise integration into predictive models, especially in regions like East Africa with distinct seasonal patterns. Consequently, schistosomiasis poses a significant threat to the well-being and livelihoods of affected populations. The urgency of addressing schistosomiasis on a local and regional scale cannot be overstated.

Therefore, the primary objectives of this thesis are named and illustrated as follows;

(i) To disentangle and identify the most important predictor parameters driving the distribution of *Bulinus* and/or *Biomphalaria* species at both local hotspot areas (smaller scale extent) in Western Uganda and regional level of entire East Africa (Uganda, Kenya, and Tanzania). Specifically, this study delves into the analyses of occurrences of these genera concerning meta-community assembly processes, including dispersal limitation, environmental filtering, and biotic interactions. These processes are crucial in influencing the successful establishment of species within an ecosystem. Systematically understanding the relationships between extrinsic factors and IH snails is essential for controlling their distribution and developing a strategic Framework for effective schistosomiasis transmission management.

(ii) To formulate mathematical models based on key stages of the *Schistosoma* life cycle (Figure 2), incorporating predictors identified from objective (i) and Figure 3, as the most important drivers of IH snails. Furthermore, these models seek to assess and appraise the most effective tiered One Health strategy including treatment, public literacy, molluscicide, mollusk diversity (non-host competitor snails) as well as potential predators.

3. Materials and Methods

The thesis utilizes two primary methodological and material components to investigate the community structure of IH snails, addressing objective (i) with an emphasis on extrinsic parameters presented in Figure 3. Additionally, it quantifies the dynamics of schistosomiasis transmission, focusing on intrinsic parameters and controls from an epidemiological perspective (see Figure 4), to fulfill objective (ii).

3.1. Factors shaping the community structure of intermediate host snails at various scales

A hypothesis was developed that distinct sets of factors determine the distribution of *Biompahalaria* and *Bulinus* IH snails across different geographies, resulting in different levels of exposure to schistosomiasis infection for different human population levels. This study examined the factors influencing the community structure of two genera across local and regional scales, with detailed descriptions of the data and methodologies provided in sections 3.1.1-3.1.2.

3.1.1. Data at local geographical scale

The beginning of my doctoral thesis was marked by data from a field study conducted in which a network of 56 crater lakes in western Uganda was surveyed. The region is considered an endemic hotspot for schistosomiasis in sub-Saharan Africa[16, 17,18,73]. The sampling strategy included three out of the four designated crater lake fields: Ndali-Kasenda (32 lakes), Fort Portal (6 lakes), and Bunyaruguru (18 lakes) fields [15]. The fourth field, known as Katwe-Kikorongo [15], containing saline lakes unsuitable for mollusks [16,28], was intentionally excluded from the survey. At one or two localities per lake, sampling techniques employed involved dredging and/or scoop netting, along with manually picking snails attached to shoreline vegetation and other solid substrates. Intermediate host snails and associated mollusk fauna at the genus level were identified and quantified, while geographical parameters (longitude, latitude, and altitude) were measured using a handheld Garmin GPS eTrex 20 device. Additionally, various physio-chemical parameters such as surface water temperature, dissolved oxygen, conductivity, and surface pH were measured using a handheld multi-meter probe.

Data on water depth, total phosphorus, calcium, and magnesium were sourced from existing literature [28,74]. Secchi depth was determined using a Secchi disk. We obtain lake surface area and variance in lake data from Google Earth Pro version 7.3 based on the latest available satellite images. Climatic data, encompassing air temperature and precipitation averaged for the period 1970–2000, were acquired from the WorldClim (v2.1) global database [75]. Assessment of human pressure on habitats, considering factors like land use, settlement, and cultivation, was assessed using satellite images from Google Earth. In this study, we used a total of 20 predictor variables, 15 were acquired during the field survey, 2 were sourced from online databases, and 3 were extracted from existing literature.

3.1.2. Data at regional and larger geographical scales

We collected geographical data (longitude and latitude coordinates) about the distribution of *Bulinus* and *Biomphalaria* across three East African countries: Uganda, Tanzania, and Kenya. In addition to the geographical data obtained through the survey at a local geographical scale, we collected information from literature sources, specifically the works of Chibwana et al. [19] and Tumwebaze et al. [17]. Additionally, we incorporated data from the Global Biodiversity Information Facility [20], which encompasses recent information derived from museum specimens and DNA barcodes. This dataset represents the most up-to-date occurrence data for the region, as depicted in Figure 1.

Bioclimatic data and elevation/altitude were obtained from the WorldClim (v2.1) database [75] utilizing the R programming language. Additionally, data on land surface temperature [76], normalized vegetation index (NDVI) [77], and land cover were extracted from MODIS [78] via the Google Earth Engine (GEE) platform. Key soil-related parameters, including sand, clay, silt, water pH (pHH2O), and nitrogen content, were sourced from ISRIC [79] via R programming.

Additional details concerning soil composition, such as soil pH, soil organic carbon content in fine earth, soil cation exchange capacity, and bulk density of the fine earth fraction, were obtained from iSDA using GEE. Slope information was derived from SRTM within GEE [80]. Distances from the closest water source were measured using FAO data through the "Extract Values to Points" tool in ArcGIS [81]. Furthermore, data on the Human Influence Index and Footprint Index were acquired from region-specific sources for Africa [82], initially in a geographic coordinate system (GCS). Later, these data were extracted at the pixel level using the "Extract Values to Points" tool in ArcGIS [81]. In this study, a total of 23 predictor variables were assessed for their importance in the distribution of IH snails across East Africa

3.1.3. Statistical-machine learning approach for data analysis

Empirical-statistical methods, particularly those leveraging machine learning, play a pivotal role in uncovering correlations among vectors, pathogens, and the environment. Random Forest (RF) [83], a machine learning technique has found broad application in various scientific domains for classification and regression analyses [13,84,85,86,87]. In classification tasks, RF has demonstrated superior predictive accuracy compared to other methods like logistic regression with forward variable selection, boosted classification trees, support vector classification, elastic net logistic regression, and multilayer perceptron classification [,88,89,90]. RF is resilient to multi-collinearity, a common issue in ecological datasets [89]. It also provides effective solutions for addressing missing data [91]. Therefore, we developed RF model algorithms to reveal the significant parameters governing the distribution of *Biomphalaria* and/or *Bulinus*. This involved analyzing individual datasets at small geographical areas initially and subsequently expanding the investigation to larger regional geographical scales. To test the hypothesis that specific parameters play a significant role in influencing the distribution of *Biomphalaria* and *Bulinus* species across diverse examined regions, this study anticipates that these two genera are regulated by different sets of parameters due to their distinct dispersal capabilities and adaptations. Moreover, substantial variations in the ranges of predictor variables are expected between larger and smaller geographical scales.

3.2. Population study of schistosomiasis prevention and management

In this subsection, we delve into the epidemiological complexities of schistosomiasis and examine how mathematical modelling contributes to our understanding of its transmission dynamics, the effectiveness of preventive measures, and the management of this persistent public health concern, as can be illustrated in Figure 4

3.2.1. Data for schistosomiasis population study

The data sources comprise empirical field surveys, clinical studies, health records, and demographic and climatological data, collectively offering insights into the characteristics and factors influencing the transmission of schistosomiasis. The integration of these diverse data sets is essential for evaluating population susceptibility and vulnerability to enable the comprehensive design of effective prevention and management strategies for schistosomiasis. Climatological (minimum and maximum temperature and rainfall patterns)

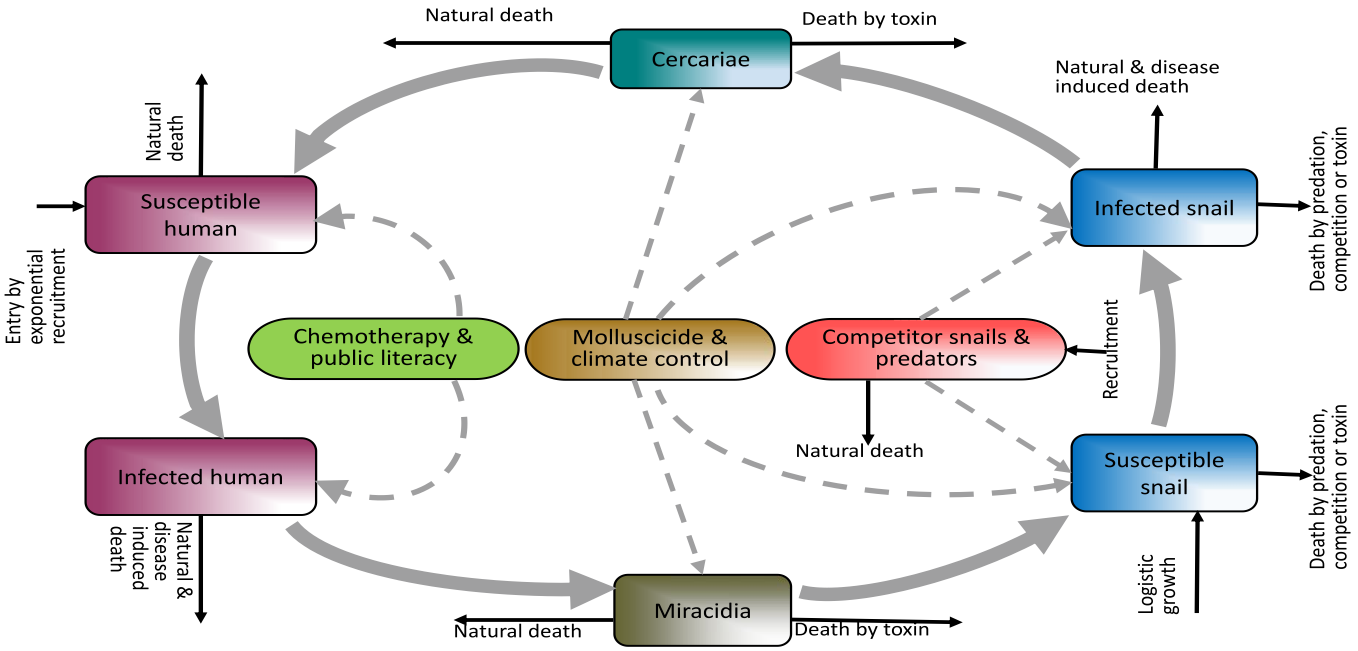

Figure 4. The life cycle of Schistosomiasis transmission serves as a model for studying population dynamics and assessing the impact of targeted control measures aimed at eradicating schistosomiasis by addressing various stages of the disease.

data for East Africa collected from the World Bank Climate change, WBC [92] was used to characterize climatically dependent traits such as human infection rate, cercaria shedding rate, snail infection rate, snail mortality rate, infected snail mortality rate, miracidia death rate, and others. The demographic and population data for Uganda, Kenya, and Tanzania were sourced from the latest UN demographic estimates and World Bank statistics from https://data.worldbank.org/indicator/sp.dyn.le00.in? and https://worldpopulationreview.com/countries, respectively. These data sets provided valuable insights for estimating various factors such as total population, life expectancy, daily recruitment rate, new infections per day, and more. The remaining parameter data (refer to figure 4) were obtained from a variety of sources, including existing literature, field and laboratory experiments [65,66,93, 94], as cited in the references). In cases where specific data were unavailable, expert estimates grounded in the current understanding of vector and disease dynamics in schistosomiasis were utilized.

3.2.2. Mathematical modelling approach

While empirical-statistical models are essential for their correlation purpose, mathematical models allow exploration of biological mechanisms and questions about the overall schistosomiasis dynamical system (see Figure 2 and 4), that cannot be adequately addressed using empirical methods. Such deterministic models not only quantify conditions for disease eradication but also aid in early detection, optimal targeting of preventive measures, and emphasizing timely treatment for at-risk individuals, among others [57, 95,96]. This study employed ordinary differential equations (ODEs) to formulate mathematical models based on the dynamics illustrated in Figure 4, incorporating specific parameters and scientific assumptions. ODEs have been widely applied in comprehending the transmission dynamics of schistosomiasis, as evidenced by various studies [57,65, 67,93,94,95]. The application of ODEs in this research provides a robust framework for analyzing and predicting the transmission patterns of schistosomiasis, contributing valuable insights to the field.

3.2.3. Mathematical model analysis

Mathematical models are analyzed numerically through techniques like center manifold theory to test the stability of equilibrium to understand the long-term behavior of the model [97]. The next-generation matrix approach is employed to evaluate disease severity [98,99]. For example, the basic reproduction number (R_0) in the model quantifies the average number of new infections caused by a single infectious individual. A $R_0 > 1$ suggests the potential for disease outbreak and persistence, while an $R_0 < 1$ indicates a likelihood of disease-free conditions. Additionally, sensitivity analyses using Rank Correlation Coefficients (PRCC) tests are applied to reveal significant parameters controlling transmission [100].

Moreover, numerical simulations are executed to simulate the model equations and visualize the dynamics over time. These analytical and numerical conditions serve as benchmarks for assessing the efficacy of control measures including climate over the transmission of the disease. The efficacy ranges from 0 to 1, it is 0 if the strategy is non effective and 1 if 100% effective.

4. Publication work outlines

This thesis comprises four peer-reviewed papers and two additional articles that have been submitted to peer-reviewed journals for publication.

4.1. Factors controlling local distribution of intermediate host snails

Tabo, Z., Neubauer, T. A., Tumwebaze, I., Stelbrink, B., Breuer, L., Hammoud, C., & Albrecht, C. (2022). Factors Controlling the Distribution of Intermediate Host Snails of Schistosoma in Crater Lakes in Uganda: A Machine Learning Approach. Frontiers in Environmental Science, 10, 871735. Doi: 10.3389/fenvs.2022.871735

The research aimed to unravel the factors influencing the distribution of *Biomphalaria* and/or *Bulinus* in Western Uganda. The region is a schistosomiasis endemic hotspot characterized by hilly uplands harboring over 90 small crater lakes, each hosting both snail species. The region also features a diverse array of potential factors that could impact the establishment of both genera. In this study, a local field

survey was conducted across three CLFs in the region, covering a total of 56 crater lakes. The survey aimed to gather data on various features in addition to the IH snail data, including associated mollusk fauna, geographical parameters (longitude, latitude, and altitude), physio-chemical parameters, absolute and Secchi depth, as well as climatic, environmental, and anthropogenic factors.

The assessment of these features for their importance in IH snail distribution was carried out by applying the RF machine learning approach. The findings indicate that distinct sets of parameters emerged as significant factors governing the presence of different IH snails across the combined and individual crater lake fields. Geography, mollusk fauna diversity, and, to a degree, climate and hydrology were key influencers for *Biomphalaria* in the combined dataset for the three CLFs. For *Bulinus*, mollusk fauna diversity, hydrology, and, to a lesser degree, geography significantly affected their distribution, while their co-existence was influenced by mollusk fauna diversity, geography, and hydrology.

At the level of each CLF, geography emerged as the primary determinant of *Biomphalaria*, while, alongside a diverse mollusk fauna, geography and hydrology played a comparatively smaller role in governing *Bulinus* snail distribution. The coexistence of both genera at this level was predominantly influenced by the diversity of associated mollusk fauna and geography. These parameters indicate meta-community assembly processes, encompassing dispersal limitation, environmental filtering, biotic interactions, and favorable conditions shaping species establishment in an ecosystem. They guide health workers and policymakers, helping prioritize interventions to interrupt local transmission for schistosomiasis control, based on identified predictors.

Contribution: *Lead author*; conceptualization, methodology, data analysis, conceived the study.

4.2. Factors controlling regional distribution of intermediate host snails

Tabo, Z., Breuer, L., Fabia, C. et al. A machine learning approach for modeling the occurrence of the major intermediate hosts for schistosomiasis in East Africa. Scientific Reports 14, 4274 (2024). Doi: 10.1038/s41598-024-54699-1

Biomphalaria and *Bulinus* snail species are key contributors to the significant disease burden of *S. mansoni* and *S. haematobium* in East Africa. This research systematically examines the significance of key factors, such as climate/environment, geography, soil composition, and human indices, associated with the two genera in East Africa utilizing an RF algorithm. Moreover, when contrasted with the previous local scale study in western Uganda, this study offers insights into potential variations in the primary factors influencing IH snail distribution across geographical scales.

The findings indicated minimal variation in the potential determinants influencing the distribution of both genera at a broad geographic scale. The findings highlight geography and climate as primary determinants for *Biomphalaria*, with *Bulinus* occurrence further linked to soil clay content and nitrogen concentration. Favorable climatic conditions in East Africa suggest a higher prevalence of IHs, while the relationship with geography suggests potential dispersal limitations or environmental filtering. The correlation between clay soils and soil nitrogen levels with *Bulinus* snails indicates favorable conditions for the survival and proliferation of these snails in their aquatic habitats. These factors represent the processes of speciation, extinction, environmental filtering, and dispersion influencing the establishment of IH snails in the region.

The study provides crucial insights into the regional framework, highlighting significant distinctions from essential factors at the local scale. This information assists health workers and policymakers in formulating targeted strategies for the prevention and control of schistosomiasis in the region, taking into account geographical variations.

Contribution: *Lead author*; conceptualization, methodology, main data analysis, conceived the study.

4.3. Exploring the interplay between climate change and schistosomiasis transmission dynamics.

Tabo, Z., Kalinda, C., Breuer, L., & Albrecht, C. (2024). Exploring the interplay between climate change and schistosomiasis transmission dynamics. Infectious Disease Modelling, 9 (1), 156-178. DOI: 10.1016/j.idm.2023.12.003

Centered on East Africa and recognizing the simultaneous increase in population growth along with the rising prevalence of schistosomiasis, this study investigates the substantial public health challenges arising from climate variability in the region. For this purpose, an autonomous climatic-mathematical model was developed, applied to the East African population, and parameterized using demographic and climatological data for this region.

The study findings highlight the substantial impact of seasonal and monthly variations on schistosomiasis transmission, demonstrating varied incidence rates among countries based on temperature and rainfall patterns. Within the region, seasonal schistosomiasis emergencies and re-emergences are noted. Conditions with temperatures between 20-27°C and precipitation ranging from 5-140 mm appear conducive for schistosomiasis transmission in East Africa. Notably, March and April pose heightened challenges with increased infections across the region, notably in Kenya, followed by Tanzania and Uganda. For each country, specific months reveal peaks in infections: April, May, and December in Kenya; February, March, and December in Uganda; and April and November in Tanzania. Conversely, June and July mark a period with fewer reported cases, attributed to adverse temperatures around 26-30°C and lower precipitation levels (5.0 to 91.8 mm).

Furthermore, the model predicts that parameters like snail reproduction rate, the unhygienic patterns of open deification, and the rate of miracidia shedding per parasite egg could significantly impact schistosomiasis infections by 2050. The model proficiently identifies hydro-meteorological conditions that increase the transmission risk of schistosomiasis across East Africa. It highlights the necessity of implementing proactive measures to mitigate the disease's impact on vulnerable populations in the region amidst climate change and developing effective management strategies.

Contribution: *Lead author*; conceptualization, methodology, data analysis, conceived the study

4.4. Modeling temperature-dependent schistosomiasis dynamics in Single and co-infections

Tabo, Z., Breuer, L., & Albrecht, C. (under review). Modelling Temperature-dependent Schistosomiasis Dynamics for Single and Co-infections with S. mansoni and S. haematobium. (Under revision in PLOS ONE)

Schistosoma mansoni and *Schistosoma haematobium* present distinct pathological profiles despite receiving limited attention in their co-infection scenario. This poses an additional challenge in understanding and addressing their impact on human health. Compelling epidemiological evidence consistently indicates a strong association between the two, emphasizing their susceptibility to temperature fluctuations in their mutual interaction and coinfection. This necessitated a temperature-dependent mathematical model to explore and compare their transmission patterns for both single and co-dynamics in the climatic setting of East Africa to address this crucial gap. Parameterized by data from two laboratory studies in the literature the results indicate that the impact of temperature on the heightened proliferation of new *S. haematobium* cases among human individuals, potentially leads to an increased likelihood of *S. mansoni* co-infection. Under moderate temperatures (20°C and 25°C), both individual and co-infected definitive hosts exhibit elevated infection levels compared to conditions at 35°C, where infections significantly decrease.

Furthermore, the recovery rates of infected individuals due to treatment increase with temperature, reaching a peak at 25°C and 35°C. *Biomphalaria* snails demonstrate higher population growth and susceptibility to infection than *Bulinus* snails, particularly below 25°C, with their populations declining above this temperature threshold. Result suggest that targeting snails during seasons below 25°C, when susceptibility is higher, and implementing human treatment interventions around 25°C-35°C, where recovery rates peak, may yield optimal results. While this suggests distinct intervention seasons for snails and humans, we propose a more effective approach by intensifying interventions during seasons with intermediate temperatures around 25°C for both snails and humans.

Contribution: *Lead author*; conceptualization, methodology, data analysis, conceived the study.

4.5. Selective competitive and predatory intervention of intermediate hosts

Tabo, Z., Luboobi, L., Kraft, P., Breuer, L., & Albrecht, C. (2024). Control of schistosomiasis by the selective competitive and predatory intervention of intermediate hosts: A mathematical modeling approach Mathematical Biosciences, 376, 109263. Doi; 10.1016/j.mbs.2024.109263

Within the ecological framework of biological control, the interaction between potential competitors and predators coexisting with IH snails becomes a pivotal factor in governing the distribution of IH snails as well as influencing the dynamics of *Schistosoma* transmission. Moreover, different competitors and predators of IH snails have different capabilities and behaviors as biological controls. This manuscript quantifies the dynamics of their interaction and assesses their consequent impact on schistosomiasis transmission, prevalence and impact of biological control. Examining the capabilities of diverse competitors indicates that particular non-host snails possess a competitive advantage that markedly reduces the population of IH snails. This, in turn, mitigates the emergence of cercariae, which pose a risk of infection to humans. Conversely, certain potential competitors demonstrate less impact, resulting in the persistence of the disease.

On the other hand, predator behaviors, especially attack and handling times, are pivotal in schistosomiasis control as they directly impact the level of predation on IH snails. Predators with faster attack rates and shorter prey-handling times are inclined to prey on and diminish the population of IH snails. This, in turn, leads to a subsequent reduction in the shedding of infectious cercariae, thereby limiting their transmission to humans and the spread of disease. Conversely, predators with longer handling times and slower attack rates for prey exhibit the opposite effect. However, employing a singular snail competitor or predator alone did not achieve complete disease eradication while their simultaneous application with controls at specific levels resulted in a noteworthy decrease in the IH snail population. This reduction brought the reproductive number below unity, signaling the effectiveness of disease control measures. Hence, by subjecting biological agents, especially native ones, to experimental assessment or screening of their competitive and predatory abilities, integrated control strategies can demonstrate cost-effectiveness and long-term efficacy. This approach is crucial for preserving ecosystem equilibrium, regulating snail population, and mitigating ecological repercussions associated with schistosomiasis

Contribution: *Lead author*; conceptualization, methodology, and data analysis conceived the study

4.6. Adapting strategies for effective schistosomiasis prevention

Tabo, Z., Kalinda, C., Breuer, L., & Albrecht, C. (2023). Adapting strategies for effective schistosomiasis prevention: a mathematical modeling approach. Mathematics, 11(12), 2609. Doi: 10.3390/math11122609

The latest WHO roadmap incorporates One Health strategies to eradicate schistosomiasis by 2030. Nonetheless, the effectiveness of both individual and layered strategies in achieving schistosomiasis eradication has not been thoroughly investigated. This study introduces a mathematical model that assesses the individual and tiered impact of chemotherapy, awareness programs, snail removal, and environmentally dependent chemical control focusing on their unique half-lives and exposure durations to the target species. Chemotherapy and chemical applications independently show significant success in reducing new cases of schistosomiasis. However, neither method individually achieves the eradication of the disease. Yet, no combination of 2-3-tiered approaches could entirely eradicate schistosomiasis, except for a four-tiered strategy that integrates all assessed interventions. Additionally, results revealed a chemical-temperature dependent efficacy, higher temperatures and prolonged chemical persistence reduce the chemically induced mortality rate of snails, necessitating the reapplication of chemicals to counter this decline.

Furthermore, increasing the half-life of various molluscicides boosts the mortality rate of snails. As a result, areas characterized by varied weather patterns and seasonal climates necessitate tailored strategies that consider the suitable/safer chemical and optimized time intervals for reapplication. The findings contribute to ongoing research on molluscicidal action and structure-activity relationships, aiming to develop suitable chemicals for schistosomiasis control. It enables the optimization of resources, and adaptation of interventions, and supports evidence-based decision-making, fostering community trust.

Contribution: *Lead author*; conceptualization, methodology, data analysis, conceived the study

5. Results and Discussion

This research centered on multi-faceted domains. Firstly, it involved the development of a statistical model for IH snails to predict factors influencing their community structure at a small geographical scale, addressing challenges and providing transmission overview at the local level in schistosomiasis hotspots in Western Uganda. Secondly, the research extended its focus to a larger geographical scale at the regional level, broader East Africa, to tackle challenges from a broader perspective. In the first and second domains. We explored the applicability of a machine learning algorithm to determine significant predictors of IH distribution and whether they differ across geographical scales. Thirdly, I introduced and crafted mechanistic models to provide a comprehensive understanding of the transmission dynamics of schistosomiasis. These models not only forecast the effects of climate variability but also assess various control strategies, as illustrated in Figure 4. Importantly, this initiative involves engaging all pertinent stakeholders. The applicability of these models extends beyond East Africa to a global context. Henceforth, the outcomes are presented and deliberated upon, delving into the factors governing the distribution of IH snails, along with the modeling of transmission dynamics, as well as strategies for the control and management of schistosomiasis.

5.1. Significant drivers of intermediate host snails across geographical scales

An expanding body of evidence indicates that targeting IH snails presents a viable strategy for effectively managing their populations and impeding the progression and dissemination of schistosomiasis [36,60,61]. However, the community structure and adaptability of IH snails play a crucial role in disease distribution [2,10]. Hence, it is vital to comprehend the major factors that affect the spread of IH snails, the primary agents responsible for the prevalence of schistosomiasis across various geographical levels. Applying empirical-statistical modeling, Tabo et al. [13] explored the distinctive parameter sets influencing the distribution of *Biomphalaria* and/or *Bulinus* at a scale of Western Uganda, and at the more confined scale of individual crater lakes field within western Uganda, a persistent schistosomiasis hotspot in East Africa [17,16,18]. Concurrently, Tabo et al. [101] provided insights into important factors influencing the distribution of IH snails on a regional scale across East Africa (refer to Figure 5 for various parameters investigated). The two studies validate the hypothesis that distinct parameters hold relevance across varying geographical scales. Within this thesis, we discuss the associations between the occurrence of IH snails and specific individual or grouped ecological parameters, with a focus on those deemed significant.

5.1.1. Geography

Geographical variables such as latitude, longitude, proximity to craters, and large lakes serve as crucial determinants for both genera across various geographical scales in general [13, 101]. However, altitude exhibits less pronounced importance for *Bulinus* distribution and lacks significant impact for *Biomphalaria* within individual crater lake fields, primarily due to the absence of altitudinal variation in these regions [13], as observed in some areas for *Bulinus*, see Abe et al. [102]. Nonetheless, Tabo et al. [101] documented that both genera thrive better below 500 meters above sea level (m a.s.l), possibly because lower altitudes favor stagnant water, facilitating breeding, while higher altitudes promote water flow [25], reflecting the dispersal patterns influenced by environmental filtering of IH snails [22,103]. The altitudinal range associated with risk exposure to schistosomiasis in East Africa spans from 3 to 2,342 m a.s.l across the two study areas, including those reported in earlier studies in Western Uganda [17,18,73] and elevations as high as 3,997 m a.s.l. at Mount Elgon in Eastern Uganda [16]. This suggests that individuals residing at these high altitudes should be considered part of the at-risk population, underscoring the necessity for targeted interventions in communities situated at high altitudes in East Africa and potentially in other countries beyond current national control activities. Furthermore, despite *Biomphalaria's* rapid dispersal, quick reproduction, and short generation times [10,104,105], the less significant association with distance (proximity to craters and large lakes) in a smaller geographical area at individual crater lake fields is not surprising. While this challenges assumptions regarding biogeographical isolation and colonization potential [106], it aligns with the island biogeography hypothesis, considering waterbodies (lakes) in highlands

and mountains as island-like systems [107]. This agreement holds, especially since crater lakes in our study area are hydrologically and hydro-geologically disconnected [15]. Moreover, the altitudinal range in habitats in western Uganda extends from 914 to above 1,566 meters, resulting in a diverse array of climate regimes [28] characterized by lower temperature, pressure, and oxygen levels, along with increased insolation [108].

5.1.2. Climate variables

Climate variables such as precipitation play a significant role in determining the suitability of snail habitats [22] and can trigger more schistosomiasis, potentially boosting breeding sites, and the frequency of disease occurrences [21,24]. Tabo et al. [109] found that climate strongly predicts the presence of IH snails at a larger geographical scale, aligning with the broader influence of climatic conditions on mollusk distribution reported [22]. Surprisingly, in smaller-scale regions like Western Uganda, the impact of climate appears to be diminished [13]. This may be attributed to the similar range of variation observed in different temperature and precipitation parameters for a smaller scale extent [13].

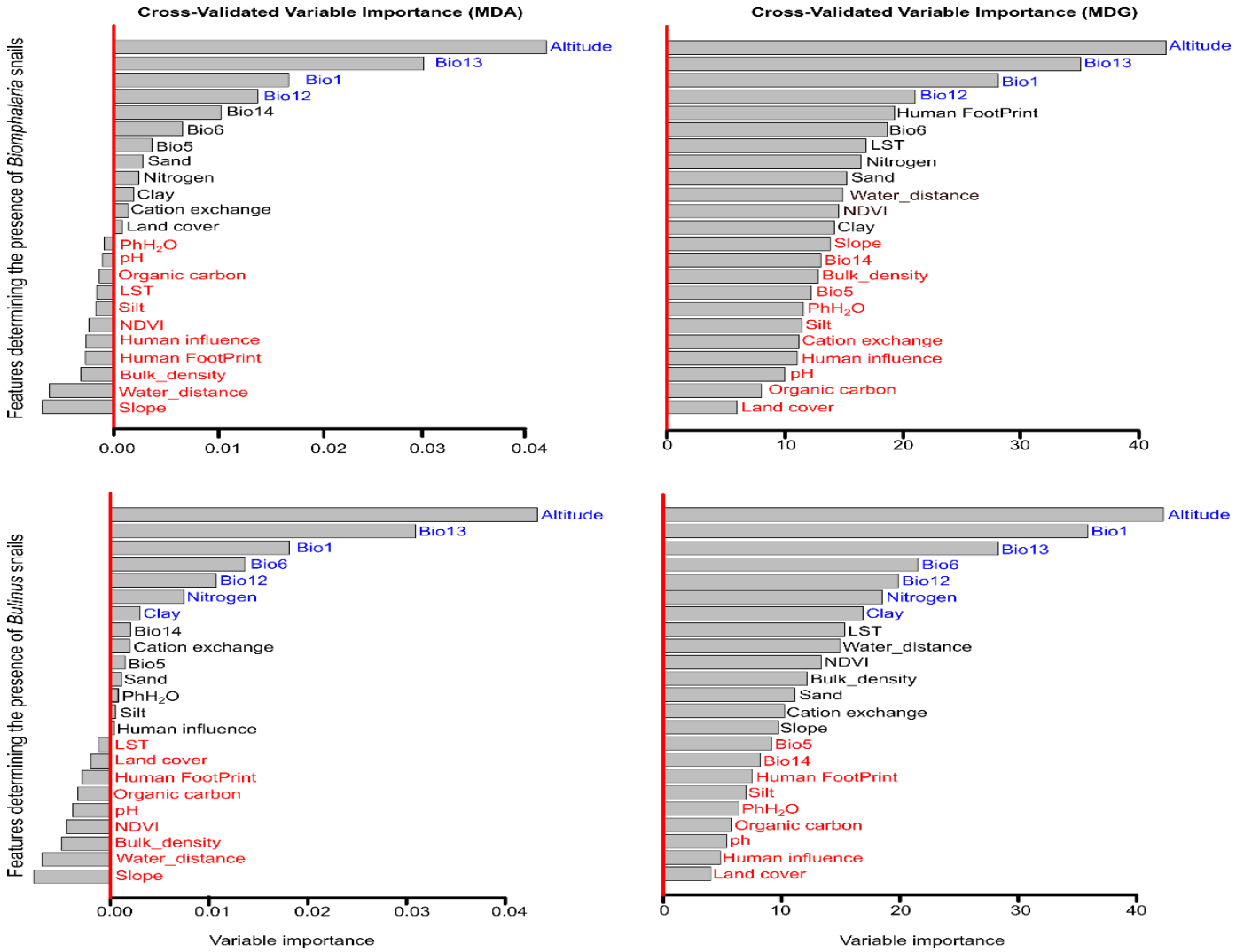

Figure 5. Contributions of the predictor features to the distribution of *Biomphalaria* (upper panel) and *Bulinus* (lower panel) across East Africa (a regional geographical scale) considering the variable importance by mean decrease in accuracy (MDA, left) and mean decrease in Gini (MDG, right) approach. The prominently significant features are highlighted in blue, those with minor influence are marked in black, and those in red are considered non-significant. Where BIO1= mean annual temperature, BIO5= temperature of the warmest month, BIO6= temperature of the coldest month, BIO12= annual precipitation, BIO13= precipitation of the wettest month, BIO14= precipitation of the driest month, LST=land surface temperature, water_distance=proxity to the nearest water body, NDVI= Normalized Difference Vegetation Index, Bulk_density=Bulk density of fine earth fraction, and PhH_2O = pH in water. Figure from Tabo et al. [101]

Thus the impact of climate change on IH snails and schistosomiasis prevalence may vary based on geographical or spatio-temporal scales [13,101,69].

Nonetheless, precipitation plays a pivotal role in assessing the presence of suitable water bodies where snails, known hosts of schistosomiasis, thrive [22], and its fluctuations due to regional climate change can alter transmission patterns and the onset of schistosomiasis [22,70,109]. An increase in precipitation levels fosters the proliferation of breeding sites by augmenting surface runoff into freshwater ecosystems which amplifies the supply of organic matter, a vital food source for snails, thereby stimulating their estivation, growth and fecundity [21,22]. Thereby influencing their populations and affecting disease transmission [110,111]. However, excessive precipitation reduces snail populations due flooding sites, displacing snails to new areas, establishing new habitats and posing a risk for the resurgence of schistosomiasis transmission [24]. Conversely, during dry seasons characterized by low precipitation levels, snails adapt by undergoing aestivation, leading to a reduction in their occurrence. Moreover, since freshwater snails are ectothermic and their temperature is subject to environmental regulation [26], temperature emerges as a key factor influencing various aspects of snail biology, including development, survival, fecundity, and reproductive rates [13,65,66,112]. Notably, Tabo et al. [109] highlights a significant prevalence of IH snails within temperature ranges of 20 to 25ºC in East Africa which complements a 20-27ºC range reported in other studies [110,111]. Thus, the inclusion of pertinent climate variables play a pivotal role in influencing the distribution of IH snail vectors in the transmission dynamic [23,65,66,67], is crucial for enhancing the accuracy of predictions [71].

5.1.3. Soil content and soil composition

Soil content and composition, including clay content and nitrogen levels, have emerged as relevant factors at the East African scale [101], with similar results observed for the same species on a larger scale extent [22]. However, conflicting findings from smaller-scale research by Mereta et al. [113], Olkeba et al. [114], and Deka [39] suggest a limited impact of clay content on snail presence. These discrepancies underscore the influence of geographical variations in defining soil types and compositions like soil nitrogen. For example, Tabo et al. [100] associated the influence of clay-rich soils with compositions ranging from 2-61% and nitrogen level of 0.5-4.6gkg^{-1} across East Africa.

Nonetheless, clay plays a significant role in shaping the distribution of IH snails, particularly *Bulinus*, by influencing soil texture, water retention, and drainage [113]. Furthermore, the robust relationship between soil nitrogen content and the distribution of *Bulinus* IH snails implies that even slight variations in soil nitrogen content can significantly affect their distribution. This connection suggests that while snails typically thrive in aquatic environments, the presence of soil nitrogen levels in the surrounding terrestrial areas may influence the spread of *Bulinus* snails. Theoretically, increased soil nitrogen often correlates with a higher likelihood of nitrogen leaching, potentially leading to elevated nitrogen levels in streams or floodplain habitats. Such conditions could favor the survival and proliferation of these snails within their aquatic environments.

Consequently, prioritizing considerations of soil type and nitrogen content becomes crucial when tailoring disease control strategies to diverse geographical settings [21,25]. However, elements such as carbon dioxide emissions from decomposing submerged vegetation and organic matter, may indirectly impact relationships with other dissolved ions, including that between nitrogen, oxygen and IH snails [115].

5.1.4. Habitat suitability

The ecological functionality depends on factors like sensitivity to hydrology and physio-chemical parameters such as pH, oxygen, conductivity, surface water temperature, magnesium, and calcium. Habitat depth, size, area, and Secchi depth are also crucial. They determine the occurrence and abundance of freshwater gastropods [22, 28, 29]. In Tabo et al. [13], among a diverse habitat parameters assessed, water conductivity emerged as a significant factor influencing *Bulinus* at individual crater lakes field scale, consistent with the majority of findings in the literature [29,116]. However, while oxygen plays a significant but relatively less critical role for *Biomphalaria*, it shows no significance for *Bulinus* in the same settings [13]. Nevertheless, the presence of other dissolved ions, such as high carbon dioxide emissions from decomposing submerged vegetation and organic matter, could indirectly influence relationships, such as that between oxygen and IH snails [115]. Furthermore, the sizes of

lakes and the seasonal variations in lake surface area serve as indicators of ecosystem stability. However, the majority of lakes in Western Uganda show minimal fluctuations over time. Even those that occasionally dry up have a lesser impact only on the distribution of *Bulinus* snails in individual crater lakes fields [13].

5.1.5. Associated mollusk diversity

The intricate ecological dynamics within freshwater ecosystems extend beyond the primary hosts of schistosomiasis, encompassing a complex interplay involving potential competitors e.g. *Thiara granifera* and *Physella acuta* [30,32,33,34], and predator's e.g. crayfish, river prawns, and the water bug *Sphaerodema urinator*, and Sciomyzidae flies in their larval stage, along with several fish and crustacean species of IH snails[30,33,34]. Tabo et al. [13] uncovered a surprising discovery in Western Uganda, where a diverse mollusk fauna ecosystem was associated with a high likelihood of encountering both *Bulinus* and *Biomphalaria* IH snails. This finding contradicts the anticipated heightened competition in environments with greater species diversity [102,117]. Despite expectations, the study identified the presence of pulmonates, known for their colonization abilities, high productivity, and shorter generation times [105]. Furthermore, IH snail species, including *Biomphalaria sudanica*, *Biomphalaria pfeifferi*, *Bulinus forskalii*, *Bulinus globosus*, and *Bulinus tropicus*, coexisted in this region [16].

Surprisingly, rather than a negative impact on IH snail survival, the positive correlation suggests that these snails thrive in environments conducive to mollusk diversity [13]. Significantly, the field survey conducted in western Uganda uncovered the presence of empty shells alongside crayfish in specific habitats [16], hinting at potential predation despite a strong positive correlation with mollusk diversity in the region [13]. These findings underscore the simultaneous interplay of competition and predation among IH snails, shaping their distribution patterns and increasing the likelihood of displacement and extinction.

5.1.6. Human activities

Tabo et al. [100] found that human activities had a minor impact on *Biomphalaria* snail distribution, with human factors such as population density, land use, and infrastructure development playing a weaker role compared to other determinants. However, Tabo et al. [13] study focusing on human settlement and land use in western Uganda did not identify human influence as a significant factor affecting IH snail distribution, in contrast to findings from studies like Olkeba et al. [114] and Krauth et al. [118] conducted at similar smaller geographical scales, which revealed a lesser significance. This discrepancy may be attributed to the limited spatial scope of the case study in Western Uganda, where many habitats are situated in protected areas like Queen Elizabeth Game Reserve, potentially limiting human activities and thus reducing their impact on snail distribution. Nevertheless, in the intricate network of human activities, the transfer of snails to different freshwater sources occurs through attachments to fishnets, seedlings during transplanting, or boats, leading to complex consequences for macroinvertebrate populations [38].

5.1.7. Non-significant parameters

Several predictor features exhibited minimal or negligible importance in influencing the distribution of *Biomphalaria* and/or *Bulinus* IH snails across different geographical scales. The parameters identified as having low relevance at a small geographical scale (Western Uganda) have been comprehensively discussed in Tabo et al. [13]. Similarly, those deemed of marginal significance at the regional level (East Africa) are categorized and extensively discussed in Tabo et al. [101].

5.2. Likelihood of genus occurrence across geographical scales

The simulated probabilities of genus occurrence, based on significant features identified across small and regional extents, revealed non-linear relationships for both *Biomphalaria* and *Bulinus* IH snails. Overall, the likelihood of encountering *Bulinus* species is generally higher than that of *Biomphalaria* species across East Africa, as indicated by their probability values, suggesting a higher potential for *S. haematobium* prevalence [101], see figure 6. However, the opposite trend is observed in western Uganda, where there are higher chances of contracting *S. mansoni* [13]. Categorizing extrinsic factors and understanding their relationships with IH snails are crucial for controlling their distribution and forming a strategic overview for successful schistosomiasis transmission at local and regional levels. However, the ultimate prevalence is also dependent on the interactions between the definitive human host population and *Schistosoma* parasite population in the life cycle [48,119]. Therefore, incorporating the direct impact of key quantifiable predictors of IH snails, identified in objective (i), such as climate variability significant at the East African scale, and biological ecological dynamics, mollusk diversity (non-host competitor snails) as well as potential predators) at the local level in Western Uganda in mathematical models, is essential in understanding the transmission dynamics of the disease in East Africa and globally.

5.3. Climate variability and the transmission dynamics of schistosomiasis

The complex interplay between climate change and disease transmission dynamics is a global challenge [120]. Deciphering the complex dynamics of schistosomiasis transmission, particularly with changing global climate patterns, involves understanding the relationship between climatic factors and *Schistosoma* life cycle stages IH snail vector, parasite eggs, miracidia, and cercaria parasites) displays sensitivity to climatic changes [22,65,66,70]. Consequently, the divergent responses of hosts and parasites to temperature

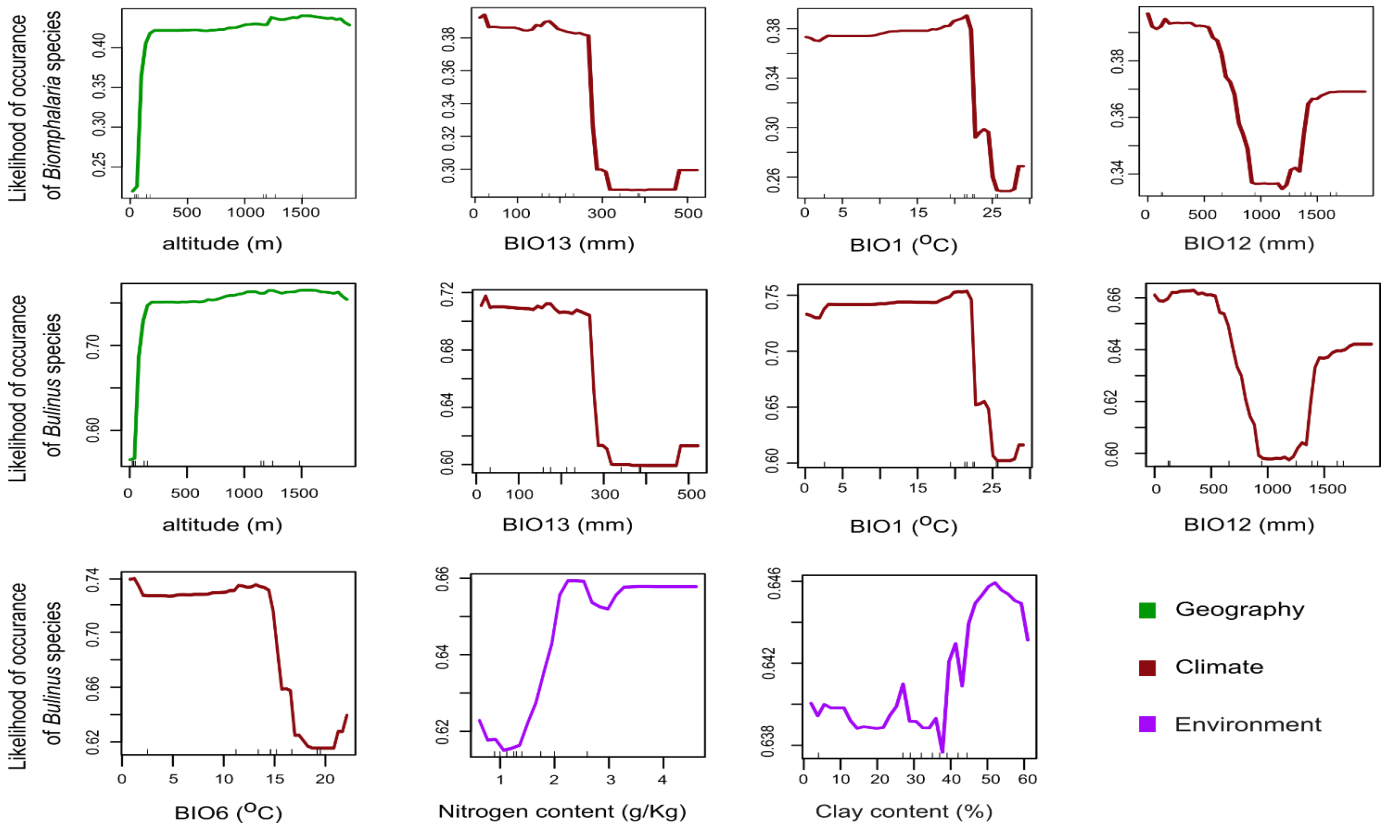

Figure 6. Likelihood of *Biomphalaria* species (1st panel) and *Bulinus* species occurrence (2nd and 3rd panels) in relation to the significant features identified by both importance metrics (MDA and MDG) in the *Biomphalaria* and *Bulinus* models across East Africa. Figure from Tabo et al. [101]

and/or rainfall fluctuations can either amplify/onset or diminish/offset the prevalence of the disease [121,122]. In specific tropical regions, including Tanzania, Kenya, Uganda, Rwanda, Burundi, and Eastern Zambia, climate changes may create favorable environments for intermediate hosts [70]. Mathematical models offer a framework to explore the direct impacts of climate change on these aspects of disease ecology [67,109,123]. Tabo et al. [109] formulated a groundbreaking climate-dependent mechanistic model to predict outbreaks and offsets of schistosomiasis across East Africa over season and time. The study reveal that the optimal conditions, (22-27°C and 50-160 mm) attributed to higher snail recruitment rates (Figure 7a), potentially by creating suitable breeding sites [124]. These conditions are linked to increased schistosomiasis activity, favouring various host snail traits [61,65,66]. While diverse conditions (27-33°C) could potentially lead to decreased schistosomiasis activities, affect ing snail mortality, fecundity, and growth rates [23, 109,110, 111]. Furthermore, the study reveals the frequencies and months of offsets and outbreaks in East Africa (Figure 7b-d). For example, cases across the region tends to increase during February-April and October-November and reaching the lowest infection levels in July (Figure 5c). Furthermore, specific temperature

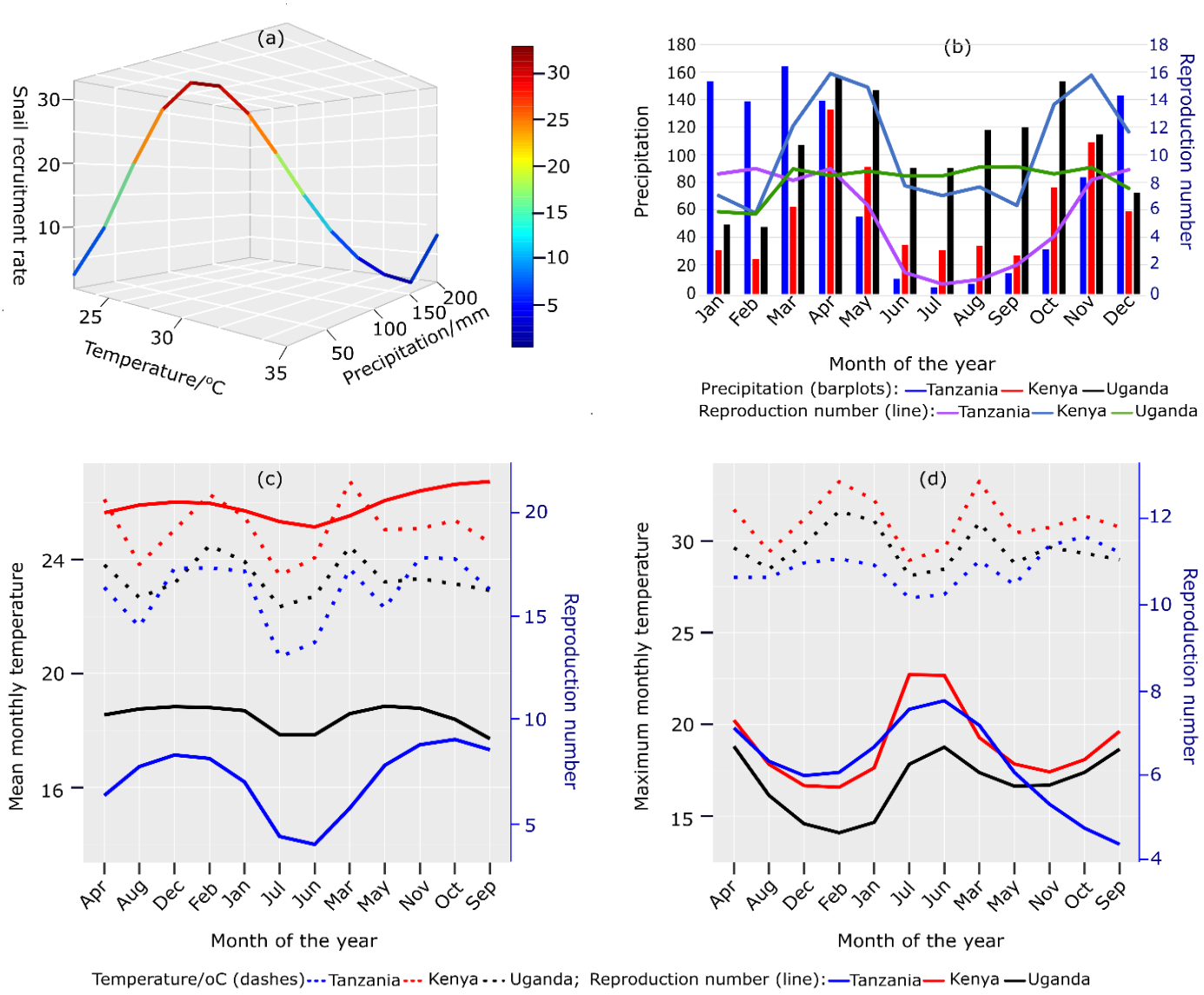

Figure 7. Individual seasonal effects of temperature and/or rainfall on (a) snail recruitment rate, and (b), (c), and (d) reproduction numbers in Tanzania (blue), Kenya (red), and Uganda (black). Figure (b-d) from Tabo et al. [109].

ranges (20-27ºC) and rainfall levels (5-140 mm) simultaneously heighten susceptibility to schistosomiasis. Surprisingly, temperatures above 27ºC, which typically known to hinder transmission [23,66,110,111], can support disease development when accompanied by suitable precipitation [109]. Conversely, certain precipitation variations may not significantly affect temperature and could limit schistosomiasis development, resulting in fewer reported cases in specific regions [23,109,120]. Thus, in regions like East Africa characterized with climate patterns shift, alterations in environmental conditions profoundly influence the distribution and abundance of IH snail, ultimately shaping the transmission dynamics of schistosomiasis. Moreover, Tabo et al. [109] suggest potential disease expansion with increased cases linked to higher snail recruitment rates in 20 years to come in the region, aligning with earlier predictions of disease spread into cooler regions [70,121].

Broadening the research scope, the complex, non-linear influence of temperatures on the *Biomphalaria-Schistosoma mansoni* [65] and *Bulinus-Schistosoma haematobium* systems [66] emphasizes the significance of climate variability for such schistosomiasis forms which share life cycle similarities and exhibit distinct infection patterns based on temperature susceptibility [48]. In their forthcoming study, Tabo et al. (2024, under revision) investigate the influence of temperature control not only on the transmission of a single species but also on the mutual interactions and co-infection dynamics of both species. Their findings suggest that *S. haematobium* increases susceptibility to *S. mansoni* co-infections. This poses an additional challenge, given its association with increased vulnerability to HIV infection [52, 125, 126,127] and bladder cancer [128,129]. Furthermore, the infection profile of *S. mansoni* demonstrates lower sensitivity to temperature changes, leading to fewer infection cases and a reduced risk of outbreaks compared to the infection profile of *S. haematobium* (Tabo et al., 2024, under revision). This observation aligns with reports indicating a higher prevalence of *S. haematobium* in regions where both species coexist [130,131,132]. Both infections peak at moderate temperatures (20-25°C), contrasting with higher temperatures (35°C). Additionally, the recovery rates of treated individuals peak at temperatures of 25°C and 35°C. Furthermore, Tabo et al. (2024, under revision) revealed that IHs, exhibit higher population growth and susceptibility to infection, especially below 25°C, with populations declining above this temperature threshold. We propose a targeted intervention strategy during seasons with intermediate temperatures around 25°C for both snails control and humans treatment. These study underscore the importance of incorporating temperature into predictive models in contrast to models neglecting temperature's influence and suggesting no difference in *Schistosoma* transmissibility between *S. mansoni* and *S. haematobium* [133].

5.4. Effects of non-host competitor snails and predators of intermediate host snails

In the pursuit of effective strategies for combating schistosomiasis, attention has turned to the fascinating realm of snail control [32,33,36,60,61]. Among these measures, the role of competitor snails and predators of IH snails emerges as a promising avenue for controlling IH snails and the spread of the disease. The competitive dynamics [30,32,33] and predation dynamics[30,33, 134] among snail species have been explored in field studies, shedding light on the potential of certain snail species to outcompete and prey on IH of schistosomes. While prior mathematical models studies have separately examined the intervention of competitor snails [135] and predators [96], except in the study by Tabo et al. [136] who simultaneously considered the impact of both non-host competitor snails and snail predators on the IH snails and the consequent disease prevalence.

Importantly, specific combinations of competitive snail species and effective predators, as highlighted by, can lead to a significant reduction in IH snail populations, signaling effective disease control [136]. However, intense competition and predation might result in complete IH snail population elimination, causing species displacement and local extinctions [136]. These results complements a number of field studies, for example effects of aggressive predation and competitiveness leading to extinctions [30,33,34]. However, appropriate balances between competitive and predatory interactions may disproportionately impact infected snails, contributing to a resilient ecosystem without species loss [136]. In an ecological dynamic with competition and predation processes, the vulnerability of infected snails, which are weaker and more immobile reducing their population

significantly, compared to healthy snails that tend to seek refuge near transmission sites [31, 137,138]. Field evidence from Pointier and McCullough [139] supports a decline in *Biomphalaria glabrata* due to competitors, *Melanoides tuberculata* and *Thiara granifera*, ultimately reducing schistosome-human interactions, the reproduction number and disease prevalence. In support of this result, Madsen [31].

In addition, overfishing reducing fish density in Lake Malawi increased schistosomiasis transmission. Furthermore, certain predators, like Marisa cornuarietis, may not effectively reduce IH snail populations due to alternative food sources [31,140,141]. Thus, selective interventions utilizing competitors and predators tailored to susceptible snails offer cost-effective and eco-friendly methods for managing schistosomiasis, backed by experimental assessments and population models, presenting a nature-based and sustainable solution for disease control.

5.5. Adapting climate based-strategies for effective schistosomiasis prevention

Today, there is a pressing need to evaluate and adapt climate-based strategies for effective schistosomiasis prevention. Hence, the adaptation of schistosomiasis prevention strategies to climate dynamics necessitates a comprehensive approach. Utilizing mathematical models is crucial for addressing schistosomiasis challenges amidst climate change. The effectiveness of various control strategies depicted in Figure 4, alongside mechanical measures (not explicitly represented in figure 4), such as physically hand-picking snails, creating deep channels as dry barriers for snail movement, enhancing flow velocity in irrigation canals, and implementing suitable cultivation practices like shorter fallow periods, modified irrigation techniques, and controlled flooding, were assessed, by Tabo et al. [112]. The evaluation considered both individual and combined impacts. The findings emphasized that relying solely on standalone approaches is insufficient for the complete eradication of schistosomiasis as highlighted in Table 1. Notably, a four-tiered approach demonstrates superior effectiveness over individual or two or three-tiered strategies and can lead to the complete eradication of schistosomiasis, with conditions where the reproduction number $R_0(P,T,M,C) < 1$ (Table 1). Additionally, a three-tiered strategy, denoted as (T,M,C), holds promise in reducing R_0 below 1. However, this can only be achieved when the efficacy of each individual control surpasses 90%, as indicated in Table 1. Nevertheless, attaining a 90% effectiveness level for each method presents practical challenges. The findings of Tabo et al. [112] align with previous research by Mangal et al. [65], King and Bertsch [142], and Zacharia et al. [54], indicating that a comprehensive approach is necessary to address schistosomiasis effectively. Instead of relying solely on a single strategy, such as drug treatment, integrated strategies are essential for combating the disease. Conversely, studies exploring the combination of chemotherapy with snail management have demonstrated incomplete eradication [37, 65, 112]. However, amidst climate change, the intricate relationship between environmental temperature, chemical degradation, and the half-life of the chemical plays a crucial role in snail control [37,123,143,144, 145]. According to Tabo et al. [112], temperature significantly influences molluscicide performance, with optimal efficacy observed at lower and moderate temperatures, specifically in the range of 15-25ºC. In the initial two weeks (14 days) of application, there is a notable increase in the chemical-induced mortality rate of snails, particularly cercariae and infected snails, and signifying effective disease control. Experimental findings from Montanari et al. [146] further support the effectiveness of molluscicides against adult snails, leading to reduced food intake and cessation of eating at temperatures of 18°C and 25ºC.

However, regions with higher temperatures exhibit lower rates of induced mortality, rendering molluscicides less effective in reducing snail populations and free-living parasite populations [109]. For example, as temperature and chemical exposure duration increase, snail mortality rates fall (Figure 8a) and may be linked to increased risks of disease transmission, which raises the R_0 value (Figure 8b). It's crucial to remember that, while no effects on survival or feeding rate have been observed at 30 ºC, no snail life may exist at very high temperatures. Hence, this study advocates for regular reapplication to sustain effectiveness, highlighting the direct correlation between half-life and active duration in water. This recommendation aligns with

ongoing research on suitable chemical development targeting IH snails [36,37,147]. However, the eradication of schistosomiasis presents challenges due to the high costs and ecological risks associated with chemical management [37], including aquatic biodiversity destruction and snail resistance, as well as limiting water use for communities. Alternatives with shorter half-lives (*C. viminalis* fruits or natural insecticides), lower toxicity (Nicotinanilide and Silver (Ag) nanopowder) offer reduced impact on biodiversity [37,148].

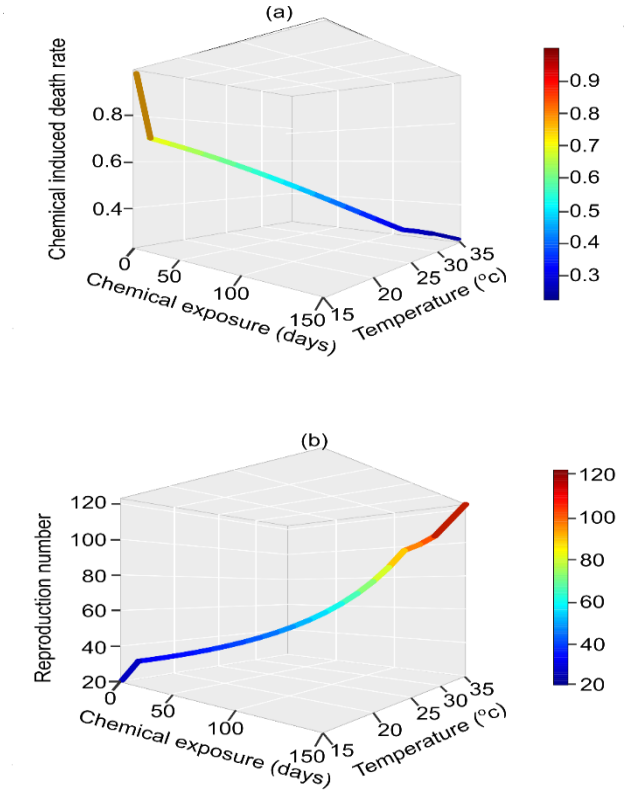

Figure 8. Combined impact of chemical exposure duration in days and the temperature on (a) the induced death rate of intermediate host snails and (b) the reproduction number

6. Conclusion and Recommendations

In conclusion, this thesis sheds light on the severe impact of schistosomiasis on impoverished rural communities in Sub-Saharan Africa, particularly in East Africa where the disease burden is highest. Despite failed efforts to eliminate schistosomiasis by 2020, ongoing research and surveillance are crucial to refine strategies for meeting the renewed elimination goals by 2030, as outlined in the new WHO roadmap. The study has identified various drivers of schistosomiasis transmission, including climatic variability, geographical factors, environmental/habitat suitability, biodiversity, and anthropogenic influences. Through data-driven case studies and mathematical modeling, the research has revealed distinct variations in the distribution of IH snails and the dynamics of schistosomiasis transmission across different geographic scales.

Additionally, the study highlights the importance of targeted prevention and control strategies, biological control measures, and proactive measures to mitigate the impact of the disease amidst climate change. Overall, this research contributes to a better understanding of IH snail community structure and the effectiveness of interventions, supporting evidence-based decision-making for schistosomiasis prevention and management in East Africa.

The study recommends a follow-up investigation at the East African level to estimate the geographic distribution of *Biomphalaria* and *Bulinus* genera, identify exposure risk zones, and quantify populations by risk level and country. The ecological environment is highly dynamic. What we observed yesterday may be different today. Therefore, regular field surveys and monitoring across East Africa, particularly in local hotspots, are essential for updating information on IH snail community structures. For effective biological control, experimental screening of potential native snail competitors and predators is crucial. Future research should explore the contrast between climate-driven snail vector management and schistosomiasis control strategies, incorporating spatially explicit transmission models for enhanced predictions of disease persistence and spread. Validation of the model through application in schistosomiasis endemic regions and comparison with available epidemiological data is an essential next step in advancing our understanding of the disease dynamics.

Table 1. Variability of R_0 across rows concerning single or different combinations of control strategies where T=treatment, P=public literacy, M=mechanical, and C=chemical control strategies with $T, P, M, C \epsilon [0, 1]$. The lower R_0, the more successful the controls are in controlling schistosomiasis. i.e. $R_0 < 1$ results for disease-free conditions. Table from Tabo et al. [112]

Control strategies as functions of R_0	Effectiveness of control strategies, $T, P, M, C \epsilon [0, 1]$										
	0	0.1	0.2	0.3	0.4	0.5	0.6	0.7	0.8	0.9	1
$R_0(T)$	10,000	1947	1390	1139	988	884	808	748	700	660	643
$R_0(P)$	10,000	9,900	9,600	9,100	8,400	7,500	6,400	5,100	3,600	1,900	975
R_0(M)	10,000	9,950	9,798	9,539	9165	8,660	8,000	7,141	6,000	4,359	3,122
$R_0(C)$	10,000	295	138	86.9	61.6	46.8	37.2	30.6	25.7	22.0	20.5
$R_0(T, P)$	10,000	1928	1334	1036	830	663	517	382	252	125	62.7
$R_0(M, C)$	10,000	294	136	82.9	56.5	40.5	29.8	21.8	15.4	9.6	6.401
$R_0(T, C$	10,000	57.4	19.3	9.9	6.1	4.1	3.0	2.3	1.8	1.5	1.3
$R_0(T, M)$	10,000	1937	1362	1086	905	766	646	534	420	288	201
$R_0(P, C)$	10,000	292	133	79.1	51.7	35.1	23.8	15.6	9.3	4.2	1.9
$R_0(P, M)$	10,000	9850	9406	8681	7699	6495	5120	3642	2160	828	304
$R_0(T, P, C)$	10,000	292	133	79.1	51.7	35.1	23.8	15.6	9.3	4.2	1.9
$R_0(T, P, M)$	10,000	9850	9406	8681	7699	6495	5120	3642	2160	828	304
$R_0(T, M, C)$	10,000	57.1	18.8	9.4	5.6	3.6	2.4	1.6	1.1	**0.63**	**0.41**
$R_0(P, C, M)$	10,000	291	130	75.5	47.4	30.4	19.1	11.1	5.5	1.8	**0.62**
$R_0(P, T, M, C)$	10,000	56.6	18.1	8.6	4.7	2.7	1.5	**0.83**	**0.39**	**0.12**	**0.04**

7. Reference list

1. WHO, World Health Organization. (2023): Combating neglected tropical disease. https://www.un.org/africarenewal/magazine/february-2023/combating-neglected-tropical-diseases. (accessed October 2023)
2. Steinmann, P., Keiser, J., Bos, R., Tanner, M., & Utzinger, J. (2006). Schistosomiasis and water resources development: systematic review, meta-analysis, and estimates of people at risk. *Lancet Infect Dis*, **6** (7), 411-425.
3. Aula, O. P., McManus, D. P., Jones, M. K., & Gordon, C. A. (2021). Schistosomiasis with a Focus on Africa. *Trop. med. infect*. **6**(3), 109.
4. Gryseels, B., Polman, K., Clerinx, J. and Kestens, L. (2006). Human schistosomiasis. *The Lancet*, **368** (9541), pp.1106-1118.
5. Tchuem Tchuenté, L. A., Rollinson, D., Stothard, J. R., & Molyneux, D. (2017). Moving from control to elimination of schistosomiasis in sub-Saharan Africa: time to change and adapt strategies. *Infect. Dis. Poverty*, **6**(1), 1-14.
6. Conteh, L., Engels, T., & Molyneux, D. H. (2010). Socioeconomic aspects of neglected tropical diseases. *The Lancet*, **375**, 239-247
7. Lu, X. T., Gu, Q. Y., Limpanont, Y., Song, L. G., Wu, Z. D., Okanurak, K., & Lv, Z. Y. (2018). Snail-borne parasitic diseases: an update on global epidemiological distribution, transmission interruption and control methods. *Infect. Dis. Poverty*, **7**(1), 1-16.
8. King, C. H. (2010). Parasites and Poverty: the Case of Schistosomiasis. *Acta Tropica* **113**, 95–104. doi:10.1016/j.actatropica.2010.11.012
9. Gray, D. J. et al. (2010). Schistosomiasis Elimination: Lessons from the Past Guide the Future. *Lancet Infect. Dis*. **10** (10), 733–736. doi:10.1016/S1473-3099(10)70099-2
10. Brown, D. S. (1994). Freshwater Snails of Africa and Their Medical Importance. Second edition. London: *Taylor & Francis*, 609.
11. Strong, E. E., Gargominy, O., Ponder, W. F., & Bouchet, P. (2008). Global diversity of gastropods (Gastropoda; Mollusca) in freshwater. *H ydrobiologia*, **595** 149-166.
12. Spigel, R. H., & Coulter, G. W. (2019). Comparison of hydrology and physical limnology of the East African great lakes: Tanganyika, Malawi, Victoria, Kivu and Turkana (with reference to some North American Great Lakes). In Limnology, climatology and paleoclimatology of the East African lakes (pp. 103-139). Routledge.
13. Tabo, Z., et al. (2022). Factors Controlling the Distribution of Intermediate Host Snails of *Schistosoma* in Crater Lakes in Uganda: A Machine Learning Approach. *Front. environ. sci.*, **10**, 871735.
14. Salzburger, W., Van Bocxlaer, B., & Cohen, A. S. Ecology and evolution of the African Great Lakes and their faunas. *Annu. Rev. Ecol. Evol. Syst.* **45,** 519-545 (2014).
15. Melack, J. M. (1978). Morphometric, physical and chemical features of the volcanic crater lakes of western Uganda.
16. Tumwebaze, I., et al.. (2019). Molecular identification of *Bulinus spp*. intermediate host snails of *Schistosoma spp*. in crater lakes of western Uganda with implications for the transmission of the *Schistosoma haematobium* group parasites. *Parasit. vectors*, **12**(1), 1-23.
17. John, R., Ezekiel, M., Philbert, C., and Andrew, A. (2008). Schistosomiasis Transmission at High Altitude Crater Lakes in Western Uganda. *BMC Infect. Dis*. **8,** (1), 1–6. doi:10.1186/1471-2334-8-110.

18. Stanton, M. C, et al. (2017). Intestinal Schistosomiasis in Uganda at High Altitude (>1400 M): Malacological and Epidemiological Surveys on Mount Elgon and in Fort Portal Crater Lakes Reveal Extra Preventive Chemotherapy Needs. *Infect. Dis. Poverty* **6,** (1), 34. doi:10.1186/s40249-017-0248-8.
19. hibwana, F. D., Tumwebaze, I., Mahulu , A., Sands, A. F., & Albrecht, C. (2020). Assessing the diversity and distribution of potential intermediate hosts snails for urogenital schistosomiasis: Bulinus spp.(Gastropoda: Planorbidae) of Lake Victoria. *Parasit. vectors*, **13**(1), 1-18.
20. Global Biodiversity Information Facility, GBIF.org (22 May 2023) GBIF Occurrence Download https://doi.org/10.15468/dl.6esfpk.
21. Madsen, H., Coulibaly, G., and Furu, P. Distribution of freshwater snails in the river Niger basin in Mali with special reference to the intermediate hosts of schistosomes. *Hydrobiologia* **146**, 77–88. doi:10.1007/bf00007580 (1987).
22. Stensgaard, A. S., et al. (2013). Large-scale determinants of intestinal schistosomiasis and intermediate host snail distribution across Africa: does climate matter? *Acta Tropica*, **128** (2), 378-390.
23. McCreesh, N., & Booth, M. (2013). Challenges in predicting the effects of climate change on *Schistosoma mansoni* and *Schistosoma haematobium* transmission potential. *Trends Parasitol*, **29** (11), 548-555.
24. David, N. F. et al. Spatial Distribution and Seasonality of *Biomphalaria* spp. In São Luís (Maranhão, Brazil). *Parasitol. Res*. **117** 1495–1502. doi:10.1007/s00436-018-5810-1 (2018).
25. Boitt, M. K., & Suleiman, M. K. (2021). Mapping of Freshwater Snails' Habitat—A Source of Transmitting Bilharzia in Mwea Sub-County, Kenya. *J. Environ. Prot. Sci*. **9**(10), 130-150.
26. Douchet, P., Gourbal, B., Loker, E. S., & Rey, O. (2023). *Schistosoma* transmission: scaling-up competence from hosts to ecosystems. *Trends Parasitol*. **39** 563-574
27. Díaz, A. V., Walker, M., & Webster, J. P. (2023). Reaching the World Health Organization elimination targets for schistosomiasis: the importance of a One Health perspective. Philos. *Trans. R. Soc*. **378**, 20220274
28. Rumes, B., Eggermont, H., and Verschuren, D. (2011). Distribution and Faunal Richness of Cladocera in Western Uganda Crater Lakes. *Hydrobiologia*. **676** (1), 39–56. doi:10.1007/s10750-011-0829-7.
29. Alhassan, A., et al. (2020). Distribution and Diversity of Freshwater Snails of Public Health Importance in Kubanni Reservoir and Weir/sediment Trap, Zaria, Nigeria. *J. Environ. Occup. Health*. **10** (1), 1–9. doi:10.5455/jeoh. 2019070409353.
30. Butler, J. M., Ferguson, F.F., Palmer, J.R. & Jobin, W.R. (1980). Displacement of a colony of *Biomphalaria glabrata* by an invading population of *Tarebia granifera* in a small stream in Puerto Rico. *Caribb. J. Sci.* **16**, 73-9
31. Madsen, H. (1990). Biological methods for the control of freshwater snails. *Parasitol. Today*. **6**, 237–241.
32. Dobson, M. (2004). Replacement of native freshwater snails by the exotic Physa acuta (Gastropoda: Physidae) in southern Mozambique; a possible control mechanism for schistosomiasis. *Ann. Trop. Med. Parasitol.* **98**. 543-548
33. Sura, S.A. & Mahon, H.K. (2011). Effects of competition and predation on the feeding rate of the freshwater snail, Helisoma trivolvis. *Am. Midl. Nat.* **166**, 358-68. https://doi.org/10.1674/0003-0031-166.2.358.
34. Sokolow, S. H, Lafferty, K. D. & Kuris, A. M. (2014). Regulation of laboratory populations of 677 snails (*Biomphalaria* and *Bulinus* spp.) by river prawns, Macrobrachium spp. (Decapoda, 678 Palaemonidae): implications for control of schistosomiasis. *Acta Trop*. **132**, 64-74
35. Sokolow, S.H. et al. (2015). Reduced transmission of human schistosomiasis after restoration of a native river prawn that preys on the snail intermediate host. *Proc. Natl. Acad. Sci.* **112**, 9650–9655.
36. Sokolow, S.H, et al. (2017) To reduce the global burden of human schistosomiasis, use 'old fashioned' snail control. *Trends Parasitol*, **34**, 23–40.
37. Zheng, L, et al. (2021). Molluscicides against the snail-intermediate host of Schistosoma: A review. *Parasitol. Res*. **120**, 3355–3393.
38. Van Bocxlaer, B., Albrecht, C., & Stauffer, J. R. (2014). Growing population and ecosystem change increase human schistosomiasis around Lake Malawi. *Trends Parasitol*, **30**(5), 217-220.
39. Deka, M. A. (2022). Predictive risk mapping of Schistosomiasis in Madagascar using ecological Niche modeling and precision mapping. *Trop. med. infect.*, **7**(2), 15.
40. Worldometer: Eastern Africa Population https://www.worldometers.info/world-population/eastern-africa-population/ 2023).
41. Hartter, J., et al. (2015). "Now There Is No Land: a story of Ethnic Migration in a Protected Area Landscape in Western Uganda." *Popul. Environ*, **36(**4), 452–479. doi:10.1007/s11111-014-0227-y.
42. Stothard, J. R., et al. (2005). Field Evaluation of the Meade Readiview Handheld Microscope for Diagnosis of Intestinal Schistosomiasis in Ugandan School Children. *J. Trop. Med. Hyg*. **73** (5), 949–955. doi:10.4269/ajtmh.2005.73.949.
43. Evan Secor, W. (2014). Water-based interventions for schistosomiasis control. *Pathog Glob Health*. **108**(5), 246-254.
44. Kalinda, C., Mindu, T., & Chimbari, M. J. (2020). A systematic review and meta-analysis quantifying schistosomiasis infection burden in pre-school aged children (PreSAC) in sub-Saharan Africa for the period 2000–2020. *PLoS One*, **15**(12), e0244695.
45. Kittur, N., et al. (2019). Persistent hotspots in schistosomiasis consortium for operational research and evaluation studies for gaining and sustaining control of schistosomiasis after four years of mass drug administration of praziquantel. *Am. J. Trop. Med. Hyg.*, **101**(3), 617.
46. Adenowo, A.F.; Oyinloye, B.E.; Ogunyinka, B.I.; Kappo, A.P. (2015). Impact of human schistosomiasis in sub-Saharan Africa. *Braz. J. Infect. Dis*. **19**, 196–205.
47. Ekpo, U. F., Oluwole, A. S., Abe, E. M., Etta, H. E., Olamiju, F., & Mafiana, C. F. (2012). Schistosomiasis in infants and preschool-aged children in sub-Saharan Africa: implication for control. *Parasitology*, **139** (7), 835-841.
48. Colley, D.G.; Bustinduy, A.L.; Secor,W.E.; King, C.H (2014). Human schistosomiasis. *Lancet*, 383, 2253–2264.
49. Mandahl-Barth, G. (1957). Intermediate hosts of Schistosoma: African Biomphalaria and Bulinus: *1. Bull. World Health Organ*. **16**(6), 1103.
50. Standley, C. J., Dobson, A. P., and Stothard, J. R. (2012). "Out of Animals and Back Again: Schistosomiasis as a Zoonosis in Africa," in Schistosomiasis (London: Intech), 209–230.
51. Lapa, M, et al. (2009) Cardiopulmonary manifestations of hepatosplenic schistosomiasis. Circulation. **119**(11) 1518-23. https://doi.org/10.1161/CIRCULATIONAHA.108.803221.
52. Khalaf, A. Shokeir, M. Shalaby. (2012). Urologic complications of genitourinary schistosomiasis. *World J Urol.* **30** 31-8. https://doi.org/10.1007/s00345-011-0751-7.
53. Barsoum RS, Esmat G, El-Baz T. (2013). Human schistosomiasis: clinical perspective. *J Adv Res*. **4**(5):433-44. https://doi.org/10.1016/j.jare.2013.01.005.
54. Zacharia A, Mushi V, Makene T. A. (2020). Systematic review and meta-analysis on the rate of human schistosomiasis reinfection. *PLoS One*. **15**(12):e0243224.
55. McManus, D. P. (2020). Recent progress in the development of liver fluke and blood fluke vaccines. *Vaccines*, **8**(3), 553.

56. Molehin, A. J. (2020). Schistosomiasis vaccine development: update on human clinical trials. *J. Biomed. Sci.* **27**(1), 1-7.
57. French, M.D. et al. (2010). Observed reductions in *Schistosoma mansoni* transmission from large-scale administration of praziquantel in Uganda: A mathematical modelling study. *PLoS Negl. Trop. Dis.* **4**, e897.
58. Bull, F.C. et al. (2020). Carty et al. World Health Organization 2020 guidelines on physical activity and sedentary behaviour. *Br J Sports Med*. **4**(24) 1451-1462.
59. Fenwick, A., & Jourdan, P. Schistosomiasis elimination by 2020 or 2030? *Int. J. Parasitol*. **46**, 385-388 (2016).
60. WHO, World Health Organization. (2021). Ending the neglect to attain the sustainable development goals: a sustainability framework for action against neglected tropical diseases 2021-2030.
61. Bergquist, R., Zhou, X. N., Rollinson, D., Reinhard-Rupp, J., & Klohe, K. (2017). Elimination of schistosomiasis: the tools required. Infect. Dis. Poverty. **6**(1), 158.
62. Gordon C, et al. (2019). Asian schistosomiasis: current status and prospects for control leading to elimination. *Trop. Med. Infect. Dis.* **4**, 40. (doi:10.3390/tropicalmed4010040).
63. Faust, C. L. et al. (2020). Schistosomiasis control: leave no age group behind. *Trends Parasitol.* **36**(7), 582-591.
64. Altizer, S., Ostfeld, R. S., Johnson, P. T., Kutz, S., & Harvell, C. D. (2013). Climate change and infectious diseases: from evidence to a predictive framework. *Science*, **341**(6145), 514-519.
65. Mangal TD, Paterson S, & Fenton A. (2008). Predicting the impact of long-term temperature changes on the epidemiology and control of schistosomiasis: a mechanistic model. *PLoS one*. **3**(1):e1438. https://doi.org/10.1371/journal.pone.0001438.
66. Kalinda C, Chimbari MJ, & Mukaratirwa S. Effect of temperature on the Bulinus globosus-Schistosoma haematobium system. Infect. Dis. Poverty. 2017;6(1):1-7. https://doi.org/10.1186/s40249-017-0260-z.
67. Kalinda, C., Mushayabasa, S., Chimbari, M. J., & Mukaratirwa, S. (2019). Optimal control applied to a temperature dependent schistosomiasis model. *Biosystems*, **175**, 47-56.
68. Benito, X, et al . (2020). Spatial and temporal ecological uniqueness of Andean diatom communities are correlated with climate, geodiversity and long-term limnological change. *Front. Ecol. Evol*., **260**.
69. Stensgaard, A.S., Booth, M., Nikulin, G., & McCreesh, N. (2016). Combining process-based and correlative models improves predictions of climate change effects on Schistosoma mansoni transmission in Eastern Africa. *Geospatial*. **11**, 94-101.
70. McCreesh, N., Nikulin, G., & Booth, M. (2015). Predicting the effects of climate change on Schistosoma mansoni transmission in eastern Africa. *Parasit. vectors*, **8**, 1-9.
71. Childs, L. M., et al. (2019). Linked within-host and between-host models and data for infectious diseases: a systematic review. *PeerJ* , **7**, e7057.
72. Exum, et al. (2019). The prevalence of schistosomiasis in Uganda: A nationally representative population estimate to inform control programs and water and sanitation interventions. *PLoS neglected tropical diseases*, *13*(8), e0007617.
73. Kabatereine, N. B., Brooker, S., Tukahebwa, E. M., Kazibwe, F., & Onapa, A. W. (2004). Epidemiology and geography of Schistosoma mansoni in Uganda: implications for planning control. *Trop. Med. Int. Health*. **9**(3), 372-380.
74. De Crop, W., and Verschuren, D. (2019). Determining Patterns of Stratification and Mixing in Tropical Crater Lakes through Intermittent Water-Column Profiling: A Case Study in Western Uganda. *J. Afr. Earth Sci.* **153,** 17–30. doi:10.1016/j.jafrearsci.2019.02.019.
75. Fick, S. E., and Hijmans, R. J. (2017). WorldClim 2: New 1-km Spatial Resolution Climate Surfaces for Global Land Areas. *Int. J. Climatol*. **37** (12), 4302–4315. doi:10.1002/joc.5086.
76. Wan, Z., Hook, S., Hulley, G. (2021). MODIS/Terra Land Surface Temperature/Emissivity Daily L3 Global 1km SIN Grid V061 [Data set]. NASA EOSDIS Land Processes DAAC. Accessed 2023-06-13 from https://doi.org/10.5067/MODIS/MOD11A1.061.
77. Didan, K. MODIS/Terra Vegetation Indices 16-Day L3 Global 250m SIN Grid V061 [Data set]. NASA EOSDIS Land Processes DAAC. Accessed 2023-06-13 from https://doi.org/10.5067/MODIS/MOD13Q1.061, 2021 (Accessed October 2023).
78. Friedl, M., Sulla-Menashe, D. (2022). MODIS/Terra+Aqua Land Cover Type Yearly L3 Global 500m SIN Grid V061 [Data set]. NASA EOSDIS Land Processes DAAC. Accessed 2023-06-13 from https://doi.org/10.5067/MODIS/MCD12Q1.061.
79. Batjes, N. H., Ribeiro, E., & Van Oostrum, A. (2020). Standardised soil profile data to support global mapping and modelling (WoSIS snapshot 2019*). Earth Syst. Sci. Data*, **12**(1), 299-320.
80. Farr, T.G., et al. (2007). The shuttle radar topography mission: *Rev. Geophys*, **45**. 2. https://doi.org/10.1029/2005RG000183.
81. Jenness, J.; Dooley, J.; Aguilar-Manjarrez, J.; Riva, C. (2007) African Water Resource Database. GIS-based tools for inland aquatic resource management. 1. Concepts and application case studies CIFA Technical Paper. No.33, Part 1. Rome, FAO. **167**p.
82. Wildlife Conservation Society - WCS, and Center for International Earth Science Information Network - CIESIN - Columbia University. 2005. Last of the Wild Project, Version 2, 2005 (LWP-2): Global Human Influence Index (HII) Dataset (Geographic). Palisades, New York: NASA Socioeconomic Data and Applications Center (SEDAC).
83. Breiman, L. (2001). Random Forests. Mach. Learn. **45** (1), 5–32. doi:10.1023/a: 1010933404324.
84. Huang, B. F. F., and Boutros, P. C. (2016). The Parameter Sensitivity of Random Forests. BMC Bioinformatics 17 (1), 1–13. doi:10.1186/s12859-016-1228-x.
85. Schonlau, M., and Zou, R. Y. (2020). The Random forest Algorithm for Statistical Learning. *Stata J.* **20** 3–29. doi:10.1177/1536867X20909688
86. Collin, F. D. et al. (2021). Extending Approximate Bayesian Computation with Supervised Machine Learning to Infer Demographic History from Genetic Polymorphisms Using DIYABC Random Forest. *Mol. Ecol. Resour.* **21** 2598–2613. doi:10.1111/1755-0998.13413
87. Georganos, S. et al. (2021). Geographical Random Forests: a Spatial Extension of the Random forest Algorithm to Address Spatial Heterogeneity in Remote Sensing and Population Modelling. *Geocarto Int.* **36**, 121–136. doi:10.1080/10106049.2019.1595177
88. Boulesteix, A.-L., Janitza, S., Kruppa, J., and König, I. R. (2012). Overview of Random Forest Methodology and Practical Guidance with Emphasis on Computational Biology and Bioinformatics. WIREs. *Data Mining Knowl. Discov*. **2**, 493–507. doi:10.1002/widm.1072
89. Bunyamin, H., and Tunys, T. A. (2016). Comparison of Retweet Prediction Approaches: the Superiority of Random Forest Learning Method. *Telkomnika* **14** 1052–1058. doi:10.12928/TELKOMNIKA.v14i3.3150
90. Zhang, J. et al. (2020). Risk Prediction of Two Types of Potential Snail Habitats in Anhui Province of China: Model-Based Approaches. *PLOS Negl. Trop. Dis.* **14**, e0008178. doi:10.1371/journal.pntd.0008178
91. Brieuc, M. S. O., Waters, C. D., Drinan, D. P., and Naish, K. A. A. (2018). Practical Introduction to Random Forest for Genetic Association Studies in Ecology and Evolution. *Mol. Ecol. Resour*. **18**, 755–766. doi:10.1111/1755-0998.12773.

92. Home | Climate Change Knowledge Portal, World Bank Climate change, WBC. (2022). Available at: https://Climateknowledgeportal.Worldbank.Org/Country . Accessed 14 Febuary 2023.
93. Abokwara, A.; Madubueze, C.E. (2021). The Role of Non-pharmacological Interventions on the Dynamics of Schistosomiasis. *J. Math. Fundam. Sci*. **53**, 243–260.
94. Nur,W.; Trisilowati; Suryanto, A.; Kusumawinahyu,W.M. (2021). Mathematical model of schistosomiasis with health education and molluscicide intervention. *J. Phys. Conf. Ser*. **1821**, 012033.
95. Gao S, Liu Y, Luo Y, & Xie D. (2011). Control problems of a mathematical model for schistosomiasis transmission dynamics. *Nonlinear Dyn*, 63, 503-512. 721 https://doi.org/10.1007/s11071-010-9818-z.
96. Das, S., Das, P. & Das P. (2021). Chemical and biological control of parasite-borne disease 737 Schistosomiasis: An impulsive optimal control approach. *Nonlinear Dyn*. 104, 603-28 738. https://doi.org/10.1007/s11071-021-06262-0.
97. Chavez, C.C., Feng, Z., Huang, W. (2002). On the computation of R0 and its role on global stability. In Mathematical Approaches for Emerging and Re-Emerging Infection Diseases: An Introduction; Springer: Berlin/Heidelberg, Germany. **125**. 229–250.
98. Diekmann, O., Heesterbeek, J.A.P., Metz, J.A.J. (1990) On the definition and the computation of the basic reproduction ratio R 0 in models for infectious diseases in heterogeneous populations. *J. Math. Biol.* **28**, 365–382.
99. Driessche, P., & Watmough, J. (2002). Reproduction numbers and sub-threshold endemic equilibria for compartmental models of disease transmission. *Math. Biosci.* **180**(1-2), 29-48. https://doi.org/10.1016/S0025-5564(02)00108-6.
100. Sanchez MA, Blower SM. (1997). Uncertainty and sensitivity analysis of the basic reproductive rate: tuberculosis as an example. *Am J Epidemiol*. 145(12) 1127-37.
101. Tabo, Z. *et al.* A machine learning approach for modeling the occurrence of the major intermediate hosts for schistosomiasis in East Africa. *Sci Rep* **14**, 4274 (2024). https://doi.org/10.1038/s41598-024-54699-1
102. Abe et al. (2012). Predicting the geospatial distribution of *Bulinus* snail vector of urinary schistosomiasis in Abeokuta, South-Western, Nigeria. *Zool* **10**, 53–60
103. Hauffe, T., Schultheiß, R., Van Bocxlaer, B., Prömmel, K., & Albrecht, C. (2016). Environmental heterogeneity predicts species richness of freshwater mollusks in sub-Saharan Africa. *Int J Earth Sci*, **105**, 1795
104. Kappes, H., and Haase, P. (2012). Slow, but Steady: Dispersal of Freshwater Molluscs. *Aquat. Sci*. **74** (1), 1–14. doi:10.1007/s00027-011-0187-6
105. Kappes, H., Tackenberg, O. ,and Haase,P.(2014). Differences in Dispersal-and Colonization-Related Traits between Taxa from the Freshwater and the Terrestrial Realm. *quat.Ecol*. **48** (1),73–83. doi:10.1007/s10452-013-9467-7.
106. Covich, A.P.(2010). Winning the Biodiversity Arms Race Among Freshwater Gastropods: Competition and Coexistence through Shell Variability and Predator Avoidance. *Hydrobiologia*. **653** (1),191–215.doi:10.1007/s10750-010-0354-0.
107. Itescu, Y. (2019).Areisland-Like Systems Biologically Similar to Islands? AReview of theEvidence Ecography. 42 (7),1298–1314. doi:10.1111/ECOG.0395.
108. Wilson, R. J., Gutiérrez, D., Gutiérrez, J., Martínez, D., Agudo, R., & Monserrat, V. J. (2005). Changes to the elevational limits and extent of species ranges associated with climate change. Ecology letters, 8(11), 1138-1146.
109. Tabo, Z., Kalinda, C., Breuer, L., & Albrecht, C. (2024). Exploring the interplay between climate change and schistosomiasis transmission dynamics. *Infect. Dis. Model*, **9**(1), 158-176.
110. Malone, J. B. (2005). Biology-based mapping of vector-borne parasites by geographic information systems and remote sensing. *Parassitologia*, **47**, 27.
111. Manyangadze, T., Chimbari, M. J., Gebreslasie, M., Ceccato, P., & Mukaratirwa, S. (2016). Modelling the spatial and seasonal distribution of suitable habitats of schistosomiasis intermediate host snails using Maxent in Ndumo area, KwaZulu-Natal Province, South Africa. *Parasit Vectors*, **9**(1), 1-10.
112. Tabo, Z., Kalinda, C., Breuer, L., & Albrecht, C. (2023). Adapting Strategies for Effective Schistosomiasis Prevention: A Mathematical Modeling Approach. *Mathematics*. **11**(12), 2609.
113. Mereta, S. T. et al. (2012). Analysis of environmental factors determining the abundance and diversity of macroinvertebrate taxa in natural wetlands of Southwest Ethiopia. *Ecol. Inform.* 7(1), 52-61.
114. Olkeba, B. K. et al. (2020). Environmental and biotic factors affecting freshwater snail intermediate hosts in the Ethiopian Rift Valley region. *Parasit. Vectors*. **13**, 1-13
115. Tchakonté, S., Ajeagah, G. A., Diomandé, D., Camara, A. I., & Ngassam, P. (2014). Diversity, dynamic and ecology of freshwater snails related to environmental factors in urban and suburban streams in Douala–Cameroon (Central Africa). *Aquat. Ecol.* **48**, 379-395.
116. Marie, M. A. S., El-Deeb, F. A. A., Hasheesh, W. S., Mohamed, R. A., & Sayed, S. S. M. (2015). Impact of seasonal water quality and trophic levels on the distribution of various freshwater snails in four Egyptian governorates. *Appl. Ecol. Environ. Sci.* 3(4), 117-126.
117. Svanbäck, R., & Bolnick, D. I. (2007). Intraspecific competition drives increased resource use diversity within a natural population. Proceedings of the Royal Society B: Biol. Sci., **274**(1611), 839-844.
118. Krauth, S. J. et al. (2017). Distribution of intermediate host snails of schistosomiasis and fascioliasis in relation to environmental factors during the dry season in the Tchologo region, Côte d'Ivoire. *Adv Water Resour*. **108** 386-396
119. Opisa, S., Odiere, M. R., Jura, W. G., Karanja, D., & Mwinzi, P. N. (2011). Malacological survey and geographical distribution of vector snails for schistosomiasis within informal settlements of Kisumu City, western Kenya. *Parasit vectors*. **4**(1), 1-9.
120. Van der Wiel, K., & Bintanja, R. (2021). Contribution of climatic changes in mean and variability to monthly temperature and precipitation extremes. *Commun. Earth Environ.* **2**(1), 1.
121. Martens, W. J. M., Jetten, T. H., Rotmans, J., & Niessen, L. W. (1995). Climate change and vector-borne diseases: a global modelling perspective. *Glob. Environ. Change.* **5**(3), 195-209. https://doi.org/10.1016/0959-3780(95)00051-O
122. Paull SH, Johnson PT. (2011). High temperature enhances host pathology in a snail–trematode system: possible consequences of climate change for the emergence of disease. *Freshw. Biol.* **56**(4):767-78. https://doi.org/10.1111/j.1365-2427.2010.02547.x
123. Feng Z, Eppert A, Milner FA, Minchella DJ. (2004). Estimation of parameters governing the transmission dynamics of schistosomes. *Appl Math Lett.* **17**(10):1105-12.
124. Xue, Z., Gebremichael, M., Ahmad, R., Weldu, M. L., & Bagtzoglou, A. C. (2011). Impact of temperature and precipitation on propagation of intestinal schistosomiasis in an irrigated region in Ethiopia: suitability of satellite datasets. *Trop. Med. Int. Health*, **16**(9), 1104-1111.
125. Mbabazi, P. S, et al. (2011). Examining the relationship between urogenital schistosomiasis and HIV infection. *PLOS Negl Trop Dis.* **5**(12):e1396. https://doi.org/10.1371/journal.pntd.0001396
126. 127. WHO, World Health Organization. Schistosomiasis. Available online: https://www.who.int/news-room/fact-sheets/detail/schistosomiasis (accessed on 3 February 2023).

127. Zirimenya, L., Mahmud-Ajeigbe, F., McQuillan, R., & Li, Y. (2020). A systematic review and meta-analysis to assess the association between urogenital schistosomiasis and HIV/AIDS infection. *PLoS Negl Trop Dis.* **14**(6), e0008383.
128. Dematei, A., Fernandes, R., Soares, R., Alves, H., Richter, J., & Botelho, M. C. (2017). Angiogenesis in Schistosoma haematobium-associated urinary bladder cancer. Apmis., 125(12), 1056-1062.
129. Efared, B. et al. (2022). Urinary bladder *Schistosoma haematobium*-related squamous cell carcinoma: a report of two fatal cases and literature review. *Trop. Dis. Travel Med. Vaccines*, **8**(1), 1-5.
130. Cunin P, Tchuem Tchuenté LA, Poste B, Djibrilla K, Martin PM. Interactions between *Schistosoma haematobium* and *Schistosoma mansoni* in humans in north Cameroon. Trop Med Int Health. 2003;8(12):1110-7. https://doi.org/10.1046/j.1360-2276.2003.01139.x
131. Garba A, et al. (2010). Schistosomiasis in infants and preschool-aged children: infection in a single *Schistosoma haematobium* and a mixed *S. haematobium-mansoni* foci of Niger. *Acta trop*. 115(3):212-9. https://doi.org/10.1016/j.actatropica.2010.03.005
132. Nassar, A. S, Adetoro, T. A, Adebimpe, W. A, Muhibi, M. A. (2015). Presumptive diagnosis of *Schistosoma haematobium* and *Schistosoma mansoni* using microscopy as gold standard in a Riverrine community of Southwestern Nigeria. African J. Clin. Exp. Microbiol. 2013;14(3):180-3. https://doi.org/10.4314/ajcem.v14i3.11
133. He YX, Chen L, Ramaswamy K. Schistosoma mansoni, S. haematobium, and S. japonicum: early events associated with penetration and migration of schistosomula through human skin. Exp Parasitol. 2002;102(2):99-108. https://doi.org/10.1016/S0014-4894(03)00024-9
134. Younes, A., El-Sherief, H., Gawish, F.& Mahmoud, M. Biological control of snail hosts transmitting schistosomiasis by the water bug, Sphaerodema urinator. Parasitol. Res. 116, 1257-64 (2017). https://doi.org/10.1007/s00436-017-5402-5
135. Allen, E.J. & Victory, Jr. HD. (2003). Modelling and simulation of a schistosomiasis infection with biological control. *Acta Trop*. **87**, 251-67 https://doi.org/10.1016/S0001-735 706X(03)00065-2
136. Tabo, Z., Luboobi, L., Kraft, P., Breuer, L., & Albrecht, C. (2024). Control of schistosomiasis by the selective competitive and predatory intervention of intermediate hosts: A mathematical modeling approach. Mathematical Biosciences, 376, 109263. Doi; 10.1016/j.mbs.2024.109263
137. Moore, J. (2002). Parasites and the behavior of animals. (Oxford University Press on Demand.
138. Swartz, S. J., De Leo, G. A., Wood, C. L. & Sokolow, S.H. (2015). Infection with schistosome parasites in snails leads to increased predation by prawns: implications for human schistosomiasis control. *J. Exp. Biol.* **218**, 3962-7. https://doi.org/10.1242/jeb.129221
139. Pointier JP, McCullough F. (1989). *Acta Trop*. **46**(3):147-55. https://doi.org/10.1016/0001-706X(89)90031-4
140. Stauffer, J. R. et al. (1997). Controlling vectors and hosts of parasitic diseases using fishes. *BioScience.* **47**, 41-9 https://www.jstor.org/stable/1313005
141. Arostegui, M. C. et al. (2019). Potential biological control of schistosomiasis by fishes in the lower Senegal river basin. *Am. J. Trop. Med. Hyg*. **100**,117 doi: 10.4269/ajtmh.18-0469
142. King CH, Bertsch D. (2015). Historical perspective: snail control to prevent schistosomiasis. *PLOS Negl. Trop. Dis.* **9**(4):e0003657.
143. Stothard, J.R.; Chitsulo, L.; Kristensen, T.K.; Utzinger, J. (2009). Control of schistosomiasis in sub-Saharan Africa: Progress made, new opportunities and remaining challenges. *Parasitology*, **136**, 1665–1675.
144. Fishel FM. (2013). Storage Limitation Statements: Temperature–Herbicides: PI123/PI160, 4/2013. EDIS. **2013**(4).
145. Ziska, L.H. (2014). Increasing minimum daily temperatures are associated with enhanced pesticide use in cultivated soybean along a latitudinal gradient in the mid-western United States. *PLoS ONE*. **9**, e98516.
146. Montanari AL, Accorsi A, Nasi M, Malagoli D. (2019). Effects of a nematode-based molluscicide on survival and antimicrobial peptide expression in Pomacea canaliculata. *Invertebr. Surviv. J.* **16**, 37.
147. King, C.; Sutherland, L.J.; Bertsch, D. (2015). Systematic review and meta-analysis of the impact of chemical-based molluscicides for control of *S. mansoni* and *S. haematobium* transmission. *PLoS Negl. Trop. Dis*. **9**, e0004290.
148. Gohar AA, Maatooq GT, Gadara SR, Aboelmaaty WS, El-Shazly AM. (2014). Molluscicidal activity of the methanol extract of Callistemon viminalis (Sol. ex Gaertner) G. Don ex Loudon fruits, bark and leaves against *Biomphalaria alexandrina* snails. *IJPR*.**13** (2):505.

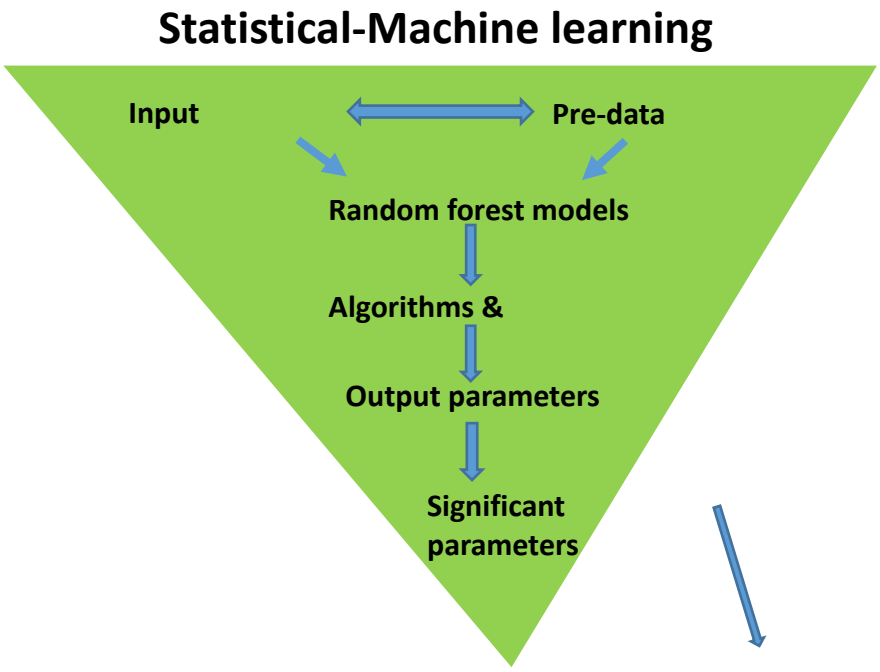

III. PUBLICATIONS

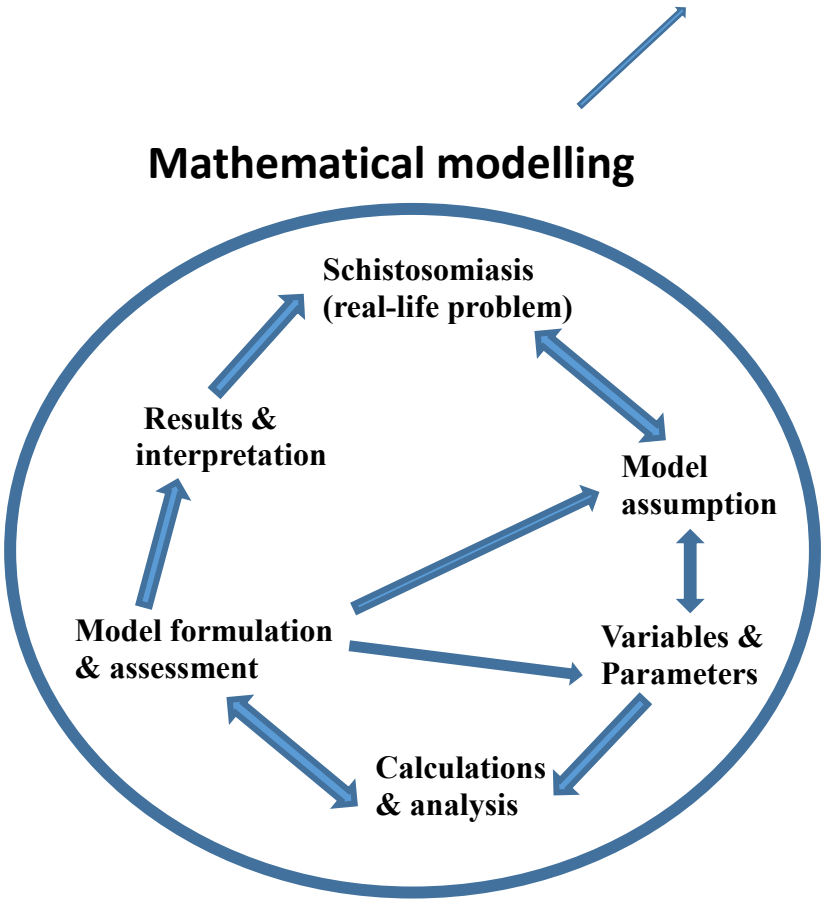

frontiers | Frontiers in Environmental Science

ORIGINAL RESEARCH
published: 14 April 2022
doi: 10.3389/fenvs.2022.871735

Factors Controlling the Distribution of Intermediate Host Snails of *Schistosoma* in Crater Lakes in Uganda: A Machine Learning Approach

Zadoki Tabo[1,2], Thomas A. Neubauer[1,3], Immaculate Tumwebaze[1], Björn Stelbrink[1†], Lutz Breuer[2,4], Cyril Hammoud[5,6] and Christian Albrecht[1]*

[1]Department of Animal Ecology and Systematics, Justus Liebig University Giessen, Giessen, Germany, [2]Department of Landscape Ecology and Resource Management, Justus Liebig University Giessen, Giessen, Germany, [3]Naturalis Biodiversity Center, Leiden, Netherlands, [4]Centre for International Development and Environmental Research (ZEU), Justus Liebig University Giessen, Giessen, Germany, [5]Limnology Research Unit, Ghent University, Ghent, Belgium, [6]Department of Biology, Royal Museum for Central Africa, Tervuren, Belgium

Schistosomiasis affects over 700 million people globally. 90% of the infected live in sub-Saharan Africa, where the trematode species *Schistosoma mansoni* and *S. haematobium* transmitted by intermediate hosts (IH) of the gastropod genera *Biomphalaria* and *Bulinus* are the major cause of the human disease burden. Understanding the factors influencing the distribution of the IH is vital towards the control of human schistosomiasis. We explored the applicability of a machine learning algorithm, random forest, to determine significant predictors of IH distribution and their variation across different geographic scales in crater lakes in western Uganda. We found distinct variation in the potential controls of IH snail distribution among the two snail genera as well as across different geographic scales. On the larger scale, geography, diversity of the associated mollusk fauna and climate are important predictors for the presence of *Biomphalaria*, whereas mollusk diversity, water chemistry and geography mainly control the occurrence of *Bulinus*. Mollusk diversity and geography are relevant for the presence of both genera combined. On the scale of an individual crater lake field, *Biomphalaria* is solely controlled by geography, while mollusk diversity is most relevant for the presence of *Bulinus*. Our study demonstrates the importance of combining a comprehensive set of predictor variables, a method that allows for variable selection and a differentiated assessment of different host genera and geographic scale to reveal relevant predictors of distribution. The results of our study contribute to making realistic predictions of IH snail distribution and schistosomiasis prevalence and can help in supporting strategies towards controlling the disease.

Keywords: schistosomisis, biotic and abiotic predictors, mollusks, random forest, Africa

OPEN ACCESS

Edited by:
Tatenda Dalu, University of Mpumalanga, South Africa

Reviewed by:
Nelson A. F. Miranda, Nelson Mandela University, South Africa
Ross Cuthbert, Queen's University Belfast, United Kingdom

***Correspondence:**
Zadoki Tabo
tabozac@gmail.com

†Present Address:
Björn Stelbrink, Museum für Naturkunde - Leibniz Institute for Evolution and Biodiversity Science, Berlin, Germany

Specialty section:
This article was submitted to Freshwater Science, a section of the journal Frontiers in Environmental Science

Received: *08 February 2022*
Accepted: *15 March 2022*
Published: *14 April 2022*

Citation:
Tabo Z, Neubauer TA, Tumwebaze I, Stelbrink B, Breuer L, Hammoud C and Albrecht C (2022) Factors Controlling the Distribution of Intermediate Host Snails of Schistosoma in Crater Lakes in Uganda: A Machine Learning Approach. Front. Environ. Sci. 10:871735. doi: 10.3389/fenvs.2022.871735

INTRODUCTION

Human schistosomiasis (bilharzia) is the second most important tropical parasitic disease after malaria (World Health Organization, 2016) and ranked the most important water-borne disease (Steinmann et al., 2006). It poses a global burden to humankind with over 700 million individuals in 78 countries at risk of infection, claiming over 200,000 lives annually (World Health Organization, 2016). In addition, more than 240 million people are infected worldwide, predominantly in sub-Saharan Africa (World Health Organization, 2016), where the disease burden is up to 90% of the global infections due to poor standards of living (Bergquist et al., 2017). Thus, schistosomiasis is commonly referred to as "the disease of the poor". Countries in sub-Saharan Africa face a challenge of high population growth, and most people live in rural or semi-rural settings associated with poverty, poor sanitation and no access to clean water (Gray et al., 2010; King, 2010; Payne and Fitchett, 2010). In such geographical settings, people might continuously be in contact with water contaminated with schistosome eggs (Stothard et al., 2005), and a large part of the population is at risk of infection.

Despite schistosomiasis being one of the most prevalent tropical diseases (Steinmann et al., 2006), it is also probably the most neglected and was given little priority by the funding bodies compared to HIV/AIDS, malaria and tuberculosis (Hotez et al., 2007; Utzinger et al., 2009). Nevertheless, a recent growing interest in neglected tropical diseases including schistosomiasis has been observed over the last decade (World Health Organization, 2012; Shiff, 2017; King et al., 2020).

So far, strategies to control the spread of the disease *via* the provision of schistosomicides and/or WASH (water, sanitation, hygiene) programmes have shown limited effectiveness, and were consequently leading to disease re-emergences in spite of the interventions (Gryseels and Polderman, 1991; Chitsulo et al., 2000; Fenwick et al., 2009). Schistosomiasis is caused by trematode worms of the genus *Schistosoma* being transmitted through intermediate host (IH) snails. The reproductive cycle of *Schistosoma* trematodes starts with parasitic eggs released into freshwater through faeces and urine by infected humans. Eventually, motile larvae called miracidia hatch from the eggs and swim in search of snails to infect as intermediate host. The parasite then reproduces asexually within the snail, before shedding to the water as cercariae, larvae that penetrate the skin of the human host to complete the cycle and eventually cause the disease (Colley et al., 2014).

Sustainable vector snail control has been suggested as a more reliable approach to the schistosomiasis problem (Gryseels et al., 2006; Steinmann et al., 2006; Wang et al., 2008; Colley et al., 2014). The control aims at interrupting the transmission and stopping the spread of infection (Rollinson et al., 2013; Walz et al., 2015; Sokolow et al., 2016), by interrupting the *Schistosoma* life cycle through eliminating potential host snails from local habitats (King and Bertsch, 2015). Yet, this approach relies on the availability of high-quality snail distribution data, which represents a major knowledge gap in most developing countries in sub-Saharan Africa.

In sub-Saharan Africa, *Schistosoma mansoni* and *S. haematobium* are the major cause of the human disease burden in Africa (Chitsulo et al., 2000; Gryseels et al., 2006). *Schistosoma mansoni* is transmitted by snails of the genus *Biomphalaria* (Planorbidae) and causes human intestinal schistosomiasis. In contrast, *S. haematobium* is transmitted by species of *Bulinus* (Bulinidae) and cause human urogenital schistosomiasis (Wang et al., 2008; Colley et al., 2014). *Schistosoma mansoni* and *S. haematobium* are mainly distributed in and around a variety of freshwater habitats such as dams, lakes and rivers (Brown, 1994; Steinmann et al., 2006; Appleton and Madsen, 2012). *Bulinus* species in particular can live in permanent or seasonal pools, rice fields and ditches. In addition, there are several other species of *Schistosoma* that are of significant veterinary importance causing schistosomiasis in livestock. They are either hosted by *Bulinus* species (*S. bovis*) or selected species of the genus (*S. magrebowiei*) (Standley et al., 2012).

Previous studies dealing with the factors that influence the distribution of *Schistosoma* IH snails included water depth (Prah and James, 1978; Utzinger and Tanner, 2000; Boelee and Laamrani, 2004), altitude (John et al., 2008; Stanton et al., 2017), temperature, precipitation, pH level, forest cover and distance to nearest water bodies (Stensgaard et al., 2013), heat waves, droughts and floods (McCreesh and Booth, 2013; Pedersen et al., 2014), calcium and salinity (Hoverman et al., 2011; Maes et al., 2021). Although the relationships with these potential predictors have been examined and tested individually, they were not quantitatively assessed for their combined importance. The contribution of these factors to the distribution of IH snails and the prevalence of schistosomiasis accordingly across different regions is far from understood.

This study focuses on two main goals: 1) to assess the significance of extrinsic (geographical, hydrological, climatic, faunistic and anthropogenic) factors for the distribution of intermediate IH snails of the genera *Bulinus* and *Biomphalaria*, being the major causes of human infections in Africa, 2) to test for differences of potential predictors and their varying impact across different geographical scales. To do so, we used a model system of 56 crater lakes in western Uganda that variably contain IH species of the two genera, along with a diverse set of geographical, climatic, hydrological, faunistic and anthropogenic parameters. We used a machine learning approach (random forest, RF) to assess the importance of the individual parameters and how they differ across the study area. Considering the geographic variation of population density (Gelorini et al., 2012; Hartter et al., 2012), land use intensity (Hartter et al., 2015), and limnological characteristics of the lakes (De Crop and Verschuren, 2019), we hypothesize that a different set of parameters is relevant in the different regions examined. Moreover, we expect that different parameters control the distributions of the two genera, since they do have different dispersal and drought resistance capacities (Brown, 1994).

MATERIALS AND METHODS

Study Area

The study area is located on the hilly uplands (>1,600 m a.s.l.) of the Edward-George branch of the East African Rift valley in western Uganda (**Figure 1**). It is bordered by the Rwenzori

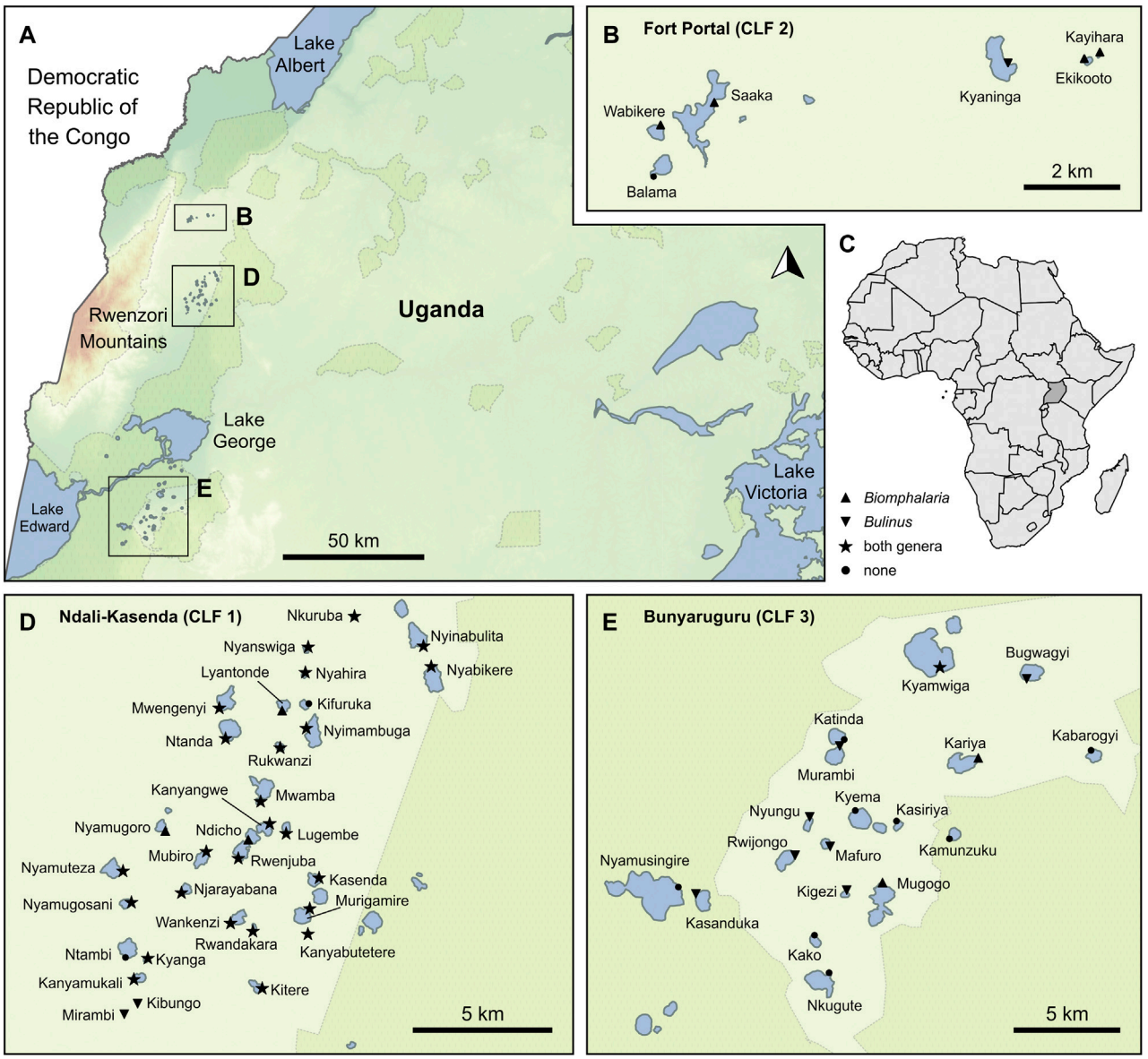

FIGURE 1 | Study area and occurrences of intermediate host (IH) snails. Three crater lake fields (CLF1–3) **(B,D,E)** in western Uganda **(A)** in Africa **(C)** were studied. Symbols at sampled lakes indicate the presence of *Biomphalaria* (triangle), *Bulinus* (inverted triangle), and both genera combined (dark star), whereas lakes marked with a small circle indicate localities where no IH snail was found.

Mountain range in the North-West, Lake Albert in the North and Queen Elizabeth National Park in the South. It contains over 90 small crater lakes, most of which formed between 4,000 and 10,000 years ago as a result of faulting and volcanic eruptions (Vinogradov, 1980; Schumann et al., 2015). Lake Ntambi, which formed c. 50,000 years ago is an exception, (Dirk Verschuren, pers. comm.).

The crater lakes of western Uganda have been repeatedly promoted as an ideal model system for studying large environmental gradients in limnological characteristics in a setting that allows meaningful comparisons due to shared geological history (e.g. Melack, 1978; Mills and Ryves, 2012; Saulnier-Talbot and Lavoie, 2018). The crater lakes region is one of the most densely populated rural areas in sub-Saharan Africa (Hartter et al., 2012), with a population growth rate of 3.3% annually (Gelorini et al., 2012). The population growth is coupled with increasing human impact through settlement, fishing, agriculture on the fertile volcano soils, swimming and water extraction for irrigation and domestic use. As a result of the high population density, the prevalence of (human) schistosomiasis in the region has dramatically increased (Kabatereine et al., 2004; Kabatereine et al., 2006; John et al., 2008; Stanton et al., 2017). In 2014, the crater lakes region covered parts of the 73 out of 112 districts of Uganda with prevalence of

schistosomiasis (Loewenberg, 2014). Nationwide, four million people are estimated to be infected and almost 20 million are at risk of infection (Loewenberg, 2014). The only preventative measures in the area are massive drug administration while environmental transmission interruption is rarely emphasized (Loewenberg, 2014).

Melack (1978) classified the region into four crater lake fields (CLFs, **Figure 1**). The Ndali-Kasenda field is locatedin the central part of the region, ~20 km from Fort Portal field in the North and ~65 km from Bunyaruguru field in the South. The fourth field of Katwe-Kikorongo contains lakes with saline waters (Rumes et al., 2011), unsuitable for mollusks (Tumwebaze et al., 2019).

Our dataset combines information from a total of 56 crater lakes in the three fields, including 32 lakes of the Ndali-Kasenda field (CLF 1), six lakes of the Fort Portal field (CLF 2) and 18 lakes of the Bunyaruguru field (CLF three; see **Supplementary Table S1**).

Data Collection

Malacological Field Data

Snails were sampled across the three regions in random months between 2010 and 2019 to account for a range of weather conditions, but mostly in dry seasons at normal or low water levels between 2010 and 2019 (**Figure 1**). Field work periods were aligned to times when highest population densities of the intermediate host snails were expected. Confounding effects by flooding and restricted accessibility during rainy seasons were avoided. Due to the steep and slippery escarpments of the crater lakes, sampling in the wet season was also avoided. Sampling methods involved dredging and/or scoop netting up to a maximum depth of 1.5 m or hand-picking snails found attached to shoreline vegetation and any solid substrates. The sampling time per lake was 40 min, and snails were collected in one to two localities (depending on the size of the respective lake). In some cases, lakes were visited more than once to ensure comprehensive representation of the local fauna. At each locality, we identified and counted the IH snails as well as the associated mollusk fauna on the genus level. The survey also revealed the presence of seven other non-host snail genera (*Radix, Gabbiella, Pila, Melanoides, Segmentorbis, Afrogyrorbis* and *Gyraulus*) as well as the bivalve genus *Sphaerium*.

Climatic and Environmental Data

We included air temperature and precipitation as proxies, because they have previously been shown to influence the distribution of freshwater mollusks (e.g., Hauffe et al., 2016a; Georgopoulou et al., 2016) and particularly those of IH snails (Appleton, 1978; Rowel et al., 2015). Specifically, temperature influences the survival and reproduction rates of snails (Paull and Johnson, 2011; McCreesh et al., 2014; Kalinda et al., 2017). Precipitation is associated with organic matter input and nutrient supply, which affects snail growth and fecundity (Madsen et al., 1987; Camara et al., 2012; Nyström Sandman et al., 2013). We retrieved the climatic data (averaged for the period 1970–2000) from the WorldClim two global database (Fick and Hijmans, 2017). We used mean annual temperature (BIO1), temperature of warmest month (BIO5), temperature of the coldest month (BIO6), annual precipitation (BIO12), precipitation of the wettest month (BIO13) and precipitation of the driest month (BIO14) to account for potential selectivity of the IH snail species to climatic fluctuations. Since the different temperature and precipitation parameters showed a similar range of variation, we calculated principal component analyses and used the first principal component for each of the two sets.

Water chemistry also plays a vital role for the occurrence and abundance of freshwater gastropods. This concerns pH, oxygen, conductivity, surface water temperature, magnesium and calcium (Rumes et al., 2011; Marie et al., 2015; Mahmoud et al., 2019; Alhassan et al., 2020; Olkeba et al., 2020). Surface water temperature, dissolved oxygen, pH and conductivity were measured using a handheld multi-meter probe. Calcium and magnesium data were retrieved from Rumes et al. (2011) and Nankabirwa et al. (2019).

Previous studies have shown the relevance of depth (both absolute lake depth and Secchi depth, i.e., a measure of water transparency) for the occurrence of both *Bulinus* and *Biomphalaria*. Absolute depth was retrieved from De Crop and Verschuren (2019), and water transparency (i.e., Secchi depth) was measured at the sampling points using a Secchi disk.

The crater lakes are characterized by seasonal fluctuations in water levels, and some lakes occasionally dry out (e.g., Lake Mirambi and Lake Kibungo). We included lake surface area and surface area variance over time as parameters in this study. The lake surface area was retrieved from satellite images from Google Earth Pro v. 7.3 taken in 2019. The lake area variance was calculated as the variance of four time slots of lake surface areas traced from satellite images taken in 2003, 2008, 2013 and 2018. Information for a few satellite images was missing, because either some lakes dried out or no records were captured in Google Earth. In such cases, we used the image of the closest time prior or after a given time slot to retrieve lake surface area.

Geographical Data

Longitude and latitude of the sampling sites were included as variables to account for potential variation in the geographical distribution of the IH snails. Altitude has been also proved relevant in the occurrence of snail hosts (John et al., 2008; Stanton et al., 2017) and was therefore considered in our study. Longitude, latitude and altitude were measured with a handheld Garmin GPS eTrex 20 device.

We used two measures for geographical distance to serve as proxies of biogeographical isolation, which might impact colonization and thus the IH presence in the area: 1) distance from a crater lake to the nearest other crater lake, and 2) distance from a crater lake to the nearest larger lake in the surrounding (i.e., lakes Victoria, Edward, Albert and George; **Figure 1**). All distances were measured "as the crow flies" in Google Earth.

Human Impact

To obtain a measure of human impact, we distinguished and quantified the proportion of land use. Since no data are available from online databases, we used the total percentage of cultivatable fields (cropland, fallow land and plantations) as a proxy and visualized a square of 0.0625 km^2 (0.25 × 0.25 km) around each

TABLE 1 | Predictor variables used in this study. Note that temperature and precipitation each represent the first principal component calculated from three climate parameters; see text for details. Sources: 1—Rumes et al. (2011), 2—Nankabirwa et al. (2019), 3—De Crop and Verschuren (2019), 4—Fick and Hijmans (2017).

Category	Predictor variables	Sources
Fauna	Species richness of associated mollusk fauna	This study
Environment/hydrology	Surface water temperature (°C)	This study
	Water pH	This study
	Dissolved oxygen (mg/L)	This study
	Electric conductivity (μS/cm)	This study
	Magnesium concentration (mg/L)	1, 2
	Calcium concentration (mg/L)	1, 2
	Secchi depth (m)	This study
	Lake depth (m)	3
	Lake surface area (km^2)	This study
	Lake area variance	This study
Climate	Temperature (°C)	4
	Precipitation (mm)	4
Geography	Longitude (°E)	This study
	Latitude (°N)	This study
	Altitude (m a.s.l.)	This study
	Distance to the nearest crater lake (km)	This study
	Distance to the nearest large lake (km)	This study
Human impact	Land use (% of area)	This study
	Population density (number of houses)	This study

crater lake in Google Earth (centered around the lake centroid). Final percentages were arcsine/square-root transformed according to Warton and Hui (2011) to limit the influence of outliers.

Additionally, the number of people living in the surroundings of a lake directly relates to the risk of schistosomiasis infection. Due to the lack of population census records in the region, we counted the number of houses in a standardized area of 0.25 km^2 (0.5 × 0.5 km) around each lake using satellite images from Google Earth taken in 2019 as a measure of population density.

A total of 20 predictor variables belonging to five categories were used in our study, 15 of which were retrieved in the course of the present survey, two were obtained from online databases and three were taken from the literature (**Table 1**, **Supplementary Table S1**).

Data Analysis

We applied a machine learning approach, i.e., random forest (RF; Breiman, 2001), to assess the combined impact of the chosen set of predictors on the distribution of IH snails. Machine learning approaches, and particularly RFs, have gained prominence in classification and regression analyses across various fields of science in recent years (e.g., Huang and Boutros, 2016; Pang et al., 2017; Schonlau and Zou, 2020; Collin et al., 2021; Georganos et al., 2021; Ruiz-AÍvarez et al., 2021). In classification problems, RFs have been demonstrated to give more accurate predictions than other approaches, such as logistic regression (Boulesteix et al., 2012; Bunyamin and Tunys, 2016; Couronné et al., 2018; Xia et al., 2019; Zhang et al., 2020). Since it is a non-parametric technique, the RF algorithm is not affected by multicollinearity among the predictor variables (Boonprong et al., 2018), which is a common problem in ecology. Also, many RF software packages come with convenient solutions to deal with missing values (Brieuc et al., 2018).

We conducted separate RF analyses to variably predict the presence of *Bulinus*, *Biomphalaria* and both genera combined. To assess variation of the potential predictors across different geographical scales, at a larger geographical extent, we ran analyses for the overall and complete dataset combining data from all the three crater lake fields. On the scale of individual crater lakes regions, we ran analyses for two subsets of CLF 1 and CLF 3. The analysis for Fort Portal field (CLF 2 subset) was not performed because it contains only six lakes. All analyses were done in the R statistical environment v. 4.0.3 (R Core Team, 2020), using the packages randomForest v. 4.6-14 (Liaw and Wiener, 2002), rfUtilities v. 2.1-5 (Evans and Murphy, 2019) and rfPermute v. 2.1.81 (Archer, 2020).

We performed imputation to fill missing data prior to further data analyses, using the function "rfImpute" in the package randomForest, which uses the RF algorithm to obtain weighted averages of the available observations. This was done for the predictors; calcium, magnesium and water depth, for which no data were available for 18, 16 and 16 lakes, respectively. Overall, missing data added up 4.7%. The "rfPermute" algorithm was used to assess variable importance in each RF model *via* permutation. The algorithm creates decision trees from the original dataset by random sampling of rows (i.e., lakes) without replacement. At each node, two-thirds of the rows are taken as training data to create the model, the remaining one-third is taken as so-called out-of-bag (OOB) sample and is used to make predictions and test for the performance of the model (Breiman, 1996; Breiman, 2001). Variables were permuted 100 times over 1,000 decision trees.

Model performance was additionally assessed *via* cross validation. This approach was chosen over the standard train–test data procedure because of the comparably low number of lakes in the dataset. Cross validation is a commonly used resampling method to assess the

TABLE 2 | Error rates and results of cross validation for all runs of the random forest (RF) models. Validation agreement was evaluated in accordance with Viera and Garrett (2005). The co-existence model for CLF three had insufficient data and is not included here. OOB, out-of-bag error.

Dataset	RF model	Error rates			Cross validation		
		OOB error	Error presence	Error absence	Kappa coefficient *K*	Validation error	Validation agreement
Complete dataset	*Biomphalaria*	0.143	0.111	0.200	0.911	0.089	excellent
	Bulinus	0.250	0.111	0.500	0.956	0.044	excellent
	Co-existence	0.179	0.148	0.207	0.919	0.081	excellent
Ndali-Kasenda (CLF 1)	*Biomphalaria*	0.063	0.000	0.500	0.633	0.367	substantial
	Bulinus	0.188	0.037	1.000	0.800	0.200	substantial
	Co-existence	0.188	0.040	0.714	0.633	0.367	substantial
Bunyaruguru (CLF 3)	*Biomphalaria*	0.222	1.000	0.067	0.633	0.367	substantial
	Bulinus	0.556	0.750	0.400	0.800	0.200	substantial

generalization potential of a model and to avoid overfitting (Berrar, 2019). We report here the kappa coefficient *K*, which determines the model's predictive accuracy, i.e., it gives the percentage of the data that is in agreement with the model (and is thus the opposite of the validation error). We adopted the suggestion of Viera and Garrett (2005), who regarded kappa values of 0.81-1 as excellent and 0.61–0.80 as substantial agreement, to evaluate our model performances.

The relevance of individual parameters to the overall RF models was assessed using two importance metrics, i.e., the mean decrease in accuracy (MDA) and the mean decrease Gini (MDG) (Calle and Urrea, 2011; Huang and Boutros, 2016). Due to discrepancies in ranking results between MDA and MDG, the results of a single metric are not completely exhaustive (Strobl et al., 2007; Liu et al., 2011). Therefore, we included both metrics but discussed in detail only those parameters that are found significant by both MDA and MDG. We used partial dependence plots to visualize the relationships and marginal effects of individual predictor variables (Friedman, 2001; Evans et al., 2011).

RESULTS

Models converged and were stable across all datasets, with those for *Biomphalaria* always performing better than those for *Bulinus* or both genera combined (**Supplementary Figure S1**). The RF models resulted in excellent to substantial classification successes for the presences of *Biomphalaria* and *Bulinus* in relation to the chosen set of predictor variables (**Table 2**). Classification errors were generally higher for false negatives compared to false positives, which is probably a result of the low number of absences in all datasets. Nonetheless, the cross validation showed that the classification agreements ranged from substantial (CLF subsets) to excellent (total dataset; **Table 2**).

For the overall and complete dataset, geographical, water chemistry and biotic parameters were the most important predictors, but their relative importance and contributions varied across the three RF models, i.e., *Biomphalaria* vs. *Bulinus* vs. both genera combined (**Figure 2**). The distribution of *Biomphalaria* was mainly controlled by latitude, longitude, diversity of the associated mollusk fauna and distance to large lake, as well as by precipitation to some extent; oxygen was only found significant by MDA. For *Bulinus*, the diversity of the associated mollusk fauna, water conductivity and latitude were most important, whereas only MDG identified altitude as a significant predictor. For the combined model, the diversity of the associated mollusk fauna, latitude, longitude and distance to large lake were found relevant. Distance to the next crater lake, magnesium and calcium played a minor role and were only found significant by MDA. Other predictors such as human impact, water pH, surface area and temperature had very little effect and were not significantly impacting the IH species distribution in the region (**Figure 2**).

A different set of parameters was found to be important for the presence of IH snails in individual crater lake fields. For CLF 1, the distance to the next crater lake was the sole important parameter for the distribution of *Biomphalaria* (**Supplementary Figure S2**). In turn, the diversity of the associated mollusk fauna seemed to be the most relevant factor shaping the distribution of *Bulinus*, in addition to distance to the next large lake and lake surface area (MDA only). The co-existence of both genera was controlled by the diversity of the associated mollusk fauna and distance from the next crater lake (**Supplementary Figure S2**). The model for CLF three yielded comparably high error rates, concerning both overall errors as well as classification errors for presences and absences (**Table 2**). Consequently, any association found for CLF 3 with individual parameters is unreliable and will not be discussed further.

The predicted probabilities for the occurrence of IH snails show non-linear relationships with individual predictor variables, with a generally positive trend being apparent in many cases (**Figure 3**). For *Biomphalaria*, the predicted probabilities of its occurrence increases with a rise in latitude, longitude, distance to the large lake (with a slight increase at the end), diversity of the associated mollusk fauna and precipitation. Increasing mollusk diversity also links with an increased probability to encounter *Bulinus*. The parameter conductivity shows a more complex relationship, featuring a steep probability increase up to ~400 µS/cm followed by a weakly, more or less gradually declining trend towards higher values (**Figure 3**). For both genera combined, similar positive trends are revealed for the relationship with the diversity of the associated mollusk fauna, latitude and longitude. The association with distance to the nearest large lake is more complex but indicates an increasing probability to encounter both genera above a distance of ~35 km.

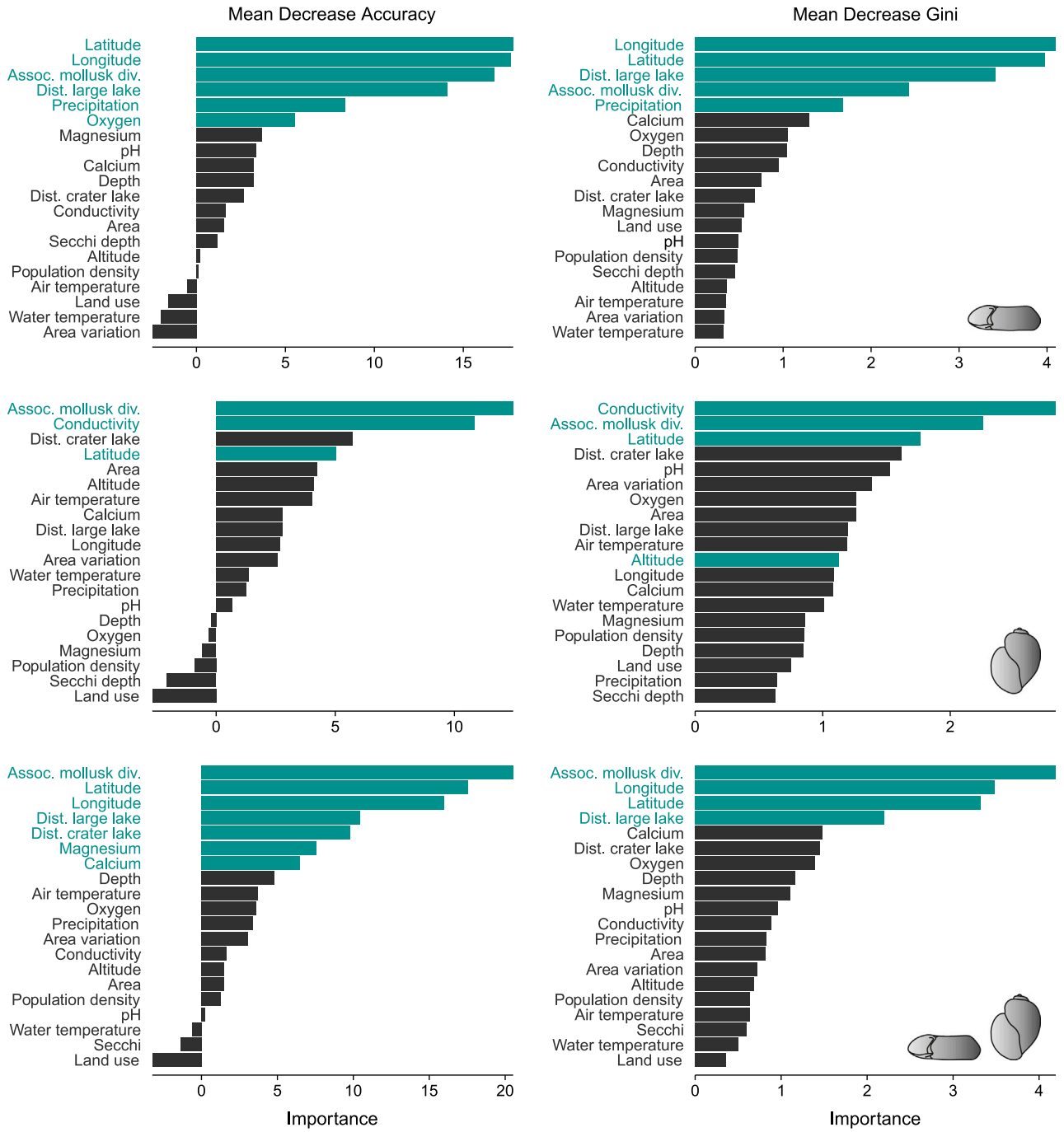

FIGURE 2 | Importance scores of predictor variables for *Biomphalaria* (upper panels), *Bulinus* (middle panels) and both genera combined (lower panels) for the complete dataset. The green bars indicate the significant predictors as determined *via* permutation tests. See **Supplementary Figure S2** for the importance scores of the subset CLF 1.

DISCUSSION

Understanding the factors influencing the distribution of snails acting as IH for *Schistosoma* is crucial for the control of human schistosomiasis. In this study, we explored the applicability of a machine learning algorithm to determine significant predictors of IH distribution and whether they differ among different Ugandan crater lakes. We found distinct variation in the potential controls of IH snail distribution. A different set of parameters is found to influence the distribution of the different genera and across different geographical scales. On the larger scale, geography, diversity of the associated mollusk fauna and

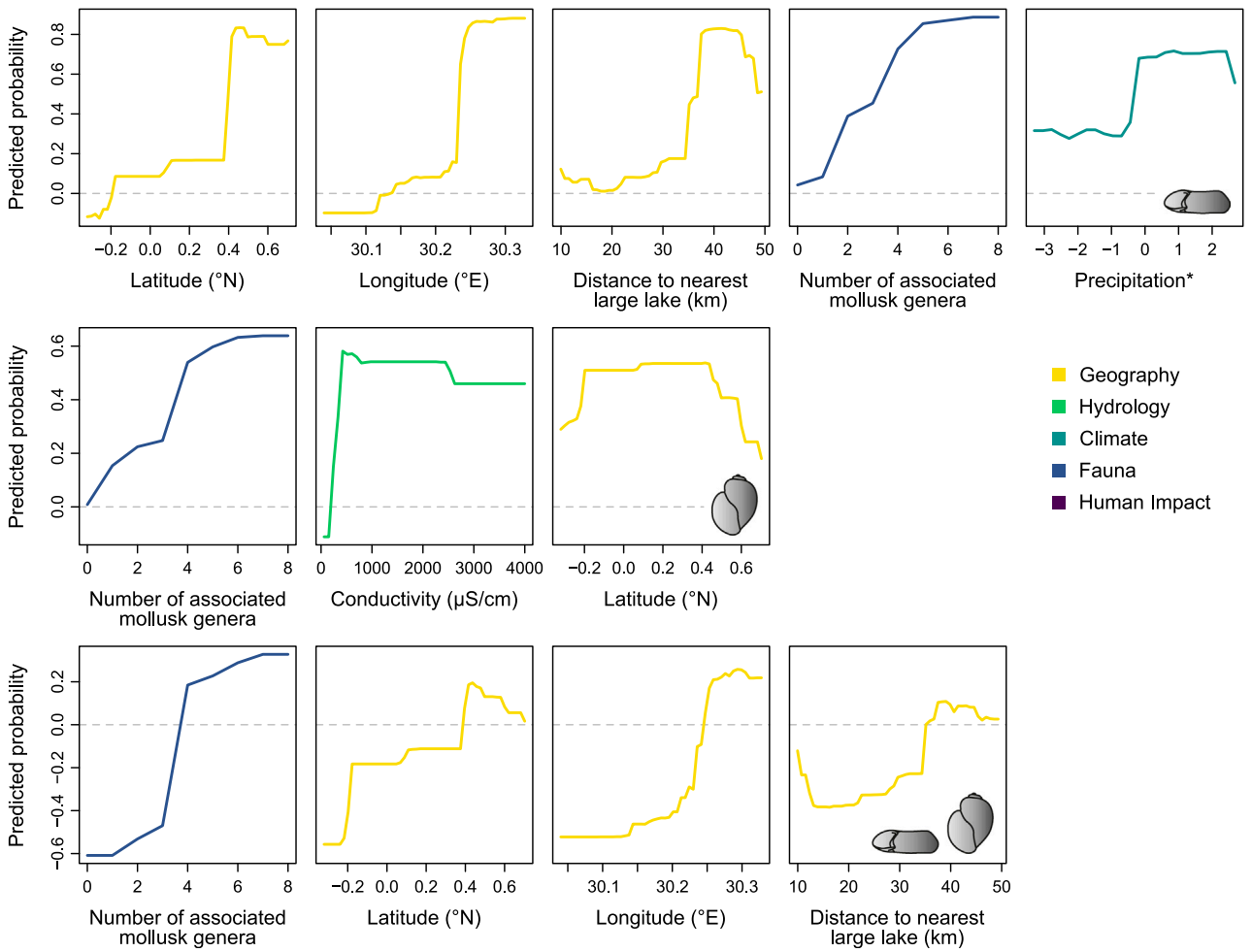

FIGURE 3 | Predicted probabilities for the presence of *Biomphalaria* (upper panels), *Bulinus* (middle panels) and both genera combined (lower panels) in relation to selected predictor variables from each dataset. Only the contributors that were found significant by both importance metrics (MDA and MDG) for the entire dataset are shown (compare **Figure 2**; see **Supplementary Figures S3–S8** for the remaining predictors as well as for the predicted probabilities for CLF 1). The asterisk denotes scaled parameters, i.e., the *x*-axis does not denote the original extent of the variable.

climate are important predictors for the presence of *Biomphalaria*, whereas mollusk diversity and water chemistry control the occurrence of *Bulinus*. Finally, mollusk diversity and geography are relevant for the presence of both genera. On the scale of an individual crater lake field (CLF1) geography (yet with a different variable) and mollusk diversity are relevant for the presence of *Bulinus* and both genera while *Biomphalaria* is solely controlled by geography. These results confirm our hypothesis that a different set of parameters is relevant on different geographical scales.

In the following sections, we discuss the relationships between IH snail occurrence and individual factors and groups of factors (geography, hydrology/water chemistry, climate, biotic and human impact) in an ecological context. Specifically, we discuss the distribution of the two genera with respect to metacommunity assembly processes, i.e., dispersal limitation, environmental filtering and biotic interactions, which limit the successful establishment of species in an ecosystem (see, e.g., Hauffe et al., 2016b for another freshwater gastropod example).

Geography: A Driver on Various Spatial Scales

Geographical variables were found to be among the most important controls for IH snail distribution, but the individual parameters depend on the scale of observation and the taxon in question. Latitude, longitude and distance to the nearest large lake are relevant for the occurrence of *Biomphalaria* as well as both genera combined. In contrast, *Bulinus* is much less influenced by geographical variables. Although latitude and altitude were identified significant, no positive relationship was found for the first (**Figure 3**), whereas the latter was of comparatively low importance (**Figure 2**). A similar trend is found in the Ndali-Kasenda crater lake field (CLF 1), where the distribution of *Biomphalaria* is strongly shaped by the distance to the nearest

crater lake, whereas the presence of *Bulinus* is mostly related to the diversity of the associated mollusk fauna (**Supplementary Figure S2**).

The strong positive relationship between the presence of *Biomphalaria* and latitude as well as longitude reflects the uneven occurrence of the genus across the study area (**Figure 1**). Particularly the rarity of the genus in the Bunyaruguru crater lake field (CLF 3) indicates that dispersal limitations and/or environmental filtering (e.g., Hauffe et al., 2016b) might constrain its distribution.

The generally positive association between the occurrence of *Biomphalaria* and distance to the nearest large lake is surprising at first, considering that distance is related to biogeographical isolation and colonization potential (Covich, 2010). Generally, these snails have a high passive dispersal capacity, a high reproduction rate and short generation times (Brown 1994). This combination is pronounced particularly in pulmonate snails such as *Biomphalaria* and makes them prime colonizers (Kappes and Haase, 2012; Kappes et al., 2014). The crater lakes are hydrologically disconnected, the possible longitudinal dispersal means are natural vectors such as birds (Kappes and Haase, 2012) and humans, through the attachment to fishing nets and/or boats.

A possible explanation for the positive association with distance concerns the taxonomic resolution. Here, we investigated the presence of genera, which may overprint patterns of dispersal and colonization of individual species of *Bulinus* and *Biomphalaria*. Also, Euclidean shore-to-shore distances might not reflect real dispersal means or pathways, because hydrological connectivity varies considerably between the large lakes and the crater lake fields. For example, the Fort Portal field (CLF 2) is connected to the Lake George–Lake Edward system *via* the Mpanga River but not to the geographically closer Lake Albert. The pattern may also results from choosing only four major lakes but disregarding smaller ones and river systems. Finally, in colonization processes, stochastic components might play an important role. For instance, regular episodes of shifting mixing regimes in some crater lakes (De Crop and Verschuren, 2021) could lead to low dissolved oxygen and consequently to the demise of most aquatic life. Based on genetic relationships of *Bulinus*, a previous study suggested that the large lakes acted as potential sources for (re)-colonization of the crater lakes (Tumwebaze et al., 2019), a scenario that cannot be tested here given the lack of genetic data. Fast re-appearance or aestivation in fluctuating environments is an intrinsic ecological feature of many *Bulinus* species, including the ones found in the study area (Watson, 1958; Brown, 1994). As such, the colonization and re-colonization patterns might be more complex and faster than previously anticipated.

Altitude was found to have limited influence on the distribution of IH snails. Several previous studies have indicated a shift in recent years of intestinal human schistosomiasis transmission towards higher altitudes (Kabatereine et al., 2004; John et al., 2008; Stanton et al., 2017). This is also supported by our findings showing that IH snails occur up to approx. 1,600 m a.s.l., and thus considerably higher than the previously presumed threshold of 1,400 m a.s.l. (Kabatereine et al., 2004). Future studies will have to establish an upper limit for both forms of schistosomiasis, because both IH snail genera have been found at altitudes above 2,000 m a.s.l. in Uganda (Stanton et al., 2017, unpubl. data).

Associated Mollusk Diversity

A strong control for the distribution of both *Bulinus* and *Biomphalaria* is the diversity of the associated mollusk fauna. The strong positive relationships in all three models (**Figure 3**) indicate that both genera are more likely encountered in generally diverse systems. One may expect the opposite, that a higher number of species (especially in a small crater lake) results in higher competition (e.g. Svanbäck and Bolnick, 2007; Hauffe et al., 2016b) and thus a lower chance of successful establishment. Instead, the positive association with diversity indicates that the IH snail genera are present in environments that provide favorable conditions for mollusks generally.

The associated mollusk fauna consists predominantly of pulmonates (*Radix natalensis* and several species of planorbids other than *Biomphalaria*), which are good colonizers in general and are characterized by a high productivity and shorter generation times (Kappes et al., 2014). Malacological surveys showed the presence of *Biomphalaria sudanica*, *Biomphalaria pfeifferi*, *Bulinus forskalii*, *Bulinus globosus*, and *Bulinus tropicus* (Tumwebaze et al., 2019; Tumwebaze et al., unpubl. data). All *Biomphalaria* species in the region are regarded susceptible to *S. mansoni*. Only *B. forskalii* and *B. globosus* were identified as host species for human schistosomes and the majority of *Bulinus* in the crater lakes region were *B. tropicus*, which is an important IH snail for livestock schistosomes. The non-pulmonate species are common and widespread regional species with no particular ecological requirements (Brown, 1994). More specialized taxa such as *Bellamya* or *Cleopatra* or unionid bivalves were not found in the crater lakes. The mollusk association in the crater lakes could still be seen as depauperate. The most obvious variation in habitat conditions and thus potentially determining mollusk associations is in the limnological characteristics of the crater lakes. Although we gathered a variety of different parameters concerning water chemistry and climatic conditions, the associations with individual parameters do not allow drawing a multifactorial picture. Moreover, the parameters measured for each crater lake do not cover seasonal variability (except for climate and lake area variation).

Hydrology and Water Chemistry

Only selected hydrochemical variables had an influence on the distribution of IH snails in our study region. Water conductivity was a significant driver across the entire study region and in CLF one for *Bulinus*. For *Biomphalaria*, oxygen was found a significant driver by one metric (MDA), but its relative importance was low (**Figure 2**). Similarly, MDA found the presence of both genera linked to magnesium and calcium, but again with low importance values.

Water conductivity determines the ionic strength of the concentration of dissolved solids including calcium and magnesium (Cormier et al., 2013). An expanding distribution with increasing conductivity was also suggested by Camara et al. (2012). This might reflect the presence of dissolved ions (e.g., calcium), which stimulate shell development for snail species

(Dillon, 2000; see also below). The non-linear relationship with a sharp increase around ~400 µS/cm followed by a nearly steady but weak decline indicates that a certain threshold must be met to allow the establishment of *Bulinus* in a lake. Higher electric conductivity is, in turn, less favorable. Conductivity as a complex factor integrating several chemical components has been identified as a determinant for *Bulinus* mortality and thus poses an important constraint on its occurrence (Brown, 1994; Marie et al., 2015).

The predicted probabilities for the presence of both genera in relation to magnesium and calcium concentrations, which were, however, only found significant by one importance metric (MDA), demonstrate that a certain threshold must be surpassed in both factors to promote the establishment of IH snails. Especially the relationship with calcium is not surprising, considering that a low concentration would constrain snail growth, fecundity, survival rate and reproduction, which, in turn, limit snail distribution (Dillon, 2000; Brodersen and Madsen, 2003). The concentration of calcium and magnesium and their ratio in the water both affect the presence and life cycle performances in southern African streams with thresholds at the lower and higher ends of concentrations (Brown, 1994).

Climate

Climatic factors seem to have surprisingly little effect on the distribution of IH snails in Ugandan crater lakes. Precipitation was found a significant but rather weak predictor in the model with *Biomphalaria*, whereas air and water temperature do not appear influential. Generally, climatic conditions and climate change are known to be important predictors for mollusk species distribution on larger geographical scales (Marcogliese, 2008; Stensgaard et al., 2019) and were also found to be relevant for IH snails. Temperature influences the survival and reproduction rates of the snails (Paull and Johnson, 2011; McCreesh et al., 2014; Kalinda et al., 2017). Higher rainfall causes more runoff into freshwater ecosystems increasing the supply of organic matter serving as food for the snails, which, in turn, promotes growth and fecundity (Madsen et al., 1987; Camara et al., 2012; Nyström Sandman et al., 2013; but see also discussion in David et al., 2018 for opposite associations). This may also explain the relationship with precipitation in our case. However, the lack of a (strong) association in our models is likely owed to the constrained geographical scale of our observations. The crater lakes are located in the same climatic zone in western Uganda, which is why precipitation and air temperature vary only little across the study region. Whereas air temperature seems to be irrelevant on that scale, the relationship with precipitation indicates that even small variations might have a significant impact on the IH snail distribution.

Non-Significant Drivers

A series of parameters was found to be non-significant in any of our models. Here, we briefly discuss the potential reasons for these findings, especially in the light of conflicting results reported in the literature. In contrast, previous studies found relationships between the distribution of *Biomphalaria* and water pH, whereas both oxygen and water pH have been suggested to determine the occurrence of *Bulinus* (Yirenya-Tawiah et al., 2011; Stensgaard et al., 2013; Marie et al., 2015; Mahmoud et al., 2019; Alhassan et al., 2020). However, no such influences were noticed despite of the influential factors of high oxygen concentration and water pH of the lakes studied (**Supplementary Table S1**). Possibly, the high carbon dioxide emission from decomposing submerged vegetation and organic matter, together with the presence of other dissolved ions could have indirectly affected such relationships (Tchakonté et al., 2014). Lake area variation, being a measure of ecosystem stability, seems also of little importance. Apparently, most of the lakes show minimal fluctuations through time, and the few that occasionally dry up could not influence the distribution or recolonization, which is facilitated by the short distances between the crater lakes. The mollusk associations of mostly opportunistic species found is also supporting this interpretation (see above).

Human impact, quantified by both land use and population density around the crater lakes, has apparently no impact on snail distribution. This result is rather unexpected, because humans are often involved in introduction of snails into new environments as passive dispersal vectors (Kappes and Haase, 2012). In the Ugandan crater lake fields, extensive anthropogenic activities (e.g., multipurpose water fetching, watering for livestock, littering and pollution) are limited to lower, relatively flat and thus more easily accessible shores of most of the crater lakes. As such, one may have expected an impact on snail occurrences. Moreover, only about 26% of the crater lakes are located in national parks (Queen Elizabeth NP and Kibale NP), thus three-quarter of the lakes are accessible and utilizable by humans. Despite these constraints, some reserves and parks like Kibale NP increasingly face migration of settlers and extensive cultivation (Hartter et al., 2015). Perhaps the prevailing population pressure affects the prevalence of infected snails, but it does not influence their presence in general. Follow-up studies should focus specifically on this aspect for mollusks communities and the prevalence of schistosomiasis. Interestingly, in other non-gastropod taxa such as cladocerans (Rumes et al., 2011) and fungi communities (Gelorini et al., 2012), negative effects of land use change and anthropogenic pressure have already been demonstrated for the crater lakes region. With increasing human activities in the Ugandan crater lakes region (including tourism), we expect further changes in biological communities of the lakes as well as increasing cases of human schistosomiasis among both local communities and visiting travelers (Lachish et al., 2013) in the near future.

Methodological Implications and Limitations

Despite the numerous advantages machine learning approaches like RFs offer, one disadvantage concerns the non-linearity of the approach, resulting in a limited prediction power outside the data range. Therefore, we cannot extrapolate our findings to other datasets or regions. Furthermore, small datasets (e.g. CLF 2,

Biomphalaria subset with CLF3), decisively limit RF classification due to insufficient data. Optimally, future studies need to include data from a larger geographical scale, involving a greater variation in the ranges of predictor variables, to provide more general predictions for the controls of IH snail distributions. Using machine-learning algorithms like RFs on a comprehensive dataset will eventually facilitate more general conclusions about the importance of individual predictors (or sets of predictors) for the presence of IH snails. Future studies may focus on applying this approach to map infection risk areas, especially in comparison to areas with actual prevalence records and those where preventative measures are in place.

CONCLUSION

The results indicate that *Biomphalaria* is mainly controlled by geography, associated mollusk diversity and climate, while fauna, hydrology and to some extent geography controlled the presence of *Bulinus*. Geography (*Biomphalaria*) and mollusk diversity (*Bulinus*) were the only significant predictors on the scale of an individual crater lake field. The intricate relationship between IH snail distribution and geography likely reflects dispersal limitations and/or environmental filtering on the hand and a complex pattern of (re-)colonization on the other hand. The positive association with the diversity of accompanying mollusks, as well as the relationship with water conductivity, indicates that IH snails are common in ecosystems offering favorable conditions for mollusks in general.

Our machine learning approach helped disentangling relevant factors in IH snail distribution. The results of this study provide baseline data that assist future research towards controlling schistosomiasis.

DATA AVAILABILITY STATEMENT

All data used in the study is available in the paper or the **Supplementary Material**.

AUTHOR CONTRIBUTIONS

CA, ZT, and IT conceived the study. CA and IT conducted field work. ZT and TN performed the analyses. ZT wrote the manuscript with contributions from TN and CA. TN, BS, and CH prepared the figures. LB and CA supervised and critically revised the study. All authors reviewed the manuscript and approved the final version.

FUNDING

Research was partly supported by German Academic Exchange Service (DAAD) in support of a PhD scholarship for ZT (Grant No. 57507871) and German Science Foundation (DFG, Grant Nos. SCHR352/9-1, AL1076/5-2 and AL1076/6-2).

ACKNOWLEDGMENTS

We thank Julius Tumusiime and Naboth Ainomugisha (Mbarara University of Science and Technology), Marie Claire Dusabe (formerly at Rwanda Wildlife Conservation Association, Kigali, Rwanda), Thies Geertz, Daniel Engelhard, and Roland Schultheiß (formerly JLU Giessen) for assistance during field work between 2010 and 2019. We also acknowledge the National Council for Science of Uganda together with Uganda Wildlife Authority granting us permits to conduct field work. We are moreover grateful to Klemens Ekschmitt (JLU Giessen) for fruitful discussions concerning classification problems and to Catharina Clewing (JLU Giessen) for creating snail reconstructions for the figures. Two reviewers are thanked for their constructive comments.

SUPPLEMENTARY MATERIAL

The Supplementary Material for this article can be found online at: https://www.frontiersin.org/articles/10.3389/fenvs.2022.871735/full#supplementary-material

REFERENCES

Alhassan, A., Abidemi, A., Gadzama, I., Shaaba, R., Wada, Y., and Kelassanthodi, R. (2020). Distribution and Diversity of Freshwater Snails of Public Health Importance in Kubanni Reservoir and Weir/sediment Trap, Zaria, Nigeria. *J. Environ. Occup. Health* 10 (1), 1–9. doi:10.5455/jeoh.20190704093531

Appleton, C. C., and Madsen, H. (2012). Human Schistosomiasis in Wetlands in Southern Africa. *Wetlands Ecol. Manage.* 20 (3), 253–269. doi:10.1007/s11273-012-9266-2

Appleton, C. C. (1978). Review of Literature on Abiotic Factors Influencing the Distribution and Life Cycles of Bilharziosis Intermediate Host Snails. *Malacol. Rev.* 11, 1–25.

Archer, E. (2020). rfPermute: Estimate Permutation P-Values for Random Forest Importance Metrics. R Package Version 2.1.81. Available at: https://cran.r-project.org/package=rfPermute. (Accessed July 1, 2021).

Bergquist, R., Zhou, X.-N., Rollinson, D., Reinhard-Rupp, J., and Klohe, K. (2017). Elimination of Schistosomiasis: the Tools Required. *Infect. Dis. Poverty* 6 (1), 1–9. doi:10.1186/s40249-017-0370-7

Berrar, D. (2019). "Cross-Validation," in *Encyclopedia of Bioinformatics and Computational Biology*. Editors S. Ranganathan, M. Gribskov, K. Nakai, and C. Schönbach (Oxford: Academic Press), 542–545. doi:10.1016/B978-0-12-809633-8.20349-X

Boelee, E., and Laamrani, H. (2004). Environmental Control of Schistosomiasis through Community Participation in a Moroccan Oasis. *Trop. Med. Int. Health* 9 (9), 997–1004. doi:10.1111/j.1365-3156.2004.01301.x

Boonprong, S., Cao, C., Chen, W., and Bao, S. (2018). Random Forest Variable Importance Spectral Indices Scheme for Burnt Forest Recovery Monitoring-Multilevel RF-VIMP. *Remote Sensing* 10 (6), 807. doi:10.3390/rs10060807

Boulesteix, A.-L., Janitza, S., Kruppa, J., and König, I. R. (2012). Overview of Random forest Methodology and Practical Guidance with Emphasis on Computational Biology and Bioinformatics. *WIREs Data Mining Knowl. Discov.* 2 (6), 493–507. doi:10.1002/widm.1072

Breiman, L. (1996). Bagging Predictors. *Mach. Learn.* 24, 123–140. doi:10.1007/bf00058655

Breiman, L. (2001). Random Forests. *Mach. Learn.* 45 (1), 5–32. doi:10.1023/a:1010933404324

Brieuc, M. S. O., Waters, C. D., Drinan, D. P., and Naish, K. A. (2018). A Practical Introduction to Random Forest for Genetic Association Studies in Ecology and Evolution. *Mol. Ecol. Resour.* 18 (4), 755–766. doi:10.1111/1755-0998.12773

Brodersen, J., and Madsen, H. (2003). The Effect of Calcium Concentration on the Crushing Resistance, Weight and Size of *Biomphalaria sudanica* (Gastropoda: Planorbidae). *Hydrobiologia* 490 (1), 181–186. doi:10.1023/a:1023495326473

Brown, D. S. (1994). *Freshwater Snails of Africa and Their Medical Importance*. Second edition. London: Taylor & Francis, 609.

Bunyamin, H., and Tunys, T. (2016). A Comparison of Retweet Prediction Approaches: the Superiority of Random Forest Learning Method. *Telkomnika* 14 (3), 1052–1058. doi:10.12928/TELKOMNIKA.v14i3.3150

Calle, M. L., and Urrea, V. (2011). Letter to the Editor: Stability of Random forest Importance Measures. *Brief. Bioinform.* 12 (1), 86–89. doi:10.1093/bib/bbq011

Camara, I. A., Bony, Y. K., Diomandé, D., Edia, O. E., Konan, F. K., Kouassi, C. N., et al. (2012). Freshwater Snail Distribution Related to Environmental Factors in Banco National Park, an Urban reserve in the Ivory Coast (West Africa). *Afr. Zoolog.* 47 (1), 160–168. doi:10.1080/15627020.2012.11407534

Chitsulo, L., Engels, D., Montresor, A., and Savioli, L. (2000). The Global Status of Schistosomiasis and its Control. *Acta Tropica* 77 (1), 41–51. doi:10.1016/S0001-706X(00)00122-4

Colley, D. G., Bustinduy, A. L., Secor, W. E., and King, C. H. (2014). Human Schistosomiasis. *Lancet* 383 (9936), 2253–2264. doi:10.1016/S0140-6736(13)61949-2

Collin, F. D., Durif, G., Raynal, L., Lombaert, E., Gautier, M., Vitalis, R., et al. (2021). Extending Approximate Bayesian Computation with Supervised Machine Learning to Infer Demographic History from Genetic Polymorphisms Using DIYABC Random Forest. *Mol. Ecol. Resour.* 21 (8), 2598–2613. doi:10.1111/1755-0998.13413

Cormier, S. M., Suter, G. W., Zheng, L., and Pond, G. J. (2013). Assessing Causation of the Extirpation of Stream Macroinvertebrates by a Mixture of Ions. *Environ. Toxicol. Chem.* 32 (2), 277–287. doi:10.1002/etc.2059

Couronné, R., Probst, P., and Boulesteix, A.-L. (2018). Random forest versus Logistic Regression: a Large-Scale Benchmark experiment. *BMC Bioinformatics* 19 (1), 1–14. doi:10.1186/s12859-018-2264-5

Covich, A. P. (2010). Winning the Biodiversity Arms Race Among Freshwater Gastropods: Competition and Coexistence through Shell Variability and Predator Avoidance. *Hydrobiologia* 653 (1), 191–215. doi:10.1007/s10750-010-0354-0

David, N. F., Cantanhede, S. P. D., Monroe, N. B., Pereira, L. P. L. A., Silva-Souza, N., Abreu-Silva, A. L., et al. (2018). Spatial Distribution and Seasonality of Biomphalaria Spp. In São Luís (Maranhão, Brazil). *Parasitol. Res.* 117 (5), 1495–1502. doi:10.1007/s00436-018-5810-1

De Crop, W., and Verschuren, D. (2019). Determining Patterns of Stratification and Mixing in Tropical Crater Lakes through Intermittent Water-Column Profiling: A Case Study in Western Uganda. *J. Afr. Earth Sci.* 153, 17–30. doi:10.1016/j.jafrearsci.2019.02.019

De Crop, W., and Verschuren, D. (2021). Mixing Regimes in the Equatorial Crater Lakes of Western Uganda. *Limnologica* 90, 125891. doi:10.1016/j.limno.2021.125891

Dillon, R. T. (2000). *The Ecology of Freshwater Mollusks*. Cambridge: Cambridge University Press.

Evans, J. S., and Murphy, M. A. (2019). rfUtilities: Random Forests Model Selection and Performance Evaluation. R Package Version 2.1-5. Available at: https://cran.r-project.org/package=rfUtilities. (Accessed July 1, 2021).

Evans, J. S., Murphy, M. A., Holden, Z. A., and Cushman, S. A. (2011). "Modeling Species Distribution and Change Using Random forest," in *Predictive Species and Habitat Modeling in Landscape Ecology* (New York, NY: Springer), 139–159. doi:10.1007/978-1-4419-7390-0_8

Fenwick, A., Webster, J. P., Bosque-Oliva, E., Blair, L., Fleming, F. M., Zhang, Y., et al. (2009). The Schistosomiasis Control Initiative (SCI): Rationale, Development and Implementation from 2002-2008. *Parasitology* 136 (13), 1719–1730. doi:10.1017/S0031182009990400

Fick, S. E., and Hijmans, R. J. (2017). WorldClim 2: New 1-km Spatial Resolution Climate Surfaces for Global Land Areas. *Int. J. Climatol* 37 (12), 4302–4315. doi:10.1002/joc.5086

Friedman, J. H. (2001). Greedy Function Approximation: a Gradient Boosting Machine. *Ann. Stat.* 29 (5), 1189–1232. doi:10.1214/aos/1013203451

Gelorini, V., Verbeken, A., Lens, L., Eggermont, H., Odgaard, B. V., and Verschuren, D. (2012). Effects of Land Use on the Fungal Spore Richness in Small Crater-lake Basins of Western Uganda. *Fungal Divers.* 55 (1), 125–142. doi:10.1007/s13225-012-0155-z

Georganos, S., Grippa, T., Niang Gadiaga, A., Linard, C., Lennert, M., Vanhuysse, S., et al. (2021). Geographical Random Forests: a Spatial Extension of the Random forest Algorithm to Address Spatial Heterogeneity in Remote Sensing and Population Modelling. *Geocarto Int.* 36 (2), 121–136. doi:10.1080/10106049.2019.1595177

Georgopoulou, E., Neubauer, T. A., Harzhauser, M., Kroh, A., and Mandic, O. (2016). Distribution Patterns of European Lacustrine Gastropods: a Result of Environmental Factors and Deglaciation History. *Hydrobiologia* 775 (1), 69–82. doi:10.1007/s10750-016-2713-y

Gray, D. J., McManus, D. P., Li, Y., Williams, G. M., Bergquist, R., and Ross, A. G. (2010). Schistosomiasis Elimination: Lessons from the Past Guide the Future. *Lancet Infect. Dis.* 10 (10), 733–736. doi:10.1016/S1473-3099(10)70099-2

Gryseels, B., and Polderman, A. M. (1991). Morbidity, Due to Schistosomiasis Mansoni, and its Control in Subsaharan Africa. *Parasitol. Today* 7 (9), 244–248. doi:10.1016/0169-4758(91)90238-J

Gryseels, B., Polman, K., Clerinx, J., and Kestens, L. (2006). Human Schistosomiasis. *Lancet* 368 (9541), 1106–1118. doi:10.1016/S0140-6736(06)69440-3

Hartter, J., Stampone, M. D., Ryan, S. J., Kirner, K., Chapman, C. A., and Goldman, A. (2012). Patterns and Perceptions of Climate Change in a Biodiversity Conservation Hotspot. *Plos One* 7 (2), e32408. doi:10.1371/journal.pone.0032408

Hartter, J., Ryan, S. J., MacKenzie, C. A., Goldman, A., Dowhaniuk, N., Palace, M., et al. (2015). Now There Is No Land: a story of Ethnic Migration in a Protected Area Landscape in Western Uganda. *Popul. Environ.* 36 (4), 452–479. doi:10.1007/s11111-014-0227-y

Hauffe, T., Schultheiß, R., Van Bocxlaer, B., Prömmel, K., and Albrecht, C. (2016a). Environmental Heterogeneity Predicts Species Richness of Freshwater Mollusks in Sub-Saharan Africa. *Int. J. Earth Sci. (Geol Rundsch)* 105 (106), 1795–1810. doi:10.1007/s00531-014-1109-3

Hauffe, T., Albrecht, C., and Wilke, T. (2016b). Assembly Processes of Gastropod Community Change with Horizontal and Vertical Zonation in Ancient Lake Ohrid: a Metacommunity Speciation Perspective. *Biogeosciences* 13, 2901–2911. doi:10.5194/bg-13-2901-2016

Hotez, P. J., Molyneux, D. H., Fenwick, A., Kumaresan, J., Sachs, S. E., Sachs, J. D., et al. (2007). Control of Neglected Tropical Diseases. *N. Engl. J. Med.* 357 (10), 1018–1027. doi:10.1056/NEJMra064142

Hoverman, J. T., Davis, C. J., Werner, E. E., Skelly, D. K., Relyea, R. A., and Yurewicz, K. L. (2011). Environmental Gradients and the Structure of Freshwater Snail Communities. *Ecography* 34 (6), 1049–1058. doi:10.1111/j.1600-0587.2011.06856.x

Huang, B. F. F., and Boutros, P. C. (2016). The Parameter Sensitivity of Random Forests. *BMC Bioinformatics* 17 (1), 1–13. doi:10.1186/s12859-016-1228-x

John, R., Ezekiel, M., Philbert, C., and Andrew, A. (2008). Schistosomiasis Transmission at High Altitude Crater Lakes in Western Uganda. *BMC Infect. Dis.* 8 (1), 1–6. doi:10.1186/1471-2334-8-110

Kabatereine, N. B., Brooker, S., Tukahebwa, E. M., Kazibwe, F., and Onapa, A. W. (2004). Epidemiology and Geography of *Schistosoma Mansoni* in Uganda: Implications for Planning Control. *Trop. Med. Int. Health* 9 (3), 372–380. doi:10.1046/j.1365-3156.2003.01176.x

Kabatereine, N. B., Tukahebwa, E., Kazibwe, F., Namwangye, H., Zaramba, S., Brooker, S., et al. (2006). Progress towards Countrywide Control of Schistosomiasis and Soil-Transmitted Helminthiasis in Uganda. *Trans. R. Soc. Trop. Med. Hyg.* 100 (3), 208–215. doi:10.1016/j.trstmh.2005.03.015

Kalinda, C., Chimbari, M. J., and Mukaratirwa, S. (2017). Effect of Temperature on the *Bulinus globosus - Schistosoma haematobium* System. *Infect. Dis. Poverty* 6 (1), 1–7. doi:10.1186/s40249-017-0260-z

Kappes, H., and Haase, P. (2012). Slow, but Steady: Dispersal of Freshwater Molluscs. *Aquat. Sci.* 74 (1), 1–14. doi:10.1007/s00027-011-0187-6

Kappes, H., Tackenberg, O., and Haase, P. (2014). Differences in Dispersal- and Colonization-Related Traits between Taxa from the Freshwater and the Terrestrial Realm. *Aquat. Ecol.* 48 (1), 73–83. doi:10.1007/s10452-013-9467-7

King, C. H., and Bertsch, D. (2015). Historical Perspective: Snail Control to Prevent Schistosomiasis. *PLOS Negl. Trop. Dis.* 9 (4), e0003657. doi:10.1371/journal.pntd.0003657

King, C. H., Yoon, N., Wang, X., Lo, N. C., Alsallaq, R., Ndeffo-Mbah, M., et al. (2020). Application of Schistosomiasis Consortium for Operational Research and Evaluation Study Findings to Refine Predictive Modeling of *Schistosoma mansoni* and *Schistosoma haematobium* Control in Sub-Saharan Africa. *J. Trop. Med. Hyg.* 103 (1 Suppl. l), 97–104. doi:10.4269/ajtmh.19-0852

King, C. H. (2010). Parasites and Poverty: the Case of Schistosomiasis. *Acta Tropica* 113, 95–104. doi:10.1016/j.actatropica.2009.11.012

Lachish, T., Tandlich, M., Grossman, T., and Schwartz, E. (2013). High Rate of Schistosomiasis in Travelers after a Brief Exposure to the High-Altitude Nyinambuga Crater lake, Uganda. *Clin. Infect. Dis.* 57 (10), 1461–1464. doi:10.1093/cid/cit559

Liaw, A., and Wiener, M. (2002). Classification and Regression by randomForest. *R. News* 2 (3), 18–22.

Liu, C., Ackerman, H. H., and Carulli, J. P. (2011). A Genome-wide Screen of Gene-Gene Interactions for Rheumatoid Arthritis Susceptibility. *Hum. Genet.* 129 (5), 473–485. doi:10.1007/s00439-010-0943-z

Loewenberg, S. (2014). Uganda's Struggle with Schistosomiasis. *Lancet* 383 (9930), 1707–1708. doi:10.1016/S0140-6736(14)60817-5

Madsen, H., Coulibaly, G., and Furu, P. (1987). Distribution of Freshwater Snails in the River Niger basin in Mali with Special Reference to the Intermediate Hosts of Schistosomes. *Hydrobiologia* 146 (1), 77–88. doi:10.1007/bf00007580

Maes, T., Hammoud, C., Volckaert, F. A. M., and Huyse, T. (2021). A Call for Standardised Snail Ecological Studies to Support Schistosomiasis Risk Assessment and Snail Control Efforts. *Hydrobiologia* 848 (8), 1773–1793. doi:10.1007/s10750-021-04547-4

Mahmoud, A., Fangary, H., Hussein, M., and Obuid-Allah, A. (2019). Population Dynamics of Freshwater Snails (Mollusca: Gastropoda) at Qena Governorate, Upper Egypt. *Egypt. Acad. J. Biol. Sci.* 3 (1), 11–22. doi:10.21608/eajbsz.2011.14309

Marcogliese, D. J. (2008). The Impact of Climate Change on the Parasites and Infectious Diseases of Aquatic Animals. *Rev. Sci. Tech.* 27 (2), 467–484. doi:10.20506/rst.27.2.1820

Marie, M. A. S., El-Deeb, F. A. A., Hasheesh, W. S., Mohamed, R. A., and Sayed, S. S. M. (2015). Impact of Seasonal Water Quality and Trophic Levels on the Distribution of Various Freshwater Snails in Four Egyptian Governorates. *Appl. Ecol. Environ. Res.* 3 (4), 117–126. doi:10.12691/aees-3-4-4

McCreesh, N., and Booth, M. (2013). Challenges in Predicting the Effects of Climate Change on *Schistosoma mansoni* and *Schistosoma haematobium* Transmission Potential. *Trends Parasitol.* 29 (11), 548–555. doi:10.1016/j.pt.2013.08.007

McCreesh, N., Arinaitwe, M., Arineitwe, W., Tukahebwa, E. M., and Booth, M. (2014). Effect of Water Temperature and Population Density on the Population Dynamics of *Schistosoma Mansoni* Intermediate Host Snails. *Parasites Vectors* 7 (1), 1–9. doi:10.1186/s13071-014-0503-9

Melack, J. M. (1978). Morphometric, Physical and Chemical Features of the Volcanic Crater Lakes of Western Uganda. *Arch. Hydrobiol.* 84, 430–453.

Mills, K., and Ryves, D. B. (2012). Diatom-based Models for Inferring Past Water Chemistry in Western Ugandan Crater Lakes. *J. Paleolimnol.* 48 (2), 383–399. doi:10.1007/s10933-012-9609-2

Nankabirwa, A., De Crop, W., Van der Meeren, T., Cocquyt, C., Plisnier, P.-D., Balirwa, J., et al. (2019). Phytoplankton Communities in the Crater Lakes of Western Uganda, and Their Indicator Species in Relation to lake Trophic Status. *Ecol. Indicators* 107, 105563. doi:10.1016/j.ecolind.2019.105563

Nyström Sandman, A., Wikström, S. A., Blomqvist, M., Kautsky, H., and Isaeus, M. (2013). Scale-dependent Influence of Environmental Variables on Species Distribution: a Case Study on Five Coastal Benthic Species in the Baltic Sea. *Ecography* 36 (3), 354–363. doi:10.1111/j.1600-0587.2012.07053.x

Olkeba, B. K., Boets, P., Mereta, S. T., Yeshigeta, M., Akessa, G. M., Ambelu, A., et al. (2020). Environmental and Biotic Factors Affecting Freshwater Snail Intermediate Hosts in the Ethiopian Rift Valley Region. *Parasites Vectors* 13, 1–13. doi:10.1186/s13071-020-04163-6

Pang, B., Yue, J., Zhao, G., and Xu, Z. (2017). Statistical Downscaling of Temperature with the Random forest Model. *Adv. Meteorology* 2017, 1–11. doi:10.1155/2017/7265178

Paull, S. H., and Johnson, P. T. J. (2011). High Temperature Enhances Host Pathology in a Snail-Trematode System: Possible Consequences of Climate Change for the Emergence of Disease. *Freshw. Biol.* 56 (4), 767–778. doi:10.1111/j.1365-2427.2010.02547.x

Payne, L., and Fitchett, J. R. (2010). Bringing Neglected Tropical Diseases into the Spotlight. *Trends Parasitol.* 26 (9), 421–423. doi:10.1016/j.pt.2010.06.002

Pedersen, U. B., Midzi, N., Mduluza, T., Soko, W., Stensgaard, A.-S., Vennervald, B. J., et al. (2014). Modelling Spatial Distribution of Snails Transmitting Parasitic Worms with Importance to Human and Animal Health and Analysis of Distributional Changes in Relation to Climate. *Geospat. Health* 8, 335–343. doi:10.4081/gh.2014.23

Prah, S. K., and James, C. (1978). The Influence of Physical Factors on the Behaviour and Infectivity of Miracidia of *Schistosoma mansoni* and *S. haematobium* II. Effect of Light and Depth. *J. Helminthol.* 52 (2), 115–120. doi:10.1017/S0022149X00005228

R Core Team (2020). *R: A Language and Environment for Statistical Computing*. Version 4.0.3. Vienna: R Foundation for Statistical Computing. Available at: http://www.R-project.org.

Rollinson, D., Knopp, S., Levitz, S., Stothard, J. R., Tchuem Tchuenté, L.-A., Garba, A., et al. (2013). Time to Set the Agenda for Schistosomiasis Elimination. *Acta Tropica* 128 (2), 423–440. doi:10.1016/j.actatropica.2012.04.013

Rowel, C., Fred, B., Betson, M., Sousa-Figueiredo, J. C., Kabatereine, N. B., and Stothard, J. R. (20152015). Environmental Epidemiology of Intestinal Schistosomiasis in Uganda: Population Dynamics of Biomphalaria (Gastropoda: Planorbidae) in Lake Albert and Lake Victoria with Observations on Natural Infections with Digenetic Trematodes. *Biomed. Res. Int.* 2015, 1–11. doi:10.1155/2015/717261

Ruiz-AÍvarez, M., Gomariz-Castillo, F., and Alonso-Sarría, F. (2021). Evapotranspiration Response to Climate Change in Semi-arid Areas: Using Random forest as Multi-Model Ensemble Method. *Water* 13 (2), 222. doi:10.3390/w13020222

Rumes, B., Eggermont, H., and Verschuren, D. (2011). Distribution and Faunal Richness of Cladocera in Western Uganda Crater Lakes. *Hydrobiologia* 676 (1), 39–56. doi:10.1007/s10750-011-0829-7

Saulnier-Talbot, É., and Lavoie, I. (2018). Uncharted Waters: the Rise of Human-Made Aquatic Environments in the Age of the "Anthropocene". *Anthropocene* 23, 29–42. doi:10.1016/j.ancene.2018.07.003

Schonlau, M., and Zou, R. Y. (2020). The Random forest Algorithm for Statistical Learning. *Stata J.* 20 (1), 3–29. doi:10.1177/1536867X20909688

Schumann, A., Muwanga, A., Lehto, T., Staudt, M., Schlüter, T., Kato, V., et al. (2015). Ugandan Geosites. *Geology. Today* 31 (2), 59–67. doi:10.1111/gto.12089

Shiff, C. (2017). Why Reinvent the Wheel? Lessons in Schistosomiasis Control from the Past. *PLOS Negl. Trop. Dis.* 11 (10), e0005812. doi:10.1371/journal.pntd.0005812

Sokolow, S. H., Wood, C. L., Jones, I. J., Swartz, S. J., Lopez, M., Hsieh, M. H., et al. (2016). Global Assessment of Schistosomiasis Control over the Past century Shows Targeting the Snail Intermediate Host Works Best. *PLOS Negl. Trop. Dis.* 10 (7), e0004794. doi:10.1371/journal.pntd.0004794

Standley, C. J., Dobson, A. P., and Stothard, J. R. (2012). "Out of Animals and Back Again: Schistosomiasis as a Zoonosis in Africa," in *Schistosomiasis* (London: Intech), 209–230.

Stanton, M. C., Adriko, M., Arinaitwe, M., Howell, A., Davies, J., Allison, G., et al. (2017). Intestinal Schistosomiasis in Uganda at High Altitude (>1400 M): Malacological and Epidemiological Surveys on Mount Elgon and in Fort Portal Crater Lakes Reveal Extra Preventive Chemotherapy Needs. *Infect. Dis. Poverty* 6 (1), 34. doi:10.1186/s40249-017-0248-8

Steinmann, P., Keiser, J., Bos, R., Tanner, M., and Utzinger, J. (2006). Schistosomiasis and Water Resources Development: Systematic Review, Meta-Analysis, and Estimates of People at Risk. *Lancet Infect. Dis.* 6 (7), 411–425. doi:10.1016/S1473-3099(06)70521-7

Stensgaard, A.-S., Utzinger, J., Vounatsou, P., Hürlimann, E., Schur, N., Saarnak, C. F. L., et al. (2013). Large-scale Determinants of Intestinal Schistosomiasis and Intermediate Host Snail Distribution across Africa: Does Climate Matter? *Acta Tropica* 128 (2), 378–390. doi:10.1016/j.actatropica.2011.11.010

Stensgaard, A.-S., Vounatsou, P., Sengupta, M. E., and Utzinger, J. (2019). Schistosomes, Snails and Climate Change: Current Trends and Future Expectations. *Acta Tropica* 190, 257–268. doi:10.1016/j.actatropica.2018.09.013

Stothard, J. R., Mathieson, W., Webster, J. P., Fenwick, A., Tukahebwa, E. M., Kazibwe, F., et al. (2005). Field Evaluation of the Meade Readiview Handheld Microscope for Diagnosis of Intestinal Schistosomiasis in Ugandan School Children. *J. Trop. Med. Hyg.* 73 (5), 949–955. doi:10.4269/ajtmh.2005.73.949

Strobl, C., Boulesteix, A.-L., Zeileis, A., and Hothorn, T. (2007). Bias in Random forest Variable Importance Measures: Illustrations, Sources and a Solution. *BMC Bioinformatics* 8 (1), 1–21. doi:10.1186/1471-2105-8-25

Svanbäck, R., and Bolnick, D. I. (2007). Intraspecific Competition Drives Increased Resource Use Diversity within a Natural Population. *Proc. R. Soc. B.* 274 (1611), 839–844. doi:10.1098/rspb.2006.0198

Tchakonté, S., Ajeagah, G. A., Diomandé, D., Camara, A. I., and Ngassam, P. (2014). Diversity, Dynamic and Ecology of Freshwater Snails Related to Environmental Factors in Urban and Suburban Streams in Douala–Cameroon (Central Africa). *Aquat. Ecol.* 48 (4), 379–395. doi:10.1007/s10452-014-9491-2

Tumwebaze, I., Clewing, C., Dusabe, M. C., Tumusiime, J., Kagoro-Rugunda, G., Hammoud, C., et al. (2019). Molecular Identification of *Bulinus* spp. Intermediate Host Snails of *Schistosoma* spp. In Crater Lakes of Western Uganda with Implications for the Transmission of the *Schistosoma haematobium* Group Parasites. *Parasites Vectors* 12 (1), 1–23. doi:10.1186/s13071-019-3811-2

Viera, A. J., and Garrett, J. M. (2005). Understanding interobserver agreement: the kappa statistic. *Fam med.* 37 (5), 360–363.

Utzinger, J., and Tanner, M. (2000). Microhabitat Preferences of *Biomphalaria Pfeifferi* and *Lymnaea Natalensis* in a Natural and a Man-Made Habitat in southeastern Tanzania. *Mem. Inst. Oswaldo Cruz* 95, 287–294. doi:10.1590/s0074-02762000000300002

Utzinger, J., Raso, G., Brooker, S., De Savigny, D., Tanner, M., Ørnbjerg, N., et al. (2009). Schistosomiasis and Neglected Tropical Diseases: towards Integrated and Sustainable Control and a Word of Caution. *Parasitology* 136 (13), 1859–1874. doi:10.1017/s0031182009991600

Vinogradov, V. I. (1980). C13/C12 and O18/O16 Ratios and C14 Concentration in Carbonatites of the Kaliango Volcano (East Africa). *Int. Geol. Rev.* 22 (1), 51–57. doi:10.1080/00206818209466862

Walz, Y., Wegmann, M., Dech, S., Vounatsou, P., Poda, J.-N., N'Goran, E. K., et al. (2015). Modeling and Validation of Environmental Suitability for Schistosomiasis Transmission Using Remote Sensing. *PLOS Negl. Trop. Dis.* 9 (11), e0004217. doi:10.1371/journal.pntd.0004217

Wang, L., Utzinger, J., and Zhou, X.-N. (2008). Schistosomiasis Control: Experiences and Lessons from China. *Lancet* 372 (9652), 1793–1795. doi:10.1016/S0140-6736(08)61358-6

Warton, D. I., and Hui, F. K. C. (2011). The Arcsine is Asinine: the Analysis of Proportions in Ecology. *Ecology* 92 (1), 3–10. doi:10.1890/10-0340.1

Watson, J. M. (1958). Ecology and Distribution of Bulinus truncatus in the Middle East; with Comments on the Effect of Some Human Activities in Their Relationship to the Snail Host on the Incidence of Bilharziasis Haematobia in the Middle East and Africa. *Bull. World Health Organ.* 18 (5-6), 833–894.

World Health Organization (2012). Elimination of Schistosomiasis. Sixty-fifth World Health Assembly, WHA65. 21, Agenda item 13.11, 26 May 2012. Available at: http://apps.who.int/gb/ebwha/pdf_files/WHA65/A65_R21-en.pdf (Accessed July, , 2021).

World Health Organization (2016). Schistosomiasis. Available at: https://www.who.int/features/factfiles/schistosomiasis/en/(Accessed July, 2021).

Xia, C., Hu, Y., Ward, M. P., Lynn, H., Li, S., Zhang, J., et al. (2019). Identification of High-Risk Habitats of *Oncomelania Hupensis*, the Intermediate Host of *Schistosoma Japonium* in the Poyang Lake Region, China: A Spatial and Ecological Analysis. *PLOS Negl. Trop. Dis.* 13 (6), e0007386. doi:10.1371/journal.pntd.0007386

Yirenya-Tawiah, D., Abdul Rashid, A., Futagbi, G., Aboagye, I., and Dade, M. (2011). Prevalence of Snail Vectors of Schistosomiasis in the Kpong Head Pond, Ghana. *West. Afr. J. Appl. Ecol.* 18, 39–45. doi:10.4314/wajae.v18i1.70310

Zhang, J., Yue, M., Hu, Y., Bergquist, R., Su, C., Gao, F., et al. (2020). Risk Prediction of Two Types of Potential Snail Habitats in Anhui Province of China: Model-Based Approaches. *PLOS Negl. Trop. Dis.* 14 (4), e0008178. doi:10.1371/journal.pntd.0008178

Conflict of Interest: The authors declare no conflict of interest. Any suggestions, results, discussions and conclusions or recommendations presented in this study are those of the authors and do not express the views of the funding agencies.

Publisher's Note: All claims expressed in this article are solely those of the authors and do not necessarily represent those of their affiliated organizations, or those of the publisher, the editors and the reviewers. Any product that may be evaluated in this article, or claim that may be made by its manufacturer, is not guaranteed or endorsed by the publisher.

scientific reports

Check for updates

OPEN

A machine learning approach for modeling the occurrence of the major intermediate hosts for schistosomiasis in East Africa

Zadoki Tabo[1,2]✉, Lutz Breuer[2,3], Codalli Fabia[2], Gorata Samuel[2,4] & Christian Albrecht[1]

Schistosomiasis, a prevalent water-borne disease second only to malaria, significantly impacts impoverished rural communities, primarily in Sub-Saharan Africa where over 90% of the severely affected population resides. The disease, majorly caused by *Schistosoma mansoni* and *S. haematobium* parasites, relies on freshwater snails, specifically *Biomphalaria* and *Bulinus* species, as crucial intermediate host (IH) snails. Targeted snail control is advisable, however, there is still limited knowledge about the community structure of the two genera especially in East Africa. Utilizing a machine learning approach, we employed random forest to identify key features influencing the distribution of both IH snails in this region. Our results reveal geography and climate as primary factors for *Biomphalaria*, while *Bulinus* occurrence is additionally influenced by soil clay content and nitrogen concentration. Favorable climate conditions indicate a high prevalence of IHs in East Africa, while the intricate connection with geography might signify either dispersal limitations or environmental filtering. Predicted probabilities demonstrate non-linear patterns, with *Bulinus* being more likely to occur than *Biomphalaria* in the region. This study provides foundational framework insights for targeted schistosomiasis prevention and control strategies in the region, assisting health workers and policymakers in their efforts.

Keywords Freshwater snails, Schistosomiasis, Predictor features, Random forest, Sub-Saharan Africa

A large number of neglected tropical diseases (NTD) in sub-Saharan Africa account for approximately 200,000 deaths annually as well as 57 million lost life-years[1].The most significant of these diseases, schistosomiasis, is the second most prevalent parasitic disease only after malaria in several sub-Saharan African countries[1,2], severely affecting low-income rural communities with poor sanitation[3]. Schistosomiasis negatively impacts child development, pregnancy outcomes, and agricultural productivity, perpetuating poverty for millions of Africans[1,3,4]. In spite of only making up 13% of the global population, sub-Saharan Africa accounted for 90% of schistosomiasis cases[5].

Human schistosomiasis is caused by species of schistosome trematode worms: *Schistosoma mansoni*, *S. haematobium*, *S. japonicum*, *S. intercalatum*, and *S. mekongi*. These infections manifest in two main forms: intestinal schistosomiasis, attributed to *S. haematobium*, and urogenital schistosomiasis, associated with other species such as *S. mansoni*[6,7]. The life cycle of *Schistosoma* initiates when parasitic eggs from infected human feces or urine enter freshwater sources. Under favorable environmental conditions, these eggs hatch into miracidia, which actively seek out and penetrate suitable IH snails. Asexual reproduction occurs within the snails, leading to the development of cercariae. At this advanced stage, the cercariae are released into the water as free-living parasites and can penetrate human skin, thereby completing the cycle and causing the disease[6]. Notably, *Bulinus* and *Biomphalaria* snails act as IHs for *S. haematobium* and *S. mansoni*, respectively[7]. *Schistosoma haematobium* and *S. mansoni* are prevalent in Sub-Saharan Africa, significantly contributing to the burden of schistosomiasis.

[1]Department of Animal Ecology and Systematics, Justus Liebig University Giessen, Heinrich-Buff-Ring 26 (iFZ), 35392 Giessen, Germany. [2]Institute for Landscape Ecology and Resource Management, Justus Liebig University Giessen, Heinrich-Buff-Ring 26 (iFZ), 35392 Giessen, Germany. [3]Centre for International Development and Environmental Research (ZEU), Justus Liebig University Giessen, Senckenbergstrasse 3, 35390 Giessen, Germany. [4]Department of Environmental Science, Faculty of Science, University of Botswana, P/Bag UB00704, Gaborone, Botswana. ✉email: tabozac@gmail.com

While the 2020 goal for schistosomiasis elimination proved elusive[8], control efforts in Sub-Saharan Africa, specifically East Africa, have predominantly relied on mass chemotherapy, particularly for school-aged children[9,10]. However, recognizing the inadequacy of this approach alone, there is an urgent call for alternative strategies[10]. The integration of One Health into the WHO 2030 NTD roadmap, encompassing human treatment, livestock treatment and/or vaccination, environmental management, and snail control, has garnered increased recognition for its potential impact[11,12]. From an ecosystem perspective, factors influencing the presences of *Schistosoma* parasites and their snail hosts can significantly impact the transmission dynamics of schistosomiasis[12]. Investigating such factors aligns with the WHO 2030 NTD elimination strategy[11]. Nonetheless, targeting IH snails, demonstrated as effective[13], holds promise. However, our understanding of various aspects related to snail hosts remains limited, with a scarcity of studies providing comprehensive prevalence data and identifying significant features influencing the distribution of *Biomphalaria* and/or *Bulinus* IH snails[14,15]. This knowledge gap is particularly pronounced in East Africa overall, with persistent schistosomiasis hotspots in Kenya and Tanzania[9].

Machine learning techniques, particularly random forest (RF)[16], have gained wide application in various scientific domains for classification and regression analyses pertaining identification of significant features[14,17–20]. In classification tasks, RF has demonstrated superior predictive accuracy compared to other methods, such as logistic regression[21–23]. RF is resilient to multicollinearity, a common issue in ecological datasets[24]. It also offers effective solutions for addressing missing data[25]. RF aids in discerning predictor variables with substantial influence on response variables, distinguishing them from those that may not contribute significantly. Therefore, this research aims to provide comprehensive insights into the distribution of IHs in the East African region using RF to identify the spatial distribution of IH snail distribution and the significant features driving their distribution.

Currently, only one documented study exists for East Africa region as a whole, albeit restricted to *Biomphalaria* IHs and a limited number of surveyed locations, considering just eight predictor features[26]. This previous study gives a first impression, however, obtaining robust results may necessitate the inclusion of a broader array of potential features in the analysis. This challenge becomes especially complex in regions like East Africa characterized by variable occurrences of both *Biomphalaria* and *Bulinus* IH species, in conjunction with diverse geographical, climatic, environmental, and anthropogenic factors. This highlights a substantial gap in understanding the distribution of the two genera, which are the primary contributors to the schistosomiasis burden in the region. To address this knowledge gap, our study has two primary objectives: a) to assess the significance of a broader array of potential features, including climatic, environmental, topographic, and human impact factors, in influencing the distribution of IH snails of both *Bulinus* and *Biomphalaria* snails in East Africa, and b) to determine the anticipated probability of occurrences for the pertinent species within the genera based on the most significant factors.

Material and methods

Description of study area

The study area spans the East African region, including Uganda, Kenya, and Tanzania, situated within the Tropics of Cancer and Capricorn. East Africa covers an extensive area of approximately 6667 Mio km^2 and is home to roughly 488 million people, making it the most densely populated sub-region in Africa[27]. This region is rich in freshwater sources, such as swamps, rivers, and (crater) lakes, but also man-made structures such as dams and irrigation schemes, serving as potential habitats for IH snails[14,28,29]. In addition, East Africa exhibits a diverse range of geographical, climatic, hydrological, and human-induced factors, all of which are highly relevant for the distribution of IH snails. Importantly, both *S. mansoni* and *S. haematobium* are major disease burdens in the region associated with the presence of both *Bulinus* and *Biomphalaria* species[14,30].

Occurrence and geographic data

The geographic distribution of occurrence data for the *Biomphalaria* and *Bulinus* IH snails in the study area can be found in the Supplementary File S1 Fig. 1. We collected geographic data (longitude and latitude), pertaining to *Bulinus* and *Biomphalaria* distribution in the three East African countries Uganda, Tanzania and Kenya, including data previously reported by Chibwana et al.[31], Tumwebaze et al.[32], Tabo et al.[14], as well as those reported in the Global Biodiversity Information Facility (GBIF), that include recent data from the museum specimens and DNA barcodes[33]. The information obtained from GBIF constitutes secondary data retrieved online, whereas the remaining three sources involve primary data collected through field surveys. This dataset encompassed all *Biomphalaria* species, universally acknowledged as hosts, and selectively featured specific well-documented host species of *Bulinus* (see the Supplementary Table S1). After obtaining the data, we imported it into the R statistical environment, version 4.0.3[34], and conducted a thorough data cleansing process by removing duplicate records. Subsequently, we harnessed the processed geographic data to extract environmental, climatic, topographic, soil content, and human influence drivers associated with occurrence data of IHs using the R programming language, Google earth engine[35], and the ArcGIS Pro geographical information systems (GIS), as briefly described in Sects. "Climatic and environmental features"–"Human impact features".

Climatic and environmental features

Climate factors such as temperature, precipitation, and natural habitat conditions are recognized for their impact on host snail distribution patterns[36–38]. To account for the potential preference of IH snail species for climatic variations, we obtained high-resolution bioclimatic data from the WorldClim (v2.1) global dataset, typically spanning records from 1970 to 2000 with a spatial resolution of 340 km^2 (10-arc minutes)[39], within the R statistical environment. We excluded most bioclimatic features and selected mean annual temperature (BIO1), temperature of the warmest month (BIO5), temperature of the coldest month (BIO6), annual precipitation (BIO12), precipitation of the wettest month (BIO13), and precipitation of the driest month (BIO14), which have been extensively

documented for their impact and the biological relevance for the presence and distribution of IH snails[14,37,38]. In addition, we computed the mean land surface temperature (LST) using the MOD11A1.061 Terra Land Surface Temperature and Emissivity Daily Global 1 km dataset within Google Earth Engine , an indicator of energy exchange at the land surface-atmosphere interface known for its influence on climate and ecosystems[40]. We have averaged all LST data for the years 2000, 2010, and 2020, accommodating any temperature and emissivity fluctuations over the past two decades. In the Google Earth Engine platform, we scripted the extraction of the Normalized Difference Vegetation Index (NDVI) from the MODIS product MOD13Q1 (2021) V6.1, offering valuable information at a 250 m pixel resolution[41]. We have averaged NDVI data for the years 2000, 2010, and 2020, accounting for any fluctuations in the index over the past two decades. The NDVI is a widely-used indicator for the quantification of vegetation health and density[42,43].

In addition, land cover, which is known to significantly impact snail habitat suitability[44], was considered and extracted from the MODIS Land Cover Type Yearly Global 500 m dataset via Google Earth Engine[45]. The land cover classification employed in this study distinguishes 17 land cover classes, including 11 natural vegetation classes (such as forests, open herbaceous areas, and wetlands), 3 human-altered classes (comprising agricultural land and built-up areas), and 3 non-vegetated classes (including snow, rocks, and water bodies). Furthermore, various physiochemical properties previously studied for their effects on IH snail distribution[14,26,46] were integrated into our analysis. This included soil pH, soil organic carbon content in fine earth, and soil cation exchange capacity obtained at a 30 m resolution at a depth of 0–20 cm and 20–50 cm from the Innovative Solutions for Decision Agriculture Ltd (iSDA) data set via Google Earth Engine[47]. Additionally, data on soil composition, including clay, sand, silt, nitrogen content, and pH (measured in H_2O) at a depth of 0-5 cm, were sourced from the International Soil Reference and Information Centre (ISRIC), the World Soil Information Service[48].

Topographic features

We included topographic metrics, such as altitude, slope, and distance to the next water body as surrogate indicators of biogeographical isolation, which can influence colonization and limit dispersal, potentially impacting IH establishment in the region[14,49]. Altitude data, a key topographic factor affecting snail host distributions and prevalence of schistosomiasis[50], was obtained from the WorldClim database. Slope was derived from the Shuttle Radar Topography Mission (SRTM) digital elevation data using Google Earth Engine at approximately 30 m resolution[51]. The nearest distance from occurrence points to surface water bodies was calculated using the "Near" tool in ArcGIS[52].

Human impact features

We integrated two significant indices, the Human Influence Index (HII) and the Human Footprint Index (HFI), to assess the impact of human activities on the distribution of IH snails. We obtained HII Data from the Last of the Wild Project (version 2, 2005) at a spatial resolution of 1 km from NASA's Socioeconomic Data and Applications Center (SEDAC). This dataset quantifies relative human impact within each terrestrial biome using scores, derived from 9 global data layers. These layers include factors such as human population pressure (population density), human land use and infrastructure (built-up areas, nighttime lights, land use/land cover), and human access (coastlines, roads, railroads, navigable rivers)[53]. Scores range from 0 to a maximum of 72, with higher scores indicating greater human influence and lower scores suggesting less human influence. Likewise, we acquired HFI data from the Last of the Wild Project (version 3, 2009) through SEDAC (NASA) with a spatial resolution of 1 km. The dataset encompasses eight variables, such as built-up environments, population density, electric power infrastructure, crop lands, pasture lands, roads, railways, and navigable waterways. Scores within the range of 0 to 50 were assigned, where higher scores signify increased human influence and lower scores indicate less human influence[53]. We acquired region-specific data for both HII and HFI in a geographic coordinate system (GCS) from the SEDAC webpage, then extracted pixel-level data for both indices using the "Extract Values to Points" tool in ArcGIS. Note that SEDAC was preferred because it provided the most recent spatial/geographic data for both HII & HFI.

Data analysis

For assessing the importance of predictor features in both *Bulinus* and *Biomphalaria* RF models, we applied a cross-validation based on presence or absence (1/0) feature sensitivity, a widely-used resampling technique to evaluate generalization capabilities and prevent overfitting[54]. Cross-validation serves to evaluate the stability of variable rankings and mitigates the influence of randomness in the assessment process. The significance of individual parameters in the overall RF models was evaluated using two crucial metrics, Mean Decrease in Accuracy (MDA) and Mean Decrease in Gini (MDG)[17]. MDA is suitable when the goal is to maximize the overall accuracy of the classification model while MDG is often used when the goal is to build decision trees that create nodes with high homogeneity, resulting in better separation of classes[17]. Notably, variations in MDA and MDG outputs are common due to distinct calculation approaches and metrics. Addressing ranking disparities between MDA and MDG, we incorporated both metrics but primarily underscored features deemed significant by both metrics. Thus, when interpreting variable importance, it is advisable to prioritize relative rankings over comparing absolute values between these two measures, ensuring a more comprehensive understanding of feature significance and analytical robustness. In addition, to visually represent how individual predictor features influence the behavior of each IH snail in the region, we employed partial dependence plots[14,55]. The plots illustrate the relationship between a specific significant variable and the occurrence of the species while keeping all other variables constant.

Results

Occurrences of IH snails and associated predictor features

The data consists of a total of 455 recorded occurrences for *Bulinus* (52%) responsible for the transmission of *S. haematobium*, and 412 (48%) for *Biomphalaria* transmitting *S. mansoni*. Specifically, the dataset encompassed 77, 69, and 309 records for *Bulinus* species and 134, 143, and 135 records for *Biomphalaria* species in Uganda, Kenya, and Tanzania, respectively.

Overall, we considered 23 predictor features for the RF model. Their spatial resolution, potential mean value, standard deviation, and range variation are shown for both genera (Table 1). Detailed occurrence data, along with corresponding geographic information for the IH snails, can be found in the Supplementary Table S1. In general, both genera share parameter values that exhibit minimal spatial variation considering range of their potential predictors. This similarity in most features is potentially influenced by the location of the region within the same tropical climate zone favoring both species. For example, the data shows that the altitudinal range for *Biomphalaria* ranges from 46 to 2342 m.a.s.l, while for *Bulinus*, it spans from 3 to 2058 m.a.s.l. Additionally, soil conditions in the region, which tend to be alkaline, reflect a complex interplay of various soil components (clay, silt, sand), soil cation exchange capacity, and the bulk density of the fine earth fraction. The high nitrogen content (0.5–4.6 g kg^{-1}) in the area can be attributed to emissions from decomposing organic matter such as vegetation (index range 0.18–0.8), land cover, and human activities like deforestation. Nevertheless, an evaluation of the significance of individual parameters in the cross-validated random forest models for *Biomphalaria* and *Bulinus* has been conducted and is presented in Sect. "Variable importance".

Parameter	Abbreviation	Spatial resolution	Sources	Mean values		Standard deviation		Range	
				Buli	Biom	Buli	Biom	Buli	Biom
Mean annual temperature (°C)	BIO1	340 km^2	WorldClim2	21.6	18.4	74.87	7.2	2–27.5	2–29.1
Temperature of the warmest month (°C)	BIO5	340 km^2	WorldClim2	22.0	23.3	13.04	11.0	28–34.3	3–36.6
Temperature of the coldest month (°C)	BIO6	340 km^2	WorldClim2	14.5	12.3	6.18	4.55	11–21.3	8–22.1
Mean annual precipitation (mm)	BIO12	340 km^2	WorldClim2	1168	718	544	604	8–1989	1–1918
Precipitation of the wettest month (mm)	BIO13	340 km^2	WorldClim2	272	163	119	83	12–522	13–522
Precipitation of the driest month (mm)	BIO14	340 km^2	WorldClim2	27	30	17.36	21.9	1–72	1–91
Land surface temperature (°C)	LST	340 km^2	MODIS	25.3	26.7	6.79	5.4	3.4–36.18	12–43.6
Normalized difference vegetation index	NDVI	250 m^2	MODIS	0.58	0.59	0.10	0.13	0.18–0.83	0.18–0.8
Land cover	Land cover	500 m	MODIS	8.26	6.9	4.46	5.21	1–14	1–14
Soil pH	pH	30 m	iSDA	5.96	5.9	0.44	0.6	5.1–7.8	5.1–9
Soil organic carbon content in fine earth (g/kg)	Organic carbon	30 m	iSDA	6.76	8.3	2.45	3.3	1.23–17.18	1.23–17.17
Soil cation exchange capacity (cmol(+)/kg)	Cation exchange	30 m	iSDA	10.88	14.6	6.74	6.5	1.23–35.59	1.23–32.12
Bulk density of fine earth fraction (g/cm^3)	Bulk_density	30 m	iSDA	1.32	1.27	0.09	0.09	1.12–1.57	1.11–1.7
Clay content (%)	Clay	340 km^2	ISRIC	29.95	36.8	12.1	11.9	2–61	3–61
Sand content (%)	Sand	340 km^2	ISRIC	38.64	33.7	16.9	13.6	3–72	2–61
Silt content (%)	Silt	340 km^2	ISRIC	19.3	19.9	6.84	8.8	1–35	2–32
Nitrogen content (g kg^{-1})	Nitrogen	340 km^2	ISRIC	1.36	1.9	0.51	0.79	0.5–4.6	0.62–4.6
pH in H_2O	pH_{H2O}	340 km^2	ISRIC	6.05	6.08	0.53	0.63	5.32–8	5.3–9.2
Altitude (m.a.s.l)	Altitude	340 km^2	WorldClim2	436	1018	581	549	3–1,895	11–2,342
Slope (°)	Slope		SRTM	4.49	4.45	3.38	4.2	0.93–26.54	0.93–26.54
Distance from the nearest water source (m)	Water_distance	1:1,000,000	FAO	1778	1890	2530	2002	0.445–15,724	1.6–8990
Human influence index	Human influence	1 km	NASA	21.2	21.3	8.74	10.8	1–52	1–52
Human footprint index	Human Footprint	1 km	NASA	15.18	15.9	8.31	9.7	1–46	1–42

Table 1. The input predictor parameters, their spatial resolution; mean values, standard deviation, and the range: *Buli Bulinus* species, and *Biom Biomphalaria* species.

Variable importance

In general, geography, precipitation patterns, temperature variations, and environmental parameters within the region play a significant role in shaping the distribution of both *Biomphalaria* and *Bulinus*, although their relative contributions to the two models vary across the region and the method for the detection of variable importance (Fig. 1). Parameters highlighted in blue are considered strong predictors with significant influence, while those in black exhibit minor influence, and those with negative variable importance values in red are considered non-significant predictors according to the MDA metric (Fig. 1, left). We based on the same order

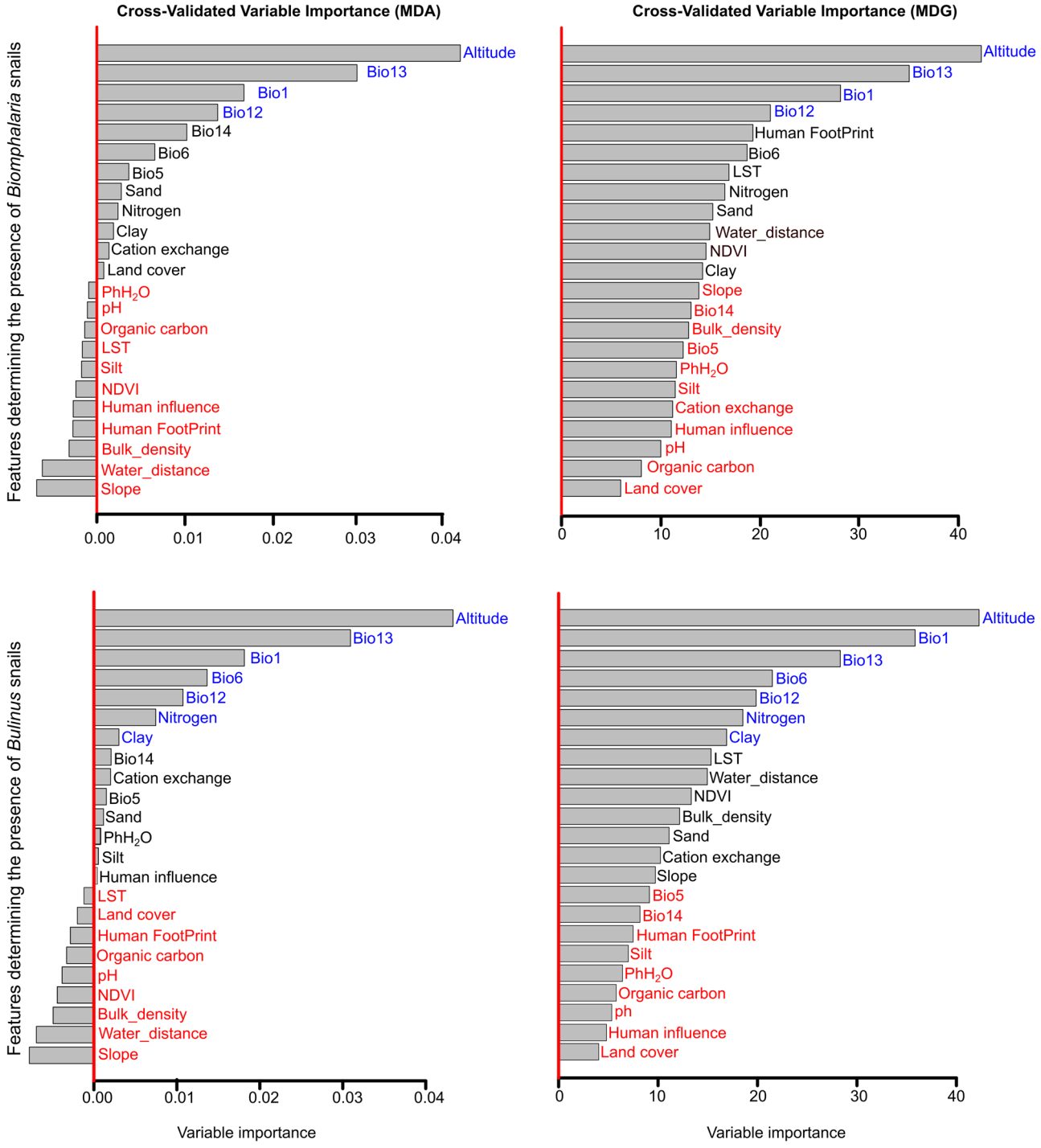

Figure 1. Contributions of the predictor features to the distribution of *Biomphalaria* (upper panel) and *Bulinus* (lower panel) considering the variable importance by mean decrease in accuracy (MDA, left)) and mean decrease in Gini (MDG, right). The prominently significant features are highlighted in blue, those with minor influence are marked in black, and those in red are considered non-significant. For abbreviations of features see Table 1.

of feature importance in MDA to categorize results in MDG into blue, black, and red (Fig. 1, right). Specifically, the most influential features affecting the distribution of *Biomphalaria* IH snails include altitude, and mainly climatic features, i.e. precipitation during the wettest month (BIO13), mean annual temperature (BIO1), and mean annual precipitation (BIO12). Features with minor contributions to the *Biomphalaria* model include the remaining climatic features like precipitation during the driest month (BIO14), temperature of the coldest month (BIO6), temperature of the warmest month (BIO5), and soil related features, as well as land cover. Additionally, the Human Footprint, land surface temperature, water distance, and vegetation index were found to have a lesser significance only with the MDA metric. The other parameters were found to be non-significant for the *Biomphalaria* model.

For *Bulinus*, the most significant parameters influencing its distribution are altitude, and again climatic features such as precipitation during the wettest month (BIO13), mean annual temperature (BIO1), mean annual precipitation (BIO12), as well as some soil features (nitrogen concentration, clay content). All other features are less relevant. Of these, parameters like land surface temperature, water distance, vegetation index, bulk density of fine earth fraction, and slope were found to be significant only when using the MDA method and only to a minor degree. Parameters that were not found to significantly impact the *Bulinus* IH species distribution at all include soil pH, organic carbon content, and the Human Footprint, amongst others (Fig. 1).

Predicted probabilities for the occurrence of IH snails

The simulated probabilities of genus occurrence in relation to the significant features identified in Fig. 1 demonstrate non-linear relationships, for both *Biomphalaria* and *Bulinus* IH snails. The likelihood of encountering *Bulinus* species is generally higher than that of *Biomphalaria* species in the region based on their probability values (Fig. 2). Nevertheless, the predicted probabilities for both genera exhibit consistent patterns concerning

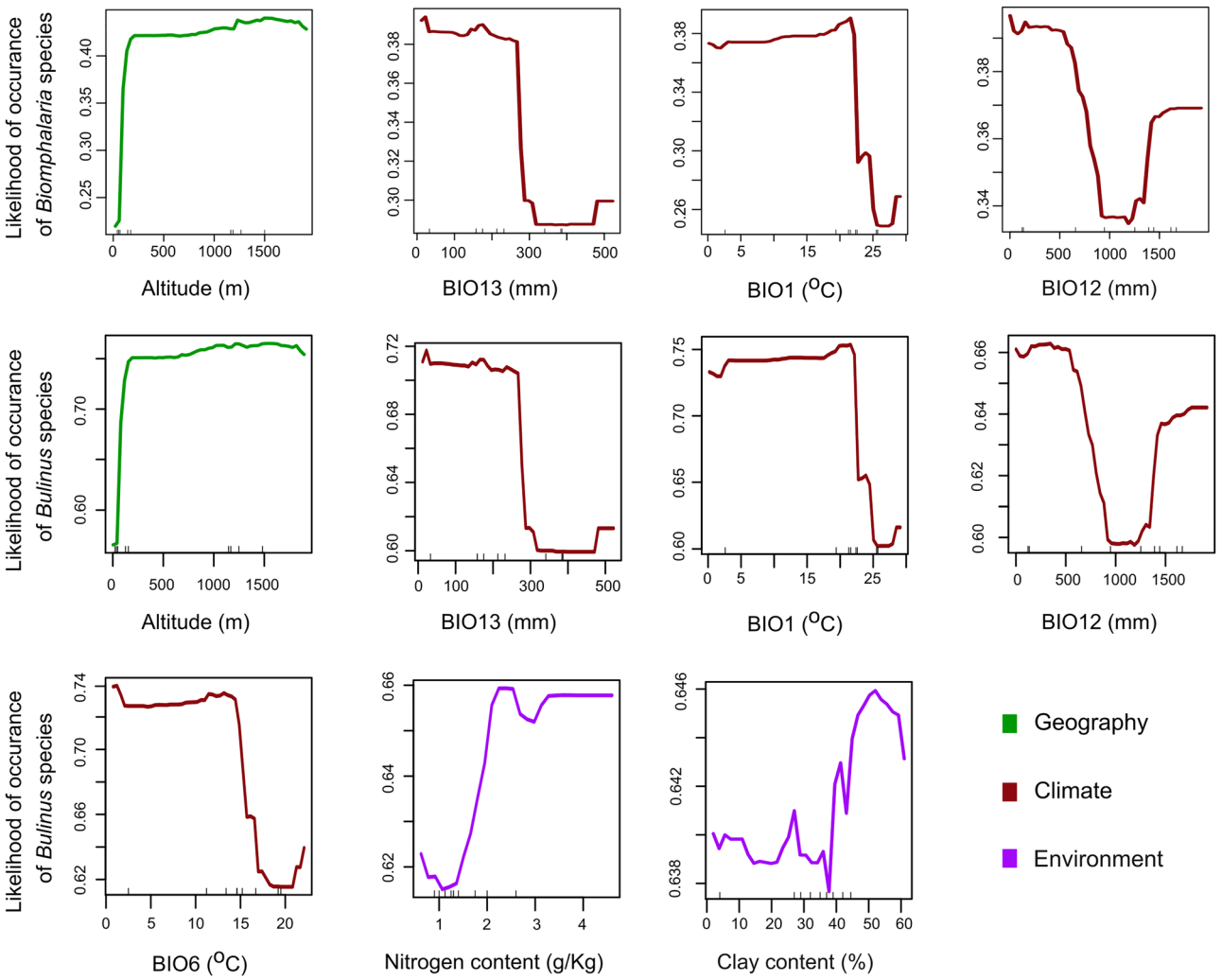

Figure 2. Likelihood of *Biomphalaria* species (1st panel) and *Bulinus* species occurrence (2nd and 3rd panels) in relation to the significant featuresfeatures identified by both importance metrics (MDA and MDG) in the *Biomphalaria* and *Bulinus* models. (Compare Fig. 1; see Supplementary S1 Fig. 2 for Biomphalaria and Fig. 3 for *Bulinus* predicted probabilities for the remaining predictors.

the importance of altitude, precipitation during the wettest month (BIO13), mean annual temperature (BIO1), and annual precipitation (BIO12). As altitude increases, the probabilities of occurrence for both IHs exhibit a steep rise up to an elevation of approximately 500 m.a.s.l. Beyond this point, the occurrence gradually increases, albeit at a very gradual rate, until approximately 1500–1800 m.a.s.l., where the trend peaks with a noticeable decrease in the likelihood of encountering these species (Fig. 2).

Conversely, for the occurrence of both IHs, the predicted probabilities decrease with a rise in precipitation levels less than 300 mm in the wettest month (BIO13) and annual precipitation (BIO12) of less than 1000 mm. This is followed by a slight increase at the end of the trend for BIO13 and a strong increase for BIO12 between around 1250 to 1900 mm. The feature mean annual temperature (BIO1) shows a complex relationship, indicating a gradual increasing trend towards higher values between 20 and 25 °C, followed by a steep probability decrease. Additionally, the association with the temperature of the coldest month (BIO6) indicates a decreasing probability of encountering *Bulinus* between 8 and 20 °C, followed by a slight increase up to 22 °C. The probability of encountering *Bulinus* increases with an increase in the soil nitrogen content, with a high probability occurring above 2 g/kg. However, the association with clay soils is complex, generally exhibiting an increasing trend that peaks at ~ 50% content of clay soils, followed by a slight decrease up to 60%.

Discussion

In this research, we relied on geographical data sourced from literature and the GBIF database to investigate the distribution of *Biomphalaria* and *Bulinus* IH snails for *Schistosoma* within the East African region. We observed minimal variation in the potential determinants of the distribution of both *Biomphalaria* and *Bulinus* snails across the regional scale. Geography and climate played a significant role in the distribution of *Biomphalaria*, while geography, climate, and to some extent, several soil factors, were crucial factors shaping the presence of *Bulinus* snails. However, it is crucial to note that the varying significance of parameters, highlights the intricate nature of snail behavior and distribution. Numerous interacting factors can convolute the straightforward impact of specific parameters potentially attenuating their effects in the model. In the following sections, we discuss IH snail occurrence in relation to the significant, minor, and non-significant predictor features within an ecological context.

Most significant predictor features of IH snail occurrences

The identification of significant features for both IH groups relied on high variable importance values, and similar results in both MDA and MDG metrics. Nonetheless our findings reveal that both genera thrive better below 500 m.a.s.l of altitude, potentially because lower altitudes promote stagnant water, facilitating breeding, while higher altitudes facilitate water flow[56], a reflection of the dispersal patterns of the IH snails[14]. Thus, the variation in the altitude of the study area plays a pivotal role, although it is important to note that Abe et al.[57] found that altitude did not significantly impact the distribution of *Bulinus* snails which they associated with the lack of altitude variation in their study area. Nonetheless, our findings complement the previous research studies which have reported differing upper altitude limits for IH snail occurrence in Uganda, with values ranging from 1400 m a.s.l[58], to more than 1600 m a.s.l[14], and even above 2000 m.a.s.l[50]. Notably, *Bulinus* species have been documented at exceptionally high altitudes (3997 m.a.s.l)[32], showing favorable conditions at such altitudes. People in high-altitude populations are at risk of disease exposure, yet often receive minimal attention from health authorities and vector control programs, posing a significant concern for their health. Therefore, dedicated research is needed to establish an upper limit for both forms of schistosomiasis and assess their potential impact on host-parasite interactions and transmission of the disease. Additionally, further investigations are required to determine whether the observed and assumed shifts in altitudinal thresholds are attributable to climate change or other factors.

Furthermore, the foremost significant drivers affecting the distribution of both *Biomphalaria* and *Bulinus* snails according to our study are the climate features, temperature, and precipitation. In contrast, a locally restricted study in western Uganda[14], assigned a lesser degree of importance to climate. This, suggests that the precise impact of climate change on IH snails and schistosomiasis is likely to exhibit variations based on geographical or spatio-temporal scales under consideration[59]. Precipitation serves as a critical metric for assessing the availability of suitable water bodies that snails are known to inhabit[36]. For example, climate change can lead to fluctuations in regional precipitation levels, which may in turn modify transmission patterns and the onset of schistosomiasis[36,38]. Nonetheless, an increase in precipitation levels contributes to the proliferation of breeding sites by increasing surface runoff into freshwater ecosystems[60], thereby enhancing the supply of organic matter, which serves as food for the snails, ultimately promoting their growth and fecundity[60,61]. Moreover, precipitation events provide suitable conditions for snails to emerge from estivation within temporary breeding sites, coinciding with a higher peak of reproduction among these organisms[62]. This would also explain the strong increase of IH snails' occurrence with precipitation features we found in our analysis. However, it is worth noting that excessive precipitation can also have adverse consequences on the distribution of IH snails[60]. Heavy rainfall can cause the breeding sites to be flooded, which dislocates snails and leads to a decline in snail populations. Consequently, snails disperse to new locations, establishing new areas for these vectors and posing a risk for the renewed transmission of schistosomiasis[60]. In contrast, during dry seasons, precipitation levels are low, and snails need to adapt, can undergo aestivation and their occurrence reduces, this may be a possible explanation for the negative correlation with the precipitation during the warmest months.

In a comparative context, our study emphasizes the importance of temperature in shaping snail distribution patterns across the broader East African region. Generally, freshwater snails are ectothermic, meaning their body temperature is regulated by the surrounding environment[12]. Temperature plays a crucial role in determining the development, survival, and reproductive rates of snails, as corroborated by multiple studies[10,36–38,56,63]. Interestingly, within the more confined geographical scope of Western Uganda, temperature exhibited a considerably

weaker influence on the distribution of IH species[14]. This could be attributed to the more consistent temperature fluctuations compared to the broader variations seen in larger-scale studies like ours. At a broader spatial scale, our study reveals a pronounced prevalence of intermediate host snails when mean annual temperatures range between 20 and 25 °C. In prior studies, a temperature of 25 °C has been associated with an increase in snail populations[64,65]. In addition, Malone[65] noticed an ideal temperature range of 20–27 °C for the intramolluscan development of *S. mansoni* within *Biomphalaria* spp. snails. On the other hand, decreased probability of IH snail presence during warm seasons exceeding 29 °C as shown in our study can be attributed to elevated snail mortality, diminished reproductive capacity, and inhibited snail growth, ultimately resulting in reduced schistosomiasis cases in such seasons[63,66].

In addition, the presence of clay in the soil was a significant factor in the *Bulinus* model, consistent with prior research by Stensgaard et al.[36], which associated clay-rich soils with higher snail prevalence. However, other studies suggested that clay content in the soil had only a minimal impact on IH snail presence[46,67]. Nonetheless, clay content in the nearby terrestrial surroundings can influence the distribution of IH snails by affecting soil texture, water retention, and drainage. The presence of heightened clay content may foster waterlogged conditions that are favorable for the proliferation of IH snails[56]. The strong relationship between soil nitrogen content and *Bulinus* IH snail distribution implies that even minor variations in soil nitrogen content can significantly impact their distribution. This connection suggests that although snails typically flourish in aquatic environments, the presence of soil nitrogen levels in the nearby terrestrial surroundings might affect the spread of *Bulinus* snails. Theoretically, increased soil nitrogen often correlates with a greater chance of nitrogen leaching, which could lead to elevated nitrogen levels in streams or floodplain habitats. These conditions could favor the survival and proliferation of these snails within their aquatic environments.

Minor and non-significant predictor features of IH snail occurrence

Certain predictor features held relatively low importance on the distribution of both genera. Discrepancies between the MDA and MDG metrics regarding these parameters were noted. A brief discussion of possible explanations for the limited and non-significant significance of these parameters on the distribution of IH snails is provided, taking into account conflicting findings in the literature. The limited impact of some climate features like BIO14 and BIO5 during the driest month can be attributed to factors including food scarcity, snail adaptations, and the possibility of aestivation/hibernation, with the likelihood of snail mortality during these driest months[62,63,66,68]. Scenarios like hibernation often occurs as most temporary breeding sites dry out[68]. Moreover, the feeding habits of freshwater snails can be influenced by cold temperatures (BIO6), leading to a potential decrease in their reproductive activity[61]. In fact, studies typically indicate that precipitation and temperature play a minimal role or lack statistical significance in influencing the distribution of intermediate host snails[14,46]. This can be linked to the smaller geographical scope examined in prior studies, where similar climatic changes were observed, resulting in collinearity in the climate data[14,46]. Consequently, there was limited variation in the data, hindering the reflection of the significance of climate variables as primary drivers for snail distribution. In contrast, our regional and larger-scale study provides a more comprehensive perspective. However, it is important to note that the distribution of IH snails may not solely be driven by all climate features but can also be influenced by a complex interplay of various factors including ecological, topological, and human factors[12,59].

Sand content, as observed, emerged as a significant yet a minor feature in both the *Biomphalaria* and *Bulinus* models. This finding is in line with the research conducted by Stensgaard et al.[36], which highlights the significance of specific levels of sand content in snail distribution. Sandy soils, due to their inherent characteristics that enhance drainage, significantly impact the suitability of habitats for snails[36]. However, sand content, representing fine soil particles, may not consistently exert a strong influence on the distribution of IH snails, with its impact varying potentially based on its content for example 34–39% in our study area. On the other hand, the significance of silt content in *Bulinus* presence was notably lower, as indicated only by MDA. This finding aligns with the results reported by Deka[46], underscoring the limited contribution of silt content to defining the presence of IH snails. On the contrary, Olkeba et al.[67] observed higher *Bulinus globosus* populations in regions with higher silt content. However, it is crucial to acknowledge that the association between soil texture (silt, clay, sand) and snail distribution represents only one aspect within a larger ecological framework. This framework includes various factors like water chemistry, vegetation, and climate.

Furthermore, we observed that soil pH (levels 5.1–9.2), had minimal significance in the distribution of *Bulinus* snails and was not significant at all in the *Biomphalaria* model. The limited impact in our study could be attributed to the varying alkaline nature of the soils. Likewise, the restricted importance of both bulk density of the fine earth fraction and soil cation exchange capacity, as constituents of soil compositions, can be linked to the limited influence exerted by the soil content parameters (sand, silt, clay). It is essential to acknowledge that land use distribution involves various classes, which vary by region and over time[69]. The potential impact of land use on the distribution of IH snails, such as waterbodies and cropland vegetation mosaics, may be limited by superimposing effects from irrelevant factors like savannah and barren land[56]. The relatively minor impact of the human footprint, which was a weaker predictor for *Biomphalaria* snail distribution (by MDA), is in line with findings from Olkeba et al.[67] and Krauth et al.[70]. Nonetheless, humans often play a crucial role in introducing snails into new environments and serve as passive dispersal vectors[70,71] through expansion of irrigation agriculture, settlement and fishing activities. Conversely, a study by Tabo et al.[14] did not identify human influence as a significant factor affecting IH snail distribution, potentially because some of the habitats are in reversed areas and in game parks where human activities are limited[14]. Furthermore, this variance may be attributed to the limited spatial scope of their case study, which may not comprehensively capture the full extent of human impact on snail distribution. While Deka[46] emphasized the importance of proximity to the nearest water body as a significant variable, our research indicates its limited influence on the distribution of both genera. Surprisingly, Tabo

et al.[14] reached a similar conclusion regarding the insignificance of this variable in IH snail distribution. These disparities may stem from the distinctive geographical and landscape characteristics considered.

In our study, with an NDVI range of 0.18 to 0.83 and an LST range of 3.4 to 43.6 °C in the region, both parameters exhibited low significance in determining the distribution of both genera (by MDG). This observation aligns with previous studies conducted by Magero et al.[26], Boitt and Suleiman[56], and Deka[46], all of which found a similar limited influence of these two parameters on the presence of IH snails. Nonetheless, it is important to consider that we have observed in this study that land cover has a limited influence at all. Moreover, Boitt and Suleiman[56] have pointed out that land surface temperature (LST) is significantly shaped by land cover, while NDVI indirectly reflects land cover characteristics. This interrelationship may help explain the relatively modest impact of both LST and NDVI on snail distribution in our study.

While the study provides valuable new insights and results, it is limited by the scarcity of accessible physico-chemical data from online spatial databases or literature in the entire region or from major parts of the study area. The sole available physico-chemical data from a survey field study[14] is constrained to a localized area in Western Uganda within our study region. Nevertheless, we advocate for extensive field sampling studies across East Africa.

Conclusion

Our comprehensive analysis highlights the significance of geographical, climatic, environmental, and human factors in understanding the distribution of IH snails for schistosomiasis. Such factors can influence not only the occurrences of the genera but specifically their speciation, extinction and dispersion processes in an ecosystem. Our machine-learning approach disentangled key drivers, revealing that topography and climate predominantly influence *Biomphalaria*, while topography, climate, soil content, and nitrogen concentration collectively affect the presence of *Bulinus*. The intricate relationship with topography (altitude) may reflect dispersal limitations or environmental filtering, while positive associations with precipitation patterns and temperature variations suggest the prevalence of IH snails in East African ecosystems, especially within the tropical climate zone. Furthermore, clayish soil content and high nitrogen levels favor IH snail distribution in freshwater habitats. It is crucial to acknowledge the multifaceted nature of IH snail distribution, influenced by diverse ecological, climatic, topological, and human factors with varying contributions. These findings provide a foundational dataset for future research and risk mapping, supporting targeted prevention and control efforts against schistosomiasis. In addition, the findings have significant implications for public health. Policy makers and stakeholders should consider habitat suitability and prioritize actions on features identified as significant for the distribution of IH snails in the region. It is crucial to integrate approaches and enhance community awareness regarding these significant factors, leading to the design and implementation of integrative measures for the control of IHs and, consequently, the prevention of schistosomiasis.

Data availability

The data generated or analyzed are present in the manuscript.

Received: 12 December 2023; Accepted: 15 February 2024
Published online: 21 February 2024

References

1. WHO, World Health Organization. Combating neglected tropical disease. https://www.un.org/africarenewal/magazine/february-2023/combating-neglected-tropical-diseases (Accesed October 2023) (2023).
2. Aula, O. P., McManus, D. P., Jones, M. K. & Gordon, C. A. Schistosomiasis with a focus on Africa. *Trop. Med. Infect.* **6**, 3 (2021).
3. Hotez, P. J. *et al.* The global burden of disease study 2010: Interpretation and implications for the neglected tropical diseases. *PLoS Negl. Trop. Dis.* **8**, e2865 (2014).
4. Conteh, L., Engels, T. & Molyneux, D. H. Socioeconomic aspects of neglected tropical diseases. *Lancet* **375**, 239–247 (2010).
5. WHO, World Health Organization. Schistosomiasis. https://www.who.int/news-room/fact-sheets/detail/schistosomiasis (Accesed October 2023) (2023).
6. Colley, D. G., Bustinduy, A. L., Secor, W. E. & King, C. H. Human schistosomiasis. *Lancet* **383**, 2253–2264 (2014).
7. Utzinger, J. *et al.* Schistosomiasis and neglected tropical diseases: Towards integrated and sustainable control and a word of caution. *J. Parasitol.* **136**, 1859–1874 (2009).
8. Fenwick, A. & Jourdan, P. Schistosomiasis elimination by 2020 or 2030?. *Int. J. Parasitol.* **46**, 385–388 (2016).
9. Kittur, N. *et al.* Persistent hotspots in schistosomiasis consortium for operational research and evaluation studies for gaining and sustaining control of schistosomiasis after four years of mass drug administration of praziquantel. *Am. J. Trop. Med. Hyg.* **101**, 617 (2019).
10. Díaz, A. V., Walker, M. & Webster, J. P. Reaching the World Health Organization elimination targets for schistosomiasis: The importance of a one health perspective. *Philos. Trans. R. Soc.* **378**, 20220274 (2023).
11. World Health Organization. Ending the neglect to attain the sustainable development goals: A road map for neglected tropical diseases 2021–2030. https://www.who.int/publications/i/item/9789240010352 (2020).
12. Douchet, P., Gourbal, B., Loker, E. S. & Rey, O. Schistosoma transmission: Scaling-up competence from hosts to ecosystems. *Trends Parasitol.* **39**, 563–574 (2023).
13. Sokolow, S. H. *et al.* Global assessment of schistosomiasis control over the past century shows targeting the snail intermediate host works best. *PLoS Negl. Trop. Dis.* **10**, 4794 (2016).
14. Tabo, Z. *et al.* Factors controlling the distribution of intermediate host snails of Schistosoma in Crater Lakes in Uganda: A machine learning approach. *Front. Environ. Sci.* **10**, 871735 (2022).
15. Bakuza, J. S. *et al.* Assessing *S. mansoni* prevalence in Biomphalaria snails in the Gombe ecosystem of western Tanzania: The importance of DNA sequence data for clarifying species identification. *Parasit. Vectors* **10**, 1 (2017).
16. Breiman, L. Random forests. *Mach. Learn.* **45**, 5–32. https://doi.org/10.1023/A:1010933404324 (2001).
17. Huang, B. F. F. & Boutros, P. C. The parameter sensitivity of random forests. *BMC Bioinform.* **17**, 1–13. https://doi.org/10.1186/s12859-016-1228-x (2016).
18. Schonlau, M. & Zou, R. Y. The random forest algorithm for statistical learning. *Stata J.* **20**, 3–29. https://doi.org/10.1177/1536867X20909688 (2020).

19. Collin, F. D. *et al.* Extending approximate Bayesian computation with supervised machine learning to infer demographic history from genetic polymorphisms using DIYABC random forest. *Mol. Ecol. Resour.* **21**, 2598–2613. https://doi.org/10.1111/1755-0998.13413 (2021).
20. Georganos, S. *et al.* Geographical random forests: A spatial extension of the random forest algorithm to address spatial heterogeneity in remote sensing and population modelling. *Geocarto Int.* **36**, 121–136. https://doi.org/10.1080/10106049.2019.1595177 (2021).
21. Boulesteix, A.-L., Janitza, S., Kruppa, J. & König, I. R. Overview of random forest methodology and practical guidance with emphasis on computational biology and bioinformatics. *WIREs Data Min. Knowl. Discov.* **2**, 493–507. https://doi.org/10.1002/widm.1072 (2012).
22. Bunyamin, H. & Tunys, T. A comparison of retweet prediction approaches: The superiority of random forest learning method. *Telkomnika* **14**, 1052–1058. https://doi.org/10.12928/TELKOMNIKA.v14i3.3150 (2016).
23. Zhang, J. *et al.* Risk prediction of two types of potential snail habitats in Anhui Province of China: Model-based approaches. *PLoS Negl. Trop. Dis.* **14**, e0008178. https://doi.org/10.1371/journal.pntd.0008178 (2020).
24. Boonprong, S., Cao, C., Chen, W. & Bao, S. Random forest variable importance spectral indices scheme for burnt forest recovery monitoring-multilevel RF-VIMP. *J. Remote Sens.* **10**(807), 2016. https://doi.org/10.3390/rs10060807 (2018).
25. Brieuc, M. S. O., Waters, C. D., Drinan, D. P. & Naish, K. A. A practical introduction to random forest for genetic association studies in ecology and evolution. *Mol. Ecol. Resour.* **18**, 755–766. https://doi.org/10.1111/1755-0998.12773 (2018).
26. Magero, V. O., Kisara, S. & Wade, C. M. Geographical distribution of *Biomphalaria* snails in East Africa. *bioRxiv* **3**, 11 (2021).
27. Worldometer: Eastern Africa Population. https://www.worldometers.info/world-population/eastern-africa-population/ (2023).
28. Salzburger, W., Van Bocxlaer, B. & Cohen, A. S. Ecology and evolution of the African Great Lakes and their faunas. *Annu. Rev. Ecol. Evol. Syst.* **45**, 519–545 (2014).
29. Spigel, R. H. & Coulter, G. W. Comparison of hydrology and physical limnology of the East African great lakes: Tanganyika, Malawi, Victoria, Kivu and Turkana (with reference to some North American Great Lakes). In *Limnology, Climatology and Paleoclimatology of the East African lakes* (eds Whittaker, K. T. *et al.*) 103–139 (Routledge, 2019).
30. Gryseels, B., Polman, K., Clerinx, J. & Kestens, L. Human schistosomiasis. *Lancet* **368**, 1106–1118 (2006).
31. Chibwana, F. D., Tumwebaze, I., Mahulu, A., Sands, A. F. & Albrecht, C. Assessing the diversity and distribution of potential intermediate hosts snails for urogenital schistosomiasis: *Bulinus* spp. (Gastropoda: Planorbidae) of Lake Victoria. *Parasit. Vectors* **13**, 1–18 (2020).
32. Tumwebaze, I., Clewing, C., Chibwana, F. D., Kipyegon, J. K. & Albrecht, C. Evolution and biogeography of freshwater snails of the genus *Bulinus* (Gastropoda) in afromontane extreme environments. *Front. Environ. Sci.* **10**, 902900 (2022).
33. GBIF.org (22 May 2023) GBIF Occurrence Download. https://doi.org/10.15468/dl.6esfpk (2023).
34. R Core Team R: A Language and Environment for Statistical Computing. Version 4.0.3. R Foundation for Statistical Computing. http://www.R-project.org (2020).
35. Gorelick, N. *et al.* Google earth engine: Planetary-scale geospatial analysis for everyone. *Remote Sens. Environ.* **202**, 18–27 (2017).
36. Stensgaard, A. S. *et al.* Large-scale determinants of intestinal schistosomiasis and intermediate host snail distribution across Africa: Does climate matter?. *Acta Trop.* **128**, 378–390 (2013).
37. McCreesh, N., Nikulin, G. & Booth, M. Predicting the effects of climate change on *Schistosoma mansoni* transmission in eastern Africa. *Parasit. Vectors* **8**, 1–9 (2015).
38. McCreesh, N., Arinaitwe, M., Arineitwe, W., Tukahebwa, E. M. & Booth, M. Effect of water temperature and population density on the population dynamics of *Schistosoma Mansoni* intermediate host snails. *Parasit. Vectors* **7**, 1–9. https://doi.org/10.1186/s13071-014-0503-9 (2014).
39. Fick, S. E. & Hijmans, R. J. WorldClim 2: New 1-km spatial resolution climate surfaces for global land areas. *Int. J. Climatol* **37**, 4302–4315. https://doi.org/10.1002/joc.5086 (2017).
40. Wan, Z., Hook, S., Hulley, G. (2021). *MODIS/Terra Land Surface Temperature/Emissivity Daily L3 Global 1km SIN Grid V061* [Data set]. NASA EOSDIS Land Processes DAAC. 10.5067/MODIS/MOD11A1.061 (Accessed October 2023) (2023).
41. Didan, K. *MODIS/Terra Vegetation Indices 16-Day L3 Global 250m SIN Grid V061*. NASA EOSDIS Land Processes DAAC. Accessed 2023-06-13 from 10.5067/MODIS/MOD13Q1.061 (Accessed October 2023) (2021).
42. Pettorelli, N. *et al.* Satellite remote sensing for applied ecologists: Opportunities and challenges. *J. Appl. Ecol.* **51**, 839–848 (2014).
43. Turner, W. *et al.* Free and open-access satellite data are key to biodiversity conservation. *Biol. Conserv.* **82**, 173–176 (2015).
44. Oso, O. G. & Odaibo, A. B. Land use/land cover change, physico-chemical parameters and freshwater snails in Yewa North, Southwestern Nigeria. *PLoS One* **16**, e0246566 (2021).
45. Friedl, M., Sulla-Menashe, D. *MODIS/Terra+Aqua Land Cover Type Yearly L3 Global 500m SIN Grid V061*. NASA EOSDIS Land Processes DAAC. 10.5067/MODIS/MCD12Q1.061 (Accessed October 2023) (2022).
46. Deka, M. A. Predictive risk mapping of Schistosomiasis in Madagascar using ecological Niche modeling and precision mapping. *Trop. Med. Infect.* **7**, 15 (2022).
47. Hengl, T. *et al.* African soil properties and nutrients mapped at 30 m spatial resolution using two-scale ensemble machine learning. *Sci. Rep.* **11**, 6130. https://doi.org/10.1038/s41598-021-85639-y (2021).
48. Batjes, N. H., Ribeiro, E. & Van Oostrum, A. Standardised soil profile data to support global mapping and modelling (WoSIS snapshot 2019). *Earth Syst. Sci. Data* **12**, 299–320 (2020).
49. Hauffe, T., Albrecht, C. & Wilke, T. Assembly processes of gastropod community change with horizontal and vertical zonation in ancient Lake Ohrid: A metacommunity speciation perspective. *Biogeosciences* **13**, 2901–2911 (2016).
50. Stanton, M. C. *et al.* Intestinal schistosomiasis in Uganda at high altitude (> 1400 m): Malacological and epidemiological surveys on Mount Elgon and in Fort Portal crater lakes reveal extra preventive chemotherapy needs. *Infect. Dis. Poverty* **6**, 1–10 (2017).
51. Farr, T. G. *et al.* The shuttle radar topography mission. *Rev. Geophys.* https://doi.org/10.1029/2005RG000183 (2007).
52. Jenness, J., Dooley, J., & Riva, C. African Water Resource Database: GIS-based tools for inland aquatic resource management: 1. Concepts and application case studies 33 (CIFA technical paper, 2007).
53. Wildlife Conservation Society - WCS, and Center for International Earth Science Information Network - CIESIN - Columbia University. Last of the Wild Project, Version 2, 2005 (LWP-2): Global Human Influence Index (HII) Dataset (Geographic). NASA Socioeconomic Data and Applications Center (SEDAC) (2005).
54. Berrar, D. Cross-validation. In *Encyclopedia of Bioinformatics and Computational Biology* (eds Ranganathan, S. *et al.*) 542–545 (Academic Press, 2019). https://doi.org/10.1016/B978-0-12-809633-8.20349-X.
55. Evans, J. S., Murphy, M. A., Holden, Z. A. & Cushman, S. A. Modeling species distribution and change using random forest. In *Predictive Species and Habitat Modeling in Landscape Ecology* (eds Drew, C. A. *et al.*) 139–159 (Springer, 2011). https://doi.org/10.1007/978-1-4419-7390-0_8.
56. Boitt, M. K. & Suleiman, M. K. Mapping of freshwater snails' habitat—A source of transmitting Bilharzia in Mwea sub-county, Kenya. *J. Geosci. Environ. Prot.* **9**, 130–150 (2021).
57. Abe, E. M. *et al.* Predicting the geospatial distribution of *Bulinus* snail vector of urinary schistosomiasis in Abeokuta, South-Western, Nigeria. *Zool* **10**, 53–60 (2012).
58. Kabatereine, N. B., Brooker, S., Tukahebwa, E. M., Kazibwe, F. & Onapa, A. W. Epidemiology and geography of *Schistosoma mansoni* in Uganda: Implications for planning control. *Trop. Med. Int. Health* **9**, 372–380 (2004).

59. Stensgaard, A. S., Vounatsou, P., Sengupta, M. E. & Utzinger, J. Schistosomes, snails and climate change: Current trends and future expectations. *Acta Trop.* **190**, 257–268 (2019).
60. David, N. F. *et al.* Spatial distribution and seasonality of biomphalaria spp. In São Luís (Maranhão, Brazil). *Parasitol. Res.* **117**(1495), 1502. https://doi.org/10.1007/s00436-018-5810-1 (2018).
61. Madsen, H., Coulibaly, G. & Furu, P. Distribution of freshwater snails in the river Niger basin in Mali with special reference to the intermediate hosts of schistosomes. *Hydrobiologia* **146**, 77–88. https://doi.org/10.1007/bf00007580 (1987).
62. Brooker, S. *et al.* Use of remote sensing and a geographical information system in a national helminth control programme in Chad. *Bull. World Health Organ.* **80**, 783–789 (2002).
63. Tabo, Z., Kalinda, C., Breuer, L. & Albrecht, C. Adapting strategies for effective schistosomiasis prevention: A mathematical modeling approach. *Mathematics* **11**, 2609 (2023).
64. Manyangadze, T., Chimbari, M. J., Gebreslasie, M., Ceccato, P. & Mukaratirwa, S. Modelling the spatial and seasonal distribution of suitable habitats of schistosomiasis intermediate host snails using Maxent in Ndumo area, KwaZulu-Natal Province, South Africa. *Parasit. Vectors* **9**, 1–10. https://doi.org/10.1186/s13071-016-1834-5 (2016).
65. Malone, J. B. Biology-based mapping of vector-borne parasites by geographic information systems and remote sensing. *Parassitologia* **47**, 27 (2005).
66. Kalinda, C., Chimbari, M. & Mukaratirwa, S. Implications of changing temperatures on the growth, fecundity and survival of intermediate host snails of schistosomiasis: A systematic review. *Int. J. Environ. Res. Public Health* **14**, 80. https://doi.org/10.3390/ijerph14010080 (2017).
67. Olkeba, B. K. *et al.* Environmental and biotic factors affecting freshwater snail intermediate hosts in the Ethiopian Rift Valley region. *Parasit. Vectors* **13**, 1–13 (2020).
68. Perez-Saez, J. *et al.* Hydrology and density feedbacks control the ecology of intermediate hosts of schistosomiasis across habitats in seasonal climates. *Proc. Natl. Acad. Sci.* **113**, 6427–6432 (2016).
69. Lambin, E. F., Geist, H. & Rindfuss, R. R. Land-use and land-cover change: Developing and implementing an agenda for local processes with global impacts. *IHDP Update* https://doi.org/10.1007/3-540-32202-7_1 (2005).
70. Krauth, S. J. *et al.* Distribution of intermediate host snails of schistosomiasis and fascioliasis in relation to environmental factors during the dry season in the Tchologo region, Côte d'Ivoire. *Adv. Water Resour.* **108**, 386–396 (2017).
71. Kappes, H. & Haase, P. Slow, but steady: Dispersal of freshwater, molluscs. *Aquat. Sci.* **74**, 1–14. https://doi.org/10.1007/s00027-011-0187-6 (2012).

Acknowledgements

The authors are thankful to the German Academic Exchange Service (DAAD) for awarding ZT a PhD scholarship (Grant No. 57507871).

Author contributions

Conceptualization: Z.T. and C.A. Methodology: Z.T., C.A., C.F. and G.S. Formal analysis: Z.T. Funding acquisition: L.B. and C.A. Supervision: C.A. and L.B. Visualization: Z.T. and C.F. Original draft: Z.T. Manuscript review and editing were conducted by all authors. The final version received approval from all authors after thorough review.

Funding

Open Access funding enabled and organized by Projekt DEAL.

Competing interests

The authors declare no competing interests.

Additional information

Supplementary Information The online version contains supplementary material available at https://doi.org/10.1038/s41598-024-54699-1.

Correspondence and requests for materials should be addressed to Z.T.

Reprints and permissions information is available at www.nature.com/reprints.

Publisher's note Springer Nature remains neutral with regard to jurisdictional claims in published maps and institutional affiliations.

Infectious Disease Modelling 9 (2024) 158–176

Contents lists available at ScienceDirect

Infectious Disease Modelling

journal homepage: www.keaipublishing.com/idm

Exploring the interplay between climate change and schistosomiasis transmission dynamics

Zadoki Tabo [a, b, *], Chester Kalinda [a, d], Lutz Breuer [b, c], Christian Albrecht [a]

[a] Department of Animal Ecology and Systematics, Justus Liebig University Giessen, Heinrich-Buff-Ring 26 (iFZ), 35392 Giessen, Germany
[b] Department of Landscape Ecology and Resource Management, Justus Liebig University Giessen, Heinrich-Buff-Ring 26 (iFZ), 35392 Giessen, Germany
[c] Centre for International Development and Environmental Research (ZEU), Justus Liebig University Giessen, Senckenbergstrasse 3, 35390 Giessen, Germany
[d] Bill and Joyce Cummings Institute of Global Health, University of Global Health Equity | Kigali Heights, Plot 772 KG 7 Ave. PO Box 6955, Kigali, Rwanda

ARTICLE INFO

Article history:
Received 30 July 2023
Received in revised form 7 November 2023
Accepted 16 December 2023
Available online 22 December 2023
Handling Editor: Dr Daihai He

Keywords:
Modeling
Schistosomiasis transmission
Temperature
Rainfall
Basic reproduction number
East Africa

ABSTRACT

Schistosomiasis, a neglected tropical disease caused by parasitic worms, poses a major public health challenge in economically disadvantaged regions, especially in Sub-Saharan Africa. Climate factors, such as temperature and rainfall patterns, play a crucial role in the transmission dynamics of the disease. This study presents a deterministic model that aims to evaluate the temporal and seasonal transmission dynamics of schistosomiasis by examining the influence of temperature and rainfall over time. Equilibrium states are examined to ascertain their existence and stability employing the center manifold theory, while the basic reproduction number is calculated using the next-generation technique. To validate the model's applicability, demographic and climatological data from Uganda, Kenya, and Tanzania, which are endemic East African countries situated in the tropical region, are utilized as a case study region. The findings of this study provide evidence that the transmission of schistosomiasis in human populations is significantly influenced by seasonal and monthly variations, with incidence rates varying across countries depending on the frequency of temperature and rainfall. Consequently, the region is marked by both schistosomiasis emergencies and re-emergences. Specifically, it is observed that monthly mean temperatures within the range of 22–27 °C create favorable conditions for the development of schistosomiasis and have a positive impact on the reproduction numbers. On the other hand, monthly maximum temperatures ranging from 27 to 33 °C have an adverse effect on transmission. Furthermore, through sensitivity analysis, it is projected that by the year 2050, factors such as the recruitment rate of snails, the presence of parasite egg-containing stools, and the rate of miracidia shedding per parasite egg will contribute significantly to the occurrence and control of schistosomiasis infections. This study highlights the significant influence of seasonal and monthly variations, driven by temperature and rainfall patterns, on the transmission dynamics of schistosomiasis. These findings underscore the importance of considering climate factors in the control and prevention strategies of schistosomiasis. Additionally, the projected impact of various factors on schistosomiasis infections by 2050 emphasizes the need for proactive measures to mitigate the disease's impact on vulnerable populations. Overall, this research provides

* Corresponding author. Department of Animal Ecology and Systematics, Justus Liebig University Giessen, Heinrich-Buff-Ring 26 (iFZ), 35392 Giessen, Germany.
E-mail address: tabozac@gmail.com (Z. Tabo).
Peer review under responsibility of KeAi Communications Co., Ltd.

https://doi.org/10.1016/j.idm.2023.12.003

valuable insights to anticipate future challenges and devise adaptive measures to address schistosomiasis transmission patterns.

1. Introduction

Schistosomiasis, classified as a neglected tropical disease and an infectious disease of poverty, primarily affects poor and marginalized communities with limited access to clean water and sanitation, exerting detrimental impacts on their health, economy, and social well-being (Gryseels et al., 2006). Transmission of the parasitic trematode worms *Schistosoma* spp. to humans relies on the presence of suitable freshwater intermediate hosts (IH) snails, where schistosomes undergo asexual reproduction, and humans, serving as the final hosts, where schistosomes undergo sexual reproduction (Steinmann et al., 2006). Globally, over 240 million individuals are infected with schistosomiasis, with approximately 90% of infections concentrated in sub-Saharan Africa (Bergquist et al., 2017). African regions exhibit high prevalence of *Schistosoma* species, such as *Schistosoma mansoni* transmitted by *Biomphalaria* snails, and *Schistosoma haematobium* transmitted by *Bulinus* snails (Utzinger et al., 2009).

Climate variables, including temperature and precipitation, have been shown to influence the presence of IH snails and schistosomiasis transmission (McCreesh & Booth, 2013; Stensgaard et al., 2016; Tabo et al., 2022). However, the impact of current and future climate changes on schistosomiasis development remains uncertain and subject to debate (McCreesh & Booth, 2013; Stensgaard et al., 2016; McCreesh et al., 2015; Kalinda et al., 2018). Temperature fluctuations and extreme weather events have been highlighted as crucial factors (McCreesh & Booth, 2013), and deterministic models incorporating temperature effects on IH snails' life history characteristics are recommended (Kalinda et al., 2018). Climate change also introduces variations in regional precipitation levels (Solomon, 2007), potentially altering transmission patterns and schistosomiasis onset (Codjoe & Larbi, 2016; Martens et al., 1995). In specific tropical regions, including Tanzania, Kenya, Uganda, Rwanda, Burundi, and Eastern Zambia, climate changes may create favorable environments for IH snails (McCreesh et al., 2015).

While these studies suggest a potential for ecological changes and thus changes in the transmission of schistosomiasis, they also increase the difficulties associated with characterizing the relationship between climate variability in terms of temperature and precipitation with the transmission of schistosomiasis because the relationship is likely, not linear. Therefore, modeling the impact of seasonal climate variations in temperature and precipitation is critical in determining how climate change will influence schistosomiasis infections. In this context, a few mathematical models for the transmission dynamics of schistosomes have been proposed (Chen et al., 2010; Feng et al., 2004; Kalinda et al., 2019; Li et al., 2017). For instance, Li et al. (Li et al., 2017) formulate a periodic model that shows a seasonal transmission pattern of schistosomiasis based on monthly human schistosomiasis cases in the lake and marsh areas of China while Schrader et al. (Schrader et al., 2013) incorporate host snail genetic structure and land use changes in a schistosomiasis predictive model. On the other hand, the results of Mangal et al. (Mangal et al., 2008) and Kalinda et al. (Kalinda et al., 2017a) [19] provide information on the relationship between temperature and schistosomiasis transmission for *Biomphalaria-S. mansoni* and *Bulinus-S. haematobium* systems. Although these models have been insightful in providing a framework for evaluating the impact of one climate variable on schistosomiasis transmission, it is still challenging to simultaneously understand how temperature and precipitation affect schistosomiasis transmission dynamics as a result of a changing climate (Van der Wiel & Bintanja, 2021).

The objective of this study is two-fold. Firstly, it aims to develop a new mechanistic model for schistosomiasis transmission, considering the coupled effects of temperature and rainfall. The model incorporates parameters accounting for population growth, temperature, precipitation, and the release of parasite eggs by infected individuals. Secondly, the study aims to assess the impact of temperature and rainfall variations on the frequency of schistosomiasis transmission in different geographical areas, considering seasonal variations. Regional model systems are specifically built for Tanzania, Kenya, and Uganda, countries where schistosomiasis is highly prevalent, and the climate supports the thriving of intermediate host snails, leading to widespread infections among the population.

2. Material and methods

2.1. Model formulation

The model describes the transmission dynamics of *Schistosoma* infection in a population consisting of humans, *Schistosoma* parasite eggs in the environment and free-living parasites, and snails. The population is divided into various compartments representing the different stages of the *Schistosoma* life cycle: Susceptible human compartment, $S_h(t)$, represents individuals who are susceptible to the *Schistosoma* infection. These individuals have not been infected previously and can

potentially become infected if they come into contact with the parasite. Infected human compartment $I_h(t)$, represents individuals who are currently infected with *Schistosoma*. These individuals can release parasite eggs into the environment through faces and urine and can contribute to the overall transmission dynamics. Parasite egg population compartment $E_h(t)$, represents the population of parasite eggs released into the environment by infected humans. These eggs can hatch into free-living stages of the parasite (miracidia) and infect snails. Free-living miracidia parasite compartment $M_f(t)$, are the first free-living stage of the *Schistosoma* life cycle. Miracidia can infect snails and continue their development. Snails serve as intermediate hosts for the parasite, facilitating its life cycle. Susceptible snail vector compartment $S_v(t)$, represents snails that are susceptible to becoming infected with schistosomiasis, while the infected snail vector compartment $I_v(t)$, represents snails that are currently infected with schistosomiasis. Infected snails release free-living cercaria *Schistosoma* parasite into the environment, contributing to the transmission of the infection to human. Free-living cercaria parasite compartment $C_f(t)$, this compartment represents the population of cercaria parasites, which are the final free-living stage of the *Schistosoma* life cycle. Cercariae can infect humans upon contact with contaminated water to complete the *Schistosoma* life cycle.

The model is developed based on the following assumptions and parameters, which govern the rates of transmission, infection, and mortality for each compartment, as well as the interactions between different compartments:

(A1) The human is recruited at the rate $\Lambda_1 e^{-\upsilon_1 x}$, where Λ_1 signifies the maximum birth rate or immigration rate per individual. The factor $e^{-\upsilon_1 x}$ takes into account that recruitment of individuals does not occur immediately at birth but rather at the age when they are first susceptible to infection, denoted as x. This age corresponds to a time when individuals have the opportunity to interact with contaminated water through activities such as swimming, fishing, farming, washing, and collecting water for domestic use. It is worth noting that this age may occur much earlier, for example, when babies below the age of two years are washed in infected freshwater. The parameter υ_1 represents the mortality rate among humans, and the probability of a child surviving up to the age of susceptibility is given by $1/\upsilon_1$. As for the recruitment of snails, the rate of maturation $\Lambda_2(T, R)$, is dependent on the prevailing temperature (T) and rainfall amount (R). This rate also takes into account the three stages of the snail life cycle, the number of eggs laid by each adult snail per day, and the survival rate of both the laid eggs and the juvenile (immature) snails until they reach adulthood.

(A2) Schistosomiasis is not passed down from an infected mother to her child through vertical transmission. In the model, the incidences of infection are represented by $\beta_1(T)S_hC_f$ for humans and $\beta_2(T)M_fS_v$ for snails. Here, $\beta_1(T)$ denotes the temperature-dependent rate of cercaria infection in humans, reflecting how the infection rate varies with temperature. Similarly, $\beta_2(T)$ represents the temperature-dependent rate of miracidia infection on snails, indicating the infection rate's dependence on temperature.

(A3) The natural mortality rates for various components in the schistosomiasis system are denoted as υ_1 for humans, υ_2 for snails, $d_v(T)$ for parasite eggs, $\upsilon_3(T)$ for miracidia, and υ_4 for cercaria. Disease-related mortality rates specific to humans and snails are represented as δ_1 and $\delta_2(T)$, respectively. It is important to note that the rates $d_v(T)$, $\upsilon_3(T)$, and $\delta_2(T)$ are temperature-dependent parameters, meaning they vary with changes in temperature. The model assumes that excreta (urine and/or feces), which includes parasite eggs, are either directly released into the freshwater or find their way into it. Infected humans, on average, excrete ρ stools per day, with each gram of stool containing an average number of eggs denoted as θ_h. The occurrence of miracidia is a result of the fact that, on average, N_E miracidia hatch from each egg, and the rate at which the eggs hatch is represented as ω_1. Additionally, infected snails shed cercariae at a rate of ω_2. Fig. 1 illustrates the transmission diagram of Schistosomiasis.

The mathematical model equation (1) is developed based on Fig. 1.

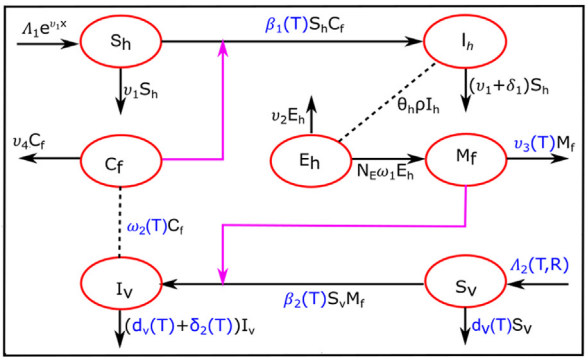

Fig. 1. Schistosomiasis transmission diagram depicting the life cycle stages of *Schistosoma*, interactions with human hosts and IH snails. Disease transmission parameters influenced by temperature and precipitation are highlighted in blue.

$$\left.\begin{aligned}
\frac{dS_h}{dt} &= \Lambda_1 e^{-\upsilon_1 x} - \beta_1(T) S_h C_f - \upsilon_1 S_h \\
\frac{dI_h}{dt} &= \beta_1(T) S_h C_f - (\upsilon_1 + \delta_1) I_h \\
\frac{dE_h}{dt} &= \theta_h \rho I_h - (\omega_1 + \upsilon_2) E_h \\
\frac{dM_f}{dt} &= N_E \omega_1 E_h - \upsilon_3(T) M_f \\
\frac{dS_v}{dt} &= \Lambda_2(T,R) - \beta_2(T) M_f S_v - d_v S_v \\
\frac{dI_v}{dt} &= \beta_2(T) M_f S_v - (d_v(T) + \delta_2(T)) I_v \\
\frac{dC_f}{dt} &= \omega_2(T) I_v - \upsilon_4 C_f
\end{aligned}\right\} \quad (1)$$

In this study, we adopt an autonomous dynamic model equation (1) to investigate the general dynamic effects of climate-driven systems on schistosomiasis. The spatial characteristics of our autonomous model output are determined by parameterization using temperature and rainfall values dependent on temperature and/or rainfall-related parameters.

2.2. Steady states and reproduction number of the model

We show that model (1) has both disease-free and endemic equilibria. The disease-free equilibrium represents a state in which the population remains free from the infection, indicating the absence of active transmission. In contrast, the endemic equilibrium represents a persistent state of disease transmission within the population, indicating an ongoing and stable level of infection. The disease-free equilibrium is crucial as it serves as a benchmark to evaluate the effectiveness of control measures. On the other hand, the endemic equilibrium provides insights into the persistence and stability of schistosomiasis transmission. In our model, the basic reproduction number (R_0) plays a fundamental role. It quantifies the average number of new infections caused by a single infectious individual in a susceptible population (Diekmann et al., 1990). If R_0 is greater than 1, it indicates that schistosomiasis has the potential to emerge, spread, and persist within the population. In contrast, if R_0 is less than 1, it suggests that, on average, less than one new case of schistosomiasis is generated during the infectious period, making the disease-free equilibrium more likely. The interplay between these equilibrium conditions and their impact under climate factors such as temperature and rainfall is crucial to forming public health strategies, as it gives insight into disease potential, the effectiveness of control measures, and the likelihood of achieving disease elimination.

We are able to calculate R_0 using model equation (1) of the autonomous dynamic model, as long as we disregard the temporal variations in temperature and rainfall (see e.g. Okuneye & Gumel, 2017; Parham & Michael, 2010). Thus, following the approach by Driessche and Watmough, (Driessche & Watmough, 2002) and Diekmann et al. (Diekmann et al., 1990), the next-generation technique is employed to determine the dominant eigenvalue, which represents the value of R_0 in the model (1). It can be expressed as:

$$R_0 = \sqrt{\left(\frac{\beta_1(T) N_E \omega_1 \theta_h \rho \Lambda_1 e^{-\upsilon_1 x}}{\upsilon_1 \upsilon_4 (d_v(T) + \delta_2(T))(\omega_1 + \upsilon_2)}\right) \cdot \left(\frac{\beta_2(T) \omega_2(T) \Lambda_2(T,R)}{\upsilon_3(T) d_v(T)\ (\upsilon_1 + \delta_1)}\right)} \quad (2)$$

Furthermore, R_0 can be represented as $R_0(T,R) = \sqrt{R_0^{S_h} R_0^{S_v}}$ where $R_0^{S_h}(T) = \frac{\beta_1(T) N_E \omega_1 \theta_h \rho(T) \Lambda_1 e^{-\upsilon_1 x}}{\upsilon_1 \upsilon_4 (d_v(T) + \delta_2(T))(\omega_1 + \upsilon_2)}$ and $R_0^{S_v}(T,R) = \frac{\beta_2(T) \omega_2(T) \Lambda_2(T,R)}{\upsilon_3(T) d_v(T)\ (\upsilon_1 + \delta_1)}$ under the square root, representing new cases of schistosomiasis infections in humans per infectious snail and cases of schistosomiasis infections in snails per infectious human, respectively. Thus, we obtained the standard expression of $R_0(T,R)$ under static environmental conditions where temperature and rainfall are constant at a given time. To determine the disease-free equilibrium E_0, we can set the equations of the model (1) to zero and solve for the respective variables when no infective compartments exist, i.e. $I_h = E_h = M_f = I_v = C_f = 0$, defined as:

$E_0 = (S_h', I_h', E_h', M_f', S_v', I_v', C_c') = \left(\frac{\Lambda_1 e^{-\upsilon_1 x}}{\upsilon_1}, 0, 0, 0, \frac{\Lambda_2(T,R)}{d_v}, 0, 0\right)$, E_0 always exists in a certain region $\Omega \in \mathscr{R}^7_{+0}$.

2.2.1. Local stability of the disease-free steady state, E_0

In this study, we analyze the local stability conditions of the disease-free equilibrium, E_0, in the model (1) based on the following theorem:

Theorem 3.1. *The disease-free steady state, E_0, in model (1) is locally asymptotically stable when $R_0 < 1$, and it is unstable when $R_0 > 1$.*

We present a proof for this theorem by demonstrating that all eigenvalues of the Jacobian matrix J(A) in (3), evaluated at E_0, are negative.

$$J(A) = \begin{pmatrix} -\upsilon_1 & 0 & 0 & 0 & 0 & 0 & -\beta_1 S_h' \\ 0 & -(\upsilon_1 + \delta_1) & 0 & 0 & 0 & 0 & \beta_1 S_h' \\ 0 & \rho\theta_h & -(\omega_1 + \upsilon_3) & 0 & 0 & 0 & 0 \\ 0 & 0 & N_E\omega_1 & -\upsilon_3 & 0 & 0 & 0 \\ 0 & 0 & 0 & -\beta_2 S_v' & -d_v & 0 & 0 \\ 0 & 0 & 0 & \beta_2 S_v' & 0 & -(d_v + \delta_2) & 0 \\ 0 & 0 & 0 & 0 & 0 & \omega_2 & -\upsilon_4 \end{pmatrix} \tag{3}$$

The Jacobian matrix $J(A)$ has seven eigenvalues, two of which by inspection in the first and fifth columns are $-\upsilon_1$ and $-d_v$. We exclude columns one and five with the corresponding rows and the resultant matrix gives the characteristic equation (4) whose roots are the remaining five eigenvalues of the Jacobian matrix

$$a_0\lambda^5 + a_1\lambda^4 + a_2\lambda^3 + a_3\lambda^2 + a_4\lambda + a_5 = 0 \tag{4}$$

where,

$$a_0 = 1, a_1 = (\upsilon_1 + \delta_1) + (\omega_1 + \upsilon_3) + \upsilon_3 + (d_v + \delta_2) + \upsilon_4$$

$$a_2 = \upsilon_3\upsilon_4 + (d_v + \delta_2)(\upsilon_3 + \upsilon_4) + ((\upsilon_1 + \delta_1) + (\omega_1 + \upsilon_3))((d_v + \delta_2) + (\upsilon_3 + \upsilon_4)) + (d_v + \delta_2)(\upsilon_3 + \upsilon_4),$$

$$a_3 = \upsilon_3\upsilon_4(d_v + \delta_2) + (\upsilon_3\upsilon_4 + (d_v + \delta_2)(\upsilon_3 + \upsilon_4))((\upsilon_1 + \delta_1) + (\omega_1 + \upsilon_3)) + (\upsilon_1 + \delta_1)(\omega_1 + \upsilon_3)((d_v + \delta_2) + (\upsilon_3 + \upsilon_4)),$$

$$a_4 = \upsilon_3\upsilon_4(d_v + \delta_2)((\upsilon_1 + \delta_1) + (\omega_1 + \upsilon_3)) + (\upsilon_1 + \delta_1)(\omega_1 + \upsilon_3)(\upsilon_3\upsilon_4 + (d_v + \delta_2)(\upsilon_3 + \upsilon_4)),$$

$$a_4 = \upsilon_3\upsilon_4(\upsilon_1 + \delta_1)(\omega_1 + \upsilon_3)(d_v + \delta_2).$$

The local stability of equilibrium point E_0 is determined by satisfying the conditions that $a_i > 0$ ($i = 1, 2, 3, 4, 5$), and $a_1a_2a_3a_4 + a_3a_5 + a_4a_5 > a_1a_2a_5 + a_1a_4^2 + a_3^2a_5$, based on the Routh-Hurwitz stability criteria for characteristic equation (4).

2.2.2. Global stability of the disease-free steady state, E_0

In accordance with Castillo-Chavez et al. (Castillo-Chavez, Feng, & Huang, 2002), our investigation focuses on the global stability of the disease-free steady state by reformulating model (1) into the following form:

$$\begin{cases} \dfrac{dX}{dt} = F(X, Z) \\ \dfrac{dZ}{dt} = G(X, Z), G(X, 0) = 0 \end{cases}$$

Here, $X = (S_h, S_v)$ represents the susceptible population, while $Z = (I_h, I_v, E_h, M_f, C_f)$ represents the infected population that is not infectious (I_h, I_v, E_h) and the infectious population (M_f, C_f). We set , $U_0 = (\tilde{X}, 0) = (\Lambda_1 e^{-\upsilon_1 x}/\upsilon_1, 0, 0, 0, \Lambda_2(T, R)/d_v, 0, 0)$ as the disease-free equilibrium of the model (1) and Theorem 3.2 holds.

Theorem 3.2. *The fixed point $U_0 = (\tilde{X}, 0)$ is globally asymptotically stable if $R_0 \leq 1$, and if the two conditions (B1) and (B2) below are fulfilled*:

(B1) $\frac{dX}{dt} = F(X, 0)$, $\tilde{X}$ is globally asymptotically stable

(B2) $G(X, Z) = AZ - \widehat{G}(X, Z)$ and $\widehat{G}(X, Z) \geq 0$ for (X, Z) ∈ R_+^7.*where $A = D_zG(\tilde{X}, 0)$ is an M-matrix and R_+^7 is the region in which model (1) makes biological sense.*

Proof: In our model (1), we have

$$F(X,0)=\begin{pmatrix}\Lambda_1 e^{-\upsilon_1 x}-\upsilon_1 S_h\\ \Lambda_2(T,R)-d_v S_v\end{pmatrix}$$

$$A=\begin{pmatrix}-(\upsilon_1+\delta_1) & 0 & 0 & 0 & \beta_1 S_h'\\ 0 & -(d_v+\delta_2) & 0 & \beta_2 S_v' & 0\\ \theta_h\rho & 0 & -(\omega_1+\upsilon_3) & 0 & 0\\ 0 & 0 & N_E\omega_1 & -\upsilon_4 & 0\\ 0 & \omega_2 & 0 & 0 & -\upsilon_5\end{pmatrix}$$

$$\widehat{G}(X,Z)=G(X,Z)-AZ=[0\quad 0\quad 0\quad 0\quad 0]^T=0.$$

In the computation, we show that

$$S_h(t)=\frac{\Lambda_1 e^{-\upsilon_1 x}}{\upsilon_1}+\left(S_h(0)-\frac{\Lambda_1 e^{-\upsilon_1 x}}{\upsilon_1}\right)e^{-\upsilon_1 t}\text{ and }S_v(t)=\frac{\Lambda_2(T,R)}{d_v}+\left(S_v(0)-\frac{\Lambda_2(T,R)}{d_v}\right)e^{-d_v t}$$

where $S_h(t)$ and $S_v(t)$, approach $\frac{\Lambda_1 e^{-\upsilon_1 x}}{\upsilon_1}$ and $\frac{\Lambda_2(T,R)}{d_v}$ as $t\to\infty$, respectively. The convergence of the solutions is global in R_+^7. Thus, $\tilde{X}$ is globally asymptotically stable, satisfying condition (A1). Moreover, matrix A is an M-matrix satisfying (A2) and as a result, Theorem 3.3 holds.

2.2.3. Existence and stability of the endemic steady state, $\boldsymbol{E_1}$

The endemic equilibrium point E_1 can be found by setting the equations of model (1) to zero, considering all compartments. The endemic equilibrium point exists when $R_0>1$ and the stability conditions for the disease-free equilibrium are not satisfied. Thus, $E_1=(S_h^*,I_h^*,E_h^*,M_f^*,S_v^*,I_v^*,C_f^*)$ and we express it in terms of I_v^* where

$$S_h^*(I_v^*)=\frac{\upsilon_4\Lambda_1 e^{-\upsilon_1 x}}{\beta_1\omega_2 I_v^*+\upsilon_1\upsilon_4}$$

$$I_h^*(I_v^*)=\frac{\beta_1\omega_2\Lambda_1 e^{-\upsilon_1 x}I_v^*}{(\beta_1\omega_2 I_v^*+\upsilon_1\upsilon_4)(\upsilon_1+\delta_1)}$$

$$E_h^*(I_v^*)=\frac{\beta_1\omega_2\rho\theta_h\Lambda_1 e^{-\upsilon_1 x}I_v^*}{(\omega_1+\upsilon_2)(\beta_1\omega_2 I_v^*+\upsilon_1\upsilon_4)(\upsilon_1+\delta_1)}$$

$$M_f^*(I_v^*)=\frac{\beta_{1\omega_1}\omega_2\rho\theta_h N_E\Lambda_1 e^{-\upsilon_1 x}I_v^*}{\upsilon_3(\omega_1+\upsilon_2)(\beta_1\omega_2 I_v^*+\upsilon_1\upsilon_4)(\upsilon_1+\delta_1)}$$

$$S_v^*(I_v^*)\frac{(\beta_1\omega_2 I_v^*+\upsilon_1\upsilon_4)\Lambda_2}{\upsilon_1\upsilon_4(d_v+\delta_2)R_0^2 I_v^*+d_v(\beta_1\omega_2 I_v^*+\upsilon_1\upsilon_4)}$$

$$C_f^*(I_v^*)=\frac{\omega_2}{\upsilon_4}I_v^*$$

By setting dI_v/dt to zero in equations of model (1) and substituting S_v^* and I_h^*, we obtain the following expression:

$$\left(\mathrm{p}_1 I_v^{*2}+\mathrm{p}_2 I_v^*+\mathrm{p}_3\right)I_v^*=0 \tag{5}$$

where $\mathrm{p}_1=\beta_1\omega_2(d_v+\delta_2)$, $\mathrm{p}_2=\mathrm{p}_1\upsilon_2(\upsilon_4(d_v+\delta_2-R_0^2)-2\upsilon_2)$ and $\mathrm{p}_3=\upsilon_1\upsilon_2(d_v+\delta_2)[\upsilon_1\upsilon_4(d_v+\delta_2)(1-\upsilon_1\upsilon_2R_0^2)+\upsilon_1\upsilon_2]$. Equation (5) has a solution where $I_v^*=0$, corresponding to the disease-free equilibrium. Additionally, the existence of an endemic equilibrium point is ensured if $R_0>1$ and $I_v^*\in\mathscr{R}_{+0}$, where I_v^* is given by $I_v^*=\frac{\mathrm{p}_2\pm\sqrt{\mathrm{p}_2{}^2-4\mathrm{p}_1\mathrm{p}_3}}{2\mathrm{p}_1}$.

2.2.4. The local stability of the endemic steady state

The condition which determines the threshold for the local stability of the endemic equilibrium, taking into account the respective parameters and values in the model is provided by the following theorem 3.3.

Theorem 3.3. *The endemic equilibrium E_1 is locally asymptotically stable if the basic reproduction number $R_0 > 1$, and the bifurcation parameter $\omega_1 = \omega_1^*$ satisfies $\omega_1 = \omega_1^* > \frac{\upsilon_1\upsilon_2\upsilon_3\upsilon_4 d_v(d_v+\delta_2)(\upsilon_1+\delta_1)}{\beta_1\beta_2\omega_2 N_E\theta_h\rho\Lambda_2\Lambda_1 e^{-\upsilon_1 x}-\upsilon_1\upsilon_3\upsilon_4 d_v(d_v+\delta_2)(\upsilon_1+\delta_1)}$.*

Proof.

We employ the manifold theorem described in Castillo-Chavez and Song, (Castillo-Chavez & Song, 2004), first, we define the variables as follows: $S_h = x_1, I_h = x_2, E_h = x_3, M_f = x_4, S_v = x_5, I_v = x_6, C_f = x_7$ and the model (1) is then transformed into the form $\frac{dx_i}{dt} = \dot{x}_i = (\dot{x_1}, \dot{x_2}\dot{x_3}, \dot{x_4}, \dot{x_5}, \dot{x_6}, \dot{x_7})^T$, where

$$\left.\begin{aligned} \dot{x_1} &:= f_1 = \Lambda_1 e^{-\upsilon_1\tau} - \beta_1 x_1 x_7 - \upsilon_1 x_1\ ;\ \dot{x_2} := f_2 = \beta_1 x_1 x_7 - (\upsilon_1+\delta_1)x_2;\\ \dot{x_3} &:= f_3 = \rho\theta_h x_2 - (\omega_1^* + \upsilon_2)x_3;\ \dot{x_4} := f_4 = N_E\omega_1^* x_3 - \upsilon_3 x_4;\\ \dot{x_5} &:= f_5 = \Lambda_2(T,R) - \beta_2 x_4 x_5 - d_v x_5;\ \dot{x_6} := f_6 = \beta_2 x_4 x_5 - (d_v+\delta_2)x_6;\\ \dot{x_7} &:= f_7 = \omega_2 x_6 - \upsilon_4 x_7 \end{aligned}\right\} \tag{6}$$

The transformed model (6) has the same disease-free equilibrium and the reproduction number R_0 as for model (1) above. Let the critical miracidia shedding be $\omega_1 = \omega_1^* = \frac{\upsilon_1\upsilon_2\upsilon_3\upsilon_4 d_v(d_v+\delta_2)(\upsilon_1+\delta_1)}{\beta_1\beta_2\omega_2 N_E\theta_h\rho\Lambda_2\Lambda_1 e^{-\upsilon_1 x}-\upsilon_1\upsilon_3\upsilon_4 d_v(d_v+\delta_2)(\upsilon_1+\delta_1)}$ as the bifurcation parameter at $R_0 = 1$. The linearized model (6) evaluated at disease-free equilibrium $(x_1^* = \Lambda_1 e^{-\upsilon_1 x}/\upsilon_1, x_2^* = 0, x_3^* = 0, x_4^* = 0, x_5^* = \Lambda_2(T,R)/d_v, x_6^* = 0, x_7^* = 0)$ with $\omega_1 = \omega_1^*$, has a simple eigenvalue associated with a right eigenvector $\boldsymbol{u} = (u_1, u_2, u_3, u_4)^T$ and a left eigenvector $\boldsymbol{v} = (\upsilon_1, \upsilon_2, \upsilon_3, \upsilon_4)$ satisfying $\boldsymbol{u}.\boldsymbol{v} = \mathbf{1}$, where

$$u_1 = \frac{-\beta_1 x_1^*}{\upsilon_1}u_7\ , u_2 = \frac{\beta_1 x_1^*}{(\upsilon_1+\delta_1)}u_7\ , u_3 = \frac{\beta_1\rho\theta_h x_1^*}{(\upsilon_1+\delta_1)(\omega_1^*+\upsilon_2)}u_7\ , u_4 = \frac{\beta_1\omega_1^*\rho\theta_h N_E x_1^*}{(\upsilon_1+\delta_1)(\omega_1^*+\upsilon_2)}u_7\ ,$$

$$u_5 = \frac{\beta_1\beta_2\omega_1^*\rho\theta_h N_E x_1^* x_5^*}{\upsilon_3 d_v(\upsilon_1+\delta_1)(\omega_1^*+\upsilon_2)}u_7\ , u_6 = \frac{\beta_1\beta_2\omega_1^*\rho\theta_h N_E x_1^* x_5^*}{\upsilon_3(d_v+\delta_2)(\upsilon_1+\delta_1)(\omega_1^*+\upsilon_2)}u_7\ , u_7 > 0$$

$$\upsilon_1 = -\upsilon_1, \upsilon_2 = \frac{\rho\theta_h}{(\upsilon_1+\delta_1)}\upsilon_3\ , \upsilon_3 > 0, \upsilon_4 = \frac{(\omega_1^*+\upsilon_2)}{N_E\omega_1^*}\upsilon_3\ , \upsilon_5 = 0, \upsilon_6 = \frac{\upsilon_3(\omega_1^*+\upsilon_2)}{N_E\omega_1^*\beta_2 x_5^*}\upsilon_3\ ,$$

$$\upsilon_7 = \frac{\upsilon_3(\omega_1^*+\upsilon_2)(d_v+\delta_2)}{\omega_1\omega_2\beta_2 N_E x_5^*}\upsilon_3\ .$$

We compute the values of coefficients a and b according to Castillo-Chavez and Song, (Castillo-Chavez & Song, 2004), and it is shown that at the disease-free equilibrium, the second-order non-zero partial derivatives associated with model (4) are as follows:

$$\frac{\partial^2 f_1}{\partial x_1\partial x_7} = -\beta_1, \frac{\partial^2 f_2}{\partial x_1\partial x_7} = \beta_1, \frac{\partial^2 f_5}{\partial x_4\partial x_5} = -\beta_2, \frac{\partial^2 f_6}{\partial x_4\partial x_5} = \beta_2, \frac{\partial^2 f_3}{\partial x_3\partial\omega_1^*} = -1, \frac{\partial^2 f_4}{\partial x_3\partial\omega_1^*} = N_E$$

The computation results in

$$a = \frac{\upsilon_3\delta_1\beta_1^2(d_v+\delta_2)(\omega_1^*+\upsilon_2)x_1^*}{\omega_1\omega_2\beta_2 N_E(\upsilon_1+\delta_1)x_1^*}u_7 > 0 \tag{7}$$

$$b = \frac{\beta_1\rho\theta_h\left(N_E^2\omega_1^* - 1\right)x_1^*}{(\upsilon_1+\delta_1)(\omega_1^*+\upsilon_2)}u_7\ \upsilon_3 \tag{8}$$

These results in equations (7) and (8) indicate the existence of an endemic equilibrium point that is locally asymptotically stable ($a > 0, b > 0$) when $N_E^2\omega_1^* > 1$. Conversely, the equilibrium is unstable when $N_E^2\omega_1^* < 1$. The proof of Theorem 3.3 is thus completed

2.3. Model datasets and model applicability

To evaluate the suitability and applicability of the model, demographic and climatological data were collected from three East African countries: Uganda, Kenya, and Tanzania (Home, 2023). These countries, located in the tropical region, are recognized for their endemicity of schistosomiasis and display a wide range of climatic conditions and parameters that have a substantial impact on disease transmission. The population data for the three countries were obtained from the most recent UN demographic estimates (https://worldpopulationreview.com/countries) and World Bank statistics (https://data.worldbank.org/indicator/sp.dyn.le00.in?). These data sources provided valuable information for estimating certain non-temperature and non-rainfall parameters in the model. For example, Uganda has a population of about 47,264,873 people with a life expectancy of 58.5 years. Consequently, in a disease-free steady state, the susceptible population is represented by $S_h' = \frac{\Lambda_1 e^{-\upsilon_1 x}}{\upsilon_1} = 47,264,873$, where $\upsilon_1 = 1/((58.5 \times 365)\,) = 0.0000468$ per day, resulting in a daily recruitment rate of $\Lambda_1 = 2212$ individuals. Similarly, Kenya has a population of 54,039,625 with a life expectancy of 64 years, yielding $\upsilon_1 = 1/((64 \times 365)\,) = 0.0000428$ and $\Lambda_1 = 2,313$ new infections per day. Tanzania, with a population of 65,519,777 and a life expectancy of 62.6 years, has $\upsilon_1 = 1/((62.6 \times 365)\,) = 0.0000444$ and $\Lambda_1 = 2,909$ new infections per day. The other non-temperature and non-rainfall parameters x, δ_1, and υ_2 of the model are derived from the literature. For instance, we assume that schistosomiasis typically first infects a child at the age of two (2), corresponding to $x = 2 \times 365 = 730$ days. The lifespan of an adult *Schistosoma* worm in a human host varies from 3 to 10.5 years according to Fulford et al. (Fulford et al., 1995) and Colley et al. (Colley et al., 2014), resulting in a range of δ_1 values from $1/(10.5 \times 365) \approx 0.000268$ to $1/\,(3 \times 365) \approx 0.000913$ per day. Additionally, the *Schistosoma* parasite egg remains viable for up to 7 days, hence $\upsilon_2 = 1/7 = 0.14286$ represents the per capita death rate of the parasite eggs (Gryseels et al., 2006; Michaels & Prata, 1968).

Furthermore, we determined temperature-dependent parameters using data from field and laboratory studies by Mangal et al. (Mangal et al., 2008) (SI Table S1) and Kalinda et al. (Kalinda et al., 2017a) (SI Table S2). These studies have demonstrated that the activity of both snails and *Schistosoma* parasites is optimized within the temperature range of 20–35 °C. We fitted temperature regression curves up to five degrees to these data and selected the results with the highest adjusted R-squared value, R-Sq (adj), along with the corresponding equations. Additionally, we developed functions for temperature- and precipitation-dependent parameters that influence snail recruitment, following methodologies described in (Okuneye & Gumel, 2017; Parham & Michael, 2010). These equations were applied to fit the climate data of the three countries. For parameters not commonly reported, we made informed assumptions based on expertise and general knowledge of vector and disease dynamics. The remaining parameters were obtained from the literature (Table 1).

Seasonal climate data for each country were obtained from the most recent World Bank Climatology (Home, 2023, Table 2). The current temperature range and rainfall variation were 21–33 °C and 5–166 mm, respectively, based on the current climate data presented in Table 2. However, it is projected that by 2050, East Africa will experience a temperature increase of approximately 2 °C (Home, 2023) due to global warming, and monthly rainfall will vary between 180 and 188 mm (Home, 2023; Ngoma et al., 2021; Najjuma et al., 2021). Based on these projections, we extrapolated rainfall ranges from 4 to 200 mm and a temperature range of 27–35 °C to represent adverse conditions for schistosomiasis transmission in future scenarios. We divided these ranges into intervals to account for future climate variability in different regions. By using the partial rank correlation coefficient (PRCC) test, we identified critical parameters that are most sensitive to disease transmission. This allowed us to analyze the relationship between climate change variables such as temperature and precipitation and the transmission of schistosomiasis, enabling us to simulate infections under hypothetical future conditions.

The numerical analyses and simulations to determine and estimate parameters and expressions for temperature and precipitation-dependent are carried out in the R statistical environment version 4.0.3 (Team, 2018), using the primary R package ODE solver Version 1.10–4 for solving ordinary differential equations (Soetaert et al., 2010). The model parameters in

Table 1
Temperature in-variant parameters, their definitions, values per day, and sources. If a parameter is computed using the references listed in the parameter estimation section, it is referenced as “Estimated”; otherwise, it is “Assumed” based on knowledge and expertise).

Symbol	Definition	Baseline value	Values/day	References
Λ_1	Human reproduction rate	2561	2213–2909	Estimated
τ	Age at first infection in a child	730	730	Estimated
δ_1	Human mortality due to infection	0.000591	0.000268-0.000913	Estimated
υ_1	Human mortality rate	0.0000448	0.0000428–0.0000468	Estimated
ρ	Portion of stool per person	115	70–160 g	Liang et al. (2005)
θ_h	Number of eggs per gram of stool	262	10-513 g^{-1}	Liang et al. (2005)
ω_1	Miracidia shedding rate	0.00232	0.00232	Estimated
υ_2	Parasite egg mortality rate	0.14286	0.14286	Estimated
υ_4	Cercaria mortality rate	1	1	Mangal et al. (2008)
N_E	Number of miracidia per parasite egg	500	500	Mangal et al. (2008)
P_E	Maximum survival probability of egg	0.8	0.8	Assumed
P_j	Maximum survival probability of juvenile	0.9	0.9	Assumed
R_m	Rainfall threshold	250	250 mm	Assumed

Table 2
The monthly mean, maximum (max.) temperatures (°C) and rainfall (mm) for Uganda (UG), Kenya (KY) and Tanzania (TZ) from World Bank Climatology Report (Home, 2023).

Countries		Jan	Feb	Mar	Apr	May	Jun	Jul	Aug	Sept	Oct	Nov	Dec
UG	Mean	23.93	24.49	24.45	23.81	23.21	22.71	22.34	22.66	22.91	23.14	23.32	23.16
	Max.	31.09	31.61	30.99	29.62	28.79	28.46	28.09	28.47	28.98	29.32	29.64	29.81
	Rainfall	50.67	48.82	108.5	157.97	148.23	91.83	91.47	119.33	121.33	154.59	116.02	73.55
KY	mean	25.5	26.28	26.74	26.11	25.05	24.06	23.44	23.83	24.59	25.37	25.08	25.03
	Max.	32.23	33.22	33.25	31.71	30.43	29.59	28.94	29.4	30.75	31.36	30.73	31.18
	Rainfall	31.78	25.36	63.53	134.19	92.52	35.61	31.81	35.06	28.09	77.44	110.48	60.20
TZ	mean	23.59	23.7	23.68	23.02	22.28	21.09	20.58	21.64	22.94	24.02	24.07	23.69
	Max.	28.68	29.02	28.92	28.01	27.61	27.08	26.89	28.01	29.38	30.24	29.75	28.8
	Rainfall	154.76	140.2	165.76	140.61	56.29	10.97	4.99	7.29	15.18	32.55	84.85	144.4

Table 1, the equations for climatic changes in temperature and precipitation from the fitted curves, and climatology data in Table 2 are used and the results are presented in Section 4 below.

3. Results and numerical simulations

3.1. Impact of temperature and/or rainfall on specific parameters and R_0

The fitted curves derived from Table S1 (Mangal et al., 2008) and Table S2 (Kalinda et al., 2017a) establish the relationship between temperature and/or rainfall with each specific parameter, while the expression in equation (2) represents the relationship between R_0 and the individual parameter. By combining these relationships, we can evaluate the impact of temperature changes on the value of R_0 for specific parameters. First, it is evident from R_0 expression in equation (2) that increasing values of $\beta_1(\mathrm{T})$, $\omega_2(\mathrm{T})$, $\beta_2(\mathrm{T})$, and $\Lambda_2(T,R)$ leads to an increase in R_0, while increasing values of $d_v(T)$, $\delta_2(\mathrm{T})$, and $\upsilon_3(\mathrm{T})$ result in a decrease in R_0. Second, we can directly observe the impact of temperature on the transmission dynamics represented by R_0. For instance, the fitted curve for the human infection rate $\beta_1(\mathrm{T})$ is given as

$$\beta_1(\mathrm{T}) = 6.300 \times 10^{-3} T - 0.0980, \tag{9}$$

where, $d\beta_1(T)/dT > 0$, indicating that human cercaria infection increases linearly with temperature. Consequently, $\frac{dR_0}{dT} = \frac{dR_0}{d\beta_1}.\frac{d\beta_1}{dT} > 0$, implying that the transmission rate of schistosomiasis will increase with increasing temperature. Moreover, the fitted curve for shedding of cercariae $\omega_2(T)$ is give as

$$\omega_2(\mathrm{T}) = 394.9\, T - 5584.1, \tag{10}$$

and $d\omega_2(\mathrm{T})/dT > 0$. As a result, cercaria is shed more often in places with increasing temperature ranges of 20–35 °C. Consequently, $\frac{dR_0}{dT} = \frac{dR_0}{d\omega_2}.\frac{d\omega_2}{dT} > 0$, which shows that R_0 increases with increasing temperature. The fitted curve for the snail infection rate, $\beta_2(\mathrm{T})$, is given by:

$$\beta_2(\mathrm{T}) = -9.830 \times 10^{-6} T^2 + 6.148 \times 10^{-4} T - 0.008257, \tag{11}$$

This curve describes a nonlinear relationship between $\beta_2(\mathrm{T})$ and temperature. The maximum snail infection rate, according to this curve, is $\beta_2(T) = 0.00136$, which occurs at a temperature of $T = 31.3^{o}C$. Consequently, snail infections increase and decrease in locations with climatic fluctuations between 20.0 to 31.3 °C and 31.3–35.0 °C, respectively. Therefore, $\frac{dR_0}{dT} = \frac{dR_0}{d\beta_2}.\frac{d\beta_2}{dT}$ shows that the transmission is increasing between 20.0 and 31.3 °C and decreasing between 31.3 and 35.0 °C. Furthermore, the fitted curve for the snail mortality rate, $d_v(T)$, is defined as follows:

$$d_v(T) = 1.120 \times 10^{-4} T^2 - 5.208 \times 10^{-3} T + 0.06332 \tag{12}$$

The result of $dd_v(T)/dT$ shows a minimum at 23.3 °C, indicating that for temperatures between 23.3 and 35 °C, $d_v(T)$ increases. On the other hand, for temperatures between 20 and 23.3 °C, $d_v(T)$ decreases. Therefore, it follows from the formula $\frac{dR_0}{dT} = \frac{dR_0}{dd_v}.\frac{dd_v}{dT}$ that the transmission decreases for temperatures between 23.3 and 35.0 °C and increases between 20.0 and 23.3 °C.

In addition, the fitted curve for snail infection mortality rate is expressed as:

$$\delta_2(\mathrm{T}) = 8 \times 10^{-5} T^2 - 1.22 \times 10^{-3} T - 0.00545 \tag{13}$$

From equation (13), it can be observed that $d\delta_2(T)/dT > 0$. Therefore, δ_2(T) increases with increasing temperature. Consequently, the transmission indicator R_0 also increases with temperature in the range of 20 to 35 °C, as indicated by $\frac{dR_0}{dT} = \frac{dR_0}{d\delta_2}.\frac{d\delta_2}{dT} > 0$. On the other hand, the fitted curve for miracidia mortality rate, υ_3(T), is mathematically represented as:

$$\upsilon_3(\mathrm{T}) = 0.18340\mathrm{T} - 1.71, \tag{14}$$

Similarly, it can be observed that $d\upsilon_3(T)/dT > 0$. Consequently, in areas where temperatures fluctuate between 20 and 35 °C, the infection of snails with miracidia increase and according to the expression $\frac{dR_0}{dT} = \frac{dR_0}{d\upsilon_3}.\frac{d\upsilon_3}{dT}$, the prevalence of the disease (R_0) also rises within the same temperature range.

Moreover, the revised formulation for the snail recruitment rate, $\Lambda_2(T,R)$, assumes that snails can withstand variations in temperature and precipitation throughout their life stages, starting from the egg stage to the juvenile and adult stages. It is mathematically represented as:

$$\Lambda_2(T,R) = \frac{E_v(T)}{d_v(T)}.P_E(R).P_J(T,R).\frac{1}{t_S(T)}, \tag{15}$$

In equation (15), $E_v(T)$ represents the number of snail eggs per snail per day, $1/d_v(T)$ denotes the average lifespan of adult snails, $P_E(T)$ and $P_J(T,R)$ represent the daily survival probabilities of eggs and juvenile snails respectively, and $t_S(T)$ represents the total time required for a snail to develop from an egg to an adult. It is evident from equation (15) that $\Lambda_2(T,R)$, increases with higher values of $E_v(T)$, $P_E(R)$, and $P_J(T,R)$, while increasing values of $d_v(T)$, and $t_S(T)$ result in a decrease in $\Lambda_2(T,R)$. The impact of temperature and/or rainfall on a specific parameter and snail recruitment rate in equation (15) can be summarized as follows:

The relationship between the number of snail eggs $E_v(T)$, and temperature T, as determined from the equation that best fits the data in Table S2, can be expressed as

$$E_v(T) = -0.09601T^2 + 5.10696T - 52.52573 \tag{16}$$

By analyzing $dE_v(T)/dT$, it can be observed that $E_v(T)$ increases until it reaches a peak at approximately 27 °C, after which it starts to decrease. Consequently, based on the formula $\frac{d\Lambda_2(T,R)}{d_T} = \frac{d\Lambda_2(T,R)}{dE_v(T)}.\frac{dE_v(T)}{dT}$, the snail recruitment rate $\Lambda_2(T,R)$ increases within the temperature range of 20 to 27 °C and decreases within the range of 27 to 35 °C.

Additionally, it is important to note that the survival rates of eggs and juvenile snails are influenced independently by both rainfall and temperature (Parham & Michael, 2010). Therefore, we can express $P_J(T,R)$ as the product of temperature-dependent daily juvenile snail survival probability, $P_J(T)$, and rainfall-dependent survival probability, $P_J(R)$. Specifically, $P_J(T)$ is defined as $P_J(T) = e^{-\upsilon_J(T)}$, where $\upsilon_J(T)$ represents the temperature-dependent natural mortality rate of juvenile snails, obtained from a line that best fits the data (SI Table S2). Thus, $P_J(T)$ can be represented as an exponential function:

$$P_J(T) = e^{-\left(8.750\times10^{-5}T^2 - 3.762\times10^{-3}T + 0.04178\right)} \tag{17}$$

In equation (17), it can be observed that $dP_J(T)/dT$ indicates that $P_J(T)$ initially decreases to a minimum around T = 22 °C and then increases with higher temperatures. Consequently, changes in $\Lambda_2(T,R)$ will follow the same trend. In contrast, $P_i(R)$ describes the probability of survival for eggs or juvenile snails on a daily basis and in comparison to Parham and Michael, (Parham & Michael, 2010), we can express $P_i(R)$ as

$$P_i(R) = \left(4P_{Mi} \Big/ R_L^2\right)R(R_L - R), i = \{E,J\}, \tag{18}$$

Here, P_{Mi} represents the maximum daily survival probability of the egg and juvenile stages, R_L represents the maximum rainfall in the region of interest, and $R_L > R(t) > 0$. When we set $P_{Mi} = 0.8$ and $R_L = 200$ mm, it can be observed that $dP_i(R)/\,dR$ indicates that $P_i(R)$ is maximum when the total amount of rainfall received is approximately 125 mm. Therefore, $\Lambda_2(T,R)$ increases with an increase in rainfall up to 125 mm, but decreases with further increases in rainfall. Additionally, the temperature-dependent egg hatching rate $\alpha_J(T)$ represents the transition from the egg stage to the juvenile stage, while the juvenile maturation rate $\theta_J(T)$ signifies the transition from the juvenile stage to the adult stage. The regression lines that best fit the temperature data in SI Table S2 for these rates are represented by equation (19):

$$\left.\begin{aligned}\alpha_J(T) &= -0.0031084T^2 + 0.1775496T - 2.3562789\\ \theta_J(T) &= -0.0006839T^2 + 0.0385458T - 0.4990643\end{aligned}\right\} \tag{19}$$

Clearly, $1/\alpha_J(T)$ and $1/\theta_J(T)$ represents the lengths of time required for an egg to survive before hatching and for a juvenile snail to mature, respectively. As a result, the total time $t_S(T)$ needed for a snail cycle to develop from an egg to an adult snail can be calculated as $t_S(T) = [\alpha_J(T) + \theta_J(T)]/\alpha_J(T).\theta_J(T)$.

The snail recruitment rate $\Lambda_2(T,R)$ in equation (20) is derived by substituting equations (16)–(19) into equation (15).

$$\Lambda_2(T,R) = \frac{\left(-0.0031084T^2 + 0.1775496T - 2.3562789\right) \times \left(-0.0006839T^2 + 0.0385458T - 0.4990643\right)}{\left(-0.0031084T^2 + 0.1775496T - 2.3562789\right) + \left(-0.0006839T^2 + 0.0385458T - 0.4990643\right)}$$
$$\times \frac{-0.09601T^2 + 5.10696T - 59.52573}{1.120 \times 10^{-4}T^2 - 5.208 \times 10^{-3}T + 0.06332}$$
$$\times \left(4P_{ME} \Big/ R_L^2\right) R(R_L - R)$$
$$\times \left(4P_{MJ} \Big/ R_L^2\right) R(R_L - R)$$
$$\times e^{-\left(8.750 \times 10^{-5}T^2 - 3.762 \times 10^{-3}T - 0.043178\right)} \tag{20}$$

Consequently, equation (20) for $\Lambda_2(T,R)$ establishes a direct relationship between temperature, rainfall, and the transmission indicator R_0. The rate of change of R_0 with respect to temperature can be determined by $\frac{dR_0}{dT} = \frac{d\Lambda_2(T,R)}{dT}.\frac{dR_0}{d\Lambda_2(T,R)}$, while the rate of change of R_0 with respect to rainfall can be assessed using $\frac{dR_0}{dR} = \frac{d\Lambda_2(T,R)}{dR}.\frac{dR_0}{d\Lambda_2(T,R)}$. When $\frac{dR_0}{dT} < 0$, an increase in temperature leads to a decrease in R_0, particularly in areas affected by global warming. However, when $\frac{dR_0}{dT} > 0$, rising temperature results in both an increase in R_0 and the prevalence of the disease. Similarly, if $\frac{dR_0}{dR} < 0$, increased precipitation leads to a decrease in R_0, whereas if $\frac{dR_0}{dR} > 0$, higher precipitation leads to an increase in R_0 and disease prevalence.

The overall impact of temperature and/or rainfall on R_0 can be assessed by examining the combined effects of these factors. The following equations mathematically connect R_0 to temperature (T) and precipitation (R)

$$\frac{dR_0}{dT,R} = \frac{d\beta_1(T)}{dT}.\frac{dR_0}{d\beta_1(T)} + \frac{d\Lambda_2(T,R)}{dT}.\frac{dR_0}{d\Lambda_2(T,R)} + \frac{d\beta_2(T)}{dT}.\frac{dR_0}{d\beta_2(T)} + \frac{dd_v(T)}{dT}.\frac{dR_0}{dd_v(T)} + \frac{d\delta_2(T)}{dT}.\frac{dR_0}{d\delta_2(T)}$$

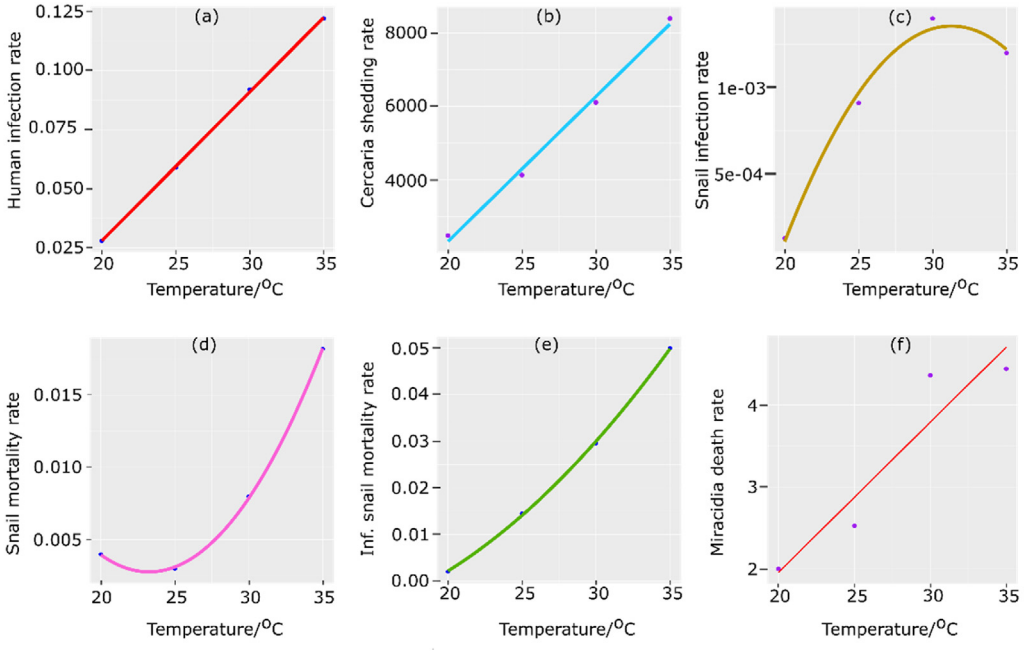

Fig. 2. Fitted models of temperature variant parameters; (a) human infection rate $\beta_1(T)$, (b) cercaria shedding rate $\omega_2(T)$, (c) snail infection rate $\beta_2(T)$, (d) snail mortality rate $d_v(T)$, (e) infected snail mortality rate $\delta_2(T)$, (f) miracidia death rate, $\upsilon_3(T)$ against temperature.

$$+\frac{d\upsilon_3(T)}{dT}\cdot\frac{dR_0}{d\upsilon_3(T)}+\frac{d\omega_2(T)}{dT}\cdot\frac{dR_0}{d\omega_2(T)}+\frac{d\Lambda_2(T,R)}{dR}\cdot\frac{dR_0}{d\Lambda_2(T,R)}$$

Furthermore, when both temperature and precipitation increase simultaneously, the combined effects on R_0 are determined by the value of $\frac{d^2R_0}{dTdR}<0$. If $\frac{d^2R_0}{dTdR}>0$, R_0 increases as both temperature and precipitation rise. A higher value of R_0 indicates greater challenges in controlling the spread of schistosomiasis, while a lower value of R_0 makes it easier to combat the disease.

3.2. Numerical simulations

In this section, numerical simulations of the model system (1) are conducted to provide support, validation, and verification of the findings presented in the numerical analysis. Specifically, Fig. 2 illustrates the influence of temperature on specific parameters within the transmission dynamics of schistosomiasis.

Fig. 3 presents the impact of temperature and rainfall on specific parameters, which in turn affect the rate of snail recruitment and subsequent changes in disease transmission. Notably, the figure highlights that an increase in rainfall, up to a threshold of approximately 140 mm, is associated with an elevated probability of survival for both snail eggs and juveniles (Fig. 3e and f). This observation underscores the importance of rainfall in influencing the reproductive success and population dynamics of snails, thereby influencing the overall transmission of the disease.

The findings indicate that mean monthly temperatures of 22–27 °C (Table 2) are typical across the three countries. These temperatures are associated with high rates of schistosomiasis activity of different host snail traits and schistosomes (Fig. 4A–C; see also SI Figures S1, S3, S5), making them ideal conditions for the development of schistosomiasis and leading to high reproduction numbers (Fig. 4D). In addition, the human infection rate (Fig. 4A), snail infection rate (Fig. 4B), and snail recruitment rate (Fig. 4C) all peak around the same time of the year across the three countries. This typically happens during February and April and between the months of October and November, respectively, when the temperatures range between 23.7 and 26.7 °C. Infection levels in the area are at their lowest in July. The region also experiences monthly maximum temperatures ranging from 27 to 33 °C (Table 2), which severely restricts the activity of various host snail traits and schistosomes (see SI Figures S2, S4, and S6). As a result, there are generally fewer new cases of schistosomiasis overall in the region during this season (Fig. 4E).

The three nations have different annual rainfall patterns (Fig. 4F). Schistosomiasis cases increase in Uganda from March to May until the second rainy season, which lasts through the warm months of June and July and the rainy months of August to November. During this period, the endemic level of the disease remains almost unchanged until November, the beginning of the dry season, when numbers tend to decrease. During the dry months from April to July in Tanzania and April to September in Kenya, schistosomiasis cases decline. In Tanzania, cases begin to rise from August and peak in December and from January

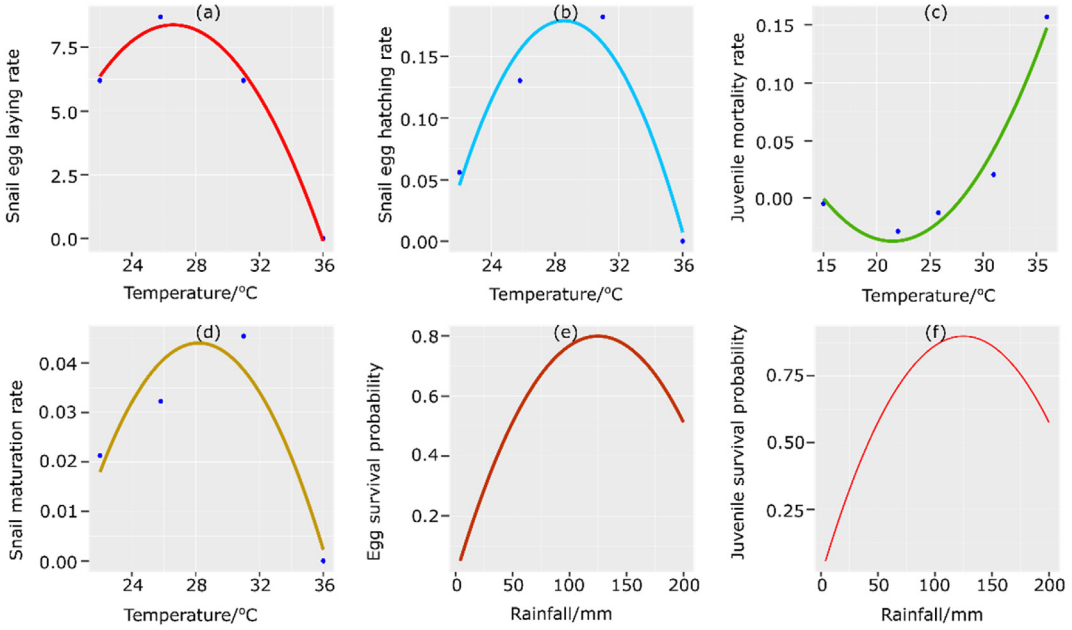

Fig. 3. Fitted model of temperature -and rainfall-dependent parameter simulations for (a) snail egg laying rate, $E_v(T)$, (b) snail egg hatching rate $\alpha_J(T)$, (c) juvenile mortality rate $\upsilon_j(T)$ (d) juvenile maturation rate $\theta_J(T)$, (f) egg survival probability $P_E(R)$, and (g) juvenile survival probability $P_j(R)$.

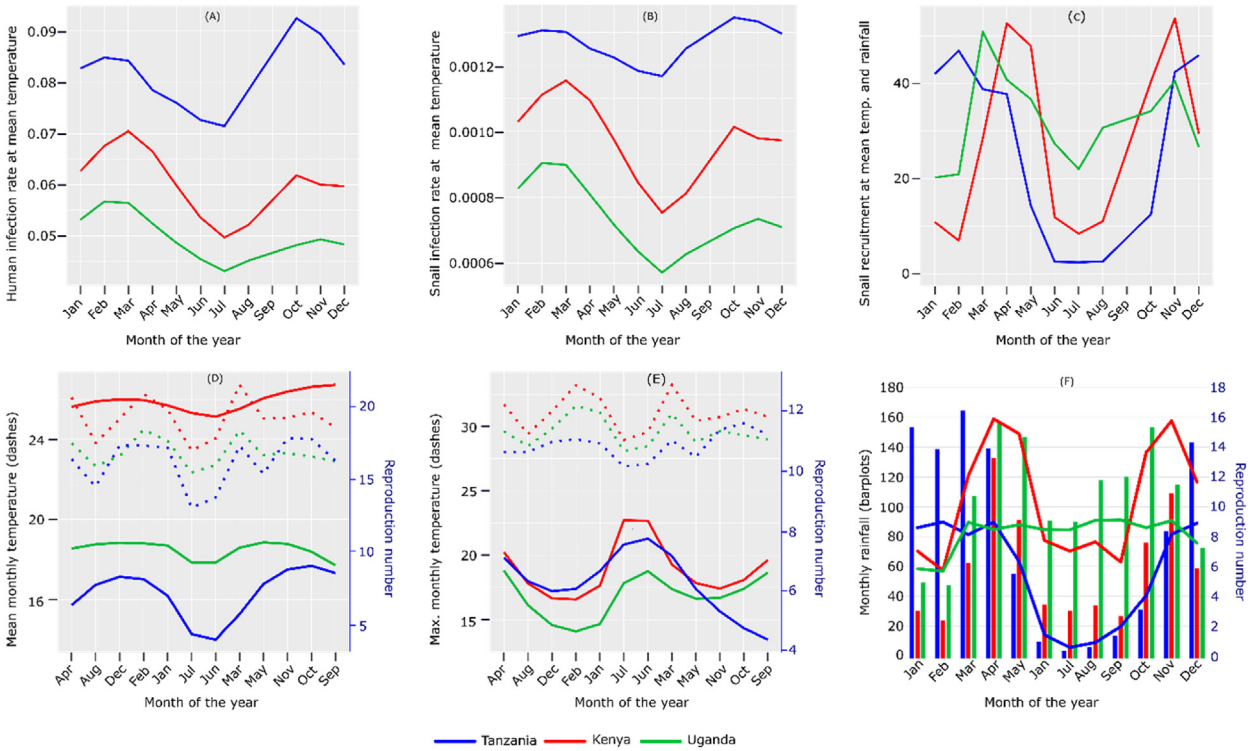

Fig. 4. Individual seasonal effects of temperature and/or rainfall on (A) human infection rate, (B) snail infection rate, (C) snail recruitment rate, and (D), (E), and (F) reproduction numbers in Tanzania (blue), Kenya (red), and Uganda (green). For other temperature- and/or precipitation-dependent parameters, see SI Figures S1–S6.

to April before they begin to decline. In Kenya, they rise from September to November and from February to April. In addition, the reproduction numbers in Kenya are so much higher (4D) and (4F) as compared to Tanzania and Uganda is associated with high rates of juvenile maturation (which enhance snail recruitment; Fig. 4C), cercaria shedding, snail egg laying and hatching rate (see SI Figures S1, S3, S5).

The schistosomiasis infection patterns are somewhat similar when temperature and rainfall are modelled together, with lowest values in July and August (Fig. 5A). However, patterns of peaks are different with two peaks for Tanzania and Kenya with rather similar phases in April (maximum) and a second maximum later in the year. A different annual pattern for Uganda with only one peak and a phase shift of the maximum towards an earlier seasonal peak through December, January till February. Surprising is the shear drop in Kenya from December to January. Fig. 5B depicts patterns that are quite similar to those in Fig. 5A for Kenya and Uganda, but behaviors in Tanzania changes after one season of infection, however, with similarly low case numbers through June, July and August as in Fig. 5A.

Schistosomiasis is a challenge across Tanzania, Kenya and Uganda, especially in March and April. For individual countries, the three months with the highest rates of infections are April, May, and December in Kenya; February, March, and December in Uganda; and April, and November in Tanzania (Fig. 5). During these months, the mean and maximum temperatures, and precipitation values in the three countries increase from 20.6 to 26.1 °C, 26.9–31.7 °C and from 5 to 165 mm, respectively. In contrast, there are relatively few cases in the three countries in June and July with mean, and maximum temperatures, and precipitation from 21.1 to 24.1 °C, 26.9–29.4 °C, and from 5.0 to 91.8 mm, respectively. For example, in Uganda, the infection numbers drop down to almost zero in Jul to Aug, while reproduction rates in Tanzania and Kenya are still around 6 to 7 during this time of the year (Fig. 5A). The maximum values in Kenya are around 50% higher in the peak season compared to Uganda and Tanzania (Fig. 5A). A comparison of precipitation with mean monthly temperatures (Fig. 5A) and maximum monthly temperatures (Fig. 5B) reveals that for Uganda, Tanzania, and Kenya, respectively, the peaks are approximately 9, 11, and 15 infections per day and 6, 7, 13 infections per day, respectively.

3.3. Expected future changes in temperature and precipitation

Tables 3 and 4 outline the temperature-and precipitation-related parameter variations across different future climate scenarios. Emphasis is placed on scenarios with severe temperatures that negatively impact schistosomiasis activity. Simulation results of crucial parameters for the persistence of schistosomiasis are presented in Table 5.

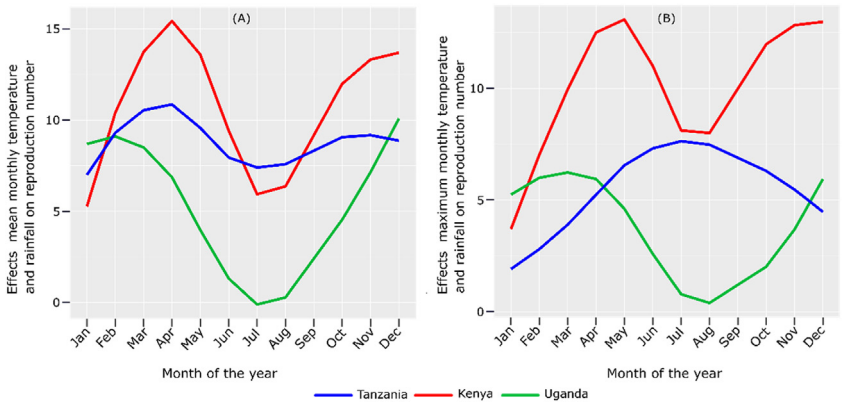

Fig. 5. Simultaneous effects of precipitation and mean temperature (A) as well as maximum temperatures (B) on reproduction numbers in Uganda (green), Kenya (red), and Tanzania (blue).

In the temperature range of [27, 35]°C, the findings indicate a decrease in parasite eggs, egg hatching rates, juvenile maturation rates, and snail recruitment rates with increasing temperatures (Table 3).

The findings demonstrate that temperatures ranging from 27 to 33 °C, combined with precipitation levels of 4–150 mm, create favorable conditions for snail recruitment. However, beyond 150 mm of rainfall, snail recruitment declines (Table 4).

The results of the PRCC test indicate that certain factors, such as the proportion of stools from infected individuals (ρ), the number of parasite eggs per gram per day (θ_h), the miracidia shedding rate per parasite egg (ω_1), and the snail recruitment rate $\Lambda_2(T,R)$, will continue to significantly influence disease transmission in the context of climate changes until 2050 (Table 5). An increase in these parameters leads to an elevated transmission of schistosomiasis. Among these factors, $\Lambda_2(T,R)$ is the only parameter that depends on both temperature and precipitation and is the most sensitive to changes. For instance, temperature ranges between 31 and 35 °C and rainfall levels between 100 and 200 mm, as well as seasons characterized by 4–50 mm of rainfall and temperatures of 27–29 °C, demonstrate that snail recruitment has a substantial impact on the reproduction number. The findings indicate that temperatures between 27 and 33 °C that occur along with precipitations of 4–150 mm are suitable for snail recruitment. Beyond 150 mm rainfall, snail recruitment declines (Table 4).

4. Discussion

Mechanistic models provide valuable insights into the incidence and burden of infectious diseases such as schistosomiasis. They enable tracking of short-term and long term effects on disease transmission and are particularly valuable for climate change assessment and projections. The mechanistic approach used in this study quantifies or understanding of relevant processes, enhancing confidence in extrapolating to various future conditions. Our model incorporates essential

Table 3
Model sensitivity of temperature- and precipitation-dependent parameter values. The full temperature range $[27,35]$°C is subdivided into intervals of 2 °C and the precipitation value is fixed at 100 mm when estimating the effect of temperature alone on snail recruitment rate $\Lambda_2(T,R)$, a temperature-and precipitation dependent parameter. Values are given a ranges and baseline values (*). Other parameter descriptions are given in SI Tables S1 and S2.

Temperature	β_1(T)	β_1^*	β_2(T)	β_2^*	d_v (T)	d_v^*	δ_2(T)	δ_2^*	ω_2(T)	ω_2^*	$\Lambda_2(T)_{100mm}$	$\Lambda_2^*(T)$
27-29 °C	0.0721	0.0784	0.001177	0.00124	0.0044	0.0055	0.0199	0.0232	5078	5473	43.7989	35.8646
	−0.0847		−0.001305		−0.0065		−0.0265		−5868		−27.9302	
29-31 °C	0.0847	0.091	0.001305	0.00133	0.0065	0.0080	0.0265	0.0301	5868	6263	27.9302	20.992
	−0.0973		−0.001355		−0.0095		−0.0336		−6658		−14.0545	
31-33 °C	0.0973	0.1036	0.001355	0.00134	0.0095	0.0115	0.0336	0.0375	6658	7053	14.0545	9.4959
	−0.1099		−0.001327		−0.0134		−0.0414		−7448		−4.9372	
33-35 °C	0.1099	0.1162	0.001327	0.00127	0.0134	0.0158	0.0414	0.0457	7448	7843	4.9372−0.5657	2.7515
	−0.1225		−00.001177		−0.0182		−0.0499		−8237			

Temperature	b_v (T)	b_v^*	$E_v(T)$	E_v^*	$\alpha_J(T)$	α_j^*	$\upsilon_j(T)$	υ_j^*	$\theta_J(T)$	θ_j^*	$u_3(T)$	u_3^*
27-29 °C	3.2418	3.4252	8.3709	8.1013	0.1715	0.1750	0.0039	0.0051	0.0432	0.0434	3.2418	3.4252
	−3.6086		−7.8317		−0.1785		−0.0062		−0.0436		−3.6086	
29-31 °C	3.6086	3.792	7.8317	7.1781	0.1785	0.1723	0.0062	0.0077	0.0436	0.0411	3.6086	3.7920
	−3.9754		−6.5244		−0.1606		−0.0092		−0.0386		−3.9754	
31-33 °C	3.9754	4.1588	6.5244	3.9867	0.1606	0.1392	0.0092	0.0110	0.0386	0.0334	3.9754	4.1588
	−4.3422		−4.4491		−0.1178		−0.0128		−0.0282		−4.3422	
33-35 °C	4.3422−4.709	4.5256	4.4491	3.02735	0.1178	0.1680	0.0128	0.0150	0.0282	0.0203	4.3422	4.5256
			−1.6056		−0.0502		−0.0172		−0.0123		−4.7090	

Table 4
Effects of precipitation at constant temperatures in the range of 27–35 °C on the snail recruitment rate. To account for variations between regions, precipitation of 4–200 mm is split into intervals of 50 mm.

T/°C	R/mm	$\Lambda_2(T,R)$	$\Lambda_2^*(T,R)$	T/°C	R/mm	$\Lambda_2(T,R)$	$\Lambda_2^*(T,R)$
	4–50	0.1885–12.4134	6.3009		4–50	0.0605–2.1943	1.1274
27-29 °C	50–100	19.4662–27.9302	23.6982	31-33 °C	50–100	6.2465–4.9372	5.5919
	100–150	43.7989–27.9302	21.8995		100–150	14.0545–4.9372	9.4959
	150–200	43.7989–12.4134	28.1062		150–200	14.0545–2.1943	8.1244
	4–50	0.1202–6.2465	3.1834		4–50	0.0212–0.2514	0.13630
29-31 °C	50–100	12.4134–14.0545	13.2339	33-35 °C	50–100	2.1943–0.5657	1.3800
	100–150	27.9302–14.0545	20.9924		100–150	4.9372–0.5657	2.751
	150–200	27.9302–6.2465	17.0884		150–200	4.9372–0.2514	2.5943

epidemiological and climate-dependent stages for intermediate hosts and *Schistosoma* parasites. Firstly, our model reveals that when the reproduction number is less than or equal to unity, a disease-free equilibrium is achieved, which is both locally and globally asymptotically stable. Conversely, when the reproduction number exceeds unity, a unique endemic equilibrium arises, which is locally asymptotically stable. Secondly, incorporating both temperature and precipitation into the model yields a better understanding of schistosomiasis transmission patterns compared to modeling them separately for the reproduction number of a given month. This demonstrates that the combined influence of temperature and precipitation provides a more comprehensive explanation of schistosomiasis transmission dynamics. The following discussions will present both the individual and combined effects of temperature and precipitation.

4.1. Effect of temperature

The study demonstrates that the transmission potential of schistosomiasis is highly sensitive to changes in the mean and maximum temperature within the region, leading to variations in the number of cases across seasons and months. This aligns with the well-established understanding that schistosomiasis, being a vector-borne disease, is greatly influenced by climatic fluctuations (Martens et al., 1995). Schistosomiasis infections exhibit changes in accordance with temperature variations within the mean monthly temperature range of 22–27 °C. Within this temperature range, there is an increase in human infection, snail infection rate, snail egg-laying rate, egg hatching, and snail maturation with rising temperatures. These findings are consistent with previous model-based studies by Ngarakana-Gwasira et al. (Ngarakana-Gwasira et al., 2016), which propose an optimal temperature range of 18–28 °C for schistosomiasis transmission. Additionally, Malone (Malone, 2005) reports a temperature range of 20–27 °C as ideal for the intramolluscan development of S. mansoni within Biomphalaria spp. snails. Moreover, Marti (Marti, 1986) and Manyangadze et al. (Manyangadze et al., 2016) observe an increase in the snail population with a slight temperature rise above 25 °C. Conversely, there are fewer cases of schistosomiasis in months with increasing mean monthly temperatures above 27 °C, corresponding to a decline in schistosomiasis activity. Similarly, monthly maximum temperatures between 27 and 33 °C are associated with reduced schistosomiasis cases, attributed to decreased survival of eggs and juveniles, lower rates of human and snail infection, and slower snail maturation. These findings align with the understanding that higher temperatures are linked to increased snail mortality, reduced fecundity, and hindered snail growth, resulting in a decline in schistosomiasis cases (McCreesh & Booth, 2013; Ngarakana-Gwasira et al., 2016; Kalinda et al., 2017b).

4.2. Effects of precipitation

The availability of suitable snail breeding sites, primarily in surface water such as ponds, is largely influenced by precipitation (Xue et al., 2011). Our findings suggest that moderate precipitation ranging from 5 to 150 mm may contribute to an increase in the number of schistosomiasis cases. This is associated with a higher snail recruitment rate, as snail eggs and juveniles have a greater chance of survival under such conditions. These results are consistent with previous studies that have shown a positive correlation between precipitation, the distribution of intermediate host snails, and the spread of schistosomiasis (Codjoe & Larbi, 2016; Stensgaard et al., 2016; Tabo et al., 2022; Xue et al., 2011). On the other hand, rainfall exceeding 150 mm has a suppressive effect on schistosomiasis transmission. This is attributed to a reduction in snail recruitment due to decreased survival of snail eggs and juveniles. This finding is supported by evidence demonstrating that decreased schistosomiasis cases result from increased streamflow velocities and associated habitat disturbance, which negatively impact the recruitment and survival of cercariae, miracidia, snail eggs, and juveniles (Adekiya et al., 2020; Xue et al., 2011). Furthermore, during the rainy season, there is a potential decrease in activities related to infested water, such as swimming, fishing, sports, and water collection for household use, due to flood-related risks. This could also contribute to a reduction in schistosomiasis transmission.

Table 5
PRCC values for the temperature and precipitation dependent parameters, with temperature values 27 – 35°C and precipitation in the range of [4, 200] mm and R_0 as a response function. The three most crucial factors affecting the dynamics of the model at such adverse temperatures are indicated in bold.

parameter	27-29 °C				29-31 °C				31-33 °C				33-35 °C			
	4 −50 mm	50 −100 mm	100 −150 mm	150 −200 mm	4 −50 mm	50 −100 mm	100 −150 mm		4 −50 mm	50 −100 mm	100 −150 mm	100 −200 mm	4 −50 mm	50 −100 mm	100 −150 mm	100 −200 mm
Λ_1	0.19062	0.18278	0.19587	0.16006	0.19081	0.19007	0.19826		0.19248	0.1939	0.20199	0.1988	0.1978	0.2033	0.1992	0.1963
τ	0.0321	0.02908	0.0297	0.03287	−0.0036	0.02412	0.01696		−0.6059	−0.6669	0.01209	0.0038	−0.001	0.00731	0.0005	0.5010
δ_1	−0.5544	−0.6483	−0.6455	−0.6139	−0.6010	−0.6602	−0.6578		−0.0035	0.0227	−0.6551	−0.632	−0.618	−0.646	0.6244	−0.6111
υ_1	−0.1351	−0.1493	−0.1491	−0.1437	−0.1469	−0.1501	−0.1518		−0.1469	−0.1528	−0.1532	−0.151	−0.148	−0.1511	−0.1485	−0.1469
ρ	**0.4875**	**0.5505**	**0.54872**	**0.52656**	**0.49145**	**0.5564**	**0.55024**		**0.4944**	**0.5599**	**0.5443**	**0.5208**	**0.5080**	**0.5359**	**0.51419**	−0.0029
θ_h	**0.75669**	**0.82174**	**0.8205**	**0.8007**	**0.7544**	**0.82665**	**0.81948**		**0.7586**	**0.8293**	**0.8133**	**0.7887**	**0.7736**	**0.8036**	**0.7805**	**0.7651**
ω_1	**0.9452**	**0.9632**	**0.9628**	**0.9577**	**0.9478**	**0.96467**	**0.9634**		**0.9491**	**0.9654**	**0.9622**	**0.9567**	**0.9528**	**0.9600**	**0.9545**	**0.9507**
υ_2	0.03214	0.0291	0.02970	0.03287	−0.0036	0.02412	0.0169		−0.0035	0.0227	0.01209	0.0038	−0.001	0.0073	0.0005	−0.0029
υ_4	0.03214	0.02908	0.02970	0.03287	−0.0036	0.02412	0.01696		−0.0034	0.0227	0.01209	0.0038	−0.001	0.0073	0.0005	−0.0029
N_E	0.03214	0.02908	0.02970	0.03287	−0.0036	0.02412	0.01696		−0.0034	0.0227	0.01209	0.0038	−0.001	0.0073	0.0005	−0.0029
$\beta_1(T)$	0.0871	0.11411	0.10389	0.09323	0.01239	0.1178	0.0926		−0.0143	0.0793	0.04083	0.0109	−0.009	0.0195	−0.0047	−0.0169
$\beta_2(T)$	0.08422	0.12706	0.12478	0.10512	0.16364	0.14316	0.15494		0.1113	0.0792	0.09726	0.1057	0.1753	0.1744	0.1754	0.1751
$d_v(T)$	−0.3147	−0.4065	−0.40306	−0.3686	−0.3772	−0.4256	−0.4275		0.3583	−0.4053	−0.4001	−0.381	−0.344	−0.3657	−0.3484	0.3373
$\delta_2(T)$	−0.1228	−0.1735	−0.17043	−0.14752	−0.2066	−0.1932	−0.2051		−0.1621	−0.1408	−0.1564	−0.161	0.147	−0.1431	−0.1466	−0.1479
$\omega_2(T)$	0.00799	0.06156	0.05783	0.03218	0.1578	0.07899	0.1065		0.1373	0.0587	0.09742	0.1212	0.1217	0.0992	0.1179	0.1265
$\upsilon_3(T)$	−0.0813	−0.0812	−0.0813	−0.0797	−0.0729	−0.0773	−0.0786		−0.0621	−0.0637	−0.0654	−0.064	−0.058	−0.0599	0.059	−0.0572
$\Lambda_2(T,R)$	**0.78953**	**0.2717**	**0.30385**	**0.63269**	**0.76732**	**0.07739**	**0.4321**		**0.7657**	**0.1584**	**0.5681**	**0.7031**	**0.7400**	**0.6382**	**0.7251**	**0.7554**

4.3. Effects of temperature and precipitation

Our study highlights the importance of suitable monthly temperature and precipitation conditions in maximizing the transmission of schistosomiasis. These findings support previous research indicating that temperature and precipitation play crucial roles in species richness (Hauffe et al., 2016), the distribution of intermediate host snails (Tabo et al., 2022), and the size of snail populations, ultimately influencing disease transmission patterns and spread (McCreesh & Booth, 2013; Stensgaard et al., 2016). We demonstrate that regions in Uganda, Tanzania, and Kenya are most susceptible to schistosomiasis transmission and spread when they experience temperature variations within the range of 20–27 °C and varying levels of rainfall between 5 and 140 mm. This aligns with observations made by Martens et al. (Martens et al., 1995), McCreesh and Booth (McCreesh & Booth, 2013), and Stensgaard et al. (Stensgaard et al., 2016), highlighting the favorable conditions for schistosomiasis transmission resulting from climate change when these specific hydrometeorological conditions are met. Interestingly, our results indicate that regions with adverse temperatures exceeding 27 °C, which are typically known to limit schistosomiasis transmission, may still facilitate disease development when accompanied by suitable precipitation. In such regions characterized by a combination of dry and wet weather conditions, episodes of precipitation followed by a drop in temperatures below 27 °C create favorable environmental conditions for schistosomiasis transmission. However, it is worth noting that certain ranges of precipitation variation may have no discernible effect on temperature and may even limit the development of schistosomiasis, resulting in a decline in reported cases. This observation provides corroboration for the findings in the scientific literature, which propose that certain weather patterns may not favor schistosomiasis transmission due to their limited influence on average temperatures in specific regions (Mas-Coma et al., 2009; McCreesh & Booth, 2013; Van der Wiel & Bintanja, 2021; Tabo et al., 2023). When considered collectively, the transmission dynamics of schistosomiasis are susceptible to seasonal variations influenced by climate factors, potentially exerting significant effects on the efficacy of control and elimination endeavors.

4.4. Future trend of schistosomiasis

The impact of climate change on schistosomiasis transmission and control measures varies depending on the frequency, temporal distribution, and range of temperature and rainfall events. Climate change-induced increases in snail recruitment rates are expected to lead to higher schistosomiasis cases during specific seasons. This finding aligns with analogous models that predict the expansion of

schistosomiasis into cooler regions and the potential for increased transmission in the future (Martens et al., 1995; McCreesh et al., 2015). Our model results suggest that seasons characterized by high snail recruitment rates present optimal opportunities to intensify intermediate host snail control efforts. However, in regions experiencing precipitation levels ranging from 50 to 150 mm and average temperature fluctuations between 27 and 35 °C, the PRCC test results indicate that snail recruitment rate values remain constrained and may not significantly drive schistosomiasis occurrence. This suggests that the impact of precipitation fluctuations within this range on the temperature-constrained snail recruitment is minimal, consistent with observations that rainfall between 50 and 150 mm is negatively correlated with a low number of *S. mansoni* patients (Xue et al., 2011). In summary, our parameterized models of schistosomiasis and climate dynamics provide insights into regions that may become more conducive to the spread of the disease in the future. This information is valuable for identifying areas that may require heightened surveillance and targeted control interventions to mitigate the potential impact of climate change on schistosomiasis transmission.

4.5. Model limitations/methodological implication and future research

It is important to acknowledge the limitations of our study. Firstly, the parameter values utilized in our model, which represent the biological aspects and real-life scenarios of schistosomiasis transmission, were sourced from the published literature. Consequently, inconsistencies and variability may exist within the data collected under diverse conditions, introducing potential uncertainties and biases into our model results. Nonetheless, the mathematical model employed in our manuscript offers a robust framework for comprehending the interplay between temperature, rainfall, and schistosomiasis transmission dynamics. It serves as a quantitative framework, with baseline parameter values providing a reasonable approximation, thereby enhancing our understanding of the impact of climate factors, seasons, and timing of interventions. By accurately predicting disease outbreaks, we facilitate the assessment of appropriate intervention strategies during specific months and seasons. Furthermore, this model has global applicability, extending its usefulness to diverse regions worldwide. In addition, our transmission model has been autonomous under static conditions. Despite insights gained, it is not exhaustive, and environmental variability and uncertainty persist. These result from natural fluctuations, parameter estimation, or external data sources. Fully addressing uncertainty and variability exceeds the scope of this paper. Future research should extend to a non-autonomous model, treating temperature and rainfall as dynamic variables. This extended model may introduce compartments for exposed, latent, and immature/juvenile snail populations and explore additional control measures other than climate.

5. Conclusion

Understanding the impact of climate change on schistosomiasis transmission requires considering the individual and combined effects of temperature and precipitation. When examined separately, the findings indicated that increasing mean monthly temperatures are associated with higher schistosomiasis cases, while increasing maximum monthly temperatures are linked to a decrease in cases. Additionally, a threshold level of rainfall is necessary to reduce the burden of schistosomiasis. However, the highest disease burden occurs when favorable temperature and precipitation conditions coincide, leading to increased prevalence of intermediate hosts, higher human and snail infection rates, enhanced survival of snail eggs and juveniles, and increased snail egg laying and hatching rates. These conditions also provide optimal opportunities for implementing control measures. Our model effectively identifies hydrometeorological conditions that increase the transmission risk of schistosomiasis, making it a valuable tool for predicting the spatial distribution of the disease under climate change and developing management strategies. This study contributes to the understanding of schistosomiasis transmission dynamics in the context of climate change and provides insights for policymakers to make informed decisions regarding disease control. Future research should explore the contrast between climate-driven management of snail vectors and schistosomiasis control strategies. Moreover, incorporating spatially explicit transmission models will enhance predictions of disease persistence and spread.

Ethics approval and consent to participate

Not applicable.

Consent for publication

Not applicable.

Funding

DAAD provided ZT with a PhD scholarship (Grant No. 57507871). As part of CK's postdoctoral training, he was awarded a scholarship from the Alexander von Humboldt Foundation (Grant No. ZMB1217528GF-P). There was no involvement of the funders in the design of the study, the collection or analysis of data, the decision to publish, or the preparation of the manuscript.

Availability of data and material

All data generated or analysed during this study are included in this published article and its supplementary information file (SI).

CRediT authorship contribution statement

Zadoki Tabo: Conceptualization, Data curation, Formal analysis, Investigation, Methodology, Software, Validation, Visualization, Writing – original draft. **Chester Kalinda:** Data curation, Methodology, Writing – review & editing. **Lutz Breuer:** Project administration, Resources, Supervision, Writing – review & editing. **Christian Albrecht:** Project administration, Resources, Supervision, Writing – review & editing.

Declaration of competing interest

The authors declare that they have no known competing financial interests or personal relationships that could have appeared to influence the work reported in this paper.

Acknowledgements

The authors extend their appreciation to the German Academic Exchange Service (DAAD) for awarding ZT a PhD scholarship (grant No. 57507871), as well as to the Alexander von Humboldt Foundation for generously supporting CK with a postdoctoral scholarship (grant No. ZMB1217528GF-P). Additionally, the authors would like to acknowledge Livingstone S. Luboobi from Makerere University for his invaluable guidance and expert advice on mathematical formulations.

Appendix A. Supplementary data

Supplementary data to this article can be found online at https://doi.org/10.1016/j.idm.2023.12.003.

References

Adekiya, T. A., Aruleba, R. T., Oyinloye, B. E., Okosun, K. O., & Kappo, A. P. (2020). The effect of climate change and the snail-schistosome cycle in transmission and bio-control of schistosomiasis in Sub-Saharan Africa. *International Journal of Environmental Research and Public Health, 17*(1), 181. https://doi.org/10.3390/ijerph17010181

Bergquist, R., Zhou, X. N., Rollinson, D., Reinhard-Rupp, J., & Klohe, K. (2017). Elimination of schistosomiasis: The tools required. *Infectious Diseases of Poverty, 6*, 1–9. https://doi.org/10.1186/s40249-017-0370-7

Castillo-Chavez, C., & Song, B. (2004). Dynamical models of tuberculosis and their applications. *Mathematical Biosciences and Engineering, 1*(2), 361–404. https://doi.org/10.3934/mbe.2004.1.361

Chavez, C. C., Feng, Z., & Huang, W. (2002). On the computation of R0 and its role on global stability. *Mathematical Approaches for Emerging and Re-emerging Infection Diseases: An Introduction, 125*, 31–65.

Chen, Z., Zou, L., Shen, D., Zhang, W., & Ruan, S. (2010). Mathematical modelling and control of schistosomiasis in hubei province, China. *Acta Tropica, 115*(1–2), 119–125. https://doi.org/10.1016/j.actatropica.2010.02.012

Codjoe, S. N. A., & Larbi, R. T. (2016). Climate change/variability and schistosomiasis transmission in Ga district, Ghana. *Climate & Development, 8*(1), 58–71. https://doi.org/10.1080/17565529.2014.998603

Colley, D. G., Bustinduy, A. L., Secor, W. E., & King, C. H. (2014). Human schistosomiasis. *The Lancet, 383*(9936), 2253–2264. https://doi.org/10.1016/S0140-6736(13)61949-2

Diekmann, O., Heesterbeek, J. A. P., & Metz, J. A. (1990). On the definition and the computation of the basic reproduction ratio R 0 in models for infectious diseases in heterogeneous populations. *Journal of Mathematical Biology, 28*, 365–382. https://doi.org/10.1007/BF00178324

Driessche, P., & Watmough, J. (2002). Reproduction numbers and sub-threshold endemic equilibria for compartmental models of disease transmission. *Mathematical Biosciences, 180*(1–2), 29–48. https://doi.org/10.1016/S0025-5564(02)00108-6

Feng, Z., Eppert, A., Milner, F. A., & Minchella, D. J. (2004). Estimation of parameters governing the transmission dynamics of schistosomes. *Applied Mathematics Letters, 17*(10), 1105–1112. https://www.sciencedirect.com/science/article/pii/S0893965904816884.

Fulford, A. J. C., Butterworth, A. E., Ouma, J. H., & Sturrock, R. F. (1995). A statistical approach to schistosome population dynamics and estimation of the life-span of Schistosoma mansoni in man. *Parasitology, 110*(3), 307–316. https://doi.org/10.1017/S0031182000080896

Gryseels, B., Polman, K., Clerinx, J., & Kestens, L. (2006). Human schistosomiasis. *The Lancet, 368*(9541), 1106–1118. https://doi.org/10.1016/S0140-6736(06)69440-3

Hauffe, T., Schultheiß, R., Van Bocxlaer, B., Prömmel, K., & Albrecht, C. (2016). Environmental heterogeneity predicts species richness of freshwater mollusks in sub-Saharan Africa. *International Journal of Earth Sciences, 105*, 1795–1810. https://doi.org/10.1007/s00531-014-1109-3

Home. (2023). *Climate change knowledge portal, World Bank climate change*. WBC. Available at: https://Climateknowledgeportal.Worldbank.Org/Country, 14 Febuary 2023.

Kalinda, C., Chimbari, M. J., Grant, W. E., Wang, H. H., Odhiambo, J. N., & Mukaratirwa, S. (2018). Simulation of population dynamics of Bulinus globosus: Effects of environmental temperature on production of Schistosoma haematobium cercariae. *PLoS Neglected Tropical Diseases, 12*(8), Article e0006651. https://doi.org/10.1371/journal.pntd.0006651

Kalinda, C., Chimbari, M. J., & Mukaratirwa, S. (2017a). Effect of temperature on the Bulinus globosus-Schistosoma haematobium system. *Infectious Diseases of Poverty, 6*(1), 1–7. https://doi.org/10.1186/S40249-017-0260-Z

Kalinda, C., Chimbari, M., & Mukaratirwa, S. (2017b). Implications of changing temperatures on the growth, fecundity and survival of intermediate host snails of schistosomiasis: A systematic review. *International Journal of Environmental Research and Public Health, 14*(1), 80. https://doi.org/10.3390/ijerph14010080

Kalinda, C., Mushayabasa, S., Chimbari, M. J., & Mukaratirwa, S. (2019). Optimal control applied to a temperature dependent schistosomiasis model. *Biosystems, 175*, 47–56. https://doi.org/10.1016/J.biosystems.2018.11.008

Liang, S., Spear, R. C., Seto, E., Hubbard, A., & Qiu, D. (2005). A multi-group model of Schistosoma japonicum transmission dynamics and control: Model calibration and control prediction. *Tropical Medicine and International Health, 10*(3), 263–278. https://doi.org/10.1111/j.1365-3156.2005.01386.x

Li, Y., Teng, Z., Ruan, S., Li, M., & Feng, X. (2017). A mathematical model for the seasonal transmission of schistosomiasis in the lake and marshland regions of China. *Mathematical Biosciences and Engineering, 14*(5–6), 1279–1299. https://doi.org/10.3934/mbe.2017066

Malone, J. B. (2005). Biology-based mapping of vector-borne parasites by geographic information systems and remote sensing. *Parassitologia, 47*(1), 27.

Mangal, T. D., Paterson, S., & Fenton, A. (2008). Predicting the impact of long-term temperature changes on the epidemiology and control of schistosomiasis: A mechanistic model. *PLoS One, 3*(1), e1438. https://doi.org/10.1371/journal.pone.0001438

Manyangadze, T., Chimbari, M. J., Gebreslasie, M., Ceccato, P., & Mukaratirwa, S. (2016). Modelling the spatial and seasonal distribution of suitable habitats of schistosomiasis intermediate host snails using Maxent in Ndumo area, KwaZulu-Natal Province, South Africa. *Parasites & Vectors, 9*(1), 1–10. https://doi.org/10.1186/s13071-016-1834-5

Martens, W. J. M., Jetten, T. H., Rotmans, J., & Niessen, L. W. (1995). Climate change and vector-borne diseases: A global modelling perspective. *Global Environmental Change, 5*(3), 195–209. https://doi.org/10.1016/0959-3780(95)00051-O

Marti, H. (1986). Field observations on the population dynamics of Bulinus globosus, the intermediate host of Schistosoma haematobium in the Ifakara area, Tanzania. *The Journal of Parasitology*, 119–124. https://doi.org/10.2307/3281803

Mas-Coma, S., Valero, M. A., & Bargues, M. D. (2009). Climate change effects on trematodiases, with emphasis on zoonotic fascioliasis and schistosomiasis. *Veterinary Parasitology, 163*(4), 264–280. https://doi.org/10.1016/j.vetpar.2009.03.024

McCreesh, N., & Booth, M. (2013). Challenges in predicting the effects of climate change on Schistosoma mansoni and Schistosoma haematobium transmission potential. *Trends in Parasitology, 29*(11), 548–555. https://doi.org/10.1016/j.pt.2013.08.007

McCreesh, N., Nikulin, G., & Booth, M. (2015). Predicting the effects of climate change on Schistosoma mansoni transmission in eastern Africa. *Parasites & Vectors, 8*, 1–9. https://doi.org/10.1186/S13071-014-0617-0

Michaels, R. M., & Prata, A. (1968). Evolution and characteristics of Schistosoma mansoni eggs laid in vitro. *The Journal of Parasitology*, 921–930. https://www.jstor.org/stable/3277120.

Najjuma, M., Nimusiima, A., Sabiiti, G., & Opio, R. (2021). Characterization of historical and future drought in central Uganda using CHIRPS rainfall and RACMO22T model data. *International Journal of Agriculture and Forestry, 11*, 9–15. https://doi.org/10.5923/j.ijaf.20211101.02

Ngarakana-Gwasira, E. T., Bhunu, C. P., Masocha, M., & Mashonjowa, E. (2016). Transmission dynamics of schistosomiasis in Zimbabwe: A mathematical and GIS approach. *Communications in Nonlinear Science and Numerical Simulation, 35*, 137–147. https://doi.org/10.1016/j.cnsns.2015.11.005

Ngoma, H., Wen, W., Ojara, M., & Ayugi, B. (2021). Assessing current and future spatiotemporal precipitation variability and trends over Uganda, East Africa, based on CHIRPS and regional climate model datasets. *Meteorology and Atmospheric Physics, 133*, 823–843. https://doi.org/10.1007/S00703-021-00784-3

Okuneye, K., & Gumel, A. B. (2017). Analysis of a temperature-and rainfall-dependent model for malaria transmission dynamics. *Mathematical Biosciences, 287*, 72–92. https://doi.org/10.1016/j.mbs.2016.03.013

Parham, P. E., & Michael, E. (2010). Modeling the effects of weather and climate change on malaria transmission. *Environmental Health Perspectives, 118*(5), 620–626. https://doi.org/10.1289/EHP.0901256

Schrader, M., Hauffe, T., Zhang, Z., Davis, G. M., Jopp, F., Remais, J. V., & Wilke, T. (2013). Spatially explicit modeling of schistosomiasis risk in eastern China based on a synthesis of epidemiological, environmental and intermediate host genetic data. *PLoS Neglected Tropical Diseases, 7*(7), Article e2327. https://doi.org/10.1371/journal.pntd.0002327

Soetaert, K., Petzoldt, T., & Setzer, R. W. (2010). Package deSolve: Solving initial value differential equations in R. *Journal of Statistical Software, 33*(9), 1–25. http://th.archive.ubuntu.com/cran/web/packages/deSolve/vignettes/deSolve.pdf.

Solomon, S. (Ed.). (2007), *Working group I contribution to the fourth assessment report of the IPCC: 4. Climate change 2007-the physical science basis*. Cambridge university press.

Steinmann, P., Keiser, J., Bos, R., Tanner, M., & Utzinger, J. (2006). Schistosomiasis and water resources development: Systematic review, meta-analysis, and estimates of people at risk. *The Lancet Infectious Diseases, 6*(7), 411–425. https://doi.org/10.1016/S1473-3099(06)70521-7

Stensgaard, A. S., Booth, M., Nikulin, G., & McCreesh, N. (2016). Combining process-based and correlative models improves predictions of climate change effects on Schistosoma mansoni transmission in eastern Africa. *Geospatial health, 11*, 94–101. https://doi.org/10.4081/gh.2016.406

Tabo, Z., Kalinda, C., Breuer, L., & Albrecht, C. (2023). Adapting strategies for effective schistosomiasis prevention: A mathematical modeling approach. *Mathematics, 11*(12), 2609. https://doi.org/10.3390/math11122609

Tabo, Z., Neubauer, T. A., Tumwebaze, I., Stelbrink, B., Breuer, L., Hammoud, C., & Albrect, A. (2022). Factors controlling the distribution of intermediate host snails of schistosoma in crater lakes in Uganda: A machine learning approach. *Frontiers in Environmental Science, 10*, Article 871735. https://doi.org/10.3389/fenvs.2022.871735

Team, R. C. (2018). *A language and environment for statistical computing*. Vienna, Austria: R Foundation for Statistical Computing. *Available online:* www.R-project.org/. (Accessed 11 September 2020).

Utzinger, J., Raso, G., Brooker, S., De Savigny, D., Tanner, M., Ørnbjerg, N., Singer, B. H., & N'goran, E. (2009). Schistosomiasis and neglected tropical diseases: Towards integrated and sustainable control and a word of caution. *Parasitology, 136*(13), 1859–1874. https://doi.org/10.1017/S0031182009991600

Van der Wiel, K., & Bintanja, R. (2021). Contribution of climatic changes in mean and variability to monthly temperature and precipitation extremes. *Communications Earth & Environment, 2*(1), 1. https://doi.org/10.1038/s43247-020-00077-4

Xue, Z., Gebremichael, M., Ahmad, R., Weldu, M. L., & Bagtzoglou, A. C. (2011). *Impact of temperature and precipitation on propagation of intestinal schistosomiasis in an irrigated region in Ethiopia: Suitability of satellite datasets*. https://doi.org/10.1111/j.1365-3156.2011.02820.x

mathematics

MDPI

Article

Adapting Strategies for Effective Schistosomiasis Prevention: A Mathematical Modeling Approach

Zadoki Tabo [1,2,*], Chester Kalinda [1,3], Lutz Breuer [2,4] and Christian Albrecht [1]

[1] Department of Animal Ecology and Systematics, Justus Liebig University Giessen, Heinrich-Buff-Ring 26 (iFZ), 35392 Giessen, Germany; ckalinda@ughe.org (C.K.); christian.albrecht@allzool.bio.uni-giessen.de (C.A.)
[2] Department of Landscape Ecology and Resource Management, Justus Liebig University Giessen, Heinrich-Buff-Ring 26 (iFZ), 35392 Giessen, Germany; lutz.breuer@umwelt.uni-giessen.de
[3] Bill and Joyce Cummings Institute of Global Health, University of Global Health Equity, Kigali Heights, Plot 772 KG 7 Ave., Kigali P.O. Box 6955, Rwanda
[4] Centre for International Development and Environmental Research (ZEU), Justus Liebig University Giessen, Senckenbergstrasse 3, 35390 Giessen, Germany
* Correspondence: tabozac@gmail.com

Abstract: One of the most deadly neglected tropical diseases known to man is schistosomiasis. Understanding how the disease spreads and evaluating the relevant control strategies are key steps in predicting its spread. We propose a mathematical model to evaluate the potential impact of four strategies: chemotherapy, awareness programs, the mechanical removal of snails and molluscicides, and the impact of a change in temperature on different molluscicide performances based on their half-lives and the length of time they persist in contact with target species. The results show that the recruitment rate of humans and the presence of cercaria and miracidia parasites are crucial factors in disease transmission. However, schistosomiasis can be entirely eradicated by combining all of the four strategies. In the face of climate change and molluscicide degradation, the results show that increasing the temperatures and the number of days a molluscicide persists in the environment before it completely degrades decreases the chemically induced mortality rate of snails while increasing the half-life of different molluscicides increases the death rate of snails. Therefore, eradicating schistosomiasis effectively necessitates a comprehensive integration of all preventative measures. Moreover, regions with different weather patterns and seasonal climates need strategies that have been adapted in terms of the appropriate molluscicide and time intervals for reapplication and effective schistosomiasis control.

Keywords: chemotherapy; public literacy; mechanical removal of snails; molluscicide performance; temperature; molluscicide degradation; half-life

MSC: 92B05

Citation: Tabo, Z.; Kalinda, C.; Breuer, L.; Albrecht, C. Adapting Strategies for Effective Schistosomiasis Prevention: A Mathematical Modeling Approach. *Mathematics* **2023**, *11*, 2609. https://doi.org/10.3390/math11122609

Academic Editor: Mikhail Kolev

Received: 8 May 2023
Revised: 30 May 2023
Accepted: 5 June 2023
Published: 7 June 2023

1. Introduction

Schistosomiasis is the second-most significant neglected tropical disease (NTD), a physically debilitating and persistent disease [1,2] that leads to severe morbidity and almost 12,000 deaths globally, of which at least 90% are from sub-Saharan Africa [2]. Human schistosomiasis infection caused by Trematoda worms depends on the availability of suitable freshwater intermediate host snails (IHs) and the final human host to be transmitted [3]. The main symptoms of infection include skin rash and itching, fever, cough, muscle pain, bloody urine, and growth retardation in children [2], while severe cases can lead to damage and failure of the liver, bladder, lungs, and intestines [1,2]. Unfortunately, unlike most NTDs, including lymphatic filariasis, leprosy, and leishmaniasis, there are currently no recommendations for intensive disease management for schistosomiasis [4], and current

disease control strategies rely on mass drug administration (MDA) chemotherapy, which, at times, is combined with health education [5,6]. Although there has been a success in the implementation of chemotherapy, especially in Africa [7,8], this may have limited the implementation of new methods to interrupt parasite transmission through snail control, leading to a resurgence of the disease following drug treatment and education efforts [6,9,10]. Therefore, there is a need to recast the current and future schistosomiasis control strategies to focus on integrated measures and enhanced surveillance response to both changes in infection and snail abundance.

Various methods have been employed in the control of schistosomiasis. For instance, intermediate hosts (IHs) can be controlled through biological, chemical/molluscicides, or environmental/ecological methods [11–13]. Biological measures include the use of predators and competitor snails [12], while chemical control measures consider the use of molluscicides to reduce IH density and abundance [14,15]. The use of molluscicides and their effectiveness has been observed to depend on their proper concentration, half-life, technique and timing of application, and length of contact time with target species, as well as the temperature of the environment where the chemical is released [16]. In addition, environmental/ecological strategies are used to lower the density and abundance of IHs and the risks of snail-to-human transmission (referred to as the mechanical control approach in this study). The approach includes excavating deep channels that act as dry buriers for snails to spread to other water outlets, increasing the flow velocity in irrigation canals, and picking IHs out of the system. Other ways include adopting appropriate cultivation methods, such as shorter fallow times, modifying irrigation techniques, and regulating flooding [11,17].

With the predicted change in global temperature due to climate change, mathematical models have become valuable tools for exploring various infection and control scenarios as they provide both theoretical and practical insights into the epidemiology of infectious diseases. In understanding the transmission and control dynamics of schistosomiasis, different models have been used to create a range of transmission and control outcomes. These models explore dynamics, including free-living parasites, miracidia, and cercariae [18], chemotherapy treatment using praziquantel drugs and the removal of snails and cercariae [19], the impact of public literacy and snail control parameters [20], as well as health education and molluscicides [21].

Our study examines whether molluscicides and/or mechanical control for snail management, combined with mass drug administration and/or health education, can eliminate schistosomiasis. In addition, we postulate that the temperature rise, as predicted by climate change models [22–24], will strongly influence the use of chemicals/molluscicides, and their performance against the target species [25,26] and the general transmission dynamics of the disease. As such, it is important to understand how temperature affects molluscicide usage for the control of schistosomiasis. This can help in the identification and control of chemical-induced environmental hazards that could be harmful to even nontarget species and human health under various environmental conditions [27–30]. The current study will evaluate four controls: mass drug administration/chemotherapy, public literacy, mechanical measures, and chemicals/molluscicides to find the most effective way to eradicate schistosomiasis. In addition, the evaluation includes the effects of temperature rise on various molluscicide performances based on half-lives and contact durations with the targeted species.

2. Materials and Methods

2.1. Schistosomiasis Model Formulation

The dynamics of schistosomiasis [2,3] and stages of intervention strategies are the basis for model formulation (Figure 1). The deterministic model formulated and represented by ordinary differential equations (ODEs) (Equations (1)–(7)) is a modification of those presented by Abokwara and Madubueze [20] and Nur et al. [21], and it is based on the compartment diagram (Figure 1). A population is represented by state time variables that

are associated with the various compartment models and change over time according to the interaction rules. t: the time variable for the sizes of susceptible humans; $S_h(t)$: infected human; $I_h(t)$: eggs released from infected humans; $E_h(t)$: free-living miracidia; $M_f(t)$: susceptible snail vector; $S_v(t)$: infected snail vector; $I_v(t)$: free-living cercariae $C_f(t)$ (Figure 1). The parameters of the model are based on the abiotic and biotic aspects of the *Schistosoma* cycle and transmission, namely the contact rates between the hosts and the free-living cercaria/miracidia population in water and the effective mortality rates.

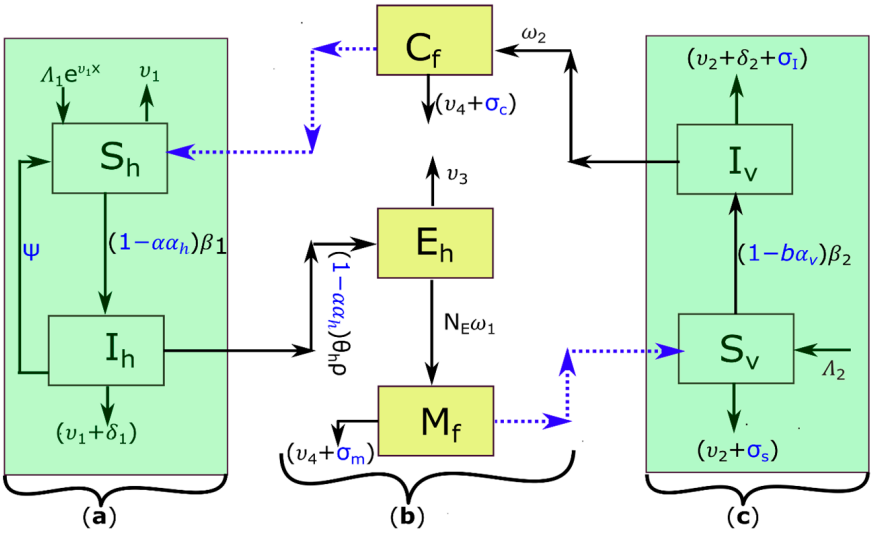

Figure 1. Transmission dynamics of schistosomiasis in (**a**) human definitive hosts (susceptible human S_h; infected human I_h), (**b**) schistosomiasis parasite forms (cercariae C_f; parasite eggs E_h; miracidia M_f), and (**c**) intermediate host snails (susceptible snail S_v; and infected snail I_v). The blue dotted arrows represent the interaction between free-living schistosomiasis parasites and the respective hosts. All parameters are as defined in Section 2.1, and the control parameters are shown in blue.

The population of susceptible human hosts S_h in the model system, Equation (1), increases by an exponential recruitment rate of $\Lambda_1 e^{-\upsilon_1 x}$, where Λ_1 is the maximum per capita birth rate/immigration rate (recruitment rate) of human individuals, υ_1 is the natural mortality rate of humans, and x is the initial age of infection in children. Susceptible human hosts, S_h, are infected only by contact with cercariae in an infested freshwater environment at a rate β_1 per contact. The saturation incidence is a Holling-type II function, which relates the rate of infection transmission and the inhibitory effect, where C_o is the saturation coefficient that represents the transmissibility of infection due to the crowding effect of the cercariae, and ε is the limitation of the growth velocity (density) of the cercaria in contaminated freshwater. Thus, model system, Equation (2) represents the infected humans, I_h. Moreover, due to schistosomiasis infection, infected people die at a rate of δ_1. Thus, our model incorporates chemotherapy treatment for deworming schistosome worms in the infected human body and to stop or limit the release of parasite eggs through urine and feces. We assume that treated infected individuals recover at a rate of ψ and return to the susceptible class because there is no lasting immunity to schistosomiasis, and reinfection is inevitable [9,31]. In addition, public literacy strategy is considered and represented by the parameters $\alpha, \alpha_h \epsilon [0, 1]$, where α is the proportion of people with knowledge/awareness about schistosomiasis, and α_h is the effectiveness of acquired knowledge. This control method focuses on managing the human population by providing access to clean water and improving sanitation and hygiene (WASH) to lower the number of humans being infected [32].

When infected humans I_h indiscriminately release parasite eggs through urine/feces into the environment, their population size increases logistically, as shown in Equation (3).

Where ρ (in grams) is the portion of stool/urine per infected person due to open defecation or urination. θ_h is the number of parasite eggs per gram of stool and/or urine, and K is the carrying capacity of the parasite eggs in the environment. The term $(1 - \alpha\alpha_h)$ represents the public literacy impact in reducing the portion of urine/feces ρ. It describes the impact of public literacy on the density of parasite eggs directly or indirectly deposited in freshwater and lowers the likelihood of human-to-snail transmission. The indirectly deposited parasite eggs find their way into a freshwater source. Each parasite egg E_h hatches, releasing N_E miracidia per parasite egg at a rate ω_1 under suitable conditions, or dies naturally at a rate v_3 when there is no IHs to penetrate, as represented in miracidia population dynamics in Equation (4).

In the model system, Equation (5), the snail host population S_v is recruited at a rate Λ_2 and is infected due to contact with miracidia at a saturation incidence given the saturation coefficient for miracidia infectivity M_o and ε the limitation of the growth velocity of the miracidia. β_2 is the rate of miracidia-to-snail transmission per contact. Both susceptible S_v and infected IH snails I_v die naturally at a rate v_2, but the infected snail (in Equation (6) may also die at a rate of δ_2 due to infection host. Infected snails I_v that survive release infectious cercariae C_f at a rate of ω_2, capable of invading and infecting humans, or dying naturally at a rate of u_5 in the absence of a human host, see Equation (7). Thus, we incorporated a snail management strategy through the mechanical measure, represented by parameter $b, \alpha_v \in [0, 1]$, where b is the proportion of snail density removed and eliminated from the system, and α_v is the effectiveness of such snail management practice. Thus, the impact of a mechanical measure $(1 - b\alpha_v)$ reduces β_2 [20,21].

In addition, we assume that the application of molluscicides into the environment causes susceptible and infected IHs to die at a chemical-induced death rate of $\sigma_s \in [0, 1]$ and $\sigma_I \epsilon [0, 1]$, respectively. Furthermore, molluscicides also reduce viability and cause the deaths of infective cercaria and miracidia at a rate of $\sigma_m \in [0, 1]$ and $\sigma_c \in [0, 1]$, respectively.

Thus, the model equations incorporating terms for control strategies highlighted in blue are given as follows:

$$\dot{S_h}(t) = \Lambda_1 e^{-v_1 x} + \psi I_h - \frac{(1 - \alpha\alpha_h)\beta_1 S_h C_f}{C_o + \varepsilon C_f} - v_1 S_h, \tag{1}$$

$$\dot{I_h}(t) = \frac{(1 - \alpha\alpha_h)\beta_1 S_h C_f}{C_o + \varepsilon C_f} - (v_1 + \delta_1 + \psi) I_h, \tag{2}$$

$$\dot{E_h}(t) = \rho\theta_h(1 - \alpha\alpha_h) I_h \left(1 - \frac{E_h}{K}\right) - (\omega_1 + v_3) E_h, \tag{3}$$

$$\dot{M_f}(t) = N_E \omega_1 E_h - (v_4 + \sigma_m) M_f, \tag{4}$$

$$\dot{S_v}(t) = \Lambda_2 - \frac{(1 - b\alpha_v)\beta_2 M_f S_v}{M_o + \varepsilon M_f} - (v_2 + \sigma_s) S_v, \tag{5}$$

$$\dot{I_v}(t) = \frac{(1 - b\alpha_v)\beta_2 M_f S_v}{M_o + \varepsilon M_f} - (v_2 + \delta_2 + \sigma_I) I_v, \tag{6}$$

$$\dot{C_f}(t) = \omega_2 I_v - (v_5 + \sigma_c) C_f. \tag{7}$$

2.2. Temperature Control

Temperature is a crucial factor for the timing of molluscicide application [16] because molluscicide efficacy is temperature-dependent [33]. The temperature has a significant effect on how quickly the half-lives of molluscicide decrease in water [27]. This has a great influence on the chemical-induced death rates σ_s, σ_I, σ_m, and σ_c and can determine the rate of transmission of the disease. We examine and evaluate the effectiveness of

temperature-dependent molluscicides on the death rates of targeted species. We derive the environmentally dependent chemical-induced deaths of species, where the effect of temperature can be reliably predicted using an Arrhenius equation [27,28,34]. The Arrhenius equation proposed and updated by the European Chemicals Agency, ECHA [29,30] to modify the half-life $t_{1/2}(T)$ at any temperature T of the environment is given as

$$t_{1/2}(T) = t_{1/2}(T_o)e^{0.08[T_o - T]} \tag{8}$$

where $t_{1/2}(T_o)$ is the factory-predetermined half-life of the chemical at the experimental temperature T_o. The preferred experimental temperature in most of the chemicals is $T_o = 20^{\circ}$C [27,35]. Furthermore, we assume that chemically induced mortalities ($\sigma_s, \sigma_I, \sigma_m, \sigma_c$) decrease exponentially with time t according to the following expressions:

$$\sigma_{s,I,m,c} = \sigma'_{s,I,m,c}e^{-kt} \tag{9}$$

where σ'_s, σ'_I, σ'_m, and σ'_c are the maximum mortality rates on the first day ($t = 0$) when the molluscicide is applied in the water. k, is the exponential decay constant of the mortality rate at degradation time t. The terms σ'_s, σ'_I, σ'_m and σ'_c were determined from the withdrawal terms $(d_v + \sigma_s)$, $(d_v + \delta_2 + \sigma_I)$, $(v_3 + \sigma_m)$, and $(v_4 + \sigma_c)$ present in the dynamics of IHs and parasite populations in the absence of humans (Equations (4)–(7)). A maximum value of one (1) is assumed for each term, the same approach as in Carvalho et al. [36]. Furthermore, we link k to the half-life ($t_{1/2}$) of the chemical released by using the following equation:

$$t_{1/2} = In2/k \tag{10}$$

where $1/k$ is the typical time the chemical persists in the environment and is, therefore, in contact with the HIs, the *Schistosoma* parasites, and other nontarget species. The results of substituting σ'_s, σ'_I, and k and substituting Equations (8) and (10) into Equation (9) are shown in Table 1.

Table 1. The continuously exponentially decreasing mortality rates for intermediate hosts and *Schistosoma* parasite forms, as functions of the half-life of the chemical $t_{1/2}$, the temperature T of the environment in which the chemical is released, and the duration t for which the targeted species are exposed to the chemicals.

Intermediate Hosts	***Schistosoma* Parasite Forms**
Susceptible snails	Free-living miracidia
$\sigma_S = (1 - d_v)e^{-\frac{\ln 2}{t_{1/2}\cdot e^{0.08[20-T]}}t}$	$\sigma_M = (1 - v_3)e^{-\frac{\ln 2}{t_{1/2}e^{0.08[20-T]}}t}$
Infected snails	Free-living cercaria
$\sigma_I = (1 - d_v - \delta_2)e^{-\frac{\ln 2}{t_{1/2}e^{0.08[20-T]}}t}$	$\sigma_C = (1 - v_4)e^{-\frac{\ln 2}{t_{1/2}e^{0.08[20-T]}}t}$

Thus, chemical control guarantees the elimination of all three water-dwelling schistosomiasis agents [16]. Furthermore, based on Matthies and Beulke [27] and the European Commission [37], the chemical is nonpersistent (NP) in the environment when $t_{1/2} = 3.1 - 40$, persistent (P) when $t_{1/2} = 41 - 60$, and very persistent (VP) when $t_{1/2} = 61 - 232$. Based on this information, we discriminate the effects of different chemical performances based on their different half-lives $t_{1/2}$, degradation k, and length of chemical exposure $1/k$ on the death rate of the targeted species.

It is worth noting that in our model, we assume that chemotherapy treatment reduces disease morbidity among humans while molluscicide increases the mortality of IHs. Public literacy and mechanical control are management strategies for humans and snails, respectively, that directly and extrinsically prevent the likelihood of parasite-host contact for the transmission of schistosomiasis. Furthermore, there is no vertical transmission of the

disease to humans nor immigration to the infected individuals. Infected snails are unable to reproduce as a side effect of infection and may die more frequently than susceptible snails.

This paper presents the model analysis first, showing that the model is epidemiologically meaningful, realistic, and of interest in a certain invariant region Ω (Appendix A). We then derive the reproduction number (Section 2.3) and show the steady states (Section 2.4).

2.3. Reproduction Number

In epidemiology, one of the most reliable indicators of infection risk is the basic reproduction number R_0, which is the average number of new cases of infection caused by an infectious individual in a fully susceptible population [38]. We derived R_0 by rewriting the model system (Equations (1)–(7)), following Chavez et al. [39], into three components: the number of susceptible individuals (U), the infected schistosomiasis agents that cannot transmit the infection (V), and the infected schistosomiasis agents that transmit the disease (W), as follows:

$$\begin{cases} \frac{dU}{dt} = f(U,V,W) \\ \frac{dV}{dt} = g(U,V,W) \\ \frac{dW}{dt} = H(U,V,W) \end{cases}$$

where $U = (S_h, S_v)$, $V = (E_h, I_h, I_V)$, and $W = \left(M_f, C_f\right)$. We let $U_0 = (U^*, 0, 0)$ represent disease-free at U_0 such that, $\widetilde{g}(U^*, Z) = (\widetilde{g}_1(U^*, W), \widetilde{g}_2(U^*, W))$, where $\widetilde{g}_1(U^*, W) = \frac{\rho\theta_h\beta_1\Lambda_1(1-\alpha\alpha_h)^2 e^{-v_1 x} C_f}{v_1 C_o(\omega_1+v_3)(v_1+\delta_1+\psi)+(1-\alpha\alpha_h)\beta_1\{v_1(v_1+\delta_1+\psi)(\omega_1+v_3)+\rho\theta_h(1-\alpha\alpha_h)\Lambda_2\}C_f}$, and $\widetilde{g}_2(U^*, W) = \frac{(1-b\alpha_v)\beta_2\Lambda_2 M_f}{v_2(v_2+\delta_2+\sigma_I)\left(M_o+\varepsilon M_f\right)}$. Suppose, $A = D_V h(U^*, \widetilde{g}(U^*, 0))$, then A is given by

$$A = \begin{bmatrix} -(v_4+\sigma_m) & \frac{\rho\theta_h N_E\omega_1\beta_1\Lambda_1(1-\alpha\alpha_h)^2 e^{-v_1 x}}{v_1 C_o(\omega_1+v_3)(v_1+\delta_1+\psi)} \\ \frac{(1-b\alpha_v)\omega_2\beta_2\Lambda_2}{v_2 M_o(v_2+\delta_2+\sigma_I)} & -(v_5+\sigma_c) \end{bmatrix}$$

Following the next-generation matrix, an approach used by van den Driessche and Watmough [40], and the concept of reproduction numbers by Diekmann et al. [38], the matrix A can be rewritten as $A = F - V$, with $F \geq 0$ (i.e., $f_{ij} \geq 0$) and $V > 0$, a diagonal matrix, where

$$F = \begin{bmatrix} 0 & \frac{\rho\theta_h N_E\omega_1\beta_1\Lambda_1(1-\alpha\alpha_h)^2 e^{-v_1 x}}{v_1 C_o(\omega_1+v_3)(v_1+\delta_1+\psi)} \\ \frac{(1-b\alpha_v)\omega_2\beta_2\Lambda_2}{v_2 M_o(v_2+\delta_2+\sigma_I)} & 0 \end{bmatrix}, V = \begin{bmatrix} (v_4+\sigma_m) & 0 \\ 0 & \left(v_5+\sigma_p\right) \end{bmatrix}$$

The basic reproduction number is the spectral radius (dominant eigenvalue) of the matrix FV^{-1} given by

$$R_0 = \rho\left(FV^{-1}\right) = \sqrt{\left(\frac{\rho\theta_h N_E\omega_1\omega_2\beta_1\beta_2\Lambda_1\Lambda_2(1-b\alpha_v)(1-\alpha\alpha_h)^2 e^{-v_1 x}}{v_1 v_2 M_o C_o(v_1+\delta_1+\psi)(v_2+\delta_2+\sigma_I)(\omega_1+v_3)(v_4+\sigma_m)(v_5+\sigma_c)}\right)}$$

2.4. Steady State

We show that the model system, Equations (1)–(7) have a disease-free state (E_0) and an endemic steady state E_1, where

$$E_0 = \left(S_h^*, I_h^*, E_h^*, M_f^* S_v^*, I_v^*, C_f^*\right) = \left(\frac{\Lambda_1 e^{-v_1 x}}{v_1}, 0, 0, 0, \frac{\Lambda_2}{v_2}, 0, 0\right)$$

It always exists in $\mathcal{R}_{+0}^7$ provided $R_0 < 1$.

$E_1 = \left(S_h^1, I_h^1, E_h^1, M_f^1 S_v^1, I_v^1, C_f^1\right)$ is expressed in terms of I_v^1 and E_h^1 by

$$S_h^1\left(I_v^1\right) = \frac{(v_1+\delta_1+\psi)\Lambda_1\left[(v_5+\sigma_c)C_o+\omega_2\varepsilon I_v^1\right]}{(v_1+\delta_1+\psi)(v_5+\sigma_c)C_o+\omega_2[(v_1+\delta_1+\psi)((1-\alpha\alpha_h)\beta_1+\varepsilon)-\psi(1-\alpha\alpha_h)\beta_1]I_v^1},$$

$$I_h^1\left(I_v^1\right) = \frac{\beta_1\omega_2(1-\alpha\alpha_h)(v_1+\delta_1+\psi)\Lambda_1\left[(v_5+\sigma_c)C_o+\omega_2\varepsilon I_v^1\right]I_v^1}{(v_1+\delta_1+\psi)\left((v_5+\sigma_c)C_o+\omega_2 I_v^1\right)\left\{(v_1+\delta_1+\psi)(v_5+\sigma_c)C_o+\omega_2[(v_1+\delta_1+\psi)((1-\alpha\alpha_h)\beta_1+\varepsilon)-\psi(1-\alpha\alpha_h)\beta_1]I_v^1\right\}}$$

$$E_h^1\left(I_v^1\right) = \frac{\beta_1\omega_2\rho\theta_h K(1-\alpha\alpha_h)(v_1+\delta_1+\psi)\Lambda_1\left[(v_5+\sigma_c)C_o+\omega_2\varepsilon I_v^1\right]I_v^1}{(v_1+\delta_1+\psi)\left(\begin{matrix}(v_5+\sigma_c)(\omega_1+v_3)KC_o+\\((\omega_1+v_3)K\omega_2+\rho\theta_h(1-\alpha\alpha_h)\omega_2)I_v^1\end{matrix}\right)\left\{\begin{matrix}(v_1+\delta_1+\psi)(v_5+\sigma_c)C_o+\\\omega_2[(v_1+\delta_1+\psi)((1-\alpha\alpha_h)\beta_1+\varepsilon)-\psi(1-\alpha\alpha_h)\beta_1]I_v^1\end{matrix}\right\}}$$

$$M_f^1\left(I_v^1\right) = \frac{\beta_1\omega_2\rho\theta_h K N_E\omega_1(1-\alpha\alpha_h)(v_1+\delta_1+\psi)\Lambda_1\left[(v_5+\sigma_c)C_o+\omega_2\varepsilon I_v^1\right]I_v^1}{(v_1+\delta_1+\psi)(v_4+\sigma_m)\left(\begin{matrix}(v_5+\sigma_c)(\omega_1+v_3)KC_o+\\((\omega_1+v_3)K\omega_2+\rho\theta_h(1-\alpha\alpha_h)\omega_2)I_v^1\end{matrix}\right)\left\{\begin{matrix}(v_1+\delta_1+\psi)(v_5+\sigma_c)C_o+\\\omega_2[(v_1+\delta_1+\psi)((1-\alpha\alpha_h)\beta_1+\varepsilon)-\psi(1-\alpha\alpha_h)\beta_1]I_v^1\end{matrix}\right\}}$$

$$S_v^1\left(E_h^1\left(I_v^1\right)\right) = \frac{\Lambda_2 M_o+\Lambda_2\varepsilon E_h^1\left(I_v^1\right)}{(v_2+\sigma_s)M_o+((v_2+\sigma_s)\varepsilon+(1-b\alpha_v)\beta_2)E_h^1\left(I_v^1\right)}$$

$$C_f^1\left(I_v^1\right) = \frac{\omega_2 I_v^1}{(v_5+\sigma_c)}$$

when $\dot{I}_v(t)$= 0, we solved I_v^1 using Equation (6) of the model Equations (1)–(7), and this leads to the substitution of $S_v^1\left(E_h^1\left(I_v^1\right)\right)$ and $M_f^1\left(I_v^1\right)$, which yields Equation (11) below.

$$\left(\mathrm{a}_4 I_v^{1^4} + \mathrm{a}_3 I_v^{1^3} + \mathrm{a}_2 I_v^{1^2} + \mathrm{a}_1 I_v^1 + \mathrm{a}_0\right) I_v^1 = 0 \tag{11}$$

where

$$\begin{aligned}
\mathrm{a}_0 &= d_1d_2d_3d_4\mathrm{d}_5d_6C_0M_0K\Lambda_1 - Kk_1k_2k_3k_4\omega_2d_1d_6M_0\Lambda_1\cdot Kd_1d_2d_3\omega_2d_6\varepsilon C_0M_0\Lambda_1\Lambda_2\\
\mathrm{a}_1 &= \mathrm{d}_5(d_1d_2d_3d_4\mathrm{d}_5d_6C_0M_0K\Lambda_1 + M_0C_0d_3d_4d_6\Lambda_1(Kd_1d_2\omega_2+k_1k_2\omega_2)+\varepsilon\omega_2M_0C_0d_6d_4d_3d_1K\Lambda_1\\
&\quad+\varepsilon\Lambda_2Kk_1k_2k_3\omega_2C_0d_1d_6\Lambda_1) - Kk_1k_2k_3k_4\omega_2d_1d_6M_0\Lambda_1\\
&\quad-Kk_1k_2k_3k_4\omega_2d_1\varepsilon C_0\Lambda_1\cdot Kd_1d_2d_3\omega_2d_6\varepsilon C_0M_0\Lambda_1\Lambda_2\\
\mathrm{a}_2 &= \mathrm{d}_5(d_1d_2d_3d_4\mathrm{d}_5d_6C_0M_0K\Lambda_1 + M_0C_0d_3d_4d_6\Lambda_1(Kd_1d_2\omega_2+k_1k_2\omega_2)+\varepsilon\omega_2M_0C_0d_6d_4d_3d_1K\Lambda_1\\
&\quad+\varepsilon\Lambda_2Kk_1k_2k_3\omega_2C_0d_1d_6\Lambda_1 + M_0C_0d_3d_4d_6\Lambda_1(Kd_1d_2\omega_2+k_1k_2\omega_2)+\varepsilon Kk_1k_2k_3\omega_2C_0d_1d_6\Lambda_1)\\
&\quad-\varepsilon M_0C_0d_1d_6\Lambda_1\Lambda_2(Kd_1d_2\omega_2+k_1k_2\omega_2)+M_0C_0d_1d_2^2d_3^2K\Lambda_2\\
&\quad+\varepsilon\Lambda_2Kk_1k_2k_3\omega_2C_0d_1d_6\Lambda_1(Kk_1k_2k_3k_4\omega_2d_1d_6M_0\Lambda_1+Kk_1k_2k_3k_4\omega_2d_1\varepsilon C_0\Lambda_1)\\
\mathrm{a}_3 &= \mathrm{d}_5(M_0C_0d_3d_4d_6\Lambda_1(Kd_1d_2\omega_2+k_1k_2\omega_2)+\varepsilon\omega_2M_0C_0d_6d_4d_3d_1K\Lambda_1+\varepsilon\Lambda_2Kk_1k_2k_3\omega_2C_0d_1d_6\Lambda_1\\
&\quad+M_0C_0d_3d_4d_6\Lambda_1(Kd_1d_2\omega_2+k_1k_2\omega_2)+\varepsilon Kk_1k_2k_3\omega_2C_0d_1d_6\Lambda_1)\\
&\quad-Kk_1k_2k_3k_4\omega_2d_1\varepsilon C_0\Lambda_1\cdot(M_0d_1d_3\varepsilon\omega_2\Lambda_1\Lambda_2(Kd_1d_2\omega_2+k_1k_2\omega_2)+\varepsilon Kk_1k_2k_3\omega_2C_0d_1d_6\Lambda_1)\\
\mathrm{a}_4 &= \mathrm{d}_5(M_0C_0d_3d_4d_6\Lambda_1(Kd_1d_2\omega_2+k_1k_2\omega_2)+\varepsilon Kk_1k_2k_3\omega_2C_0d_1d_6\Lambda_1)(M_0C_0d_3d_4d_6\Lambda_1(Kd_1d_2\omega_2+k_1k_2\omega_2)\\
&\quad+\varepsilon\omega_2M_0C_0d_6d_4d_3d_1K\Lambda_1)\\
k_1 &= (1-\alpha\alpha_h)\beta_1, k_2 = \rho\theta_h(1-\alpha\alpha_h), k_3 = N_E\omega_1, k_4 = (1-b\alpha_v)\beta_2, d_1 = (v_1+\delta_1+\psi),
\end{aligned}$$

$d_2 = (\omega_1+v_3), d_3 = (v_4+\sigma_m), d_4 = (v_2+\sigma_s), \mathrm{d}_5 = (v_2+\delta_2+\sigma_I), \mathrm{d}_6 = (v_5+\sigma_c)$. Equation (11) has one of the solutions $I_v^1 = 0$, which corresponds to a disease-free equilibrium. Other solutions can be determined according to the sign rule of Descartes [41], which states that depending on the change in the sign of the coefficients, a_0, a_1, a_2, and a_3, 3, 2, or 1 positive solutions exist; thus, the proof for existing conditions for E_1 for the model Equations (1)–(7) is complete.

In addition, the stability of the model system depends on the parameters used to build the model and the changes in these parameters affect R_0, with numerous scientific and biological implications for the transmission and control of the disease. For instance, if we use $\beta_1 = \beta^*$ as the bifurcation parameter for model Equations (1)–(7), then $R_0 = 1$ and

$$\beta^* = \frac{\upsilon_1\upsilon_2 M_o C_o(\upsilon_1+\delta_1+\psi)(\upsilon_2+\delta_2+\sigma_I)(\omega_1+\upsilon_3)(\upsilon_4+\sigma_m)(\upsilon_5+\sigma_c)}{\rho\theta_h N_E\omega_1\omega_2\beta_2\Lambda_1\Lambda_2(1-b\alpha_v)(1-\alpha\alpha_h)^2 e^{-\upsilon_1 x}}$$

is the crucial bifurcation value for cercaria-to-human transmission. When $R_0 < 1$ and $\beta_1 < \beta^*$, for instance, only the asymptotically stable disease-free equilibrium point (E_0) can exist, and R_0 provides conditions for disease extinction. The disease-free equilibrium is unstable, whereas the endemic equilibrium (E_1) is asymptotically stable, and both equilibrium points exist when $R_0 > 1$ and $\beta_1 > \beta^*$ [40], and in this case, R_0 provides the conditions for the disease to persist. Thus, the asymptotic dynamic behavior of the infectious disease, which determines whether it will vanish or persist in the future, can be inferred from the steady states. Although we do not provide a stability analysis of the equilibrium points, we acknowledge that control strategies have a role to play in reducing R_0 and possibly eliminating schistosomiasis.

2.5. Parameter Data

For our study, we use data collected in the literature related to *Bulinus* and *Biomphalaria* (Table 2). In the absence of published data, parameter values are assumed or estimated based on expert knowledge using what is commonly known about vector and disease dynamics, as follows. The life expectancy of an adult *Schistosoma* worm within a human host is 3–10.5 years [42–44]; thus, δ_1 vary from $1/(10.5\times 365) \approx 0.000268$ to $1/(3\times 365) \approx 0.000913$. In addition, Dabo et al. [45] establish schistosomiasis infection in preschool children aged 1–4 years through both passive and active exposure to infected water bodies. On average, a child's initial infection age is 2 years [43]; thus, $x = 2\times 365 = 730$ days. Gryseels et al. [46] reported 2–10 weeks as the period a schistosomiasis patient takes to recover after chemotherapy treatment. Thus, we assume that the recovery period for a schistosomiasis patient varies between 14 and 70 days, which sets ψ between $\psi = 1/14 \approx 0.0714$ and $\psi = 1/70 \approx 0.0143$ individuals per day. The *Schistosoma* parasite egg can stay for 7 days, with a 0.14286 per egg death rate, and miracidia survive 12 days in freshwater ($\upsilon_3 = 1/12 \approx 0.0833$) [46,47]. Cercaria can only spend 10–40 h in freshwater [48], which sets υ_4 between $\upsilon_4 = 1/(10\times 24) \approx 0.00417$ and $\upsilon_4 = 1/(40\times 24) \approx 0.00104$. Table 2 shows the numerical values (and potential ranges) of parameters set for the model system Equations (1)–(7) from the literature and estimations.

Table 2. Model parameters, their definition, baseline values, potential ranges, and sources.

Parameter	Definition	Baseline Value	Values Range/Day	References
Λ_1	Human recruitment rate	4127	254–8000	[18,49]
Λ_2	Snail recruitment rate	200	200	[18]
x	Initial age of infection in children	730 d	730 d	[33,46]
δ_1	The human death rate due to infection	0.0039	0.0039	[50]
υ_1	Natural death rate of human	0.00004025	0.0000384–0.0000421	[18,41]
ρ	Proportion of stool/urine per person	115 g	70–160 g	[51]
θ_h	Number of egg parasites in stool/urine	262 g^{-1}	10–513 g^{-1}	[51]
ω_1	Miracidia emergence rate	0.00232	0.00232	[52]
υ_2	Natural death rate of IHs	0.01110	0.004–0.0182	[52]
υ_3	Natural death rate of parasite eggs	0.07193	0.001–0.14286	[44,46,49]
υ_4	Natural death rate of miracidia	0.49165	0.0833–0.9	[46,49]
υ_5	Nautral death rate of cercaria	0.002605	0.00104–0.00417	[52]

Table 2. *Cont.*

Parameter	Definition	Baseline Value	Values Range/Day	References
N_E	Number of miracidia released per egg	500	500	[52]
β_1	Cercaria-human infection rate	0.0750	0.028–0.122	[52]
β_2	Miracidia-snail infection rate	0.001235	0.000127–0.615	[52]
ω_2	Cercaria shedding rate	2.6	2.6	[19,49]
δ_2	Snail death rate due to infection	0.026	0.002–0.05	[52]
K	Parasite egg carrying capacity	100,000	100,000	Estimated
C_o	Saturation coefficient for miracidia infectivity	1,000,000		Estimated
M_o	Saturation coefficient for cercaria infectivity	1,000,000		[19]
ε	limitation of miracidia the growth velocity	0.25	0.2–0.3	[18,19]
$\psi, \alpha, \alpha_h, b, \alpha_v$	Effective rates of control strategies	0.5	0–1	Varied
$\sigma_s, \sigma_I, \sigma_m, \sigma_c$	Chemical-induced death rates	0.5	0–1	Varied

We performed a numerical simulation using the main R package ODE solver Version 1.10-4 for solving ordinary differential equations [53] in the R statistical environment version 4.0.3 [54]. The baseline values in Table 2 were used for all simulations and predictions. We conducted a sensitivity analysis of R_0 with respect to the baseline value using the Partial Rank Correlation Coefficients (PRCC) test to determine how robust our predictions are to changes in parameter values. In this way, we can determine quantitatively which key parameters can be targeted by control measures to reduce disease the most. For instance, R_0 increases when parameters with positive PRCC values are increased, increasing the likelihood of infection.

3. Results

The results show that the key parameters (bold in Table 3) that have the greatest influence on the transmission of the disease include the recruitment rate of human individuals Λ_1, a portion of stool/urine per infected person ρ, number of miracidia per parasite egg N_E, cercaria-to-human transmission per contact β_1, rate of miracidia-to-snail transmission per contact β_2, and rate of cercaria emergence from infected snails ω_2.

Table 3. The partial rank correlation coefficients for the baseline parameter values for R_0 (without control) as a response function, with the most significant parameters that influence the dynamics of the model highlighted in bold.

Parameter	$\mathbf{\Lambda_1}$	Λ_2	x	δ_1	υ_1	$\boldsymbol{\rho}$	θ_h	ω_1	υ_2	υ_3
R_0	**+0.8338**	+0.0451	+0.0195	−0.0089	−0.7899	**+0.7725**	+0.7545	+0.5504	−0.8636	−0.7537
Parameter	υ_5	N_E	$\boldsymbol{\beta_1}$	$\boldsymbol{\beta_2}$	$\boldsymbol{\omega_2}$	δ_2	C_o	M_o	ε	υ_4
R_0	−0.5777	**+0.8186**	**+0.7607**	**+0.7928**	**+0.8005**	−0.6731	−0.7799	−0.8032	−0.0481	−0.8303

The model system Equations (1)–(7) is solved numerically using the initial conditions $S_h(0) = 100,000$, $S_h(0) = 100,000$, $I_h(0) = 1$, $E_h(0) = 0$, $M_f(0) = 0$, $S_v(0) = 100,000$, $I_v(0) = 1$, and $C_f(0) = 0$, and the effects of different control strategies on the targetted human and snail populations are shown graphically in Figure 2. When a chemotherapy treatment of the infected humans is integrated with public literacy (two-tiered approach), the strategy is more successful in managing and reducing disease morbidity in the human population than when each strategy is carried out separately, i.e., the number of infected humans who recover, reduce, and join the susceptible humans, who grow in number

(Figure 2a,b). Chemical/molluscicide control significantly increases IHs mortality, and when paired with a mechanical technique, this effect is essentially identical (Figure 2c,d).

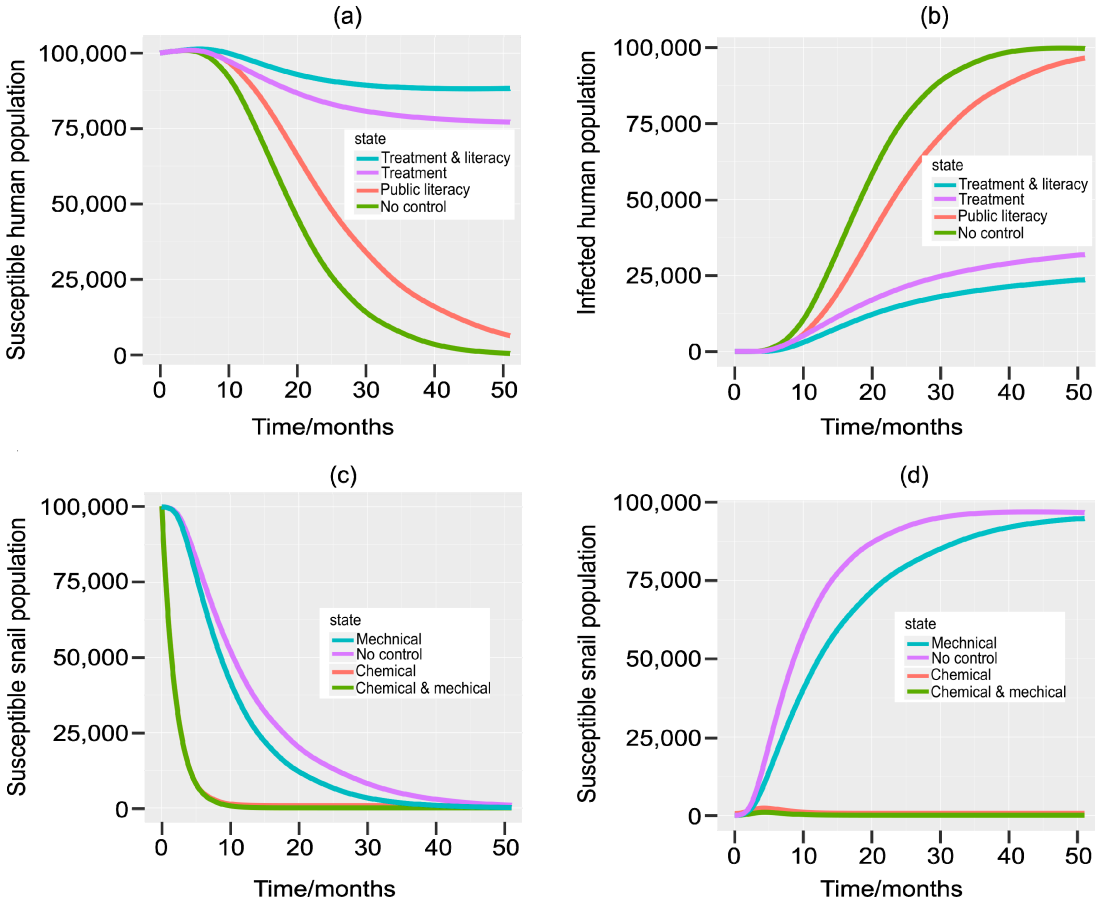

Figure 2. Comparisons between treatment and public literacy targeting the populations of (**a**) susceptible humans, (**b**) infected humans, and molluscicide (chemical) and the mechanical strategies targeting (**c**) susceptible snails and (**d**) infected snails of schistosomiasis in contrast with no control measures.

The impact of individual control measures and various combinations of all control measures on disease transmission is determined by the value of R_0, as shown in Table 4. The more successful a certain level of control is, the smaller the value of R_0. We show that when a single control strategy is used, the chemical/molluscicides strategy ($\sigma_{I,M,C}$) has a greater impact on reducing the value of R_0 followed by the chemotherapy treatment strategy (ψ), public literacy ($\alpha\alpha_h$), and finally mechanical control ($b\alpha_v$). However, a single intervention cannot eradicate the disease, $R_0 \not< 1$: see Table 4. The results of integrating the various strategies show that a combination of two-tiered control measures, treatment strategies (ψ), and molluscicides ($\sigma_{I,M,C}$) have the greatest impact compared to any other pair of strategies (Table 4). Moreover, a combination of a three-tiered approach: treatment (ψ), molluscicides ($\sigma_{I,M,C}$), and mechanical ($b\alpha_v$), as well as another three-tiered approach: public literacy ($\alpha\alpha_h$), molluscicides ($\sigma_{I,M,C}$), and mechanical ($b\alpha_v$) have the potential to lower R_0 below 1, but only if the effectiveness of each separate control is greater than 90% (Table 4). However, schistosomiasis can be eradicated, $R_0 < 1$, if a four-tiered approach (treatment, public literacy, molluscicides, and mechanical) is applied, with each method being more than 70% effective when combined (Table 4).

Table 4. The variability of R_0 across rows for a single or different combination of control strategies, $\psi, \alpha, \alpha_h, \sigma_I, \sigma_M, \sigma_C, b, \alpha_v \in [0,1]$. The lower the R_0, the more successful the strategy(s) are in controlling schistosomiasis.

Control strategies as Functions of R_0	**Effectiveness of Control Strategies; ψ, α, α_h, σ_I, σ_M, σ_C, b, and α_v**										
	0	**0.1**	**0.2**	**0.3**	**0.4**	**0.5**	**0.6**	**0.7**	**0.8**	**0.9**	**1**
$R_0(\psi)$	10,000	1947	1390	1139	988	884	808	748	700	660	643
$R_0(\alpha\alpha_h)$	10,000	9900	9600	9100	8400	7500	6400	5100	3600	1900	975
$R_0(b\alpha_v)$	10,000	9950	9798	9539	9165	8660	8000	7141	6000	4359	3122
$R_0(\sigma_{I,M,C})$	10,000	295	138	86.9	61.6	46.8	37.2	30.6	25.7	22.0	20.5
$R_0(\psi, \alpha\alpha_h)$	10,000	1928	1334	1036	830	663	517	382	252	125	62.7
$R_0(b\alpha_v, \sigma_{I,M,C})$	10,000	294	136	82.9	56.5	40.5	29.8	21.8	15.4	9.6	6.401
$R_0(\psi, \sigma_{I,M,C})$	10,000	57.4	19.3	9.9	6.1	4.1	3.0	2.3	1.8	1.5	1.3
$R_0(\psi, b\alpha_v)$	10,000	1937	1362	1086	905	766	646	534	420	288	201
$R_0(\alpha\alpha_h, \sigma_{I,M,C})$	10,000	292	133	79.1	51.7	35.1	23.8	15.6	9.3	4.2	1.9
$R_0(\alpha\alpha_h, b\alpha_v)$	10,000	9850	9406	8681	7699	6495	5120	3642	2160	828	304
$R_0(\psi, \alpha\alpha_h, \sigma_{I,M,C})$	10,000	292	133	79.1	51.7	35.1	23.8	15.6	9.3	4.2	1.9
$R_0(\psi, \alpha\alpha_h, b\alpha_v)$	10,000	9850	9406	8681	7699	6495	5120	3642	2160	828	304
$R_0(\psi, \sigma_{I,M,C}, b\alpha_v)$	10,000	57.1	18.8	9.4	5.6	3.6	2.4	1.6	1.1	0.63	0.41
$R_0(\alpha\alpha_h, \sigma_{I,M,C}, b\alpha_v)$	10,000	291	130	75.5	47.4	30.4	19.1	11.1	5.5	1.8	0.62
$R_0(\psi, \alpha\alpha_h, \sigma_{I,M,C}, b\alpha_v)$	10,000	56.6	18.1	8.6	4.7	2.7	1.5	0.83	0.39	0.12	0.04

When considering mortality rate functions (Table 1), we show that temperature, the length of chemical exposure, and the chemical's half-life affect the molluscicide performance on the death rates of targeted species. In general, chemical-induced mortality rates for targeted species (host snails and free-living *Schistosoma* cercaria and miracidia) decline as the temperature increases. However, the decline is more rapid when the half-life of molluscicides decreases, i.e., shorter half-lived molluscicides (e.g., non-persistent and persistent molluscicides) lose their toxicity sooner, leading to lower mortality rates. For instance, Figure 3a shows how temperature control impacts the half-life of molluscicides and the consequent mortality rate of susceptible snails. In the same context, chemical-induced mortality rates decrease with an increase in the duration of molluscicide exposure. Molluscicides with a longer half-life (very persistent molluscicides) remain in the environment longer, resulting in a higher mortality rate compared to molluscicides with a shorter half-life (Figure 3b). Thus, increasing the half-life of molluscicides increases the chemically induced mortality rates, especially for cercariae σ_c, and infected snails σ_I (Figure 3c). As a result, increasing the temperature and days of chemical exposure decreases the mortality rate of snails (Figure 3d) associated with higher risks of disease transmission, thus increasing the R_0 value (Figure 3e).

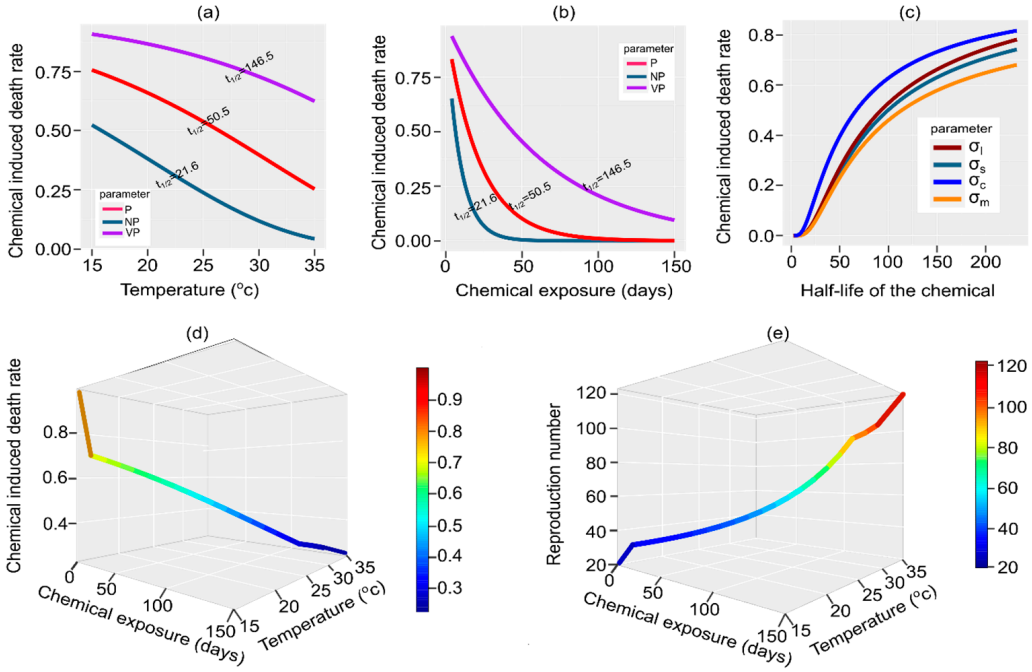

Figure 3. Various molluscicides are regulated by temperature according to their half-lives and durations of chemical exposure to snails. A molluscicide is classified as a non-permanent molluscicide (NP) with a half-life of $t_{1/2} = 21.6$, a persistent molluscicide (P) with a half-life of $t_{1/2} = 50.5$, or a very-permanent molluscicide (VP) with a half-life of $t_{1/2} = 146.5$. (**a**) Shows variations in the temperature of the environment and the duration of chemical exposure (**b**) for different chemicals affecting the death rate of targeted host snails. (**c**) Shows the effect of chemicals with different half-lives on the death rate of different target species (susceptible snails σ_s, infected snails σ_I, cercaria σ_c, and miracidia σ_m). At the same time, the effect of combined chemical exposure and temperature on the death rate of host snails and the subsequent reproduction number is shown in (**d**,**e**).

4. Discussion

We formulate a mathematical model to assess the effectiveness of methods that target humans and those targeting IHs in the control of schistosomiasis. The results of the PRCC test suggest that control strategies focusing on the key parameters N_E, β_1, β_2, and ω_2 in the transmission dynamics may be more effective in reducing R_0 and may result in disease-free conditions of $R_0 < 1$, indicating disease control. Our results show that the chemotherapy treatment strategy (reducing N_E) and application of molluscicides (reducing β_1, β_2, and ω_2) are the most successful methods for reducing R_0 and disease morbidity among the human population and increasing snail mortality, respectively, when applied independently and compared to mechanical control (reducing ω_2) and public literacy (reducing β_1 and β_2) with limited impact. But each strategy cannot eradicate schistosomiasis individually, which complements the finding by Mangal et al. [52], King and Bertsch [9], and Zacharia et al. [10]. Thus, a single approach may reduce morbidity [2,55] but often without reducing the local and environmental transmission of parasites [6], which contributes to the development of the disease. In addition, chemotherapy has shown ineffectiveness against juvenile worms within the body. This is the reason why worms inside infected and treated children can continue to release eggs, observed in their feces three weeks after the drug has been administered [56–58]. This thus perpetuates local transmission, and residents who stay in endemic areas run the risk of re-infection [6,59]. The fragility of drug control alone is demonstrated by this.

On the other hand, mechanical control practices like the physical picking of snails are considered old-fashioned but prove to be a good complementary strategy to drugs, molluscicides, and public literacy [17]. However, its use may be limited, especially in large water bodies, such as lakes, rivers, and streams, or where a larger number of aquatic

inhabitants must be controlled. In addition, public literacy advocates for significant behavior change in water use and contact. However, this ultimately requires the provision of safe and hygienic alternative water supplies, latrines, and washing facilities. When compared to using individual control strategies, integrated strategies are far more effective. Our study further shows that when a four-tiered control strategy is used, the results are much better than using one-, two- or three-tiered controls. Although a three-tiered strategy would be effective as well, it is practically difficult to achieve 90% effectiveness from each method. These findings support, to a certain extent, the findings of Mangal et al. [52], Thétiot-Laurent et al. [56], Lo et al. [58], and Zheng et al. [13], which suggest that the integrated intervention of chemotherapy and snail management has a greater impact on schistosomiasis control than a single method like chemotherapy treatment alone.

However, in such integrated efforts to control schistosomiasis, the time and season of application of molluscicides are crucial. This is relevant in providing a realistic assessment of the spread of schistosomiasis under the current and projected temperature increases in areas like sub-Saharan Africa, where the disease is most prevalent. Our results corroborate with the reports by Feng et al. [60], Fishel [25], Ziska [26], and Zheng et al. [13] that the temperature of the environment, chemical degradation, and half-life of the chemical are important factors in the chemical control of snails. Regardless of the chemical type used, non-persistent (NP), persistent (P), or very persistent (VP), the results show that the chemical strategy may be more effective in areas with low temperatures (15–25 °C). In the first two weeks (14 days) of application, the chemically induced mortality rate of snails is significantly higher, especially for cercariae and infected snails, and consequently, R_0 is less than at unity, indicating disease control. This corroborates the finding by Montanari et al. [33] that, at a standard temperature of 25 °C, molluscicides proved to be effective against adult snails; the snails reduced their food intake and stopped eating, whereas the same effects were significantly stronger at 18 °C. No effects on survival or feeding rate have been recorded at incubations of 30 °C. In regions with higher temperatures, an even longer treatment period using NP chemicals is associated with low rates of induced mortality and is, therefore, less effective in reducing snails, free-living parasite populations, and R_0. The results also show that the molluscicides NP, P, and VP with increasing half-lives reduce species mortality by more than 50% only up to 2 weeks, 3 weeks, and 6 weeks, respectively, suggesting that the chemical should be reapplied regularly thereafter. Thus, the half-life of the molluscicide is directly proportional to the active length of the molluscicides in the water. This result supports the finding of Seligman et al. [61], who observed that the half-lives/chemical degradation of different chemicals ranges from 4 to 19 days and up to several months under specific conditions. For efficient snail management, integration efforts, and schistosomiasis control, different areas with varying weather patterns and seasonal variations may require different molluscicide-type and variable time intervals of reapplication.

Therefore, it is critical to quantify the use of chemical control agents in response to climatic conditions to determine alternative changes in the target intermediate host population and the best season (temperature) for control. This result complements the efforts to investigate molluscicidal action, the structure-activity relationship, and the potential mechanisms of several molluscicides [13,14,62] toward developing suitable chemicals.

Our findings, thus, demonstrate that effective schistosomiasis control programs necessitate a co-ordinated effort and comprehensive integration of preventative treatment, public literacy, and mechanical and molluscicide controls. Despite the promising results, we believe that controlling schistosomiasis with fewer than three different combinations of control strategies will be challenging and may not be worth the effort to eradicate schistosomiasis compared to when the four strategies are integrated and carried out simultaneously. However, achieving the schistosomiasis eradication goal may require a large investment of resources (high cost, which severely limits the use of the molluscicide on a big scale), time, and commitment, and also has associated ecological risks. For instance, chemical management has several negative effects, including the destruction of aquatic biodiversity due to toxicity [63] and the emergence of snail resistance to the chemicals are very likely.

If chemicals are released into the environment, local people will not be able to use the water [13,64]. Several molluscicides have a half-life that ranges from 3.17 to 223 days [65], while others have a half-life of up to 2 years. This means that the presence of molluscicides in water would continue to pose a health risk to people for more than 30 years before it decays completely [61].

Furthermore, the development and use of molluscicide need to be blended with an increase in health education and an assessment of their levels of toxicity when ingested by humans and domestic animals through agricultural products and their effect on non-target aquatic fauna and flora [13]. However, our results suggest that chemicals with shorter half-lives, such as an extract from *C. viminalis* fruits, or natural insecticides, such as *Nereistoxin,* are effective in killing snails at low concentrations in a shorter amount of time [13,66]. They could provide an alternative to long-term exposures to common molluscicides with less effects on biodiversity. Furthermore, specific molluscicides, such as nicotinanilide molluscicides and silver (Ag) nanopowder (Ag-NPs) molluscicides [13], have been shown to exhibit strong molluscicidal effects with less toxicity to humans, animals, fish, and plants, can be applied in small waterbodies to manage snail populations despite their high cost and strong human skin irritant effects. The effect of change in temperature on the environment on molluscicide performance greatly affects the mortality rate of the targeted organism (IHs, cercariae, and miracidia) and general disease transmission. Therefore, better molluscicide performance should be achieved by developing harmless, low-toxicity, and temperature-dependent molluscicides, with low environmental impact to control the targeted species holistically.

Our study has some limitations given that the parameters that best reflect the biological representation and real-life situations of schistosomiasis disease and transmission had to be used based on the published record. Since neither the *Biomphalaria-S. mansoni* nor the *Bulinus-S. haematobium* infection system had a complete list of genus-specific model parameters, we used published parameter values for both infection systems. Due to the absence of specifically published data relating to the two systems, two parameter values were estimated, and two others were assumed based on expert knowledge. Furthermore, the literature data are not always consistent and are collected under different conditions. Nonetheless, the baseline values of such parameters provide a good first approximation of the parameter values, and the model can be used generally to develop a better understanding of the effects of interventions. This model can be improved to incorporate more features, such as the effect of temperature and molluscicides on the development of eggs into miracidia, snail recruitment, and biodiversity of nontarget species.

5. Conclusions

We conclude that the proposed model provides valuable mechanistic insights into how the impact of schistosomiasis and future control programs will depend on the integration of chemotherapy, public literacy, and mechanical and molluscicide types in different endemic regions. In addition, molluscicide performances in different regions with changing temperatures will vary depending on their type and half-life, degradation rate, and reapplication frequency.

Author Contributions: Conceptualization, Z.T.; Methodology, Z.T. and C.K.; Formal analysis, Z.T.; Funding acquisition, L.B. and C.A.; Supervision, C.A. and L.B.; Visualization, Z.T.; Writing—original draft, Z.T.; Writing—review & editing, Z.T., C.K., L.B. and C.A. All authors have read and agreed to the published version of the manuscript.

Funding: The German Academic Exchange Service (DAAD) supported Z.T with a Ph.D. scholarship (Grant No. 57507871). The Alexander von Humboldt Foundation supported C.K as a Georg Forster Research Fellow with a scholarship for his research visit and stay at Justus Liebig University Giessen. (Grant No. ZMB1217528GF-P). The funders had no role in study design, data collection or analysis, the decision to publish, or the preparation of the manuscript.

Data Availability Statement: All data generated or analyzed during this study are included in this published article.

Acknowledgments: It is with great gratitude that the authors acknowledge the German Academic Exchange Service (DAAD) for providing Z.T. with a Ph.D. scholarship, as well as Alexander von Humboldt Foundation for providing C.K. with a scholarship.

Conflicts of Interest: The authors declare that they do not have any competing interests.

Appendix A

Invariant region

In model system Equations (1)–(7), we prove that non-negative and bounded solutions exist in Ω, as follows:

Let $\mathcal{L}(t) = \Big[S_h(t), I_h(t), E_h(t), M_f(t), S_v(t), I_v(t), C_f(t)\Big]^T \subset \mathbb{R}^7_+$ be the solution set of the model equations Equations (1)–(7) from which $\mathcal{L}(0) \geq 0$ are the non-negative initial conditions.

Lemma A1. *$\mathcal{L}(t)$is non-negative in $\Omega \subset \mathbb{R}^7_+$ with $\mathcal{L}(0) \geq 0$ for $\forall t \geq 0$.*

Proof. It is evident from model equation Equation (1) that

$\dot{S_h}(t) \geq -\Big(\frac{(1-\alpha\alpha_h)\beta_1 C_f}{C_o+\varepsilon C_f} + v_1\Big)S_h$, where $S_h(t) \geq S_h(0)e^{(\frac{(1-\alpha\alpha_h)\beta_1 C_f}{C_o+\varepsilon C_f}+v_1)t}$, $\forall t \geq 0$.

Thus, $S_h(t) \geq 0$ is non-negative and, in the same way, it can be shown that $I_h(t) \geq 0$, $E_h(t) \geq 0, M_f(t) \geq 0, S_v(t) \geq 0, I_v(t) \geq 0$, and $C_f(t) \geq 0$. Therefore, $\mathcal{L}(t)$ in the region $\Omega \subset \mathbb{R}^7_+$ is positively invariant. □

Lemma A2. *$\mathcal{L}(t)$ remains bounded in $\Omega \subset \mathbb{R}^7_+$.*

Proof. Let the total human population $S_h(t) + I_h(t) = N_h(t)$, and the total snail population $S_v(t) + I_v(t) = N_v(t)$, such that $\dot{N_h}(t) \leqslant \Lambda_1 e^{-v_1 x} - v_1 N_h(t)$ and $\dot{N_v}(t) \leqslant \Lambda_2 - v_2 N_v(t)$ and $\mathcal{L}(t) = \Big[N_h(t), E_h(t), M_f(t), N_v(t), C_f(t)\Big]^T$. Thus, $\mathcal{L}(t)$ can be expressed analytically as follows:

$$\mathcal{L}(t) = \begin{cases} N_h(t) \leqslant \frac{\Lambda_1 e^{-v_1 x}}{v_1} - \Big(\frac{\Lambda_1 e^{-v_1 x}}{v_1} - N_h(0)\Big)e^{-v_1 t} \\ E_h(t) \leqslant K - (K - E_h(0))e^{\rho\theta_h(1-\alpha\alpha_h)I_h t} \\ M_f(t) \leqslant \frac{N_E\omega_1 E_h}{(v_4+\sigma_m)} - \Big(\frac{N_E\omega_1 E_h}{(v_4+\sigma_m)} - M_f(0)\Big)e^{-(v_4+\sigma_m)t} \\ N_v(t) \leqslant \frac{\Lambda_2}{v_2} - \Big(\frac{\Lambda_2}{v_2} - N_v(0)\Big)e^{-v_2 t} \\ C_f(t) \leqslant \frac{\omega_2 I_v}{(v_5+\sigma_c)} - \Big(\frac{\omega_2 I_v}{(v_5+\sigma_c)} - C_f(0)\Big)e^{-(v_5+\sigma_c)t} \end{cases}$$

Assuming $N_h(0) \leqslant \frac{\Lambda_1 e^{-v_1 x}}{v_1}$, and $N_v(0) \leqslant \frac{\Lambda_2}{v_2}$, we conclude that $\lim_{t\to\infty} Sup N_h(t) = \frac{\Lambda_1 e^{-v_1 x}}{v_1}$, and $\lim_{t\to\infty} Sup N_v(t) = \frac{\Lambda_2}{v_2}$, and therefore, both human ($S_h(t), I_h(t)$) and snail ($S_v(t)$, $I_v(t)$) populations are biologically feasible. Similarly $\lim_{t\to\infty} Sup\Big[E_h(t), M_f(t), C_f(t)\Big]^T = \Big[K, \frac{N_E\omega_1 E_h}{(v_4+\sigma_m)}, \frac{\omega_2 I_v}{(v_5+\sigma_c)}\Big]^T$, shows that the egg, miracidia, and cercaria populations are biologically feasible. Thus, $\mathcal{L}(t)$ with initial conditions remains bounded for all $t \geq 0$. □

As a result of Lemmas A1 and A2, our model is epidemiologically and mathematically well-posed.

References

1. Adenowo, A.F.; Oyinloye, B.E.; Ogunyinka, B.I.; Kappo, A.P. Impact of human schistosomiasis in sub-Saharan Africa. *Braz. J. Infect. Dis.* **2015**, *19*, 196–205. [CrossRef]
2. WHO, World Health Organization. Schistosomiasis. Available online: https://www.who.int/news-room/fact-sheets/detail/schistosomiasis (accessed on 3 February 2023).
3. Wang, L.; Utzinger, J.; Zhou, X.-N. Schistosomiasis control: Experiences and lessons from China. *Lancet* **2008**, *372*, 1793–1795. [CrossRef]
4. Rosenberg, M.; Utzinger, J.; Addiss, D.G. Preventive chemotherapy versus innovative and intensified disease management in neglected tropical diseases: A distinction whose shelf life has expired. *PLoS Negl. Trop. Dis.* **2016**, *10*, e0004521. [CrossRef] [PubMed]
5. WHO, World Health Organization. Elimination of Schistosomiasis. *Sixty-Fifth World Health Assembly, WHA65. 21, Agenda item 13.11*. 26 May 2012. Available online: http://apps.who.int/gb/ebwha/pdf_files/WHA65/A65_R21-en.pdf (accessed on 23 February 2023).
6. French, M.D.; Churcher, T.S.; Gambhir, M.; Fenwick, A.; Webster, J.P.; Kabatereine, N.B.; Basáñez, M.-G. Observed reductions in *Schistosoma mansoni* transmission from large-scale administration of praziquantel in Uganda: A mathematical modelling study. *PLoS Negl. Trop. Dis.* **2010**, *4*, e897. [CrossRef] [PubMed]
7. Stothard, J.R.; Chitsulo, L.; Kristensen, T.K.; Utzinger, J. Control of schistosomiasis in sub-Saharan Africa: Progress made, new opportunities and remaining challenges. *Parasitology* **2009**, *136*, 1665–1675. [CrossRef]
8. Hotez, P.J.; Molyneux, D.H.; Fenwick, A.; Kumaresan, J.; Sachs, S.E.; Sachs, J.D.; Savioli, L. Control of neglected tropical diseases. *N. Engl. J. Med.* **2007**, *357*, 1018–1027. [CrossRef] [PubMed]
9. King, C.H.; Bertsch, D. Historical perspective: Snail control to prevent schistosomiasis. *PLoS Negl. Trop. Dis.* **2015**, *9*, e0003657. [CrossRef]
10. Zacharia, A.; Mushi, V.; Makene, T. A systematic review and meta-analysis on the rate of human schistosomiasis reinfection. *PLoS ONE* **2020**, *15*, e0243224. [CrossRef] [PubMed]
11. Madsen, H. Biological methods for the control of freshwater snails. *Parasitol. Today* **1990**, *6*, 237–241. [CrossRef]
12. Sokolow, S.H.; Huttinger, E.; Jouanard, N.; Hsieh, M.H.; Lafferty, K.D.; Kuris, A.M.; Riveau, G.; Senghor, S.; Thiam, C.; N'Diaye, A.; et al. Reduced transmission of human schistosomiasis after restoration of a native river prawn that preys on the snail intermediate host. *Proc. Natl. Acad. Sci. USA* **2015**, *112*, 9650–9655. [CrossRef]
13. Zheng, L.; Deng, L.; Zhong, Y.; Wang, Y.; Guo, W.; Fan, X. Molluscicides against the snail-intermediate host of Schistosoma: A review. *Parasitol. Res.* **2021**, *120*, 3355–3393. [CrossRef] [PubMed]
14. King, C.; Sutherland, L.J.; Bertsch, D. Systematic review and meta-analysis of the impact of chemical-based molluscicide for control of *Schistosoma mansoni* and *S. haematobium* transmission. *PLoS Negl. Trop. Dis.* **2015**, *9*, e0004290. [CrossRef]
15. Lo, N.C.; Gurarie, D.; Yoon, N.; Coulibaly, J.T.; Bendavid, E.; Andrews, J.R.; King, C.H. Impact and cost-effectiveness of snail control to achieve disease control targets for schistosomiasis. *Proc. Natl. Acad. Sci. USA* **2018**, *115*, E584–E591. [CrossRef]
16. WHO, World Health Organization. *Field Use of Molluscicides in Schistosomiasis Control Programmes: An Operational Manual for Programme Managers*; Licence: CC BY-NC-SA 3.0 IGO; World Health Organization: Geneva, Switzerland, 2017.
17. Sokolow, S.H.; Wood, C.L.; Jones, I.J.; Lafferty, K.D.; Kuris, A.M.; Hsieh, M.H.; De Leo, G.A. To reduce the global burden of human schistosomiasis, use 'old fashioned' snail control. *Trends Parasitol.* **2017**, *34*, 23–40. [CrossRef]
18. Chiyaka, E.T.; Garira, W. Mathematical analysis of the transmission dynamics of schistosomiasis in the human-snail hosts. *J. Biol. Syst.* **2009**, *17*, 397–423. [CrossRef]
19. Gao, S.; Liu, Y.; Luo, Y.; Xie, D. Control problems of a mathematical model for schistosomiasis transmission dynamics. *Nonlinear Dyn.* **2010**, *63*, 503–512. [CrossRef]
20. Abokwara, A.; Madubueze, C.E. The Role of Non-pharmacological Interventions on the Dynamics of Schistosomiasis. *J. Math. Fundam. Sci.* **2021**, *53*, 243–260. [CrossRef]
21. Nur, W.; Trisilowati; Suryanto, A.; Kusumawinahyu, W.M. Mathematical model of schistosomiasis with health education and molluscicide intervention. *J. Phys. Conf. Ser.* **2021**, *1821*, 012033. [CrossRef]
22. Stensgaard, A.-S.; Booth, M.; Nikulin, G.; McCreesh, N. Combining process-based and correlative models improves predictions of climate change effects on Schistosoma mansoni transmission in eastern Africa. *Geospat. Health* **2016**, *11*, 406. [CrossRef]
23. De Leo, G.A.; Stensgaard, A.-S.; Sokolow, S.H.; N'goran, E.K.; Chamberlin, A.J.; Yang, G.-J.; Utzinger, J. Schistosomiasis and climate change. *BMJ* **2020**, *371*, m4324. [CrossRef]
24. Tabo, Z.; Neubauer, T.A.; Tumwebaze, I.; Stelbrink, B.; Breuer, L.; Hammoud, C.; Albrecht, C. Factors controlling the distribution of intermediate host snails of *Schistosoma* in crater lakes in Uganda: A machine learning approach. *Front. Environ. Sci.* **2022**, *10*, 871735. [CrossRef]
25. Fishel, F.M. Storage Limitation Statements: Temperature–Herbicides: PI123/PI160, 4/2013. *EDIS* **2013**, *4*, 123–160.
26. Ziska, L.H. Increasing minimum daily temperatures are associated with enhanced pesticide use in cultivated soybean along a latitudinal gradient in the mid-western United States. *PLoS ONE* **2014**, *9*, e98516. [CrossRef] [PubMed]
27. Matthies, M.; Beulke, S. Considerations of temperature in the context of the persistence classification in the EU. *Environ. Sci. Eur.* **2017**, *29*, 15. [CrossRef]

28. European Food Safety Authority (EFSA). Opinion on a request from EFSA related to the default Q10 value used to describe the temperature effect on transformation rates of pesticides in soil-Scientific Opinion of the Panel on Plant Protection Products and their Residues (PPR Panel). *EFSA J.* **2008**, *6*, 622. [CrossRef]
29. ECHA. *Guidance on Information Requirements and Chemical Safety Assessment*; Chapter R.11: PBT/vPvB Assessment; Version 2; Technical Report ECHA-14-G-07-EN; European Chemicals Agency: Helsinki, Finland, 2014.
30. ECHA. *Guidance for Information Requirements and Chemical Safety Assessment*; Chapter R.7b: Endpoint Specific Guidance; Draft Version 4.0 (Public); European Chemicals Agency: Helsinki, Finland, 2016.
31. Ronoh, M.; Chirove, F.; Pedro, S.A.; Tchamga, M.S.S.; Madubueze, C.E.; Madubueze, S.C.; Addawe, J.; Mwamtobe, P.M.; Mbra, K.R. Modelling the spread of schistosomiasis in humans with environmental transmission. *Appl. Math. Model.* **2021**, *95*, 159–175. [CrossRef]
32. Grimes, J.E.T.; Croll, D.; Harrison, W.E.; Utzinger, J.; Freeman, M.C.; Templeton, M.R. The roles of water, sanitation and hygiene in reducing schistosomiasis: A review. *Parasites Vectors* **2015**, *8*, 156. [CrossRef]
33. Montanari, A.L.; Accorsi, A.; Nasi, M.; Malagoli, D. Effects of a nematode-based molluscicide on survival and antimicrobial peptide expression in *Pomacea canaliculata*. *Invertebr. Surviv. J.* **2019**, *16*, 37.
34. Laidler, K.J.; Chen, H.; Ling, M.; Hencz, L.; Ling, H.Y.; Li, G.; Lin, Z.; Liu, G.; Zhang, S.; Abyazisani, M.; et al. The development of the Arrhenius equation. *J. Chem. Educ.* **1984**, *61*, 494. [CrossRef]
35. Lewis, K.; Tzilivakis, J.; Green, A.; Warner, D. Pesticide Properties DataBase (PPDB). 2006. Available online: http://hdl.handle.net/2299/15375 (accessed on 14 February 2023).
36. Carvalho, S.A.; da Silva, S.O.; Charret, I.D.C. Mathematical modeling of dengue epidemic: Control methods and vaccination strategies. *Theory Biosci.* **2019**, *138*, 223–239. [CrossRef]
37. European Commission EC. Technical Guidance Document on Risk Assessment in Support of Commission Directive 93/67/EEC on Risk Assessment for New Notified Substances Part II. In *Commission Regulation (EC) No 1488/94 on Risk Assessment for Existing Substances and of Directive 98/8/EC of the European Parliament and of the Council Concerning the Placing of Biocidal Products on the Market*; Technical Report EUR 20418 EN/2; European Commission EC: Luxembourg, 2003.
38. Diekmann, O.; Heesterbeek, J.A.P.; Metz, J.A.J. On the definition and the computation of the basic reproduction ratio R 0 in models for infectious diseases in heterogeneous populations. *J. Math. Biol.* **1990**, *28*, 365–382. [CrossRef] [PubMed]
39. Chavez, C.C.; Feng, Z.; Huang, W. On the computation of R_0 and its role on global stability. In *Mathematical Approaches for Emerging and Re-Emerging Infection Diseases: An Introduction*; Springer: Berlin/Heidelberg, Germany, 2002; Volume IMA 125, pp. 229–250.
40. Driessche, P.V.D.; Watmough, J. Reproduction numbers and sub-threshold endemic equilibria for compartmental models of disease transmission. *Math. Biosci.* **2002**, *180*, 29–48. [CrossRef] [PubMed]
41. Anderson, B.; Jackson, J.; Sitharam, M. Descartes' rule of signs revisited. *Am. Math. Mon.* **1998**, *105*, 447. [CrossRef]
42. Fulford, A.J.C.; Butterworth, A.E.; Ouma, J.H.; Sturrock, R.F. A statistical approach to schistosome population dynamics and estimation of the life-span of *Schistosoma mansoni* in man. *Parasitology* **1995**, *110*, 307–316. [CrossRef]
43. Colley, D.G.; Bustinduy, A.L.; Secor, W.E.; King, C.H. Human schistosomiasis. *Lancet* **2014**, *383*, 2253–2264. [CrossRef]
44. Anderson, R.; Turner, H.; Farrell, S.; Truscott, J. Studies of the transmission dynamics, mathematical model development and the control of schistosome parasites by mass drug administration in human communities. *Adv. Parasitol.* **2016**, *94*, 199–246. [CrossRef]
45. Dabo, A.; Badawi, H.M.; Bary, B.; Doumbo, O.K. Urinary schistosomiasis among preschool-aged children in Sahelian rural communities in Mali. *Parasites Vectors* **2011**, *4*, 21. [CrossRef]
46. Gryseels, B.; Polman, K.; Clerinx, J.; Kestens, L. Human schistosomiasis. *Lancet* **2006**, *368*, 1106–1118. [CrossRef]
47. Michaels, R.M.; Prata, A. Evolution and characteristics of *Schistosoma mansoni* eggs laid in vitro. *J. Parasitol.* **1968**, *54*, 921. [CrossRef]
48. Braun, L.; Grimes, J.E.T.; Templeton, M.R. The effectiveness of water treatment processes against schistosome cercariae: A systematic review. *PLoS Negl. Trop. Dis.* **2018**, *12*, e0006364. [CrossRef]
49. Kanyi, E.; Afolabi, A.S.; Onyango, N.O. Mathematical modelling and analysis of transmission dynamics and control of schistosomiasis. *J. Appl. Math.* **2021**, *2021*, 1–20. [CrossRef]
50. Feng, Z.; Eppert, A.; Milner, F.; Minchella, D. Estimation of parameters governing the transmission dynamics of schistosomes. *Appl. Math. Lett.* **2004**, *17*, 1105–1112. [CrossRef]
51. Liang, S.; Spear, R.C.; Seto, E.; Hubbard, A.; Qiu, D. A multi-group model of Schistosoma japonicum transmission dynamics and control: Model calibration and control prediction. *Trop. Med. Int. Health* **2005**, *10*, 263–278. [CrossRef]
52. Mangal, T.D.; Paterson, S.; Fenton, A. Predicting the impact of long-term temperature changes on the epidemiology and control of schistosomiasis: A mechanistic model. *PLoS ONE* **2008**, *3*, e1438. [CrossRef]
53. Soetaert, K.; Petzoldt, T.; Setzer, R.W. Solving differential equations in R: Package deSolve. *J. Stat. Softw.* **2010**, *33*, 1–25. [CrossRef]
54. R Core Team. R: A Language and Environment for Statistical Computing. R Foundation for Statistical Computing, Vienna, Austria. 2016. Available online: http://www.R-project.org/ (accessed on 6 March 2021).
55. Andrade, G.; Bertsch, D.J.; Gazzinelli, A.; King, C.H. Decline in infection-related morbidities following drug-mediated reductions in the intensity of *Schistosoma* infection: A systematic review and meta-analysis. *PLoS Negl. Trop. Dis.* **2017**, *11*, e0005372. [CrossRef] [PubMed]

56. Thétiot-Laurent, S.A.-L.; Boissier, J.; Robert, A.; Meunier, B. Schistosomiasis chemotherapy. *Angew. Chem. Int. Ed.* **2013**, *52*, 7936–7956. [CrossRef]
57. Faust, C.L.; Osakunor, D.N.; Downs, J.A.; Kayuni, S.; Stothard, J.R.; Lamberton, P.H.; Reinhard-Rupp, J.; Rollinson, D. Schistosomiasis control: Leave no age group behind. *Trends Parasitol.* **2020**, *36*, 582–591. [CrossRef]
58. Lo, N.C.; Bezerra, F.S.M.; Colley, D.G.; Fleming, F.M.; Homeida, M.; Kabatereine, N.; Kabole, F.M.; King, C.H.; Mafe, M.A.; Midzi, N.; et al. Review of 2022 WHO guidelines on the control and elimination of schistosomiasis. *Lancet Infect. Dis.* **2022**, *22*, e327–e335. [CrossRef]
59. Satayathum, S.A.; King, C.; Muchiri, E.M.; Ouma, J.H.; Whalen, C.C. Factors affecting infection or reinfection with *Schistosoma haematobium* in coastal Kenya: Survival analysis during a nine-year, school-based treatment program. *Am. J. Trop. Med. Hyg.* **2006**, *75*, 83–92. [CrossRef]
60. Feng, W. Progress of research on molluscicidal effect of nereistoxin pesticide. *Chin. J. Schistosomiasis Control* **2012**, *19*, 482.
61. Seligman, P.F.; Maguire, R.J.; Lee, R.F.; Hinga, K.R.; Valkirs, A.O.; Stang, P.M. Persistence and fate of tributyltin in aquatic ecosystems. In *Organotin*; Springer: Dordrecht, The Netherlands, 1996; Volume 20, pp. 429–457. [CrossRef]
62. Sokolow, S.H.; Wood, C.L.; Jones, I.J.; Swartz, S.J.; Lopez, M.; Hsieh, M.H.; Lafferty, K.D.; Kuris, A.M.; Rickards, C.; De Leo, G.A. Global assessment of schistosomiasis control over the past century shows targeting the snail intermediate host works best. *PLoS Negl. Trop. Dis.* **2016**, *10*, e0004794. [CrossRef] [PubMed]
63. Sprecher, S.L.; Getsinger, K.D. *Zebra Mussel Chemical Control Guide*; ERDC/EL TR-00-1; U.S. Army Engineer Research and Development Center: Vicksburg, MS, USA, 2000; 114p.
64. Zayed, K.M.; Guo, Y.-H.; Lv, S.; Zhang, Y.; Zhou, X.-N. Molluscicidal and antioxidant activities of silver nanoparticles on the multi-species of snail intermediate hosts of schistosomiasis. *PLoS Negl. Trop. Dis.* **2022**, *16*, e0010667. [CrossRef]
65. Castle, G.D.; Mills, G.A.; Gravell, A.; Jones, L.; Townsend, I.; Cameron, D.G.; Fones, G.R. Review of the molluscicide metaldehyde in the environment. *Environ. Sci. Water Res. Technol.* **2017**, *3*, 415–428. [CrossRef]
66. Gohar, A.A.; Maatooq, G.T.; Gadara, S.R.; Aboelmaaty, W.S.; El-Shazly, A.M. Molluscicidal activity of the methanol extract of *Callistemon viminalis* (Sol. ex Gaertner) G. Don ex Loudon fruits, bark and leaves against *Biomphalaria alexandrina* snails. *Iran. J. Pharm. Res.* **2014**, *13*, 505.

Mathematical Biosciences 376 (2024) 109263

Contents lists available at ScienceDirect

Mathematical Biosciences

journal homepage: www.elsevier.com/locate/mbs

Control of schistosomiasis by the selective competitive and predatory intervention of intermediate hosts: A mathematical modeling approach

Zadoki Tabo [a,b,*], Livingstone Luboobi [d], Philipp Kraft [b], Lutz Breuer [b,c], Christian Albrecht [a]

[a] Department of Animal Ecology and Systematics, Justus Liebig University Giessen, Heinrich-Buff-Ring 26 (iFZ), 35392, Giessen, Germany
[b] Department of Landscape Ecology and Resource Management, Justus Liebig University Giessen, Heinrich-Buff-Ring 26 (iFZ), 35392, Giessen, Germany
[c] Centre for International Development and Environmental Research (ZEU), Justus Liebig University Giessen, Senckenbergstrasse 3, 35390, Giessen, Germany
[d] Independent Researcher, C/O Department of Mathematics, Makerere University, Kampala, Uganda

ARTICLE INFO

Keywords:
Schistosomiasis
Snail competitor
Snail predator
Mathematical model
Neglected tropical disease
Elimination

ABSTRACT

Schistosomiasis, a freshwater-borne neglected tropical disease, disproportionately affects impoverished communities mainly in the tropical regions. Transmission involves humans and intermediate host (IH) snails. This manuscript introduces a mathematical model to probe schistosomiasis dynamics and the role of non-host snail competitors and predators as biological control agents for IH snails. The numerical analyses include investigations into steady-state conditions and reproduction numbers associated with uncontrolled scenarios, as well as scenarios involving non-host snail competitors and/or predators. Sensitivity analysis reveals that increasing snail mortality rates is a key to reducing the IH snail population and control of the transmission. Results show that specific snail competitors and/or predators with strong competition/predation abilities reduce IH snails and the subsequent infectious cercaria populations, reduce the transmission, and possibly eradicate the disease, while those with weaker abilities allow disease persistence. Hence our findings advocate for the effectiveness of snail competitors with suitable competitive pressures and/or predators with appropriate predatory abilities as nature-based solutions for combating schistosomiasis, all while preserving IH snail biodiversity. However, if these strategies are implemented at insignificant levels, IH snails can dominate, and disease persistence may pose challenges. Thus, experimental screening of potential (native) snail competitors and/or predators is crucial to assess the likely behavior of biological agents and determine the optimal biological control measures for IH snails.

1. Introduction

Schistosomiasis, a prevalent disease in tropical regions, is caused by parasites known as *Schistosoma*. These parasitic trematode worms rely on two primary hosts: the humans, within whom it matures into an adult, leading to schistosomiasis infection, and intermediate host (IH) snails, which aid in the early stages of its development. The propagation of this ailment hinges on the interactions between these hosts, intricately connecting the life cycle of the parasite with both human and snail organisms [1,2]. This disease is closely associated with impoverished living conditions resulting from factors such as poverty, inadequate sanitation, and limited access to clean water sources [3]. Schistosomiasis imposes a considerable toll in terms of mortality and morbidity [4]. On a global scale, more than 700 million individuals are at risk of infection, and over 200,000 people lose their lives to it annually, with the highest burden experienced in sub-Saharan Africa, where it accounts for up to 90 % of infections worldwide [5,6].

In terms of disease control, it is important to note that there is currently no vaccine available to prevent schistosomiasis. However, the primary interventions for managing the transmission of this disease at the human population level involve mass drug administration and/or the implementation of WASH (water, sanitation, and hygiene) measures [7]. However, despite these efforts, schistosomiasis frequently re-emerges shortly after interventions, presenting significant challenges at the human level and limited impact in affected regions. In contrast, there is a growing body of evidence suggests that targeting IH snails as a control strategy could effectively manage their populations and curb the spread of schistosomiasis [8–11]. This approach has achieved substantial success in various Asian regions [9]. In support of this approach, the 65th World Health Assembly took a crucial step by passing a resolution

* Corresponding author.
E-mail address: Tabo.Zadoki@umwelt.uni-giessen.de (Z. Tabo).

https://doi.org/10.1016/j.mbs.2024.109263
Received 22 September 2023; Received in revised form 24 June 2024; Accepted 24 July 2024
Available online 31 July 2024

advocating for the integration of biological controls in the management of IH snails [8]. Within this context, studies have revealed that coexisting with potential competitors and predators of various species plays a crucial role in regulating the distribution of these snails, emerging as a critical ecological factor in the development of diseases [12,13]. Significantly, numerous potential competitors to IH snails have been documented, including species such as *Thiara granifera and Physella acuta* [14]. In the presence of many competitors, snails intensify their feeding behavior, and species out-competition could potentially lead to colonization by non-host invasive species [15]. Previous research has reported instances of displacement and/or colonization of IH snails by non-host snails, as documented by Butler et al. [16], who observed the colonization of IH *Biomphalaria* species by the presence of *Thiara granifera*.

On the contrary, potential predators within the ecosystem encompass a diverse array of species, including crayfish, river prawns, the water bug *Sphaerodema urinator*, various insect species, selected leech species, Sciomyzidae flies in their larval stage, as well as several fish and crustacean species [15–19]. The presence of these snail predators exerts a remarkable influence on the IH snail population, inducing heightened stress and instigating observable behavioral modifications. For instance, IH snails possess the ability to detect the presence of these predators, prompting them to seek refuge. This behavioral shift subsequently leads to a decrease in their feeding rate, thereby leading to consequential alterations in the patterns of disease dissemination [15,20]. For example, the study conducted by Sokolow et al. [10] documented a decrease in human schistosomiasis transmission following the reintroduction of a native river prawn, known to prey on the IH snails. Furthermore, recent research by Mathers et al. [21] has unveiled considerable variations in the handling time and attack rate exhibited by predators when preying upon different gastropod species. These observed variations may lead to shifts in the predation dynamics, affecting the strategies and effectiveness of predators in capturing their prey.

Consequently, the roles played by both snail competitors and predators emerge as key components within the ecological framework. These elements play significant roles in the complex ecological interactions within the system, influencing the dynamics of *Schistosoma* transmission. Nonetheless, the development of mathematical models has significantly enhanced our comprehension of population dynamics and facilitated the evaluation of various control programs. The utilization of mathematical models for assessing the relative effectiveness of different biological interventions and the elimination of schistosomiasis transmission holds paramount importance in informing policy decisions. Several studies, including those conducted by Altizer et al. [22], Chiyaka and Garira [23], Gao et al. [24], and Abokwara and Madubueze [25], have explored the dynamics and control of schistosomiasis at the human population level. Additionally, research has provided valuable insights into temperature control for different aspects of the *Schistosoma* life cycle, as seen in studies conducted by Mangal et al. [26], Kalinda et al. [27] and Tabo et al. [28]. To the best of our knowledge, a few mathematical models have investigated biological control strategies for the management of IH snails and the control of schistosomiasis [29,30], but none have examined the influence of non-host competitor snails and snail predators concerning concurrent disease propagation. In our present model, we formulate ordinary differential equations (ODEs) to represent the principal stages of the *Schistosoma* life cycle. Within this model, we incorporate non-host competitors and predators as integral biological components. Consequently, we utilize this model as a tool to illuminate the control of schistosomiasis and quantify the anticipated impacts of snail competitors and predators in the effective management of IH snail vectors and the control of schistosomiasis.

2. Materials and methods

2.1. Model formulation

The primary stages of the *Schistosoma* spp. life and transmission cycle (Fig 1) served as the basis for our mathematical model. The key stages include the human host, free-living parasites (cercaria and miracidia), and the IH snail. Within the human population, individuals can be classified into two distinct groups: individuals who exhibit susceptibility denoted as $H(t)$, and those who have been infected, denoted as $I(t)$. The infected individuals represented by $I(t)$, expel parasite eggs $E(t)$ through feces or urine, which may either be directly excreted or introduced into freshwater sources. In favorable freshwater environments, the parasite eggs undergo hatching, giving rise to miracidia $\mathrm{M}(t)$, which function as hosts for IH snails. These IH snails can be classified as either susceptible, denoted as $S(t)$, or infected, labeled as $Is(t)$. Infected IH snails, $Is(t)$, release infectious cercaria parasites $C(t)$, which subsequently initiate infection in humans to complete the *Schistosoma* life cycle. Furthermore, the model incorporates biological control agents, denoted as $X(t)$, which represent potential competitor for IH snail, and $Y(t)$, which represent potential predator.

We assume that newborns are not recruited untill a certain age (τ) when they can interact or be washed in water. The IH snail and human host are infected through contact with miracidia and cercariae, respectively, in an infested freshwater environment. The competitor snail is not an infectious host and is not a vector. Snails grow logistically in the absence of the disease. The infected snails do not reproduce as a side effect of miracidia infection and due to infection, their mortality is potentially higher than for susceptible snails. The competitor snail is a superior competitor with the advantage of impacting more strongly on available resources than the IH snails. There are various potential predators with specific capabilities, and the only food available in the environment is the IH snails, especially the infected IH snails. The effort and time required by the predator to handle infected IH snails is less than that required time to handle the susceptible IH snails. Thus, the model equations, which depict the dynamic interactions of schistosomiasis in the presence of biological control agents, are presented in Eqs. (1)-(9):

$$\dot{H}(t) = \Lambda_1 - \frac{\beta_1 HC}{C_o + \varepsilon C} - \upsilon_1 H \tag{1}$$

$$\dot{I}(t) = \frac{\beta_1 HC}{C_o + \varepsilon C} - (\upsilon_1 + \delta_1) I \tag{2}$$

$$\dot{E}(t) = \rho\theta_h I\left(1 - \frac{E}{K}\right) - (\omega_1 + \upsilon_3) E \tag{3}$$

$$\dot{\mathrm{M}}(t) = \omega_1 E - \upsilon_4 \mathrm{M} \tag{4}$$

$$\dot{S}(t) = r_1 S\left(1 - \frac{S + e_1(I_s + X)}{K_1}\right) - \frac{\beta_2 MS}{M_o + \varepsilon M} - f_1(S)Y \tag{5}$$

$$\dot{I}_s(t) = \frac{\beta_2 MS}{M_o + \varepsilon M} - (\upsilon_2 + \delta_2 + e_2(S + X + I_s))I_s - f_2(I_s)Y \tag{6}$$

$$\dot{C}(t) = \omega_2 I_s - \upsilon_5 C \tag{7}$$

$$\dot{X}(t) = r_2 X\left(1 - \frac{X + e_3(S + I_s)}{K_2}\right) \tag{8}$$

$$\dot{Y}(t) = \eta_1 f_1(S)Y + \eta_2 f_2(I_s) - \upsilon_6 Y \tag{9}$$

Here, $\Lambda_1 = \lambda e^{-\upsilon_1 \tau}$ represents human recruitment through birth, which follows an exponentially distributed waiting time function. It has a maximum per capita birth rate of λ, a natural death rate of υ_1, and τ represents the age of first schistosomiasis infection in children. The term $e^{-\upsilon_1 \tau}$ represents the fraction of children waiting to be recruited at time τ,

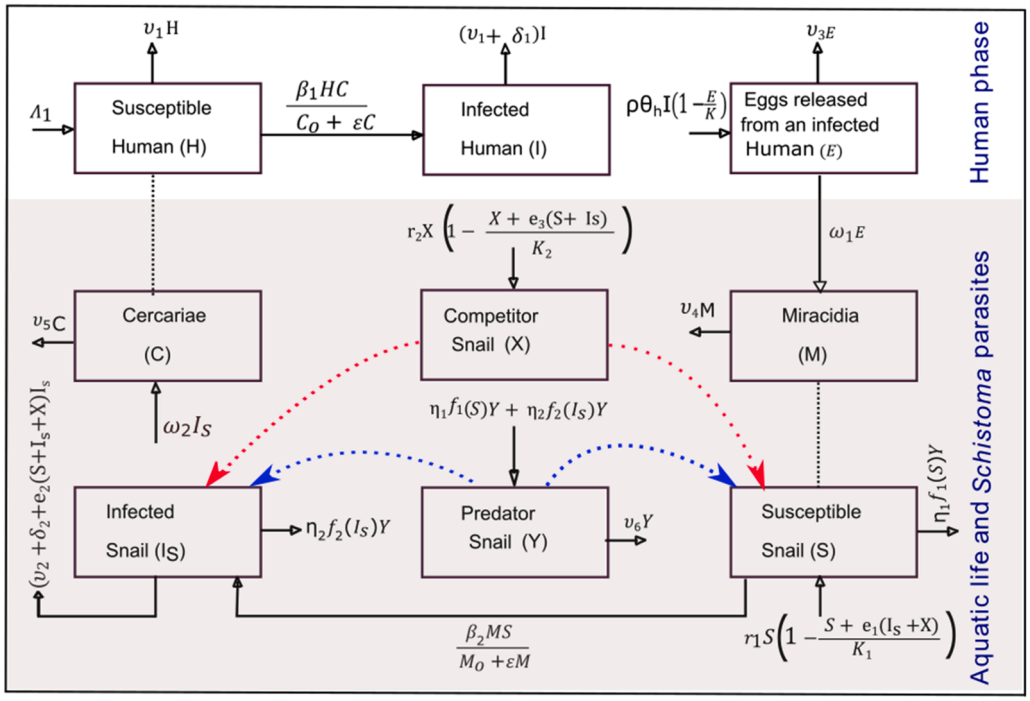

Fig. 1. A schematic description of the schistosomiasis transmission cycle. Interactions between snail competitors and predators with intermediate host snails are shown by the dashed arrows in red and blue, respectively. The parameter descriptions are provided in Table 1. (For interpretation of the references to color in this figure legend, the reader is referred to the web version of this article.)

with a $\frac{1}{\upsilon_1}$ chance of survival. The non-linear infection incidences in the model are denoted as $\beta_1 HC/(C_o + \varepsilon C)$ for human hosts and $\beta_2 MS/(M_o + \varepsilon M)$ for snail hosts. Here, β_1 and β_2 represent the infection rates of human and snail hosts. ε represents the crowding effect which encapsulates environmental and ecological constraints (temperature, competition, predation, water quality, etc.) that may limit the effective contact rate between hosts (human and snail) and parasites (cercaria and miracidia). C_o and M_o are saturation coefficients for cercariae and miracidia infectivity, respectively, and ensure that the incidence rate increases with C and M, but asymptotically approaches a maximum value. Thus, C_o and M_o represent the carrying capacity of the environment and the biological limits of the humans and snails that can be infected. Furthermore, infected humans excrete an average of ρ stool (volume of urine) per day, containing an average number of parasite eggs θ_h per gram of stool (*S. mansoni*) or per liter of urine per day (*S. haematobium*). Miracidia emerge from parasite eggs at an average rate of N_E miracidia per egg, and ω_1 represents the rate of parasite egg hatching. The populations of IH snails and competitor snails grow intrinsically at rates r_1 and r_2, respectively. Meanwhile, the predator population increases due to conversion factors η_1 and η_2, which represent susceptible snail-to-predator conversion and infected snail-to-predator conversion, respectively. Note that the intrinsic growth of parasite egg, IH snails, and competitor snails populations are constrained by their respective carrying capacity of K, $K_1$and K_2 respectively. Predators feed on host snails with a saturating Holling type II functional response to susceptible snail density, represented by $f_1(S) = \frac{t_1 S}{1+at_1 S}$, and to infected snail density, represented by $f_2(I_s) = \frac{t_2 I_s}{1+bt_2 I_s}$. The parameters (a, b), and (t_1, t_2) are handling times and attack rates of the susceptible and infected IH snails, respectively. Additionally, the cercaria population is shed from infected snails at a rate of ω_2. The snail, parasite egg, miracidia, cercaria, and predator populations naturally die at rates υ_2, υ_3, υ_5, and υ_6, respectively. Disease-related mortality rates for humans and snails are indicated by δ_1 and δ_2.

2.2. Positivity of the solution and biologically invariant region

We show that our model is of epidemiological interest and can be analyzed in a region $\Omega \subset R_+^6$, if all parameters and state variables are non-negative for all future time, $\forall t > 0$ and, given non-negative initial conditions, all solutions remain non-negative and bounded.

Theorem 1. *Let* $\pounds(t) = [H(t), I(t), E(t), M(t), S(t), I_s(t), C(t), X(t), Y(t)]^T \subset \mathscr{R}_+^9$, *for initial conditions* $\pounds(0) \geq 0$, *then the solution set* $\pounds(t)$ *of the model equations Eqs. (1)-(9) is non-negative for* $\forall t > 0$ *and eventually enters the invariant attracting region* $\Omega \subset R_+^9$.

Proof. Consider equation (Eq. (1)) of the model equations Eqs. (1)-(9). It is obvious that $\dot{H}(t) \geq -\left(\frac{\beta_1 C}{C_0+\varepsilon C} - \upsilon_1\right)H$. By integration, we get $H(t) \geq H(0)$. This implies that as t approaches negative infinity, the lower bound of $H(t)$ tends towards zero, i.e., $\lim_{t\to-\infty} Inf(H(t)) \geq 0$. Consequently, the solution H(t) remains non-negative. Similarly, through analogous reasoning, we can show that $I(t) \geq 0$, $E(t) \geq 0$, $M(t) \geq 0$, $S(t) \geq 0$, $I_s(t) \geq 0$, $C(t) \geq 0$, $X(t) \geq 0$, $Y(t) \geq 0$. Thus, all state variables maintain non-negative values. This confirms that the feasible region Ω is positively invariant, since the solution trajectory of the system always remains within this non-negative region over time. This leads to the conclusion that the solution set $\pounds(t)$ of the model equations Eqs. (1)-(9) eventually enters and remains in the attracting invariant region $\Omega \subset R_+^9$.

Theorem 2. *Let the initial conditions* $\pounds(0) \geq 0$, *then all solutions to the set* $\pounds(t)$ *remain bounded for all future time*

Proof. Let's consider the total human population $N_h(t) = H(t) + I(t)$, $\forall t > 0$. The differential equation governing this population is given by: $\frac{dN_h}{dt} = \Lambda_1 - \upsilon_1 N_h - \delta_1 I$. If we have $\frac{dN_h}{dt} \leq \Lambda_1 - \upsilon_1 N_h$, integrating this inequality yields $N_h(t) \leq \frac{\Lambda_1}{\upsilon_1} - \left(\frac{\Lambda_1}{\upsilon_1} - N_h(0)\right)e^{-\upsilon_1 t}$. As t approaches

infinity, the supremum of $N_h(t)$ becomes bounded by $max\left\{N_h(o),\ \frac{\Lambda_1}{\upsilon_1}\right\}$, thus ensuring that $N_h(t)$ remains bounded above.

Now, consider the total host snail population $N_s(t) = S(t) + I_s(t)$ for $\forall\ t > 0$. The differential equation governing this population is given by: $\frac{dN_s(t)}{dt} = r_1 N_s\left(1 - \frac{N_s}{K_1}\right)$. Solving this equation gives $N_s(t) = \frac{K_1 N_s(o)}{N_s(o) + ((K_1 - N_s(0))e^{-r_1 t}}$, where $N_s(0) = S(0) + I_s(0)$. By setting $\underset{t\to\infty}{limSup}(N_s(t)) \le Q_1$, for $\forall t > 0$ where $Q_1 = max\{N_s(o), K_1\}$, we deduce that $N_s(t) \le Q_1$ for $\forall t > 0$. Additionally, by introducing the variable $Z = S + I_s + Y$, where Y represents some other components, we find that $\frac{dZ}{dt} + \gamma Z \le \delta$, where $\delta = (1 + r_1)Q_1$ and $\gamma = min\{1,\ (\upsilon_1 + \delta_1),\ \upsilon_5\}$. Solving this inequality gives $Z(t) \le Q_2 = \frac{\delta}{\gamma} + \left(Z(0) - \frac{\delta}{\gamma}\right)e^{-\delta t}$ for $\forall t > 0$. Hence $Q_2 = max\left\{Z(0),\ \frac{\delta}{\gamma}\right\}$. This guarantees that the solutions for $S(t)$, $I_s(t)$ and $Y(t)$ remain bounded above. Furthermore, this bound can be extended to $E(t)$, $M(t)$, $C(t)$ and $X(t)$, ensuring the boundedness of all variables. Consequently, feasible solutions converge within the region Ω. Thus, Theorems 1 and 2 together demonstrate that the system of model equations is both mathematically and epidemiologically well-posed. The well-posed nature of the model enables us to proceed with additional mathematical analyses of the model.

3. Analysis of the model (Eqs. (1)-(9))

In this section, we conduct our analyses and offer insights into the disease-free equilibria, including associated reproduction numbers for the model without control measures, with one control implemented separately and with the two controls implemented simultaneously. Furthermore, we present the endemic equilibrium for a complete model system and carry out a bifurcation analysis.

3.1. Disease-free equilibrium points

When all the populations are disease free, we assumed that $I(t) = E(t) = M(t) = I_s(t) = C(t) = 0$. By equating the left-hand side (LHS) of the model equation (Eqs. (1)-(9)) to zero, we present the disease-free equilibria in the following scenarios:

(i) We start with the scenario where no biological control measures are applied, resulting in a model with no competitor snails and no predators. In this case, we derive two disease-free equilibrium points:

$$D_{fe1} = \left(\frac{\lambda e^{-\upsilon_1 \tau}}{\upsilon_1},\ 0,0,0,0,0,0\right) \text{ and } D_{fe2} = \left(\frac{\lambda e^{-\upsilon_1 \tau}}{\upsilon_1}, 0,0,0,\ K_1, 0,0\right)$$

(ii) Next, we consider the scenario where there are no snail predators, and competitor snails continue to exist. In this competition-only model, we obtain four disease-free equilibrium points categorized as follows:

(a) Human-trial equilibrium: $\left(\frac{\lambda e^{-\upsilon_1 \tau}}{\upsilon_1}\ 0,0,0,0,0,0,\ 0\right)$,

(b) Two boundary equilibria: $\left(\frac{\lambda e^{-\upsilon_1 \tau}}{\upsilon_1}, 0,0,0,\ K_1, 0,0,\ 0\right)$ and $\left(\frac{\lambda e^{-\upsilon_1 \tau}}{\upsilon_1},\ 0,0,0,0,0,\ 0,\ K_2\right)$,

(c) Interior equilibrium point: $E_o^X = \left(\frac{\lambda e^{-\upsilon_1 \tau}}{\upsilon_1},\ 0,\ 0,\ 0,\ \frac{K_1 - e_1 K_2}{1 - e_1 e_3},\ 0,\ 0,\ \frac{K_2 - e_3 K_1}{1 - e_1 e_3}\right)$, provided $\frac{K_1}{e_1 K_2} > 1$ for $e_1, e_3 \in [0,1]$.

(iii) In the absence of competitor snails and the presence of snail predators, we describe a predation-only model. In this scenario, we obtain up to four disease-free equilibrium points:

(a) Human-trivial equilibrium $\left(\frac{\lambda e^{-\upsilon_1 \tau}}{\upsilon_1},\ 0,0,0,0,0,0,0\right)$,

(b) Two boundary equilibria $\left(\frac{\lambda e^{-\upsilon_1 \tau}}{\upsilon_1}, 0,0,0,\ K_1,\ 0,0,\ 0\right)$ and $\left(\frac{\lambda e^{-\upsilon_1 \tau}}{\upsilon_1},\ 0,0,0,0,0,\ 0,\ \frac{r_1}{t_1}\right)$,

(c) Interior equilibrium point $E_o^Y = \left(\frac{\lambda e^{-\upsilon_1 \tau}}{\upsilon_1},\ 0,0,0, \frac{u_6}{t_1(\eta_1 - au_6)},\ 0,\ 0,\ \frac{r_1 \eta_1 K_1 t_1 (\eta_1 - au_6) - u_6}{t_1 K_1}\right)$ provided $\frac{\eta_1}{au_6} > 1$ and $\frac{r_1 \eta_1 K_1 t_1 (\eta_1 - au_6)}{u_6} > 1$.

(iv) Lastly, in the presence of both snail competitor and snail predator, we have a competition-predation model. In this case, we identify a single disease-free equilibrium point denoted as:

$E_o^{XY} = \left(\frac{\lambda e^{-\upsilon_1 \tau}}{\upsilon_1},\ 0,\ 0,\ 0,\ \frac{u_6}{t_1(\eta_1 - au_6)},\ 0,\ 0,\ \frac{K_1 t_1 (\eta_1 - au_6) - e_3 u_6}{t_1(\eta_1 - au_6)},\ \eta_1 \left[\frac{r_1 t_1 (\eta_1 - au_6)(K_1 - e_1 K_2) - (1 - e_1 e_2)u_6}{K_1 (t_1(\eta_1 - au_6)^2)}\right]\right)$, provided $\frac{\eta_1}{au_6} > 1$, $\frac{K_1 t_1 (\eta_1 - au_6)}{e_3 u_6} > 1$, $\frac{K_1}{e_1 K_2} > 1$, and $\frac{r_1 t_1 (\eta_1 - au_6)(K_1 - e_1 K_2)}{(1 - e_1 e_2)u_6} > 1$.

The interior equilibrium points, specifically E_o^X, E_o^Y, and E_o^{XY}, play a significant role in our study as they signify the presence of IHs and the dynamic interactions between the hosts and control agents across different scenarios. These equilibrium points hold biological significance in our assessment of control strategies. In contrast, the trivial and boundary equilibrium points typically indicate scenarios where both snail and control agent populations either go extinct or reach their maximum carrying capacity. These points are not suitable for evaluating control strategies.

3.1.1. Reproduction number for model Eqs. (1)-(9)

This represents the number of new secondary schistosomiasis cases caused by an infected human/snail with both biological interventions in place. It is the effective reproduction number (R_{XY}) used to assess the impact of interventions on reducing disease transmission. We use the next-generation approach according to Diekmann et al. [31], Castillo-Chavez et al. [32], and Van den Driessche and Watmough [33], to calculate R_{XY}. Let $E_{XY} = (H^*,\ 0,0,0,\ S^*,\ 0,\ 0,\ X^*, Y^*)$ represent the disease-free equilibrium point for the model incorporating biological interventions. The result R_{XY} can be expressed as follows:

$$R_{XY} = \sqrt{\left(\frac{\beta_1 \omega_2 H^*}{C_o \upsilon_5 (\upsilon_2 + \delta_2 + e_2(S^* + X^*) + t_2 Y^*)}\right) \cdot \left(\frac{\beta_2 \omega_1 \rho \theta_h S^*}{M_o \upsilon_4 (\upsilon_1 + \delta_1)(\omega_1 + \upsilon_3)}\right)} \tag{10}$$

In this equation (Eq. (10)), $R_{XY}^H = \frac{\beta_1 \omega_2 H^*}{C_o \upsilon_5 (\upsilon_2 + \delta_2 + e_2(S^* + X^*) + t_2 Y^*)}$ and $R_{XY}^S = \frac{\beta_2 \omega_1 \rho \theta_h S^*}{M_o \upsilon_4 (\upsilon_1 + \delta_1)(\omega_1 + \upsilon_3)}$ represent the number of new human infections per infected IH snail and the number of new snail infections per infected human, respectively, under both biological interventions. Epidemiologically, schistosomiasis can emerge and spread in the population depending on the value of the bifurcation parameter, which corresponds to the threshold value $R_0 = 1$. Taking the snail infection rate $\beta_2 = \beta_{XY}^*$ as the bifurcation parameter with $R_{XY} = 1$, the critical value β_{XY}^* can be expressed as:

$$\beta_{XY}^* = \frac{\upsilon_4 \upsilon_5 C_o M_o (\upsilon_1 + \delta_1)(\omega_1 + \upsilon_3)(\upsilon_2 + \delta_2 + e_2(S^* + X^*) + t_2 Y^*)}{\beta_1 \omega_1 \omega_2 \rho \theta_h H^* S^*} \tag{11}$$

This critical value (Eq. (11)) represents the threshold below which the susceptible snails are not infected by miracidia and the infection

cannot progress in the presence of both the competitor snail and the predator, and vice versa. In particular, increasing the competition term $e_2(S^* + X^*)$ and the predation term $t_2 Y^*$ in Equation (Eq. (11)), increases β^*_{XY}. This, in turn, limits how far the infection can spread. Furthermore, in Equation Eq. (10), R_{XY} is a decreasing function of $e_2(S^* + X^*)$ and $t_2 Y^*$, suggesting that R_{XY} decreases with increase in the intervention.

In addition, we substitute for (H^*, S^*, X^*, Y^*) at the equilibrium point E_o^{XY} with both biological interventions to obtain

$$R_{XY} = \sqrt{\left(\frac{\beta_1\omega_2 K_1\lambda(t_1(\eta_1 - au_6))^2 e^{-\upsilon_1\tau}}{C_o\upsilon_1\upsilon_5((\upsilon_2+\delta_2)K_1(t_1\eta_1 - au_6))^2 + e_2t_1((\eta_1 - au_6)q_1 + t_2\eta_1 q_2)}\right)\cdot\left(\frac{\beta_2\omega_1\rho\theta_h u_6}{M_o\upsilon_4 t_1(\upsilon_1+\delta_1)(\omega_1+\upsilon_3)(\eta_1 - au_6)}\right)}$$

stands as the critical value for the rate of miracidial infection on susceptible snails.

3.1.3. Reproduction number with a snail competitor

This is an effective reproduction number for the model with a snail competitor intervention. It is used to assess the impact of the snail competitor intervention on reducing disease transmission. Similarly, in the presence of the snail competitor and when the predator goes extinct ($Y^* = 0$), we introduce the equilibrium terms of the variables (H^*, S^*, X^*) at E_X into equation Eq. (10), resulting in:

$$R_X = \sqrt{\left(\frac{(1-e_1e_3)\beta_1\omega_2\lambda e^{-\upsilon_1\tau}}{\upsilon_1\upsilon_5 C_o[(1-e_1e_3)(\upsilon_2+\delta_2) + e_2(K_1+K_2-e_3K_1-e_1K_2)]}\right)\cdot\left(\frac{\beta_2\omega_1\rho\theta_h(K_1-e_1K_2)}{\upsilon_4 M_o(1-e_1e_3)(\upsilon_1+\delta_1)(\omega_1+\upsilon_3)}\right)} \tag{13}$$

where,

$q_1 = K_1(K_1t_1(\eta_1 - au_6)) + (1-e_3)u_6$

$q_2 = r_1t_1(\eta_1 - au_6)(K_1 - e_1K_2) - (1-e_1e_2)u_6.$

Consequently, by substituting the variables (H^*, S^*, X^*, Y^*) into Equation (Eq. (10)) at distinct disease-free equilibrium points E_o, E_o^X, and E_o^Y, we obtain the corresponding reproduction numbers R_o, R_X, and R_Y for the sub-models as described in the Sections 3.1.2-3.1.4.

3.1.2. Basic reproduction number with no control

This provides insight into the potential for disease spread in a population without any interventions. It quantifies the initial disease transmission, allowing us to understand the inherent transmissibility of a disease. This value is obtained when we substitute $X^* = Y^* = 0$ and the equilibrium terms for the variables (H^*, S^*) at the disease free equilibrium with no control, E_o into Equation (Eq. (10)). The result is expressed as:

$$R_0 = \sqrt{\left(\frac{\beta_1\omega_2\lambda e^{-\upsilon_1\tau}}{\upsilon_1\upsilon_5 C_o(\upsilon_2+\delta_2)}\right)\cdot\left(\frac{\beta_2\omega_1\rho\theta_h K_1}{\upsilon_4 M_o(\upsilon_1+\delta_1)(\omega_1+\upsilon_3)}\right)} \tag{12}$$

Here, $R_H = \frac{\beta_1\omega_2\lambda e^{-\upsilon_1\tau}}{\upsilon_1\upsilon_5 C_o(\upsilon_2+\delta_2)}$ represents the number of human infections caused by one infectious snail and $R_S = \frac{\beta_2\omega_1\rho\theta_h K_1}{\upsilon_4 M_o(\upsilon_1+\delta_1)(\omega_1+\upsilon_3)}$ represents the number of snail infections caused by one infectious human, assuming no interventions are in place. If we assume $\beta_2 = \beta^*$ as the bifurcation parameter for model, then $R_0 = 1$ and $\beta^* = \frac{\upsilon_1\upsilon_4\upsilon_5 C_o M_o K(\upsilon_1+\delta_1)(\upsilon_2+\delta_2)(\omega_1+\upsilon_3)}{\beta_1\omega_1\omega_2\rho\theta_h K_1\lambda e^{-\upsilon_1\tau}}$

where $R_X^H = \frac{(1-e_1e_3)\beta_1\omega_2\lambda e^{-\upsilon_1\tau}}{\upsilon_1\upsilon_5 C_o[(1-e_1e_3)(\upsilon_2+\delta_2)+e_2(K_1+K_2-e_3K_1-e_1K_2)]}$ and $R_X^S = \frac{\beta_2\omega_1\rho\theta_h(K_1-e_1K_2)}{\upsilon_4 M_o(1-e_1e_3)(\upsilon_1+\delta_1)(\omega_1+\upsilon_3)}$ is the number of possible new human infections per infected snail and the number of possible new snail infections per infected human, respectively if the snail competitor survives. Considering $\beta_2 = \beta_X^*$ as the bifurcation parameter and setting $R_X = 1$, the critical value $\beta_2 = \beta_X^*$ is determined as $\beta_X^* = \frac{\upsilon_1\upsilon_4\upsilon_5 C_o M_o[(1-e_1e_3)(\upsilon_2+\delta_2)+e_2(K_1+K_2-e_3K_1-e_1K_2)](\upsilon_1+\delta_1)(\omega_1+\upsilon_3)}{\beta_1\omega_1\omega_2\rho\theta_h\lambda(K_1-e_1K_2)e^{-\upsilon_1\tau}}$. This critical value represents the rate at which susceptible snails become infected by miracidia in the presence of only a snail competitor.

3.1.4. Reproduction number with a predator

This represents the effective reproduction number within the model involving a snail predator intervention, and isused to evaluate the impact of introducing predatory snails in reducing disease transmission. In this scenario, the competition term in Eq. (10), specifically $e_2(S^* + X^*)$, is set to zero. The resulting specific reproduction number, denoted as R_Y, is determined at the equilibrium point E_o^Y for the predator-only model, and it is given by:

$$R_Y = \sqrt{\left(\frac{\beta_1\omega_2\lambda e^{-\upsilon_1\tau}}{C_o\upsilon_1\upsilon_5(\upsilon_2+\delta_2+r_1\eta_1K_1t_1t_2(\eta_1 - au_6) - (t_2u_6/t_1K_1))}\right)\cdot\left(\frac{\beta_2\omega_1\rho\theta_h u_6}{M_o\upsilon_4 t_1(\upsilon_1+\delta_1)(\omega_1+\upsilon_3)(\eta_1 - au_6)}\right)} \tag{14}$$

Here, $R_Y^H = \frac{\beta_1\omega_2\lambda e^{-\upsilon_1\tau}}{C_o\upsilon_1\upsilon_5(\upsilon_2+\delta_2+r_1\eta_1K_1t_1t_2(\eta_1-au_6)-(t_2u_6/t_1K_1))}$ represents the potential number of new human infections per infected snail, and $R_Y^S = \frac{\beta_2\omega_1\rho\theta_h u_6}{M_o\upsilon_4 t_1(\upsilon_1+\delta_1)(\omega_1+\upsilon_3)(\eta_1-au_6)}$ represents the potential number of new snail infections per infected human, specifically in case where snail predation

is the only control strategy. If we consider $\beta_2 = \beta_Y^*$ as the bifurcation parameter with $R_Y = 1$, then $\beta_Y^* = \frac{\upsilon_1\upsilon_4\upsilon_5 C_o M_o t_1(\upsilon_2+\delta_2+r_1\eta_1 K_1 t_1 t_2(\eta_1-a\upsilon_6)-(t_2\upsilon_6/t_1K_1))(\upsilon_1+\delta_1)(\omega_1+\upsilon_3)(\eta_1-a\upsilon_6)}{\beta_1\omega_1\omega_2\upsilon_6\rho\theta_h\lambda e^{-\upsilon_1\tau}}$ represents the rate at which susceptible snails become infected by miracidia when only a snail predator is present in the environment.

$$J(XY) = \begin{bmatrix} -\upsilon_1 & 0 & 0 & 0 & 0 & 0 & -\frac{\beta_1 H^*}{C_o} & 0 & 0 \\ 0 & -(\upsilon_1+\delta_1) & 0 & 0 & 0 & 0 & \frac{\beta_1 H^*}{C_o} & 0 & 0 \\ 0 & \rho\theta_h & -(\omega_1+\upsilon_3) & 0 & 0 & 0 & 0 & 0 & 0 \\ 0 & 0 & \omega_1 & -\upsilon_4 & 0 & 0 & 0 & 0 & 0 \\ 0 & 0 & 0 & -\frac{\beta_2 S^*}{M_o} & g_1 & \frac{-r_1 S^*}{K_1} & 0 & \frac{-r_1 S^*}{K_1} & \frac{-t_1 S^*}{1+at_1 S^*} \\ 0 & 0 & 0 & \frac{\beta_2 S^*}{M_o} & 0 & g_2 & 0 & 0 & t_2 Y^* \\ 0 & 0 & 0 & 0 & 0 & \omega_2 & -\upsilon_5 & 0 & 0 \\ 0 & 0 & 0 & 0 & \frac{-r_2 X^*}{K_2} & \frac{-r_2 X^*}{K_2} & 0 & g_3 & 0 \\ 0 & 0 & 0 & 0 & \frac{\eta_1 t_1 S^*}{(1+at_1 S^*)^2} & \eta_2 t_2 Y^* & 0 & 0 & g_4 \end{bmatrix}$$

3.2. The local stability of the disease-free equilibrium E_o^{XY} for model Eqs. (1)-(9)

We present Theorem 3, which addresses the stability of the disease-free equilibrium for the complete model system.

Theorem 3. *The disease-free equilibrium point E_o^{XY} is locally asymptotically stable if $R_{XY} < 1$ and unstable if $R_{XY} > 1$*

Proof. We show that Jacobian matrix $J(XY)$ of the model equation Eqs. (1)-(9) has negative eigenvalue. The $J(XY)$ at E_o^{XY} is given by

Here $g_1 = r_1\left(1 - \frac{2S^*+X^*}{K_1}\right) - \frac{t_1\alpha_1 Y^*}{(1+at_1S^*)^2}$, $g_2 = -(\upsilon_2 + \delta_2 + e_1(S^* + X^*) + t_2Y^*)$, $g_3 = r_2\left(1 - \frac{2X^*+S^*}{K_2}\right)$, and $g_4 = \frac{\eta_1 t_1 S^*}{1+at_1S^*} - \upsilon_6$. The negative eigenvalues of $J(XY)$ are: $-\upsilon_1, -(\upsilon_1+\delta_1), -(\omega_1+\upsilon_3), -\upsilon_4$ and $-\upsilon_5$. The remaining eigenvalues can be obtained from a reduced 4×4 matrix which results from $J(XY)$, and its characteristic equation is expressed as:

$$\lambda^4 - d_1\lambda^3 + d_2\lambda^2 + d_3\lambda + d_4 = 0 \tag{15}$$

Table 1
Model parameters and their descriptions.

Symbol	Definition	Symbol	Definition
λ	Human reproduction rate	C_0	Saturation coefficient for cercaria infectivity
β_1	Human infection rate	M_0	Saturation coefficient for miracidia infectivity
β_2	Snail infection rate	ρ	Portion of stool per person
τ	Initial age of infection in children	θ_h	Number of eggs per gram of stool
δ_1	Human mortality due to infection	K	Egg carrying capacity
δ_2	IH snail mortality due to infection	K_1	Carrying capacity of host snails
υ_1	Human mortality rate	K_2	Carrying capacity of competitor snail
υ_3	Parasite egg mortality rate	r_1	Intrinsic growth rate of snails
υ_2	IH snail mortality rate	r_2	Intrinsic growth rate of competitor snails
υ_4	Miracidia death rate	ε	Crowding effect of miracidia/cercaria
b_s	IH snail birth rate	t_1	Attack rate of susceptible snail by a predator
υ_5	Cercaria mortality rate	t_2	Attack rate of infected snail by a predator
ω_1	Miracidia production rate	a	Handling time for susceptible snails by a predator
ω_2	Cercariae emergence rate	b	Handling time of infected snail by a predator
e_1	Competition factor against susceptible snails	η_1	Susceptible snail-to-predator conversion factor
e_2	Competition factor against infected snails	η_2	Infected snail-to-predator conversion factor
e_3	Competition factor against snail competitor	υ_6	Death rate of the predator

where,

$$
\begin{cases}
d_1 = \left(r_1\left(1-\dfrac{2S^*+X^*}{K_1}\right)+\dfrac{t_1Y^*}{(1+at_1S^*)^2}\right)+\left(r_2\left(1-\dfrac{2X^*+S^*}{K_2}\right)\right)+\left(\dfrac{\eta_1t_1S^*}{1+at_1S^*}+\upsilon_6\right)-(\upsilon_2+\delta_2+e_1(S^*+X^*)+t_2Y^*),\\
d_2 = \left[\left(r_1\left(1-\dfrac{2S^*+X^*}{K_1}\right)+\dfrac{t_1Y^*}{(1+at_1S^*)^2}\right)+\left(r_2\left(1-\dfrac{2X^*+S^*}{K_2}\right)\right)\right]\left[\left(\dfrac{\eta_1t_1S^*}{1+at_1S^*}+\upsilon_6\right)-(\upsilon_2+\delta_2+e_1(S^*+X^*)+t_2Y^*)\right]\\
-\left[\left(\dfrac{\eta_1t_1S^*}{1+at_1S^*}+\upsilon_6\right)\left(\upsilon_2+\delta_2+e_1(S^*+X^*)+\dfrac{t_2Y^*}{\alpha_2}\right)+\eta_2t_2^{*2}Y^{*2}\right],\\
d_3 = \left[\left(r_1\left(1-\dfrac{2S^*+X^*}{K_1}\right)+\dfrac{t_1\alpha_1Y^*}{(1+at_1S^*)^2}\right)+\left(r_2\left(1-\dfrac{2X^*+S^*}{K_2}\right)\right)\right]\left[\left(\dfrac{\eta_1t_1S^*}{1+at_1S^*}+\upsilon_6\right)(\upsilon_2+\delta_2+e_1(S^*+X^*)+t_2Y^*)+\eta_2t_2^{*2}Y^{*2}\right]\\
-\left[\left(\dfrac{\eta_1t_1S^*}{1+at_1S^*}+\upsilon_6\right)-\left(\upsilon_2+\delta_2+e_1(S^*+X^*)+\dfrac{t_2Y^*}{\alpha_2}\right)\right]\left[\left(r_1\left(1-\dfrac{2S^*+X^*}{K_1}\right)+\dfrac{t_1\alpha_1Y^*}{(1+at_1S^*)^2}\right)\left(r_2\left(1-\dfrac{2X^*+S^*}{K_2}\right)\right)-\dfrac{r_1r_2X^*}{K_1K_2}\right]\\
+\dfrac{\eta_1\alpha_1t_1S^*}{(\alpha_1+S^*)^2}\left(\dfrac{r_1t_2S^*Y^*}{K_1\alpha_2}-\dfrac{t_1S^*}{1+at_1S^*}\right),\\
d_4 = \dfrac{\eta_1\alpha_1r_1t_1t_2X^*YS^{*2}}{K_1K_2\alpha_2(1+at_1S^*)^2}+\dfrac{r_1r_2X^*}{K_1K_2}\left(\dfrac{\eta_1t_1S^*}{\alpha_1+S^*}+\upsilon_6\right)(\upsilon_2+\delta_2+e_1(S^*+X^*)+t_2Y^*)-\dfrac{\eta_1\alpha_1r_1t_1t_2X^*YS^{*2}}{K_1K_2\alpha_2(1+at_1S^*)^2}r_2\left(1-\dfrac{2X^*+S^*}{K_2}\right)-\\
\dfrac{\eta_1\alpha_1(t_1S^*)^2}{(1+at_1S^*)^3}\left(r_2\left(1-\dfrac{2X^*+S^*}{K_2}\right)\right)-\\
\left(r_1\left(1-\dfrac{2S^*+X^*}{K_1}\right)+\dfrac{t_1\alpha_1Y^*}{(1+at_1S^*)^2}\right)\left(r_2\left(1-\dfrac{2X^*+S^*}{K_2}\right)\right)\left[\left(\dfrac{\eta_1t_1S^*}{1+at_1S^*}+\upsilon_6\right)(\upsilon_2+\delta_2+e_1(S^*+X^*)+t_2Y^*)+\eta_2t_2^{*2}Y^{*2}\right].
\end{cases}
$$

The Ruth-Hurwitz criterion serves as both the necessary and sufficient condition for establishing the asymptotic stability of E_o^{XY}. This criterion ensures that all roots of the characteristic polynomial (Eq. (15)) have negative real components. This condition is fulfilled if the inequality $(d_1d_2+d_3)d_3+d_1^2d_4\le 0$ is satisfied. Consequently, for the matrix J(XY) to have all eigenvalues negative, it is essential that $R_{XY}\le 1$, and E_o^{XY} achieves local asymptotic stability if $R_{XY}<1$.

Table 2
Model parameters, possible values and their sources.

Symbol	Baseline value	Ranges	References
λ	8000/**day**	6000–10,000	[39]
β_1	0.075/ **day**	0.028–0.122	[26]
β_2	0.0006635/ **day**	0.000127–0.0012	[26]
τ	730**days**	730	[28]
δ_1	0.0227/**d ay**	0.00039- 0.0227	[27,40]
δ_2	0.018805/**day**	0.00122–0.03639	[27]
υ_1	0.0028/**day**	0–0.5	[40]
υ_3	0.004/**day**	0.004–0.0182	[26]
υ_2	0.000569/**day**	0.0001–0.04	[23]
υ_4	2 /**day**	2–10	[26]
b_s	0.08/**day**	0.08–0.118	[26]
υ_5	1/**day**	1–5	[26,41]
ω_1	500/**day**		[26]
ω_2	4615/**day**	829–8400	[26,27]
e_1	0–0.5/**day**	0–0.5	Varied
e_2	0–0.5/**day**	0–0.5	Varied
e_3	0.001/**day**	0.001	Estimated
C_o	1000,000	1000,000	[24]
M_o	1000,000	1000,000	[28]
ρ	115 grams/**day**	70–160	[42]
θ_h	262/grams/**day**	10–513	[42]
K	1×10^5	1×10^5	[28]
K_s	1×10^5	1×10^5	[27]
K_2	1×10^5	1×10^5	Estimated
r_1	0.16 /**day**	0–0.5	Estimated
r_2	1.5 r_1/**day**	0–0.5	Estimated
ε	0.2	0.2–0.3	[24,39]
t_1	0–4/**day**	0–4	Varied
t_2	0–4/**day**	0–4	Varied
a	0- 3/**day**	0- 3	Varied
b	0–3/**day**	0- 3	Varied
η_1	0.07	0–1	[10]
η_2	0.09	0–1	[10]
υ_6	0.02/**day**	0.0001–0.04	[23,30]

3.3. Endemic equilibrium point of model Eqs. (1)-(9)

This represents a steady state solution that occurs when the disease persists in the community, and is calculated by equating the derivatives of the model equations (Eqs. (1)-(9)) to zero. Let $E_1^{XY}=(H_1^*,I_1^*,E^*,M^*,S_1^*,I_s^*,C^*,X_1^*,Y_1^*)$ be the endemic equilibrium with variables expressed in terms of I_s^* as follows:

$$
\begin{cases}
H^*(I_s^*)=\dfrac{\lambda(\upsilon_5C_o+\varepsilon\omega_2I_s^*)e^{-\upsilon_1\tau}}{\upsilon_1^2\upsilon_5C_o+\upsilon_1(\omega_2\beta_1+\varepsilon\upsilon_1\omega_2)I_s^*},\\
I^*(I_s^*)=\dfrac{\beta_1\omega_1\lambda e^{-\upsilon_1\tau}I_s^*}{\upsilon_1(\upsilon_1+\delta_1)[\upsilon_1\upsilon_5C_o+(\beta_1\omega_2+\varepsilon\upsilon_1\omega_2)I_s^*]}\\
\#\\
E^*(I_s^*)=\dfrac{\beta_1\omega_1\rho\theta_hK\lambda e^{-\upsilon_1\tau}I_s^*}{\upsilon_1\upsilon_5C_oK(\upsilon_1+\delta_1)(\omega_1+\upsilon_3)+(\beta_1\omega_1\rho\theta_hK\lambda e^{-\upsilon_1\tau}+\beta_1\omega_2+\varepsilon\upsilon_1\omega_2)I_s^*},\\
\#\\
M^*(I_s^*)=\dfrac{\beta_1\omega_1^2\rho\theta_hK\lambda e^{-\upsilon_1\tau}I_s^*}{\upsilon_1\upsilon_4\upsilon_5C_oK(\upsilon_1+\delta_1)(\omega_1+\upsilon_3)+\beta_1\omega_1\rho\theta_hK\lambda e^{-\upsilon_1\tau}+\omega_2\upsilon_4(\beta_1+\varepsilon\upsilon_1)I_s^*},\\
S_1^*(I_s^*)=\dfrac{\upsilon_6+t_2(b\upsilon_6-\eta_2)I_s^*}{t_1(\eta_1-a\upsilon_6)+t_1t_2(\eta_1+a\eta_2-ab\upsilon_6)I_s^*},\\
C^*(I_s^*)=\dfrac{\omega_2}{\upsilon_5}I_s^*,\\
X_1^*(I_s^*)=K_2-e_3\left(\dfrac{\upsilon_6+t_2(b\upsilon_6-\eta_2)I_s^*}{t_1(\eta_1-a\upsilon_6)+t_1t_2(\eta_1+a\eta_2-ab\upsilon_6)I_s^*}+I_s^*\right)\\
Y_1^*(S_1^*,I_s^*,X_1^*)=\dfrac{\beta_2S_1^*I_1^*-(I_{0s}+\varepsilon_1I_s^*)(\upsilon_2+\delta_2+e_2(S^*+I_s^*+X^*))I_s^*}{(1+bt_2I_s^*)(I_{0s}+\varepsilon_1I_s^*)}
\end{cases}
$$

To determine I_s^*, we use Eq. (5) of model (Eqs. (1)-(9)) at endemic equilibrium when $dX/dt=0$. Substituting $S_1^*(I_s^*)$ and $X_1^*(I_s^*)$, we obtain

an equation in the form

$$A_1 I_s^{*2} + A_2 I_s^{*} - A_3 = 0 \tag{16}$$

where

$$A_1 = e_3 t_1 t_2 (1 - e_3)(\eta_1 + a\eta_2 - ab\upsilon_6),$$

$$A_2 = t_1 t_2 K_2 (1 + e_3)(\eta_1 + a\eta_2 - ab\upsilon_6) + e_3 t_1 (1 - e_3)(\eta_1 - a\upsilon_6) - t_2 (1 + e_3^2)(b\upsilon_6 - \eta_2)$$

$$A_3 = t_1 K_2 (1 + e_3)(\eta_1 - a\upsilon_6) - (1 + e_3^2)\upsilon_6.$$

The positive root of Eq. (14) provides the solution for I_s^*, specifically:

$$I_s^* = \frac{-A_2 \pm \sqrt{{A_2}^2 + 4A_1A_3}}{2A_1}.$$

This solution is valid and the endemic equilibrium point exists if $I_s^* \in R_{+0}$, the set of non-negative real numbers.

3.4. Bifurcation analysis

To investigate both the type of bifurcation exhibited and the local stability of the endemic equilibrium, E_1^{XY} of the model (Eqs. (1)-(9)), we use the center manifold theory described by Castillo-Chavez and Song [34]. To apply this theory, a change of variables is introduced for the normalized version of model (Eqs. (1)-(9)). i.e., introducing $H = x_1$, $I = x_2$, $E = x_3$, $M = x_4$, $S = x_5$, $I_s = x_6$, $X = x_8$, $Y = x_9$, the model is transformed to:

$$\left.\begin{aligned}
\dot{x}_1 &= \Lambda_1 - \frac{\beta_1 x_1 x_7}{C_o + \varepsilon x_7} - \upsilon_1 x_1 := f_1,\\
\dot{x}_2 &= \frac{\beta_1 x_1 x_7}{C_o + \varepsilon x_7} - (\upsilon_1 + \delta_1)x_2 := f_2\\
\dot{x}_3 &= \rho\theta_h x_2\left(1 - \frac{x_3}{K}\right) - (\omega_1 + \upsilon_3)x_3 := f_3,\\
\dot{x}_4 &= \omega_1 x_3 - \upsilon_4 x_4 := f_4\\
\dot{x}_5 &= r_1 x_5\left(1 - \frac{x_5 + e_1(x_6 + x_8)}{K_1}\right) - \frac{\beta_2 x_4 x_5}{M_o + \varepsilon x_4} - \frac{t_1 x_5 x_9}{1 + at_1 x_5} := f_5,\\
\dot{x}_6 &= \frac{\beta_2 x_4 x_5}{M_o + \varepsilon x_4} - (\upsilon_2 + \delta_2 + e_2(x_5 + x_8) + x_6)x_6 - \frac{t_2 x_6 x_9}{1 + bt_2 x_6} := f_6\\
\dot{x}_7 &= \omega_2 x_6 - \upsilon_5 x_7 := f_7,\\
\dot{x}_8 &= r_2 x_8\left(1 - \frac{x_8 + e_3(x_5 + x_6)}{K_2}\right) := f_8\\
\dot{x}_9 &= \frac{\eta_1 t_1 x_5 x_9}{1 + at_1 x_5} + \frac{\eta_2 t_2 x_6 x_9}{\alpha_2 + x_6} - \upsilon_6 x_9 := f_9
\end{aligned}\right\} \tag{17}$$

The transformed model has the disease-free equilibrium given as $E_0^d = \left({x_1}^* = \frac{\lambda e^{-\upsilon_1 \tau}}{\upsilon_1},\ {x_2}^* = 0,\ {x_3}^* = 0,\ {x_4}^* = 0,\ {x_5}^* = {x_5}^*,\ {x_6}^* = 0,\ {x_7}^* = 0,\ {x_8}^* = {x_8}^*,\ {x_9}^* = {x_9}^*\right)$. Let $\beta_2 = \beta^{**}$ be the bifurcation parameter, with $R_{XY} = 1$, Subsequently, we have $\beta^{**} = \frac{\upsilon_1\upsilon_4\upsilon_5 C_o M_o K(\upsilon_1+\delta_1)(\upsilon_2+\delta_2+e_2(S^*+X^*)+t_2Y^*)}{\beta_1\omega_2\rho\theta_h\lambda e^{-\upsilon_1\tau}}$ and the corresponding Jacobian matrix of the model (Eq. (17)) at the E_0^d is:

$$J(E_0^d) = \begin{bmatrix}
-\upsilon_1 & 0 & 0 & 0 & 0 & 0 & -\frac{\beta_1 {x_1}^*}{C_o} & 0 & 0\\
0 & -(\upsilon_1 + \delta_1) & 0 & 0 & 0 & 0 & \frac{\beta_1 {x_1}^*}{C_o} & 0 & 0\\
0 & \rho\theta_h & -(\omega_1 + \upsilon_3) & 0 & 0 & 0 & 0 & 0 & 0\\
0 & 0 & \omega_1 & -\upsilon_4 & 0 & 0 & 0 & 0 & 0\\
0 & 0 & 0 & -\frac{\beta^{**} {x_5}^*}{M_o} & g_1 & \frac{-r_1 {x_5}^*}{K_1} & 0 & \frac{-r_1 {x_5}^*}{K_1} & \frac{-t_1 {x_5}^*}{1 + at_1 {x_5}^*}\\
0 & 0 & 0 & \frac{\beta^{**} {x_5}^*}{M_o} & 0 & g_2 & 0 & 0 & t_2 {x_9}^*\\
0 & 0 & 0 & 0 & 0 & \omega_2 & -\upsilon_5 & 0 & 0\\
0 & 0 & 0 & 0 & \frac{-r_2 {x_8}^*}{K_2} & \frac{-r_2 {x_8}^*}{K_2} & 0 & g_3 & 0\\
0 & 0 & 0 & 0 & \frac{\eta_1 t_1 {x_5}^*}{(1 + at_1 {x_5}^*)^2} & \eta_2 t_2 {x_9}^* & 0 & 0 & g_4
\end{bmatrix}$$

where $g_1 = r_1\left(1 - \frac{2{x_5}^* + {x_8}^*}{K_1}\right) - \frac{t_1 {x_9}^*}{(1+at_1 {x_5}^*)^2}$, $g_2 = -(\upsilon_2 + \delta_2 + e_2({x_5}^* + {x_8}^*) + t_2 {x_9}^*)$, $g_3 = r_2\left(1 - \frac{2{x_8}^* + {x_5}^*}{K_2}\right)$, and $g_4 = \frac{\eta_1 t_1 {x_5}^*}{1+at_1 {x_5}^*} - \upsilon_6$. It is clear

that zero is a simple eigenvalue of the Jacobian matrix, $J(E_0^d)$. The corresponding eigenvectors represent an approximate rate of infected human/snails in an endemic state when the disease-free state is unstable and the asymptotic distribution of the infected human/snails as the disease dies out. Thus $J(E_0^d)$ has a right eigenvector $u = (u_1, u_2, u_3, u_4, u_5, u_6, u_7, u_8, u_9)$ and a left eigenvector $v = (v_1, v_2, v_3, v_4, v_5, v_6, v_7, v_8, v_9)$ associated with zero eigenvalue satisfying the condition $u.v = 1$, where

$$\begin{pmatrix} u_1 \\ u_2 \\ u_3 \\ u_4 \\ u_5 \\ u_6 \\ u_7 \\ u_8 \\ u_9 \end{pmatrix} = \begin{pmatrix} -\frac{\beta_1 {x_1}^*}{C_o} u_7, \\ \frac{\beta_1 {x_1}^*}{C_o(v_1+\delta_1)} u_7, \\ \frac{\beta_1 \rho \theta_h {x_1}^*}{C_o(v_1+\delta_1)(\omega_1+v_3)} u_7, \\ \frac{\beta_1 \omega_1 \rho \theta_h {x_1}^*}{C_o v_4(v_1+\delta_1)(\omega_1+v_3)} u_7, \\ -\frac{r_1 r_2 K_1 v_5 {x_8}^*}{r_1 \omega_2 (r_1 K_2 {x_5}^* + r_2 K_1 {x_8}^*)} u_7, \\ \frac{v_5}{\omega_2} u_7, \\ u_7 > 0 \\ -\frac{r_1 r_2 K_1 v_5 (1+ \mathrm{at}_1 {x_5}^*)^2 {x_5}^* {x_8}^*}{\omega_2 g_3 \eta_1 t_1 {x_5}^* (r_1 K_2 {x_5}^* + r_2 K_1 {x_8}^*)} u_7, \\ -\frac{r_1 r_2 K_1 v_5 (1+ \mathrm{at}_1 {x_5}^*)^2 {x_5}^* {x_8}^*}{\omega_2 g_3 \eta_1 t_1 {x_5}^* (r_1 K_2 {x_5}^* + r_2 K_1 {x_8}^*)} u_7, \end{pmatrix} = \begin{pmatrix} 0 \\ \frac{C_o v_5}{\beta_1 {x_1}^*} v_7 \\ \frac{C_o v_5 (v_1+\delta_1)}{\rho \theta_{h\beta_1} {x_1}^*} v_7 \\ \frac{C_o v_5 (v_1+\delta_1)(\omega_1+v_3)}{\omega_1 \rho \theta_{h\beta_1} {x_1}^*} v_7 \\ \frac{g_3 C_o M_o v_5^2 (v_1+\delta_1)(\omega_1+v_3)}{K_1 \omega_1 \rho \theta_{h\beta_1 (r_1 {x_5}^* - g_3 K_1) {x_1}^*}} v_7 \\ \frac{\omega_2 {x_5}^*}{(v_2+\delta_2)} v_7 \\ v_7 > 0 \\ \frac{C_o M_o v_5^2 (v_1+\delta_1)(\omega_1+v_3)}{r_1 \omega_1 \rho \theta_{h\beta_1 (r_1 {x_5}^* - g_3 K_1) {x_1}^{*2}}} v_7 \\ \mathscr{M} \left(\frac{r_2 {x_5}^*}{K_2} - \frac{g_1 g_3 K_1}{r_1 {x_5}^*} \right) v_7 \end{pmatrix}$$

where $\mathscr{M} = \frac{C_o M_o r_1 v_5^2 (1+ \mathrm{at}_1 {x_5}^*)^2 (v_1+\delta_1)(\omega_1+v_3)(1+ \mathrm{at}_1 {x_5}^*)^2}{K_1 \omega_1 \rho \theta_h \beta_1 \eta_1 t_1 (r_1 {x_5}^* - g_3 K_1) {x_1}^*}$.

$$\begin{cases} \frac{\partial^2 f_1}{\partial x_1 \partial x_7} = \frac{-\beta_1}{C_o}, \ \frac{\partial^2 f_2}{\partial x_1 \partial x_7} = \frac{\beta_1}{C_o}, \ \frac{\partial^2 f_3}{\partial x_2 \partial x_3} = \frac{-\rho \theta_h}{K}, \ \frac{\partial^2 f_5}{\partial x_4 \partial x_5} = \frac{-\beta^{**}}{M_o}, \ \frac{\partial^2 f_5}{\partial {x_5}^2} = \frac{-2r_1}{K_1}, \ \frac{\partial^2 f_5}{\partial x_5 \partial x_6} = \frac{-r_1}{K_1}, \\ \frac{\partial^2 f_5}{\partial x_5 \partial x_9} = \frac{-t_1}{(1+ \mathrm{at}_1 {x_5}^*)^2}, \frac{\partial^2 f_6}{\partial x_4 \partial x_5} = \frac{\beta^{**}}{M_o}, \ \frac{\partial^2 f_6}{\partial x_5 \partial x_6} = \frac{\partial^2 f_6}{\partial x_6 \partial x_8} = -e_2, \ \frac{\partial^2 f_6}{\partial x_6 \partial x_6} = -2e_2, \\ \# \\ \frac{\partial^2 f_6}{\partial x_6 \partial x_9} = \frac{t_2}{\alpha_2}, \ \frac{\partial^2 f_8}{\partial x_5 \partial x_8} = \ \frac{\partial^2 f_8}{\partial x_6 \partial x_8} = \frac{-r_2}{K_2}, \frac{\partial^2 f_6}{\partial {x_8}^2} = \frac{-2r_2}{K_2}, \ \frac{\partial^2 f_5}{\partial x_4 \partial \beta^*} = \frac{-{x_5}^*}{M_o}, \ \frac{\partial^2 f_6}{\partial x_4 \partial \beta^*} = \frac{{x_5}^*}{M_o} \end{cases}$$

We compute the values of the coefficients a and b according to the formulae in Castillo-Chavez and Song [34], where:

$$a = \sum_{k,\ i,\ j=1}^{9} v_k u_i u_j \frac{\partial^2 f_k}{\partial x_i \partial x_j} \left(E_1^d, \beta^{**}\right)$$

$$b = \sum_{k,\ j=1}^{9} v_k u_i \frac{\partial^2 f_k}{\partial x_i \beta^{**}} \left(E_1^d, \beta^{**}\right)$$

where the non-vanishing second-order partial derivatives at the disease-free equilibrium E_0^d, are algebraically given by

Thus, considering the signs and combining similar terms we obtain

$$a = \left(v_5 u_4 u_5 \frac{\beta^{**}}{M_o} + v_5 u_5 u_6 \frac{r_1}{K_1} + v_6 u_5 u_6 e_2 + v_5 u_5 u_6 \frac{r_2}{K_2} \right)$$
$$- \left(v_2 u_1 u_7 \frac{\beta_1}{C_o} + v_3 u_2 u_3 \frac{\rho \theta_h}{K} + 2 v_5 {u_5}^2 \frac{-t_1}{(1+ \mathrm{at}_1 {x_5}^*)^2} + v_6 u_6 u_8 e_2 + 2 v_6 {u_6}^2 e_2 + v_6 u_6 u_9 \frac{t_2}{\alpha_2} + 2 v_6 {u_8}^2 \frac{r_2}{K_2} \right)$$

$$b = \frac{u_4 x_5^*}{M_o}(v_5 + v_6)$$

The positivity of the coefficient b has been established. As pointed out by Castillo-Chavez and Song [34], the behavior of coefficient a determines the specific characteristics of the local dynamics of the equilibrium points. Consequently, if $a < 0$, the model system (Eq. (17)) will exhibit forward bifurcation where the endemic equilibrium is locally asymptotically stable. Conversely, if $a > 0$, it will undergo backward bifurcation. This can lead to the coexistence of stable and endemic equilibria, and reducing the reproduction number $R_{XY} < 1$ at disease free equilibrium does not guarantee disease eradication. This makes disease control more difficult, as both competition and predation measures may still result in persistent low endemicity. To anticipate and manage backward bifurcation, in addition to competition and predation of snail-vector control measures, it is essential to implement more interventions such as increased treatment coverage and public health education. In addition, in order to respond to the dynamic changes in the system and to prevent the disease from re-emerging, monitoring and adaptive management strategies should be put in place.

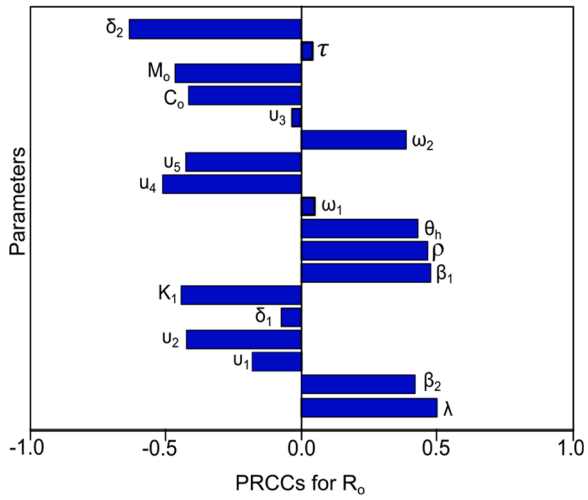

Fig. 2. Partial rank correlation coefficients (PRCC) for sensitivity analysis of R_0 with respect to each model parameter when no control measures are implemented.

4. Numerical simulations

We use the R statistical environment version 4.0.3 [35], and the main R package for executing ordinary differential equations [36]. We use information from relevant literature to determine the parameters of the model (Table 2). Parameters not typically found in the literature are replicated using expert knowledge, taking into account the prevailing understanding of vector and disease dynamics in schistosomiasis. For instance, the documented initial age of infection in children is typically around 2 years (730 days) [37]. However, it is worth noting that the disease can also affect very young children who are under the age of 2 if they come into contact with contaminated freshwater sources through activities such as washing. Furthermore, as reported by Cross and Benke [38], the interaction between species in competitive scenarios can exert

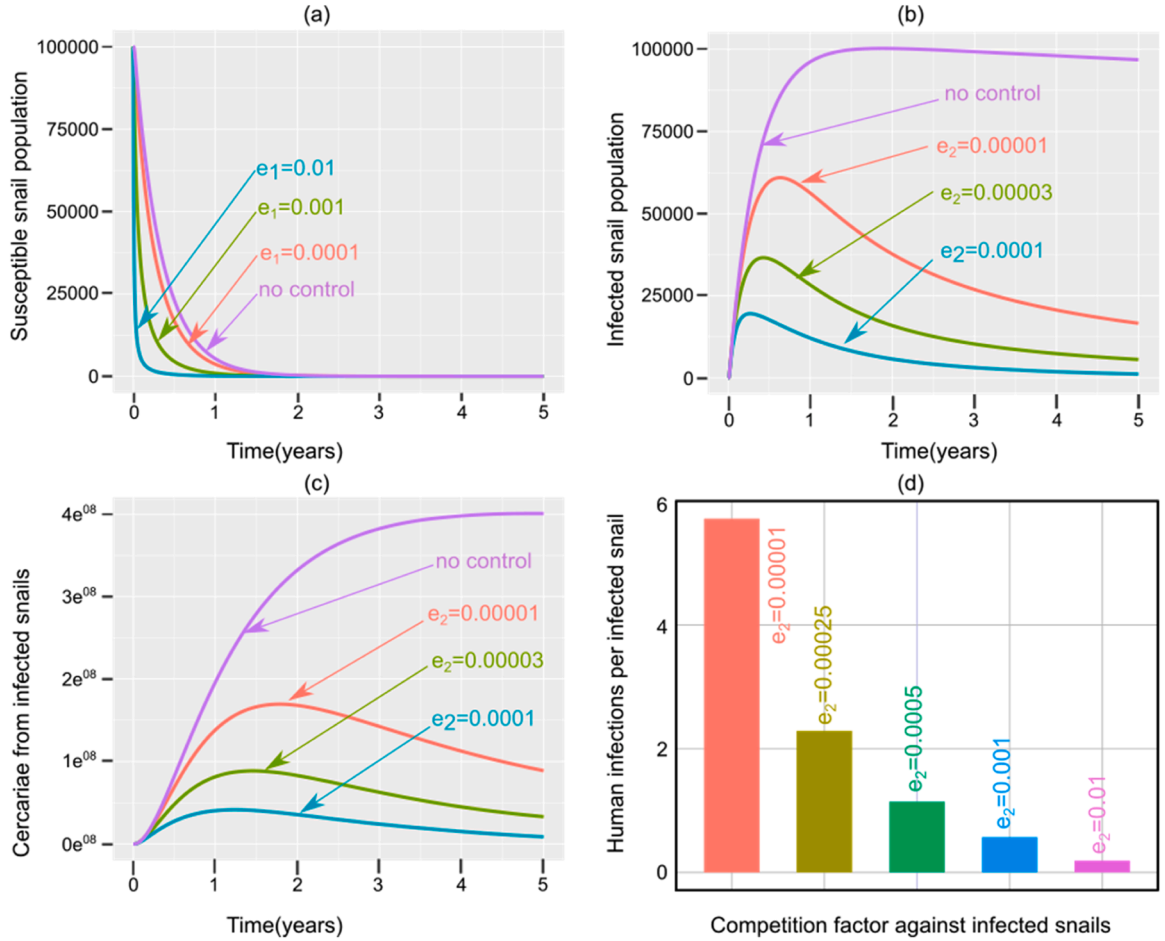

Fig. 3. Impact of varying competition against (a) susceptible snail population, and (b) infected snail population. The subsequent influence on (c) infectious cercariae emerging from infected snails, and (d) human infections per infected snail.

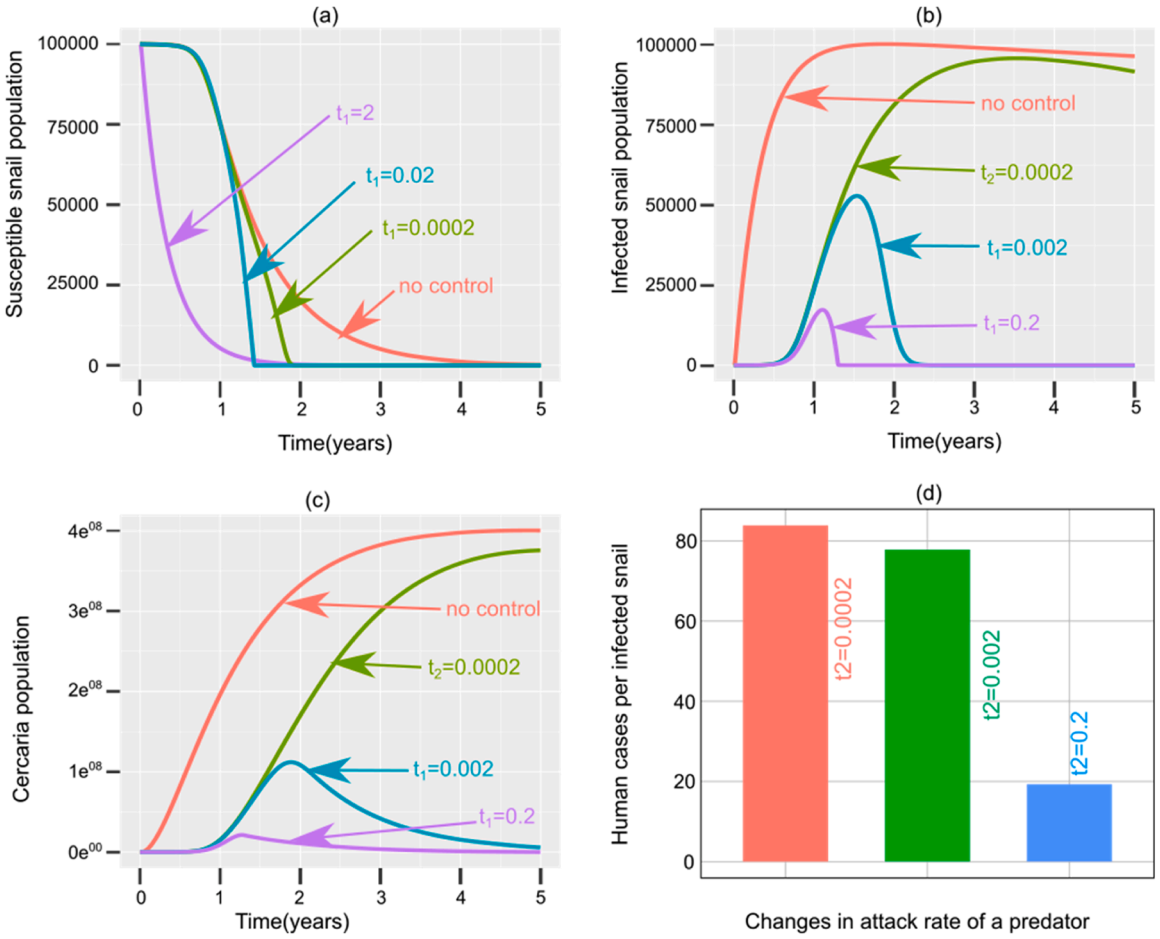

Fig. 4. Impact of varying the attack rate (t_1, t_2) of a predator on (a) susceptible snail population, and (b) infected snail population. The subsequent influence on (c) infectious cercaria emerging from infected snail population, and (d) human infections per infected snail.

a substantial influence on the disparities observed in their respective growth rates. Therefore, for comparison purposes, we assume that inherent natural increase (r_2) of the competitor snail will exhibit a 15 % increment over the inherent natural increase (r_1) of the IH snail. This is closer to the 10 % assumed in a similar study conducted by Allen and Victory [29]. In addition, we assume that $r_1, r_2 \in [0, 0.5]$ because values outside this range would indicate a doubling of the population within less than two time units, and this may not be realistic given reproduction and survival characteristics of snails. In addition, we assume that both the competitor and the IH snail have the same carrying capacities. Furthermore, we assume that infected snails are more impacted by competition and that the competition coefficients are such that $e_3 < e_2 < e_1 \in [0, 1]$ when the non-host competing snail outcompetes, otherwise the control agent is outcompeted. In addition, due to the limited availability of data regarding IH snail predation, the corresponding parameter values were adjusted over a range such that a, $b \in [0, 3]$, and $t_1, t_2 \in [0, 4]$ to account for different potential predator behaviors. For example, a predator's interest in its next prey may decrease as the number of prey items consumed increases, and some may typically require a longer period of handling before they resume hunting their next prey.

4.1. Sensitivity analysis of the model parameters

We performed a Partial Rank Correlation Coefficient (PRCC) test to measure the robustness of the model to parameter values and support the qualitative results of our analyses. PRCC helps identify which input parameters have the most significant impact on the output (R_0) of the model. This information can be crucial in understanding the behavior of the model, identifying influential factors, and making informed decisions, such as determining which parameters should be targeted for intervention strategies. Hence, we used the range of parameter values in Table 2 and the expression for the basic reproduction number, R_0, in equation Eq. (12) to compute the PRCC (Fig. 2).

Parameters with positive PRCC values increase R_0 when increased and therefore lead to higher risk of infection and vice versa (Fig. 2). However, an increase in parameters with negative PRCC values including δ_2, υ_2, K_1, υ_4, υ_5, C_o, and M_o (Fig. 2) results in R_0 reduction, critical for disease extinction. Notably, snail mortality parameter, δ_2 has a greater influence on reducing R_0, suggesting that increasing δ_2 could potentially decrease the endemicity of the disease. In addition, R_0 is a decreasing function of δ_2 and υ_2 therefore it makes sense that control intervention targeting δ_2 and υ_2 would be an accepted strategy. This study underscores the incorporation of biological control measures for IH snails, with a particular focus on assessing how snail competitors and predators influence the IH snail populations. Additionally, it examines the subsequent impact on the cercaria population originating from infected IH snails, which, in turn, poses a risk of disease transmission to humans.

4.2. Impact of a snail competitor on the population dynamics of IH snails and cercariae

We use a pure competition model with a snail competitor as a control strategy to mitigate IH snail and the subsequent cercaria populations. We fix $e_3 = 0.001$ and vary the competition factors e_1 and e_2 to account

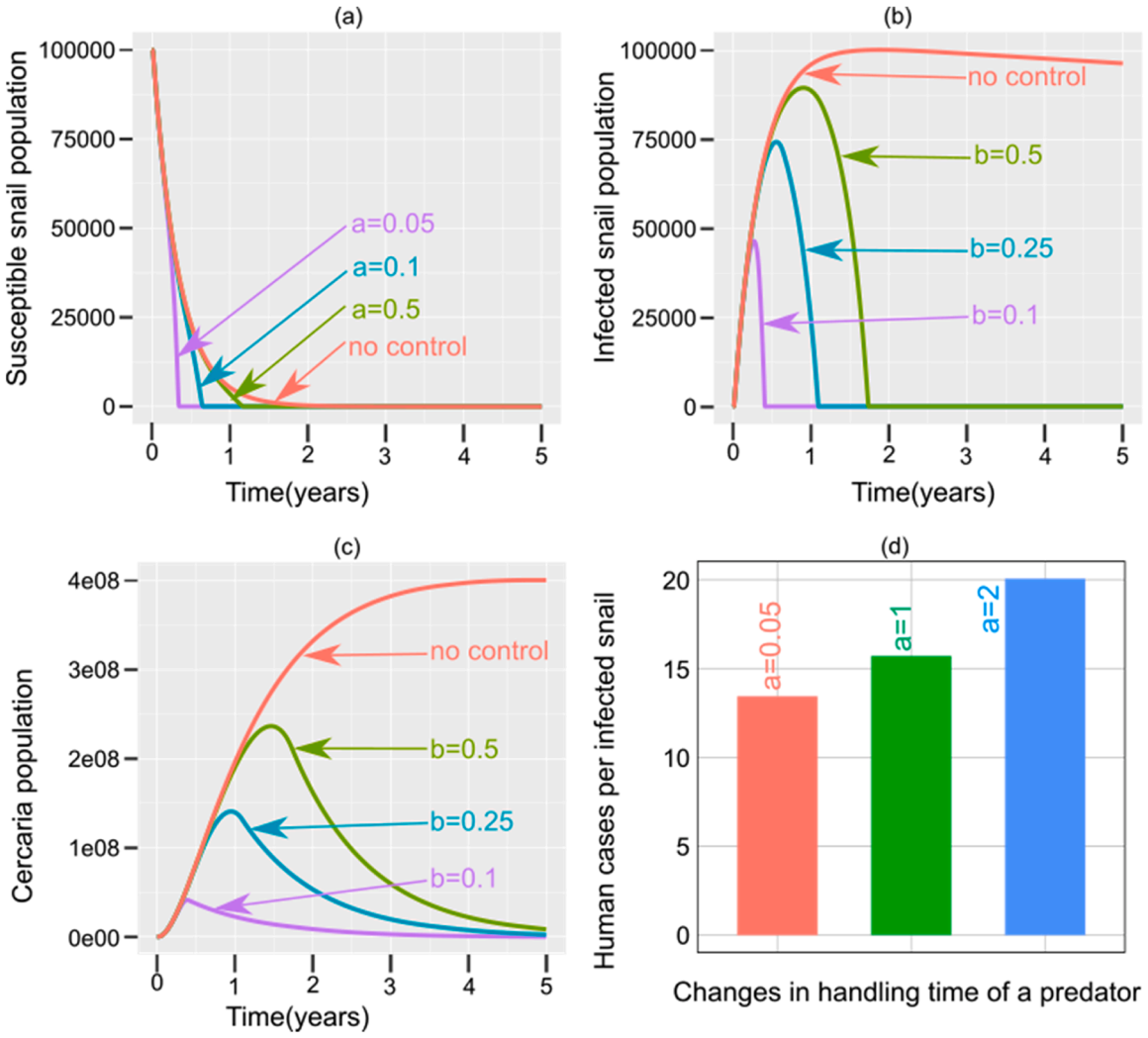

Fig. 5. Impact of varying the handling time (a, b) of a predator on (a) susceptible snail population, and (b) infected snail population. The subsequent influence on (c) infectious cercaria emerging from infected snail population, and (d) human infections per infected snail.

Table 3
Various parameter sets representing distinct combinations of both snail competitors and snail predators.

	e_1	e_2	t_1	t_2	a	b
Set 1	0.001	0.00001	0.002	2	3	0.5
Set 2	0.0001	0.00003	0.02	1	0.5	0.1
Set 3	0.00003	0.0001	0.2	0.04	0.05	0.5
Set 4	0.000001	0.001	2	0.004	0.005	1

for the variability in competition against the IH snail populations. This accounts for different potential competitive snails that may behave more specifically and competitively than the intermediate host in an ecosystem. Our findings demonstrate a substantial reduction in the number of susceptible IH snail population with increasing values of e_1 (Fig. 3a) and a reduction in infected snail population, as well as the subsequent emergence of cercaria population from infected snails, with increasing values of e_2 (Fig. 3b, 3c). As a result, there is a corresponding decrease in the number of infected individuals per infected snail (Fig. 3d). Based on our observations, snail competitors with higher competitive abilities, such as $e_1, e_2 > 0.001$, are promising as effective biological control agents. In particular, these competitors have the potential to suppress especially the population of infected IH snails. Consequently, the subsequent infective cercaria population from infected snails is reduced leading to a potential reduction in human infections and the transmission of schistosomiasis. This reduction could potentially drive the reproduction number below 1, indicating a potential for disease extinction. However, it is worth noting that some snail competitors with lower competitive abilities ($e_1, e_2 < 0.00025$) are ineffective control agents. Their coexistence can only bring about a partial reduction in the IH snail population. The number of subsequent infectious cercaria population and the corresponding human infection per infected snail are still high. Thus, the reproduction number remains higher than one, allowing the disease to persist.

4.3. Impact of a predator on the population dynamics of IH snails and cercariae

We use the predator-only model with the predator as the only control strategy. To account for variation in predation caused by several potential predators of IH snails with specific predation abilities, we vary the predation parameters. First, we investigate the effects of varying the attack rates t_1 and t_2 of susceptible and infected snails, respectively. This is done by fixing the handing times $a = 0.25$ and $b = 0.175$. The results show that increasing the predator attack rate has a negative effect on the IH susceptible snail population (Fig. 4a) and the infected snail population as well as the subsequent cercaria population (Fig. 4b, 4c). Consequently, there is a concurrent reduction in the number of infected

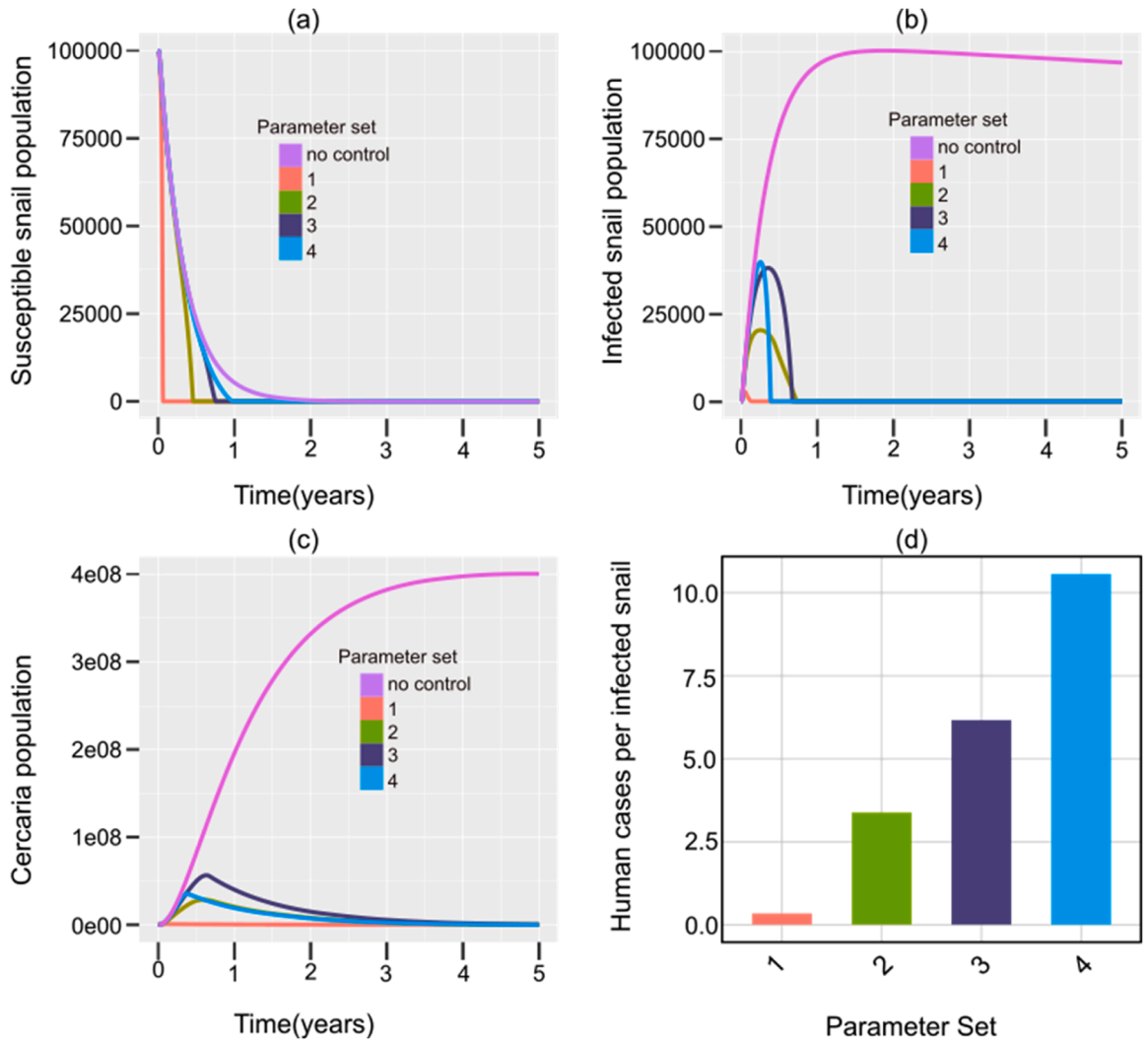

Fig. 6. Impact of varying competition factors (e_1, e_2), attack rates (t_1, t_2), and handling times (a, b) on (a) susceptible snail population, and (b) infected snail population. The subsequent influence on (c) infectious cercaria emerging from infected snail population, and (d) human infections per infected snail.

individuals per infected snail (Fig. 4d) and the disease is less prevalent. Thus, predators with higher attack rates tend to be more effective as biological control agents for IH snails (Fig. 4d). On the contrary, predators characterized by a low attack rate ($t_2 < 0.0002$ hour/day) exhibit reduced efficiency in regulating snail populations and achieving a reduction of human infections to less than one individual (Fig. 4d) and schistosomiasis may persist in the population.

Second, the effects of changing the handling times a and b of susceptible and infected snails, respectively, are examined. This is done by fixing the attack rate $t_1 = 0.02$ and $t_2 = 0.4$.

The findings indicate that reducing the handling time of the IH snail by the predator has adverse effects on both the IH susceptible snail population (Fig. 5a) and the infected snail population, together with the subsequent cercaria population (5b, 5c). In our findings, predators with shorter handling times, exemplified by values where $a = b < 0.05$, consistently prove to be more effective biological control agents in reducing the IH snail population (Fig. 5a, b), consequently leading to a reduction in the subsequent infectious cercaria population (Fig. 5c). Consequently, the occurrence of human infections per infected snail is notably lower (Fig. 5d), thereby alleviating the burden of schistosomiasis. Conversely, predators characterized by longer handling times ($b >$ 1 hour/day) have limited efficacy as control agents. They are less efficient in reducing the number of snail hosts, which, in turn, results in the persistence of high human infection rates even in the presence of such control measures (Fig. 5d). This persistence suggests that schistosomiasis may endure within the population. Thus, the dynamics ofschistosomiasis can be greatly determined by the handling time (a, b) and attack rate (t_1,t_2) of the IH snails by the potential predator.

4.4. Impact of both a snail competitor and a predator on the population dynamics of IH snails and cercariae

We investigate various scenarios employing both biological control agents. We use randomized sets of competition and predation parameters to simulate situations in which competition and/or predation can exert either a strong or weak influence, or achieve intermediate impact on IH snail populations. We use four sets of parameters as defined in Table 3.

The findings reveal that the presence of potential snail competitors and snail predators alongside IH snails can have a substantial impact on their populations, leading to variations in emerging cercariae populations and a reduction in the subsequent number of human infections per infected snail, depending on the specific parameter sets (Fig. 6). In general, decreasing e_1, t_2, a, and increasing e_2, t_1, b were found to be optimal for effective management of IH snail populations and controlling schistosomiasis. For instance, in Set 4, the combination of a snail competitor with high competitive abilities and a snail predator with strong predation capabilities, especially against infected snail

populations, results in a lower incidence of human infections compared to unity (Fig. 6d). This suggests that schistosomiasis transmission is significantly less likely to occur, potentially creating disease-free environments in areas where both biological agents are introduced or coexist naturally. However, it is important to note that certain combinations of snail competitors and snail predators can lead to high numbers of IH snails, subsequent infectious cercariae, and human infections per infected snail (Fig. 6d), which may contribute to disease persistence. In such cases, these agents are less effective in controlling the disease.

5. Discussion

We formulated and analyzed a deterministic model for the control of schistosomiasis by competitive and predatory control of the IH snails. In the analysis, we explored the feasible region, and computed the stability and characteristics of disease-free and endemic equilibrium points. Additionally, bifurcation analyses were conducted, revealing instances of backward bifurcation for specific parameter values. Sensitivity analysis of the basic reproduction number (R_0) highlighted δ_2 as the most negatively influential sensitivity parameter, thus identifying it as a potential intervention target. Therefore, the primary intervention strategy was to introducenon-host competiting snails and/or snail predators to reduce the population of IH snails and the infectious cercariae emerging from the infected snail population.

Our study reveals that the distinct competitive advantage demonstrated by competitor snails over IH snails significantly diminishes the population size of IH snails, particularly among the infected subgroup, along with a subsequent reduction in the emergence of cercariae. This finding is consistent with empirical observations from field and laboratory investigations, indicating that within a competitive ecological context, characterized by resource scarcity, outcompeted populations remain constrained in size. s As a result, some species within the population die off, while the survivors have reduced diminished reproductive rates and produce fewer infectious cercariae [45–48]. In some cases of species shift, displacement, and invasion are most likely. In particular, Pointier and McCullough [47] specifically documented a decline in the population of IH snails *Biomphalaria glabrata*, coinciding with the proliferation of competitors such as *Melanoides tuberculata* and *Thiara granifera* in certain habitats. This phenomenon results in limited interaction of the schistosomes with humans and reduced disease prevalence. Our findings are consistent with mathematical models suggesting that the use of a suitable snail competitor as a biological control can strongly influence infection dynamics, stop local transmission, and potentially eradicate schistosomiasis [10,29]. However, the reverse case is also proven, certain potential competitors are only less/average competitors and that competition has less impact on susceptible IH snails, As a result, cercariae-human interaction is high and disease can potentially spread. This result complements a field study in which *Lanistes carinatus* species were introduced into water canals and only a small decrease in the density of *B. pfeifferi* was subsequently observed [49].

Predator attack and handling times are also important factors affecting the control of schistosomiasis because they determine the extent of predation on IH snails. According to our results, schistosomiasis prevalence correlates with handling time and inversely with attack time. According to our results, predators making quick handling decisions and attacking quickly may prey more on infected IH snails than on healthy or susceptible IH snails, thus reducing their population and shedding infectious cercariae. The findings of our study are supported by studies showing that infected prey (snails) tend to be weaker, more immobile, live in more accessible areas, and change their appearances or behaviors, leaving them more vulnerable to predators [50,51], whereas healthy snails may seek refuge beneath submerged aquatic plants near transmission sites [29,15,49]. The presence of predators therefore plays a significant role in both regulating and contributing to the success of schistosomiasis control at transmission sites. A higher abundance of potential snail-eating predators increases the effectiveness of schistosomiasis control. Conversely, the low presence or absence disease control predators explains the persistence of schistosomiasis in certain areas [44,19]. For example, Madsen and Stauffer [44] observed that the decline in fish density due to overfishing in Lake Malawi was linked to increased schistosomiasis transmission in that region. On the other hand, certain predators tend to opt for alternative food sources, failing to effectively impact and reduce IH snail populations, thus limiting their potential as effective biological control agents [49]. For example, *Marisa cornuarietis* consumes not only juvenile and potentially adult vector snails but also other snails [52].

Our study shows that specific combinations involving the competitive abilities of a snail competitor and the predatory effectiveness of certain species lead to a significant reduction in the population of IH snails, with the reproductive numbers falling below unity, indicating effective disease control measures. However, a notable observation is that heightened levels of competition and predation, especially when IH snails face intense competitive pressure and exploitative predation, could potentially lead to the complete elimination of IH snail populations. This outcome is characterized by instances of species displacement and local extinction, underscoring the delicate balance between competitive and predatory interactions. Furthermore, specific scenarios emerge where the interaction disproportionately impacts infected snails rather than susceptible IH snails. This unique dynamic sustains the diversity of susceptible IH snails without triggering species loss, potentially contributing to a more resilient ecosystem. However, it is essential to acknowledge that certain predators exert a more restricted influence on IH snails, allowing infected individuals to persist. Consequently, this facilitation of infected snails' survival maintains the presence of the disease in their vicinity, emphasizing the complexity of predator-prey relationships within this context. Our findings are substantiated by several studies that demonstrated aggressive predation (e.g., by some crustaceans) and competition between potential competitor snails (e.g., *Thiara granifera* and *Melanoides tuberculata*). This led to ecosystem invasions, which resulted in extinctions and the loss of species, especially in the genera *Biomphalaria* and *Bulinus* [10,15,16,53]. Furthermore, ecologists and parasitologists have criticized some snail predators for to their consumption of non-target gastropod species and aquatic plant communities (water lilies). Consequently, the presence of non-specific predators in large natural water bodies (lakes), poses a threat to freshwater biodiversity, as seen in Lake Malawi and East African lakes [17,43]. Nevertheless, some predatory fish, such as the cichlid *Astatoreochromis alluaudi*, demonstrated only initial success and proved ineffective in sustaining long-term snail control efforts, which is likely due to their slow reproduction rate, which makes them less suitable for large-scale biocontrol initiatives [54]. This can be associated with the fact that fish reproduce too slowly to be useful in large-scale biocontrol efforts. However, it has also been reported that the reintroduction of native predators, e.g., river prawns or crayfish, has further reduced the density of IH snails [10]. Consequently, if biological agents, especially native ones, are experimentally evaluated for their competitive and predatory capabilities, integrated control measures may prove to be both cost-effective and long-lasting. This outcome aligns with the discovery that certain natural predators of disease vectors offer viable ecological approaches to disease control [55]. For instance, an optimal approach could involve using snails as competitors only when their competitive abilities match those of susceptible IH snails and to use predators with average attack rates and quicker handling times. This approach offers a naturally cost-effective in implementation, environmentally friendly, and self-sustaining strategy for managing IH snails and eliminating schistosomiasis. Thus, population growth models such as the one presented here can be helpful in hypothesis testing, landscape planning, or scenario analysis prior to the management of predator and competitor snail populations. We conclude that selective competitor-predator intervention is a way forward to control schistosomiasis in style of a nature-based and sustainable manner.

6. Future work

We propose three important tasks for the future. First, despite the benefits of using a population growth model for *a priori* testing of schistosomiasis dynamics, field and laboratory research is needed to gain a better understanding of the mechanisms responsible for generating these dynamics. Native snail competitors and snail predators need to be tested under controlled and in situ conditions to determine whether their effects on IH snails are minor and ineffective, or whether they exploit them, resulting in invasive, colonizing, or extinction behaviors.

Secondly, the structure and setup of the population growth model and its parameter values can influence the results. For example, adding a climate component to the model could be useful, as climatic variables may affect the schistosomiasis life cycle over time. Furthermore, the lack of experimental parameter values in the literature is a challenge for model parameterization.

Thirdly, there is a need to explore alternative vector control methods, including molluscicides, physical removal, and environmental modifications.

Therefore, our model with its competition rates, attack and handling times should be seen as a tool to test the effects and hypotheses of biological control methods in relation to the spread of schistosomiasis.

Supporting information

All the data used in the study are available in the paper.

CRediT authorship contribution statement

Zadoki Tabo: Writing – original draft, Validation, Software, Methodology, Formal analysis, Data curation, Conceptualization. **Livingstone Luboobi:** Writing – review & editing, Methodology, Investigation, Conceptualization. **Philipp Kraft:** Writing – review & editing, Visualization, Data curation. **Lutz Breuer:** Writing – review & editing, Supervision, Funding acquisition. **Christian Albrecht:** Writing – review & editing, Supervision, Project administration, Funding acquisition, Conceptualization.

Declaration of competing interest

The authors declare that they have no known competing financial interests or personal relationships that could have appeared to influence the work reported in this paper.

Funding and acknowledgements

The authors would like to express their gratitude to the German Academic Exchange Service (DAAD) for providing ZT with a PhD scholarship (Grant No. 57507871).

References

[1] D.G. Colley, A.L. Bustinduy, W.E. Secor, C.H. King, Human schistosomiasis, Lancet 383 (2014) 2253–2264, https://doi.org/10.1016/S0140-6736(13)61949-2.
[2] A.S. Stensgaard, et al., Large-scale determinants of intestinal schistosomiasis and intermediate host snail distribution across Africa: does climate matter? Acta Trop. 128 (2013) 378–390, https://doi.org/10.1016/j.actatropica.2011.11.010.
[3] C.H. King, Parasites and poverty: the case of schistosomiasis, Acta Trop. 113 (2010) 95–104, https://doi.org/10.1016/j.actatropica.2009.11.012.
[4] P. Steinmann, J. Keiser, R. Bos, M. Tanner, J. Utzinger, Schistosomiasis and water resources development: systematic review, meta-analysis, and estimates of people at risk, *Lancet* Infect. Dis 6 (2006) 411–425, https://doi.org/10.1016/S1473-3099(06)70521-7.
[5] R. Bergquist, X.N. Zhou, D. Rollinson, J. Reinhard-Rupp, K. Klohe, Elimination of schistosomiasis: the tools required, Infect. Dis. Poverty. 6 (2017) 1–9, https://doi.org/10.1186/s40249-017-0370-7.
[6] J.R. Stothard, L. Chitsulo, T.K. Kristensen, J. Utzinger, Control of schistosomiasis in sub-Saharan Africa: progress made, new opportunities and remaining challenges, J. Parasitol. 136 (2009) 1665–1675, https://doi.org/10.1017/S0031182009991272.
[7] L. Chitsulo, D. Engels, A. Montresor, L. Savioli, The global status of schistosomiasis and its control, Acta Trop. 77 (2000) 41–51, https://doi.org/10.1016/S0001-706X(00)00122-4.
[8] WHO. World Health Organization, Elimination of Schistosomiasis, Sixty-Fifth World Health Assembly, 2012. WHA65. 21, Agenda item 13.11, 26 May 2012, http://apps.who.int/gb/ebwha/pdf_files/WHA65/A65_R21-en.pdf.
[9] D. Rollinson, et al., Time to set the agenda for schistosomiasis elimination, Acta Trop. 128 (2013) 423–440, https://doi.org/10.1016/j.actatropica.2012.04.013.
[10] S.H. Sokolow, K.D. Lafferty, A.M. Kuris, Regulation of laboratory populations of snails (*Biomphalaria* and *Bulinus* spp.) by river prawns, *Macrobrachium* spp. (Decapoda, Palaemonidae): implications for control of schistosomiasis, Acta Trop. 132 (2014) 64–74, https://doi.org/10.1016/j.actatropica.2013.12.013.
[11] A.S. Stensgaard, L. Rinaldi, R. Bergquist, The future is now: new United Nations' Sustainable Development Goals report provides a perspective on vector-borne diseases, *Geospat. Health* 14 (2019).
[12] A.B. Pedersen, T.J. Greives, The interaction of parasites and resources cause crashes in a wild mouse population, J. Anim. Ecol. 77 (2008) 370–377, https://doi.org/10.1111/j.1365-2656.2007.01321.x.
[13] D.J. Becker, D.G. Streicker, S. Altizer, Linking anthropogenic resources to wildlife–pathogen dynamics: a review and meta-analysis, Ecol. Lett. 18 (2015) 483–495, https://doi.org/10.1111/ele.12428.
[14] M. Dobson, Replacement of native freshwater snails by the exotic Physa acuta (Gastropoda: physidae) in southern Mozambique; a possible control mechanism for schistosomiasis, Ann. Trop. Med. Parasitol. 98 (2004) 543–548.
[15] S.A. Sura, H.K. Mahon, Effects of competition and predation on the feeding rate of the freshwater snail, *Helisoma trivolvis*, Am. Midl. Nat. 166 (2011) 358–368, https://doi.org/10.1674/0003-0031-166.2.358.
[16] J.M. Butler, F.F. Ferguson, J.R. Palmer, W.R. Jobin, Displacement of a colony of *Biomphalaria glabrata* by an invading population of *Tarebia granifera* in a small stream in Puerto Rico, Caribb. J. Sci. 16 (1980) 73–79.
[17] D.M. Lodge, et al., Louisiana crayfish (*Procambarus clarkii*) (Crustacea: Cambaridae) in Kenyan ponds: non-target effects of a potential biological control agent for schistosomiasis, Afr. J. Aquat. Sci. 30 (2005) 119–124, https://doi.org/10.2989/16085910509503845.
[18] A. Younes, H. El-Sherief, F. Gawish, M. Mahmoud, Biological control of snail hosts transmitting schistosomiasis by the water bug, *Sphaerodema urinator*, Parasitol. Res. 116 (2017) 1257–1264, https://doi.org/10.1007/s00436-017-5402-5.
[19] M.C. Arostegui, et al., Potential biological control of schistosomiasis by fishes in the lower Senegal river basin, Am. J. Trop. Med. Hyg. 100 (2019) 117, https://doi.org/10.4269/ajtmh.18-0469.
[20] D.B. Lewis, Trade-offs between growth and survival: responses of freshwater snails to predacious crayfish, Ecol 82 (2001) 758–765, https://doi.org/10.1890/0012-9658(2001)082[0758:TOBGAS]2.0.CO;2.
[21] K.L. Mathers, S. Guareschi, C. Patel, P.J. Wood, Response of freshwater snails to invasive crayfish varies with physiochemical exposure cues and predator experience, Freshw. Biol. 67 (3) (2022) 473–486, https://doi.org/10.1111/fwb.13855.
[22] Dobson A Altizer, P. Hosseini, P. Hudson, M. Pascual, P Rohani, Seasonality and the dynamics of infectious diseases, Ecol. Let. 9 (4) (2006) 467–484, https://doi.org/10.1111/j.1461-0248.2005.00879.x.
[23] E.T. Chiyaka, W. Garira, Mathematical analysis of the transmission dynamics of schistosomiasis in the human-snail hosts, J. Biol. Syst. 17 (2009) 397–423, https://doi.org/10.1142/S0218339009002910.
[24] S. Gao, Y. Liu, Y. Luo, D. Xie, Control problems of a mathematical model for schistosomiasis transmission dynamics, Nonlinear. Dyn. 63 (2011) 503–512, https://doi.org/10.1007/s11071-010-9818-z.
[25] A. Abokwara, C.E. Madubueze, The role of non-pharmacological interventions on the dynamics of schistosomiasis, J. Math. Fundam. Sci. 53 (2021) 243–260.
[26] T.D. Mangal, S. Paterson, A. Fenton, Predicting the impact of long-term temperature changes on the epidemiology and control of schistosomiasis: a mechanistic model, PLoS. One 3 (2008) e1438, https://doi.org/10.1371/journal.pone.0001438.
[27] C. Kalinda, M.J. Chimbari, S. Mukaratirwa, Effect of temperature on the *Bulinus globosus-Schistosoma haematobium* system, Infect. Dis. *Poverty* 6 (1) (2017) 1–7, https://doi.org/10.1186/s40249-017-0260-z.
[28] Z. Tabo, C. Kalinda, L. Breuer, C. Albrecht, Adapting strategies for effective schistosomiasis prevention: a mathematical modeling approach, Mathematics 11 (12) (2023) 2609, https://doi.org/10.3390/math11122609.
[29] E.J. Allen, H.D. Victory Jr., Modelling and simulation of a schistosomiasis infection with biological control, Acta Trop. 87 (2003) 251–267, https://doi.org/10.1016/S0001-706X(03)00065-2.
[30] S. Das, P. Das, P. Das, Chemical and biological control of parasite-borne disease schistosomiasis: an impulsive optimal control approach, Nonlinear. Dyn. 104 (2021) 603–628, https://doi.org/10.1007/s11071-021-06262-0.
[31] O. Diekmann, J.A. Heesterbeek, J.A. Metz, On the definition and the computation of the basic reproduction ratio R0 in models for infectious diseases in heterogeneous populations, J. Math. Biol. 28 (1990) 365–382.
[32] C. Castillo-Chavez, S. Blower, P. van den Driessche, D. Kirschner, A.A. Yakubu, Mathematical Approaches For Emerging and Reemerging Infectious Diseases: Models, Methods, and Theory, Springer Science & Business Media, 2002, 126.
[33] P. Van den Driessche, J. Watmough, Reproduction numbers and sub-threshold endemic equilibria for compartmental models of disease transmission, Math. Biosci. 180 (2002) 29–48, https://doi.org/10.1016/S0025-5564(02)00108-6.

[34] C. Castillo-Chavez, B. Song, Dynamical models of tuberculosis and their applications, Math. Biosci. Eng. 1 (2004) 361–404, https://doi.org/10.3934/mbe.2004.1.361.
[35] R.C. Team, A Language and Environment For Statistical Computing, R Foundation for Statistical Computing, Vienna, Austria, 2014. http://www.R-project.org.
[36] K. Soetaert, T. Petzoldt, R.W. Setzer, Solving differential equations in R: package deSolve, J. Stat. Softw. 33 (2010) 1–25, https://doi.org/10.18637/jss.v033.i09.
[37] B. Gryseels, K. Polman, J. Clerinx, L. Kestens, Human schistosomiasis, Lancet 368 (2006) 1106–1118, https://doi.org/10.1016/S0140-6736(06)69440-3.
[38] W.F. Cross, A.C. Benke, Intra-and interspecific competition among coexisting lotic snails, Oikos. 96 (2) (2002) 251–264, https://doi.org/10.1034/j.1600-0706.2002.960207.x.
[39] E.T. Chiyaka, G. Magombedze, L. Mutimbu, Modelling within host parasite dynamics of schistosomiasis, Comput. Math. Methods Med. (2010) 255–280, https://doi.org/10.1080/17486701003614336.
[40] Z. Feng, C.C. Li, F.A. Milner, Schistosomiasis models with two migrating human groups, Math. Comput. Model. 41 (11–12) (2005) 1213–1230, https://doi.org/10.1016/j.mcm.2004.10.023.
[41] E.T. Ngarakana-Gwasira, C.P. Bhunu, M. Masocha, E. Mashonjowa, Transmission dynamics of schistosomiasis in Zimbabwe: a mathematical and GIS approach, Commun. Nonlinear Sci. Numer. Simul. 35 (2016) 137–147.
[42] S. Liang, R.C. Spear, E. Seto, A. Hubbard, D. Qiu, A multi-group model of *Schistosoma japonicum* transmission dynamics and control: model calibration and control prediction, Trop. Med. Int. Health 10 (2005) 263–278, https://doi.org/10.1111/j.1365-3156.2005.01386.x.
[43] B.V. Hofkin, D.M. Hofinger, D.K. Koech, E.S. Loker, Predation of *Biomphalaria* and non-target molluscs by the crayfish *Procambarus clarkii*: implications for the biological control of schistosomiasis, Ann. Trop. Med. Parasitol. 86 (1992) 663–670, https://doi.org/10.1080/00034983.1992.11812723.
[44] J.R. Stauffer, et al., Controlling vectors and hosts of parasitic diseases using fishes, Bioscience 47 (1997) 41–49. https://www.jstor.org/stable/1313005.
[45] D.J. Civitello, L.H. Baker, S. Maduraiveeran, R.B. Hartman, Resource fluctuations inhibit the reproduction and virulence of the human parasite *Schistosoma mansoni* in its snail intermediate host, Proc. R. Soc. B 287 (2020) 20192446, https://doi.org/10.1098/rspb.2019.2446.
[46] D.J. Civitello, et al., Transmission potential of human schistosomes can be driven by resource competition among snail intermediate hosts, Proc. Natl. Acad. Sci. 119 (2022) e2116512119, https://doi.org/10.1073/pnas.2116512119.
[47] J.P. Pointier, F. McCullough, Biological control of the snail hosts of *Schistosoma mansoni* in the Caribbean area using *Thiara* spp, Acta Trop. 46 (3) (1989) 147–155, https://doi.org/10.1016/0001-706X(89)90031-4.
[48] G.C. Coles, The effect of diet and crowding on the shedding of *Schistosoma mansoni* cercariae by *Biomphalaria glabrata*, Am. J. Trop. Med. Hyg. 67 (1973) 419–423, https://doi.org/10.1080/00034983.1973.11686909.
[49] H. Madsen, Biological methods for the control of freshwater snails, Parasitol. Today. 6 (7) (1990) 237–241, https://doi.org/10.1016/0169-4758(90)90204-H.
[50] J. Moore, Parasites and the Behavior of Animals, Oxford University Press on Demand, 2002.
[51] S.J. Swartz, G.A. De Leo, C.L. Wood, S.H. Sokolow, Infection with schistosome parasites in snails leads to increased predation by prawns: implications for human schistosomiasis control, J. Exp. Biol. 218 (2015) 3962–3967, https://doi.org/10.1242/jeb.129221.
[52] J.F. Nguma, F.S. McCullough, E. Masha, Elimination of *Biomphalaria pfeifferi, Bulinus tropicus* and *Lymnaea natalensis* by the ampullarid snail, *Marisa cornuarietis*, in a man-made dam in northern Tanzania, Acta Trop. 39 (1982) 85–90.
[53] J.P. Pointier, The introduction of *Melanoides tubercu*lata (Mollusca: *Thiaridae*) to the island of Saint Lucia (West Indies) and its role in the decline of *Biomphalaria glabrata*, the snail intermediate host of *Schistosoma mansoni*, Acta Trop. 54 (1993) 13–18, https://doi.org/10.1016/0001-706X(93)90064-I.
[54] R. Slootweg, E.A. Malek, F.S. McCullough, The biological control of snail intermediate hosts of schistosomiasis by fish, Rev. Fish Biol. Fish. 4 (1994) 67–90.
[55] I.J. Jones, S.H. Sokolow, G.A De Leo, Three reasons why expanded use of natural enemy solutions may offer sustainable control of human infections, People Nat. 4 (2022) 32–43, https://doi.org/10.1002/pan3.10264.

Modelling Temperature-dependent Schistosomiasis Dynamics for Single and Co-infections with *S. mansoni* and *S. haematobium*

Zadoki Tabo[1,2*], Lutz Breuer[2,3] & Christian Albrecht[1]

[1]Department of Animal Ecology and Systematics, Justus Liebig University Giessen, Heinrich-Buff-Ring 26 (iFZ), 35392 Giessen, Germany.
[2]Department of Landscape Ecology and Resource Management, Justus Liebig University Giessen, Heinrich-Buff-Ring 26 (iFZ), 35392 Giessen, Germany.
[3]Centre for International Development and Environmental Research (ZEU), Justus Liebig University Giessen, Senckenbergstrasse 3, 35390 Giessen, Germany.

[*]Corresponding Author
E-mail: Tabo.Zadoki@umwelt.uni-giessen.de (ZT)

Abstract

Schistosomiasis, a prevalent public health issue specifically in sub-Saharan Africa, is primarily attributed to *Schistosoma haematobium* and *Schistosoma mansoni*, often occurring concurrently. These schistosome species share similarities in life cycles and transmission, manifesting comparable infection patterns and susceptibility to temperature variations. This study investigates the influence of temperature control not only on the transmission of individual species but also on their mutual interactions and co-infection dynamics using a mathematical model. Sub-models and co-dynamic properties, including reproduction numbers, equilibrium states, and stability conditions, are derived. Sensitivity analysis is performed to clarify the impact of parameter variations on model stability. Results suggest that temperature variation increases the spread of *S. haematobium*, which enhances susceptibility to *S. mansoni* co-infection, possibly by altering the immune response. At moderate temperatures (20°C and 25°C), infection levels in both single and co-infected individuals are higher, while recovery rates increase with temperature, peaking at 25°C and 35°C as infections significantly decrease. *Biomphalaria* snails exhibit greater population growth and susceptibility to infection than *Bulinus* snails, particularly below 25°C. Above this temperature, *Biomphalaria* population decreases while *Bulinus* species are more likely to experience faster mortality. These temperature-related variations differently impact mortality rates of intermediate snails and snail-to-human transmissibility rates for schistosome species, holding significant health implications. Targeting snails during seasons below 25°C, when susceptibility is higher, and intensifying human treatment interventions around 25°C-35°C, where recovery rates peak, may yield optimal results, particularly during seasons with intermediate temperatures around 25°C for both snails and humans. The results underscore the importance of integrating temperature into models for predicting and managing schistosomiasis dynamics for both genera. Therefore, this model is applicable not only to sub-Saharan Africa, but also to other regions where the described temperature ranges match with the local climate.

Key Words: Neglected tropical disease**,** temperature, mutual interaction, co-infection, reproduction number, control.

1. Introduction

Schistosomiasis, a neglected tropical disease (NTD), is widely prevalent in sub-Saharan Africa characterized by poverty and limited access to safe drinking water and proper sanitation facilities [1]. The disease poses a significant health risk to the population, with annual death rates estimated

to be around 200,000 to 280,000 deaths per year [2]. It is important to note that these figures are subject to change as new data becomes available as efforts to control and treat schistosomiasis continue to progress [1]. Schistosomiasis is caused by parasitic worms known as *Schistosoma* trematodes, or blood flukes. These worms are transmitted to humans through intermediate host snails [3, 4]. While various species of schistosomes can infect humans [5], *Schistosoma mansoni* and *Schistosoma haematobium* are particularly prevalent and exert a significant burden on countries in sub-Saharan Africa [4]. These two types of schistosomes are closely related and have similar complex life cycles and transmission dynamics, but they differ in their distinct pathological profiles. *Schistosoma mansoni* causes intestinal schistosomiasis and is transmitted by various snail species of the *Biomphalaria* genus within the Planorbidae family [6]. On the other hand, *S. haematobium* causes urogenital schistosomiasis and is transmitted by specific snails belonging to the *Bulinus* genus within the Bulinidae family [7].

The life cycle of the schistosome begins with cercaria shedding from infected snails into the water. Within a few seconds of contact with the human host, they can penetrate through the skin and invade the body. The cercaria larvae enter the circulatory system and migrate through the lungs to the liver where they transform into adult schistosomes and mate inside the body. Subsequently, adult couples migrate to their final destination to reproduce. *Schistosoma mansoni* moves to the blood arteries and the portal system where the females release their eggs through the intestinal walls and are expelled from the body in feces into freshwater sources. Conversely, *S. haematobium* migrates to the vessels of the urinary bladder, where females produce eggs that pass through the bladder wall and are excreted in the urine contaminating freshwater sources. The eggs of both schistosome species hatch into miracidia larvae in freshwater. These larvae exclusively infect respective intermediate host snails, where they undergo transformation into cercaria larvae. Subsequently, these cercariae infect humans, completing the life cycle [8, 9].

Human schistosomiasis has a wide-ranging impact on various organ systems, affecting the cardiopulmonary, gastrointestinal, genital, and central nervous systems. Infections caused by *S. mansoni* may result in complications such as pulmonary hypertension and schistosomal appendicitis, and many other [1, 10,11]. In contrast, *S. haematobium* infection manifests with symptoms including, but not limited to, hematuria, bladder cancer, anemia, and infertility [1, 12]. Additionally, co-infection with both *S. haematobium* and *S. mansoni* can lead to a more complicated immune-mediated glomerulopathies [13]. Currently, the anthelmintic praziquantel is the primary treatment for both schistosomiasis forms, given its efficacy against adult worms, while no effective vaccine is available yet [14]. Although praziquantel reduces worm burden, it may not eliminate immature worms or eggs, and concerns about drug resistance and re-infections following treatment have been raised [15]. To manage schistosomiasis effectively, continued research and surveillance are essential [16]. Hence, accounting for the particular species involved in both single infections and mixed co-infections of schistosomiasis becomes critical for disease treatment, control, and overall human health, given that humans serve as the definitive host.

In sub-Saharan Africa, persistent transmission of both single and mixed schistosomiasis can be influenced by various factors, including climate change and global warming. Among these factors, temperature plays a significant role in snail distribution and population size, affecting some traits of the schistosome life cycle and overall human infection dynamics [17, 18]. The differing responses of hosts and parasites to temperature fluctuations can either elevate or reduce disease prevalence [19]. While literature links schistosomiasis to various diseases [20, 21, 22], existing mathematical models focus on co-infections but lack consideration of climate change. These models explore schistosomiasis interactions with other diseases but overlook climate factors [23],

[24, 25, 26, 27]. Furthermore, laboratory experiments conducted by Mangal et al. [17] on the *Biomphalaria-S. mansoni* system and Kalinda et al. [18] on the *Bulinus-S. haematobium* system have yielded crucial temperature-dependent data regarding schistosome life cycle traits. Utilizing models parameterized by such data becomes imperative, especially in regions like Sub-Saharan Africa, particularly East Africa, where local temperatures align with the temperature ranges observed in these experiments and where both infections coexist [2, 22]. Despite the significance of this data, a noticeable gap exists in the absence of a mathematical model that employs this information to elucidate the impact of temperature variations on schistosomiasis transmission, distinguishing between single-species infections and their mixed co-infection interactions. This study aims to develop a globally applicable mathematical model, inspired by the classic SIR model, to quantitatively predict temperature control over the trends, interactions, and differences in *S. mansoni* and *S. haematobium* co-infection dynamics for effective disease control planning. The selection of the SIR model for investigating the spread of single and mixed schistosomiasis infections at the population level agrees with similar co-dynamic models found in the existing literature [25, 26, 27]. However, our study uniquely incorporates temperature as a crucial factor influencing transmission rates, *Schistosoma* species interaction, and co-infection dynamics, which provides new insights into the optimisation of intervention strategies based on climatic variations.

2. Material and Methods

2.1. Co-dynamics model formulation and equations

In our co-dynamics model studying the interactions between *S. mansoni* and *S. haematobium*, we divide the total human population (N_h) into different subpopulations. These subpopulations include susceptible humans (H), individuals infected with only *S. mansoni* (I_m), individuals infected with only *S. haematobium* (I_h), individuals infected with both strains (I_{hm}), individuals who have recovered from *S. mansoni* (R_m), individuals who have recovered from S. *haematobium* (R_h), and individuals who have recovered from both strains (R_{hm}). Similarly, the total population of *Biomphalaria* snails (N_1) is divided into susceptible snails (S_1) and infected snails (I_1), while the total population of *Bulinus* snails (N_2) is divided into susceptible snails (S_2) and infected snails (I_2). Mathematically, we can express these subdivisions as follows: $N_h = H + I_m + I_h + +I_{hm} + R_m + R_h + R_{hm}$, $N_1 = S_1 + I_1$, and $N_2 = S_2 + I_2$. Consequently, we describe a co-dynamics model using a system of ordinary differential equations Eq. (1-11).

$$H' = \Lambda_h + \varepsilon R_h + \alpha R_m + \theta R_{hm} - (\beta_i(T)I_2 + \beta_u(T)I_1)H - \upsilon_1 H \quad (1)$$

$$I_m' = \beta_i(T)I_2 H - \beta_u(T)I_1 I_m - (\gamma + \delta_i + \upsilon_1)I_m \quad (2)$$

$$I_h' = \beta_u(T)I_1 H - \beta_i(T)I_2 I_h - (\omega + \delta_u + \upsilon_1)I_h \quad (3)$$

$$I_{hm}' = \beta_u(T)I_1 I_m + \beta_i(T)I_2 I_h - (\delta + \delta_i + \delta_u + \upsilon_1)I_{hm} \quad (4)$$

$$R_m' = \gamma I_m + \tau_1(1-\delta)I_{hm} - (\alpha + \upsilon_1)R_m \quad (5)$$

$$R_h' = \omega I_h + (1-\tau_1)(1-\delta)I_{hm} - (\varepsilon + \upsilon_1)R_h \quad (6)$$

$$R_{hm}' = \delta I_{hm} - (\theta + \upsilon_1)R_{hm} \quad (7)$$

$$S_1' = \Lambda_1 - \beta_1(T)(I_h + I_{hm})S_1 - \gamma_1(T)S_1 \quad (8)$$

$$I_1' = \beta_1(T)(I_h + I_{hm})S_1 - (\gamma_1(T) + \alpha_1(T))I_1 \quad (9)$$

$$S_2' = \Lambda_2 - \beta_2(T)(I_m + I_{hm})S_2 - \gamma_2(T)S_2 \quad (10)$$

$$I_2' = \beta_2(T)(I_m + I_{hm})S_2 - (\gamma_2(T) + \alpha_2(T))I_2 \quad (11)$$

All temperature variant parameters are given as functions of temperature, T. Human population increase exponentially with a recruitment rate given by $\Lambda_h = \Lambda_r e^{-\upsilon_1 \tau}$, where Λ_r is the maximum per capita birth rate/immigration rate of human individuals, υ_1 is the natural mortality rate of humans and τ is the earliest age at which an individual is infected. Reproduction rates for *Bulinus* and *Biomphalara* snails are respectively, Λ_1 and Λ_2, while the corresponding natural death rates are $\gamma_1(T)$ and $\gamma_2(T)$. The transmissibility of *S. haematobium* and *S. mansoni* is, respectively, $\beta_u(T)$ and $\beta_i(T)$ to humans, $\beta_1(T)$ and $\beta_2(T)$ to snails. In humans, *S. mansoni* and *S. haematobium*-related death rates are δ_i and δ_u, whereas in *Bulinus* snails and *Biomphalaria*, they are $\alpha_1(T)$ and $\alpha_2(T)$. The recovery rates from *S. mansoni*, *S. haematobium* and co-infection are denoted as γ, ω, and δ respectively, while the immunity waning rates are represented by α, ε, and θ. The portion of co-infected individuals who recover from *S. mansoni* is given by the term $\tau_1(1-\delta)$, and the co-infected individuals who recover from *S. haematobium* only are described by $(1-\tau_1)(1-\delta)$. Hence, the model investigates the comprehensive dynamic effects of a temperature-driven system on schistosomiasis. The model was parameterized using both real experimental temperature variants and non-temperature variants from the literature.

2.2. Temperature variant parameters

We collected temperature-dependent data from real experimental and laboratory studies conducted by Mangal et al.[17] for the *Biomphalaria-S. mansoni* system and Kalinda et al. [18] for the *Bulinus-S. haematobium* system. Data from Mangal et al. 2008 [17] included temperature-dependent parameters $\beta_i(T)$, $\beta_2(T)$, $\alpha_2(T)$, $\gamma_2(T)$ at each with distinct values at 20, 25, 30, and 35 °C (see Table A.1 in Appendix A). Similarly, data from Kalinda et al. 2017 [18] covered temperature-dependent parameters $\beta_u(T)$, $\beta_1(T)$, $\alpha_1(T)$, $\gamma_1(T)$ across 15, 22, 25.8, 31, and 36 °C (Table A.2 in Appendix A). The data underwent analysis to formulate equations capturing the impact of temperature control on the two systems in actual static environmental conditions. For data analysis, we selected a common temperature range of 20 to 35 °C for both systems. We computed R-squared values and determined the regression equations that produced the highest adjusted value for each temperature-dependent parameter. The regression equations, representing the best fit for the data (curve fitting), are provided in Table 1. Note that Kalinda et al. 2017 [18] excluded Schistosomiasis transmission to snails. Yet, statistical comparisons [28, 29, 30] suggest higher *S. haematobium* prevalence where both species coexist, therefore, we assumed implying $\beta_1(T) > \beta_2(T)$.

Table 1: Temperature-dependent parameters, symbols, derived curves, ranges, and their sources

Parameter	***Biomphalaria-S. mansoni* system**		**Values/day**	**References**
Definition	Symbol	Derived regression equations	range of values	

Transmissibility of Schistosomiasis to humans	$\beta_i(T)$	$0.000066T^2 + 0.00259T - 0.0488$	$0.03469 - 0.12270$	[17]
Transmissibility of Schistosomiasis to snails	$\beta_2(T)$	$-0.000009830T^2 + 0.0006148T - 0.00826$	$0.00032 - 0.00135$	[17]
Schistosomiasis-induced death in snails	$\alpha_2(T)$	$0.00008T^2 - 0.00122T - 0.00545$	$0.04985 - 0.07744$	[17]
Natural death rate of snails	$\gamma_2(T)$	$0.000112T^2 - 0.00521T + 0.0633$	$0.00271 - 0.01815$	[17]
	***Bulinus-S. haematobium* system**			
Transmissibility of Schistosomiasis to humans	$\beta_u(T)$	$0.0063T - 0.098$	$0.0280 - 0.12250$	[18]
Transmissibility of Schistosomiasis to snails	$\beta_1(T)$	$1.2\beta_2(\mathrm{T})$	$0.00037 - 0.00162$	[18]
Schistosomiasis-induced death in snails	$\alpha_1(T)$	$0.0000732T^2 - 0.00203T + 0.01484$	$0.00449 - 0.03346$	[18]
Natural death rate of snails	$\gamma_1(T)$	$0.0000794T^2 - 0.002608T + 0.02215$	$0.00239 - 0.02814$	[18]

The derived equations serve as valuable tools for assessing, comparing, and differentiating between the two genera under prevailing or anticipated climatic conditions. They provide a means to evaluate transmissibility, survival rates, and mortality rates for both genera within areas characterized by temperatures ranging from [20, 35]°C. The applicability of these equations is particularly relevant in Sub-Saharan Africa, specifically East Africa, where *Biomphalaria* and *Bulinus* species are common, and both *S. mansoni* and *S. haematobium* infections are prevalent. The specified temperature ranges align with the local climate in the region, making the equations pertinent for studies and assessments such settings at local or global geographical context.

2.3. Temperature invariant parameters

All non-temperature-dependent parameters used in the model were either derived from existing literature or estimated based on expert knowledge (Table 2). For instance, previous observations by Gryseels et al. [4] indicated that schistosomiasis commonly initiates infection in a child at the age of two years. In our model, we represented this age of infection using the parameter τ, set to correspond to 730 days. Nevertheless, it is important to acknowledge that infants younger than two years can also contract the disease if they come into contact with infected freshwater during activities such as bathing babies. Additionally, the research by Cunin et al. [28], Garba et al. [29], and Nassar et al. [30] reveal a higher occurrence of *S. haematobium* in areas of coexistence with *S. mansoni*. Therefore, based on this knowledge, we assume that $\delta_u > \delta_i\ \gamma > \omega > \delta$, and $\alpha > \varepsilon > \theta$. Note that the values of waning immunity α, ε, and θ lie between 0 and 1 because they reflect a proportion or fraction of the original immunity that remains effective at a given point in time. As ε approaches 1, immunity remains strong, while as ε approaches 0, immunity weakens or fades away. Similarly, the values of the recovery rates after treatment (γ, ω) lie between 0 and 1 because they represent a proportion or fraction of the original individuals that remain effective at a given point in time. As γ, ω approaches 1, treatment becomes 100% effective, while as γ, ω approaches 0, no individuals recover, and the treatment is not effective. Note that there is no existing epidemic data for both genera to cross-verify their, waning immunity, treatment effectiveness and recovery rates. We incorporated certain values from the literature and estimated others within the range of [0, 1].

Table 2: Temperature-invariant parameters, symbols, ranges and baseline values, and sources

Symbol	Definition	Range of values/day	Baseline values	References
Λ_h	Human reproduction rate	100-8,000	100	[31, 32]
Λ_1	*Bulinus* snail reproduction rates	100	100	[33]
Λ_2	*Biomphalaria* snail reproduction rates	100	100	[33]

τ	Age at first infection in a child	730	730	[4]
υ_1	Human mortality rate	0.0000428-0.0000468	0.0000448	[34]
δ_i	S. mansion-human-related death rate	0.000591-0.0039	0.000591	[32, 34]
δ_u	*S. haematobium*-human-related death rate	0.000591-0.0039	0.0039	[32, 34]
γ	Recovery rates of *S. mansoni*-infected individuals	$0 < \gamma < 1$	0.050	Estimated
ω	Recovery rates of *S. haematobium*-infected individuals	$0 < \omega < 1$	0.0181	[26]
δ	Recovery rates of co-infected individuals from both infections	$0 < \delta < 1$	0.012	Estimated
τ_1	Recovery rates of co-infected individuals from *S. mansoni* infection only	$0 < \tau_1 < 1$	0.4	Estimated
ε	*Schistosoma haematobium* waning immunity	$0 < \varepsilon < 1$	0.013	[26]
α	*Schistosoma mansoni* waning immunity	$0 < \alpha < 1$	0.04	Estimated
θ	Co-infection waning rate	$0 < \theta < 1$	0.009	Estimated

2.4. Steady states and the transmissibility of infections

In this study, we examined the stability of infections using both the disease-free equilibrium (E_0) and the endemic equilibrium (E_1) and assessed the transmissibility of the infections using the basic reproduction number (R_0). The disease-free equilibrium represents a state with no active transmission, while the endemic equilibrium signifies ongoing and stable disease transmission within the population. The disease-free equilibrium E_0 provides a basis for evaluating the effectiveness of control measures, whereas E_1 offers insights into the persistence and stability of schistosomiasis, while R_0 quantifies the average number of new infections caused by a single infectious individual in a susceptible population [35]. If $R_0 > 1$, schistosomiasis can emerge, spread, and persist. Conversely, if $R_0 < 1$, the disease-free equilibrium is more likely, as on average, less than one new case is generated during the infectious period. The interplay of the equilibria and R_0 conditions under climate factors like temperature is vital for shaping public health strategies, providing insight into disease potential, control measure effectiveness, and disease elimination likelihood.

2.5. Sensitivity of transmissibility to model parameters

We performed a sensitivity analysis using the partial rank correlation coefficient (PRCC) to assess the impact of individual input parameters on the output variable R_0. In this analysis, the data is reorganized in ascending order, and the ranks of the variables are substituted. The parameters exhibiting a positive (negative) sign result in an increase (decrease) in the output when they are increased (decreased), and vice versa. The PRCC provides a measure of the monotonic relationship after removing the linear effects of each model parameter while holding all other parameters constant [36]. By employing this approach, one can identify parameters that exert the most significant influence and should be the target of interventions. Note that all the simulations methods and the statistical analysis were generated using the R statistical environment v. 4.0.3 [37].

3. Qualitative results

In this study, we formulated a co-dynamic model Eq. (1-11) which can be subdivided into variables H, I_h, R_h, S_1, and I_1 to create a specific sub-model for *S. haematobium* (SH) infection dynamics and variables H, I_m, R_m, S_2, and I_2 to create a specific sub-model for *S. mansoni* (SM) infection dynamics (see the separate sub-model equations in the Appendix B). The sub-models facilitated

independent analyses of the dynamics of single infections by each *Schistosoma* species. Sections 3.1-3.6 present analyses of the disease-free equilibrium, reproduction number, establishment of endemic equilibria, mutual interaction, and treatment impact for both sub-models and the co-dynamic model. The numerical stability analysis for the equilibrium points in the sub-models and co-dynamics is shown in Appendix B. Note that for simplicity, we use the notations; $\beta_1(T) = \beta_1, \beta_2(T) = \beta_2, \gamma_2(T) = \gamma_2, \beta_u(T) = \beta_u, \beta_i(T) = \beta_i, \alpha_1(T) = \alpha_1, \alpha_2(T) = \alpha_2, \gamma_1(T) = \gamma_1$ and $\gamma_2(T) = \gamma_2$ in all the sections that follow

3.1. *Schistosoma haematobium* (SH) sub-model

To analyze the stability of the SH sub-model, we first established the disease-free equilibrium (E_{0h}) and reproduction number (R_{0h}) of the *S.haematobium* infection. The SH sub-model has a disease-free equilibrium point given as

$$E_{0h} = (H^*, I_h^*, R_h^*, S_1^*; I_1^*) = \left(\frac{\Lambda_h}{\upsilon_1}, 0, 0, \frac{S_1}{\gamma_1}, 0\right)$$

Using a method and next-generation matrix approach [35, 38], we show that

$$F = \begin{pmatrix} 0 & \frac{\beta_u \Lambda_h}{\upsilon_1} \\ \frac{\beta_1 \Lambda_1}{\gamma_1} & 0 \end{pmatrix}, \; V = \begin{pmatrix} (\omega + \delta_u + \upsilon_1) & 0 \\ 0 & (\gamma_1 + \alpha_1) \end{pmatrix}$$

where F is the rate at which new infections arise in one compartment, and V is the rate at which people and *Biomphalaria* snails are transferred into that compartment. According to a Jacobian matrix evaluated at E_{0h}, R_{0h} is the dominant eigenvalue of FV^{-1} given as

$$R_{0h} = \sqrt{\frac{\beta_1 \beta_u \Lambda_1 \Lambda_h}{\upsilon_1 \gamma_1 (\gamma_1 + \alpha_1)(\omega + \delta_u + \upsilon_1)}} \qquad (12)$$

At different temperatures, R_{0h} in equation Eq. (12) depends on temperature T, portraying the standard expression of $R_{0h}(T)$ for *Schistosoma haematobium* new cases, governed by temperature-sensitive parameters β_1, β_u, γ_1, and α_1. When $R_{0h} < 1$ for specific temperature values, the SH sub-model shows a disease-free equilibrium, countering infection. Conversely, when $R_{0h} > 1$, an endemic equilibrium point E_h appears in the SH sub-model, promoting infection persistence and establishment. By setting the system of differential equations in the SH sub-model to zero allows for the computation of the endemic equilibrium point $E_h = (H^{"}, I_h^{"}, R_h^{"}, S_1^{"}; I_1^{"})$, expressed in terms of I_h, where

$$H^{"} = \frac{(\gamma_1+\alpha_1)\left((\varepsilon+\upsilon_1)\Lambda_1+\varepsilon\omega I_h^{"}\right)(\beta_1 I_h^{"}+\gamma_1)}{(\varepsilon+\upsilon_1)(\gamma_1+\alpha_1)(\beta_1 I_h^{"}+\gamma_1)}, R_h^{"} = \frac{\omega}{(\varepsilon+\upsilon_1)} I_h^{"}, S_1^{"} = \frac{\Lambda_1}{(\beta_1 I_h^{"}+\gamma_1)} I_h^{"}, I_1^{"} = \frac{\beta_1 \Lambda_1 I_h^{"}}{(\gamma_1+\alpha_1)(\beta_1 I_h^{"}+\gamma_1)} I_h^{"},$$

By substituting the values of $H^{"}$ and $I_1^{"}$ into the equation representing *S. haematobium* infected humans (I_h) from the SH sub-model, we can obtain the solution for $I_h^{"}$. The resulting polynomial, given by equation Eq. (13), satisfies the endemic equilibrium of the SH sub-model.

$$\lambda^3 + a_2\lambda^2 + a_1\lambda + a_0 = 0 \qquad (13)$$

where $a_0 = -\frac{\gamma_1\beta_u\beta_1\Lambda_1\Lambda_h}{\beta_1(\gamma_1+\alpha_1)(\omega+\delta_u+\upsilon_1)}$, $a_1 = \frac{(\gamma_1+\alpha_1)(\omega+\delta_u+\upsilon_1)(\gamma_1-\beta_1\Lambda_h)-\gamma_1\beta_u\beta_1\Lambda_1}{\beta_1(\gamma_1+\alpha_1)(\omega+\delta_u+\upsilon_1)}$,

$a_2 = \frac{(\gamma_1+\alpha_1)(\omega+\delta_u+\upsilon_1)(\gamma_1-\beta_1\Lambda_h)-(\gamma_1+\alpha_1)\varepsilon\omega\gamma_1\beta_u\beta_1\Lambda_1}{\beta_1\gamma_1(\gamma_1+\alpha_1)(\omega+\delta_u+\upsilon_1)}$.

There is no doubt that $a_0 < 0$, and in accordance with Descartes' rule of signs [39], if any or both of a_1 and/or a_2, at least one positive root results, and endemic equilibrium exists. Note that the prevalence of endemicity and infection levels across subpopulations fluctuates with environmental shifts caused by temperature variations.

3.2. *Schistosoma mansoni* (SM) sub-model

A disease-free equilibrium point for the SM sub-model is given as

$$E_{0m} = (H^*, I_m^*, R_m^*, S_2^*, I_2^*) = \left(\frac{\Lambda_h}{\upsilon_1}, 0, 0, \frac{S_2}{\gamma_2}, 0\right)$$

Similarly, we show that the SM sub-model has a reproduction number R_{0m} given as

$$R_{0m} = \sqrt{\frac{\beta_2\beta_i\Lambda_2\Lambda_h}{\upsilon_1\gamma_2(\gamma_2+\alpha_2)(\gamma+\delta_i+\upsilon_1)}} \qquad (14)$$

Similarly, as described in Section 3.1, R_{0m} in Eq. (14) reflects temperature-dependent *Schistosoma mansoni* new case influenced by β_2, β_i, γ_2, and α_2. When $R_{0m} < 1$, the SM sub-model reaches a disease-free equilibrium, and such temperature conditions hinders infection. Under favorable temperature conditions, $R_{0m} > 1$, indicating the presence of an endemic equilibrium point $E_h = (H^*, I_m^*, R_m^*, S_2^*; I_2^*)$ in the SM sub-model, expressed as follows:

$H^* = \frac{(\gamma_2+\alpha_2)((\alpha+\upsilon_1)\Lambda_2+\gamma\omega I_m^*)(\beta_2 I_m^*+\gamma_2)}{(\alpha+\upsilon_1)(\gamma_2+\alpha_2)(\beta_2 I_m^*+\gamma_2)}$, $R_m^* = \frac{\gamma}{(\alpha+\upsilon_1)} I_m^*$, $S_2^* = \frac{\Lambda_2}{(\beta_2 I_m+\gamma_2)} I_m^*$, $I_2^* = \frac{\beta_2\Lambda_2 I_m^*}{(\gamma_2+\alpha_2)(\beta_2 I_m^*+\gamma_2)} I_m^*$,

where the solution for I_m^*, representing *S. mansoni* infected humans in the SM sub-model, is derived by substituting the values of H^* and $I_2^{"}$ into the equation. The resulting polynomial, described by equation Eq. (15), establishes the endemic equilibrium of the SM sub-model.

$$\lambda^3 + b_2\lambda^2 + b_1\lambda + b_0 = 0 \qquad (15)$$

where $b_0 = -\frac{\gamma_2\beta_i\beta_2\Lambda_2\Lambda_h}{\beta_2(\gamma_2+\alpha_2)(\gamma+\delta_i+\upsilon_1)}$, $b_1 = \frac{(\gamma_2+\alpha_2)(\omega\gamma+\delta_i+\upsilon_1)(\gamma_2-\beta_2\Lambda_h)-\gamma_2\beta_i\beta_2\Lambda_2}{\beta_2(\gamma_2+\alpha_2)(\gamma+\delta_i+\upsilon_1)}$,

$b_2 = \frac{(\gamma_2+\alpha_2)(\gamma+\delta_i+\upsilon_1)\big((\gamma_2-\beta_2\Lambda_h)\big)-(\gamma_2+\alpha_2)\gamma\gamma_2\beta_i\beta_2\Lambda_2}{\beta_2\gamma_2(\gamma_2+\alpha_2)(\gamma+\delta_i+\upsilon_1)}$.

Thus, it is clear that $b_0 < 0$. Following Descartes' rule of signs [39], if either or both of $b_i > 0, i = 1,2$, there will be at least one positive root, leading to the existence of an endemic equilibrium. Similarly, fluctuating temperatures alters infection prevalence at an endemic state triggered by β_2, β_i, γ_2, and α_2.

3.3. Co-dynamics model

The co-dynamics model in equations Eq. (1-11) has a disease-free equilibrium point given by

$$E_{0hm} = (H^{**}, I_m^{**}, I_h^{**}, I_{hm}^{**}, R_m^{**}, R_h^{**}, R_{hm}^{**}, S_1^{**}, I_1^{**}, S_2^{**}, I_2^{**})$$

$$= \left(\frac{\Lambda_h}{\upsilon_1}, 0, 0, 0, 0, 0, 0, \frac{\Lambda_1}{\gamma_1}, 0, \frac{\Lambda_2}{\gamma_2}, 0\right)$$

Similarly, linearization of the co-dynamic model at E_{0hm} can be ascertained where,

$$F = \begin{pmatrix} 0 & 0 & 0 & 0 & \frac{\beta_i \Lambda_h}{\upsilon_1} \\ 0 & 0 & 0 & \frac{\beta_u \Lambda_h}{\upsilon_1} & 0 \\ 0 & 0 & 0 & 0 & 0 \\ 0 & \frac{\beta_1 \Lambda_1}{\gamma_1} & \frac{\beta_1 \Lambda_1}{\gamma_1} & 0 & 0 \\ \frac{\beta_2 \Lambda_2}{\gamma_2} & 0 & \frac{\beta_2 \Lambda_2}{\gamma_2} & 0 & 0 \end{pmatrix}$$

$$V = \begin{pmatrix} (\gamma + \delta_i + \upsilon_1) & 0 & 0 & 0 & 0 \\ 0 & (\omega + \delta_u + \upsilon_1) & 0 & 0 & 0 \\ 0 & 0 & (\delta + \delta_i + \delta_u + \upsilon_1) & 0 & 0 \\ 0 & 0 & 0 & (\gamma_1 + \alpha_1) & 0 \\ 0 & 0 & 0 & 0 & (\gamma_2 + \alpha_2) \end{pmatrix}$$

Similarly, we can get the next generation matrix and R_{0hm} for the co-dynamics model:

$$FV^{-1} = \begin{pmatrix} 0 & 0 & 0 & 0 & \frac{\beta_i \Lambda_h}{\upsilon_1(\gamma_2 + \alpha_2)} \\ 0 & 0 & 0 & \frac{\beta_u \Lambda_h}{\upsilon_1(\gamma_1 + \alpha_1)} & 0 \\ 0 & 0 & 0 & 0 & 0 \\ 0 & \frac{\beta_1 \Lambda_1}{\gamma_1(\omega + \delta_u + \upsilon_1)} & \frac{\beta_1 \Lambda_1}{\gamma_1(\delta + \delta_i + \delta_u + \upsilon_1)} & 0 & 0 \\ \frac{\beta_2 \Lambda_2}{\gamma_2(\gamma + \delta_i + \upsilon_1)} & 0 & \frac{\beta_2 \Lambda_2}{\gamma_2(\delta + \delta_i + \delta_u + \upsilon_1)} & 0 & 0 \end{pmatrix}$$

There are two eigenvalues that, depending on the parameter values, could both be the largest/dominant [38, 40],

$$R_{0h}^2 = \frac{\beta_1 \beta_u \Lambda_1 \Lambda_h}{\upsilon_1 \gamma_1 (\gamma_1 + \alpha_1)(\omega + \delta_u + \upsilon_1)}, \text{ and } R_{0m}^2 = \frac{\beta_2 \beta_i \Lambda_2 \Lambda_h}{\upsilon_1 \gamma_2 (\gamma_2 + \alpha_2)(\gamma + \delta_i + \upsilon_1)}$$

Consequently, the basic reproductive number is the largest of these two eigenvalues.

$$R_{0hm} = max\{R_{0h}, R_{0m}\}$$

Thus, the emergence of *Schistosoma* co-infection cases hinges on the influence of temperature on either R_{0h} or R_{0m}. The subsequent Theorem 1 establishes this dependency.

Theorem 1: *The disease free equilibrium E_{0hm} in co-dynamic model is locally asymptotically stable whenever $R_{0hm} < 1$ and unstable otherwise* (see the proof in Appendix B)

3.4. Mutual interactions: Impact of *S. haematobium* on *S. Mansoni* and vice versa

This section explores mutual effects of *S. haematobium* and *S. mansoni* by expressing their reproduction numbers bidirectionally. This will allow us to explore the relationship between the reproduction numbers of the two infections and gain insights into their mutual interactions. We begin by expressing R_{0h} in equation Eq. (12) in terms of R_{0m} given in equation Eq. (14), where we solve for υ_1 in R_{0m} and substitute in R_{0h}, to get

$$\upsilon_1 = \frac{-q_1 R_{0m} + \sqrt{(q_1 R_{0m})^2 + 4p_1 r_1}}{2p_1 R_{0m}}$$

where $p_1 = \gamma_2(\gamma_2 + \alpha_2)$, $q_1 = \gamma_2(\gamma_2 + \alpha_2)(\gamma + \delta_i)$, and $r_1 = \beta_i \beta_2 \Lambda_2 \Lambda_h$. Substituting υ_1 into expression for R_{0h}, we obtain

$$R_{0h} = \sqrt{\left(\frac{2r_2 p_1^2}{q_1(q_1 p_2 - p_1 q_2)R_{0m} + (p_1 q_2 - q_1 p_2)\sqrt{(q_1 R_{0m})^2 + 4p_1 r_1} + 2p_1 p_2 r_1 R_{0m}^{-1}}\right)} \quad (16)$$

where $p_2 = \gamma_1(\gamma_1 + \alpha_1)$, $q_2 = \gamma_1(\gamma_1 + \alpha_1)(\omega + \delta_u)$, and $r_2 = \beta_u \beta_1 \Lambda_1 \Lambda_h$.

Similarly, expressing υ_1 in terms of R_{0h} leads to

$$\upsilon_1 = \frac{-q_2 R_{0h} + \sqrt{(q_2 R_{0h})^2 + 4p_2 r_2}}{2p_2 R_{0h}}$$

Substituting υ_1 into expression for R_{0m}, we get

$$R_{0m} = \sqrt{\left(\frac{2r_1 p_2^2}{q_2(q_2 p_1 - p_2 q_1)R_{0h} + (p_2 q_1 - q_2 p_1)\sqrt{(q_2 R_{0h})^2 + 4p_2 r_2} + 2p_1 p_2 r_2 R_{0h}^{-1}}\right)} \quad (17)$$

Partial derivatives of R_{0h} in equation Eq. (16) and R_{0m} in equation Eq. (17), determine the co-infection impact of *S. mansoni* on *S. haematobium* and *haematobium* on *S. mansoni*, respectively, in a population. By partially differentiating R_{0h} in Eq. (16) with respect to R_{0h}, we obtain

$$\frac{\partial R_{0h}}{\partial R_{0m}} = \frac{\sqrt{2r_2 p_1^2}\left\{q_1(q_2 p_1 - p_2 q_1) + 2q_1(q_2 p_1 - p_2 q_1)R_{0m}\left(\sqrt{(q_1 R_{0m})^2 + 4p_1 r_1}\right)^{-1} - 2p_1 p_2 r_1 R_{0m}^{-2}\right\}}{\left\{q_1(q_1 p_2 - p_1 q_2)R_{0m} + (p_2 q_1 - q_2 p_1)\sqrt{(q_1 R_{0m})^2 + 4p_1 r_1} + 2p_1 r_1 R_{0m}^{-1} + 2p_1 p_2 r_1 R_{0m}^{-1}\right\}^{3/2}} \quad (18)$$

Similarly, by partially differentiating R_{0m} in equation Eq. (17) with respect to R_{0h}, we are able to derive

$$\frac{\partial R_{0m}}{\partial R_{0h}} = \frac{\sqrt{2r_1p_2^2}\left\{q_2(q_1p_2-p_1q_2)+2q_2(q_1p_2-p_1q_2)R_{0h}\left(\sqrt{(q_2R_{0h})^2+4p_2r_2}\right)^{-1}-2p_1p_2r_2R_{0h}^{-2}\right\}}{\left\{q_2(q_2p_1-p_2q_1)R_{0h}+(p_1q_2-q_1p_2)\sqrt{(q_2R_{0h})^2+4p_2r_2}+2p_2r_2R_{0h}^{-1}+2p_1p_2r_2R_{0h}^{-1}\right\}^{3/2}} \quad (19)$$

The partial derivatives in equations Eq. (18) and Eq. (19) reveal distinct scenarios. Equation Eq. (18) determines the temperature-driven influence of *S. haematobium* on *S. mansoni*. If $(\partial R_{0h}/\partial R_{0m}) > 0$ under specific environmental conditions, an increase in *S. mansoni* cases boosts *S. haematobium* infection, favoring both. Conversely, $(\partial R_{0h}/\partial R_{0m}) = 0$ signifies no significant impact of *S. mansoni* changes on *S. haematobium* transmission. If $(\partial R_{0h}/\partial R_{0m}) < 0$, an increase in *S. mansoni* cases reduces *S. haematobium* cases, negatively affecting *S. haematobium* but favoring emerging *S. mansoni* cases. Equation Eq. (19) similarly assesses the temperature-dependent impact of *S. mansoni* on *S. haematobium*.

3.5. Impacts on treatment inferred from the recovery rate

Furthermore, our model assumes that infected individuals recover due to treatment. Consequently, in individuals co-infected with both *S. mansoni* and *S. haematobium*, the effect of treatment with praziquantel is likely to be a reduction of worm burdens for both forms in the human body. The effect can be determined by evaluating the partial derivatives of $R_{0hm} = max\{R_{0h}, R_{0m}\}$ with respect to the recovery rate (γ) of individuals from *S. mansoni* and (ω) of individuals from *S. haematobium*. . For example, if $R_{0h} > R_{0m}$ then $R_{0hm} = R_{0h}$, the derivation yields insights into.

$$\frac{\partial R_{0hm}}{\partial \gamma \partial \omega} = \sqrt{2r_2p_1^2}\left(\frac{D_2q_1p_1\left\{R_{0m}-\left[(q_1R_{0m})^2+4p_1r_1\right]^{-1/2}\right\}+3D_1p_1\left\{q_1R_{0m}-\left[(q_1R_{0m})^2+4p_1r_1\right]^{-1/2}\right\}}{4(D_2)^2}\right) \quad (20)$$

$$D_1 = q_1(p_1q_2 - 2q_1p_2)R_{0m} + p_2\sqrt{(q_1R_{0m})^2 + 4p_1r_1} + q_1(q_1p_2 - p_1q_2)[(q_1R_{0m})^2 + 4p_1r_1]^{-1/2}$$

$$D_2 = 2(q_1(q_1p_2 - p_1q_2)R_{0m} + (p_1q_2 - q_1p_2)\sqrt{(q_1R_{0m})^2 + 4p_1r_1} + 2p_1p_2r_1R_{0m}^{-1})^3$$

Thus depending on environmental conditions, the cost-effectiveness of treating both *S. mansoni* and *S. haematobium* in a mixed infection model holds different implications depending on the sign of equation Eq. (20). A negative value, Eq. (20) < 0 indicates a potential synergy, reducing the transmission potential against a mixed infection. A value of zero, Eq. (20) $= 0$ implies no substantial impact on schistosomiasis co-infection dynamics. Conversely, a positive value, Eq. (20) > 0 suggests a potential increase in the transmission potential of a mixed infection, indicating an antagonistic effect or heightened risk of when treating both *S. mansoni* and *S. haematobium* using a single praziquantel treaetment alone. Similarly, we can assess the treatment impact, as indicated by the recovery rate γ for individuals infected with *S. mansoni*, through the partial derivative $\partial R_{0m}/\partial \gamma$. Additionally, we can examine the treatment impact, determined by the recovery rate ω for individuals infected with *S. haematobium*, using the partial derivative $\partial R_{0h}/\partial \omega$. These analytical insights can assist in determining an appropriate treatment strategy based on specific seasonal or monthly temperature conditions. However, it is important to note that the effectiveness of treatment may be influenced by other factors such as the stage of each infection, the severity of the disease, and individual variations in response to the drug.

4. Numerical simulations

Based on the parameter values in Table 1 and Table 2, we simulate the dynamics of co-infection between *S. haematobium* and *S. mansoni*. The simulation outcomes demonstrate a linear relationship between the transmissibility rate of *S. haematobium* (β_u) and *S. mansoni* (β_i) to humans (Fig. 1a). These results also show a similar pattern of changes in temperature for both infections. However, the transmissibility of *S. mansoni* to *Biomphalaria* snails (β_2) displays greater sensitivity to temperature variations compared to the transmissibility of *S. haematobium* to *Bulinus* snails (β_1), as shown in Fig. 1b. Furthermore, it is observed that the natural death rate (γ_1) and *S. haematobium*-induced death (α_1) in *Bulinus* snails exhibit higher sensitivity to temperature changes than the natural death rate (γ_2) and *S. mansoni*-induced death (α_2) in *Biomphalaria* snails as depicted in Fig. 1c and Fig. 1d. This indicates that the two species respond differently to environmental temperature variations, leading to distinct impacts on the dissemination of the single and mixed infections within the populations.

Figure 1: Temperature-dependent model parameters in the life history of *Schistosoma* species between human and intermediate host genera.

In the sensitivity analysis, we further identify the most sensitive and significant parameters in R_{0h} and R_{0m} concerning their mutual interaction, which is influenced by the interplay of other parameters in the co-dynamics model. Specifically, we consider $|\text{PRCC}| \geq 0.5$ as the threshold, which is indicated by the horizontal lines in Fig. 2a and Fig. 2b. Our findings show that the reproduction number of *S. haematobium* (R_{0h}) is highly sensitive to changes in the transmissibility of *S. haematobium* to humans (β_u), the transmissibility of *S. haematobium* to snails (β_1), the natural death rate of *Biomphalaria* snails (γ_2), the transmissibility of *S. mansoni* to humans (β_i), and the transmissibility of *S. mansoni* to snails (β_2), in that order as depicted in Fig. 2a. Similarly, the reproduction number of *S. mansoni* (R_{0m}) exhibits sensitivity to changes in the transmissibility of *S. mansoni* to humans (β_i), the natural death rate of *Bulinus* snails (γ_1), the transmissibility of *S. mansoni* to snails (β_2), and the transmissibility of *S. haematobium* to snails (β_1), in that order, as depicted in Fig. 2b. These parameters stand out as crucial and could serve as potential targets for controlling both infections. In general, within an endemically co-infected community, R_{0h} shows greater sensitivity to S. *mansoni* parameters, whereas R_{0m} demonstrates lesser sensitivity to *S. haematobium* parameters. This indicates that changes in *S. mansoni* infections, R_{0m} have a lesser impact on transmission of haematobium, R_{0h} compared to the reverse scenario. Thus, it can be inferred that *S. haematobium* has a positive impact on *S. mansoni* dynamics, suggesting that *S. haematobium* may modulate the immune response to increase susceptibility. Consequently, $R_{0h} > R_{0m}$ in endemically co-infected communities, especially when considering how temperature-dependent parameters vary simultaneously due to climate change in such regions; see Fig. 2c and Fig. 2d. Furthermore, regions or seasons characterized by temperature fluctuations of approximately 23-26ºC tend to exhibit the highest number of infection cases from both species (Figure 2c, 2d). However, in the presence of temperature fluctuations above 26ºC degrees, a notable decrease in the number of infections and burden is observed; see Fig. 2c and Fig. 2d. This phenomenon can likely be attributed to a higher mortality rate among the intermediate hosts (Fig. 1c, Fig. 1d) and a concurrent decline in their infection rates (Fig. 1b).

Figure 2: Impacts of individual input parameters on the output variables (a) R_{0h} as a function of R_{0m} and (b) R_{0m} as a function of R_{0h}. (c) Variations in *S. haematobium* infection cases, and (d) *S. mansoni*

infection cases due to changes in temperature-dependent model parameters (note different scales for infection cases for *S. haematobium and S. mansoni* in (c) and (d).

Furthermore, we utilized the temperature-dependent parameter curves (in Table 1) to derive temperature variant parameter values at 20°C, 25°C, and 35°C, representing distinct seasons and geographical regions with potentially diverse climatic conditions, as outlined in Table 3. Subsequently, simulations of the co-dynamic model Eq. (1-11) were conducted to depict the progression of single and mixed infections across a 5-year period.

Table 3: Temperature-dependent parameter values under stable temperatures conditions

	β_i	β_u	β_1	β_2	γ_1	γ_2	α_1	α_2
20°C	0.0294	0.0280	0.000125	0.000104	0.00175	0.0039	0.00352	0.00215
25°C	0.0572	0.0595	0.00116	0.00097	0.006575	0.00305	0.00305	0.01405
35°C	0.01227	0.1225	0.001459	0.001216	0.02814	0.01815	0.03346	0.04985

Our study underscores temperature-dependent variations in infection levels among hosts and individuals, particularly at moderate temperatures (20°C and 25°C) compared to higher temperatures (35°C), resulting in decreased infections (Fig. 3a-c). Notably, we observe different temperature-related impacts on dissemination, with *S. haematobium* exhibiting higher rates at 20°C in the short term (1-3 years) but experiencing a higher co-infection burden in the long term (Fig. 3a). Conversely, rapid dissemination occurs in a shorter time with increased co-infection cases at 25°C and 35°C (Fig. 3c-b). The recovery rates differ with temperature, notably more individuals recovering from *S. haematobium* than *S. mansoni* and mixed infections (Fig. 3d-f). This underscores variations in response to treatment and recovery patterns across different infection types, with recovery being lower at 20°C but higher at 25°C and 35°C (Fig. 3d-f). Additionally, our simulations reveal that despite the increase in the *Biomphalaria* snail population, they exhibit higher susceptibility to infection compared to *Bulinus* snails at 25°C, resulting in more *Biomphalaria* infections than *Bulinus* cases (Fig. 3g-j). Additionally, *Biomphalaria* snails show a more pronounced decrease in population at temperatures between 25°C and 35°C compared to *Bulinus* snails (Fig. 3h-l), suggesting potential differences in sensitivity and resistance to temperature changes between these snail species. These variations stem from the non-linear impact of temperature on *Schistosoma* traits within their life history.

Figure 3: Temperature effects on populations of *S. haematobium* and *S. mansoni* infections. (a-c) Susceptible and infected human populations; (d-f) Recovered human population; (g-i) Susceptible snail population; (j-l) Infected snail population.

5. Discussion

Climate-induced challenges like drought, population displacements, poverty, and poor sanitation hinder disease control in endemic regions such as Sub-Saharan Africa, where schistosomiasis is prevalent [1, 2, 4]. Integrating climatic variability into complex multi-host disease models, like schistosomiasis, is challenging and debatable. The scarcity of climatic experimental and epidemiological data for model parameterization adds to the complexity. Nevertheless, two existing laboratory studies providing comprehensive temperature-related data in the literature

served as inspiration for this study, see [17, 18]. This study employs a mathematical model to comprehensively explore the co-dynamics between *S. mansoni* and *S. haematobium*, revealing temperature-related variations in their transmission dynamics, interactions, and implications for both single and mixed schistosomiasis infections. Standard mathematical techniques are applied to calculate and present theoretical properties of the single species sub-models and co-dynamic model, including disease-free and endemic states as functions of temperature. The study derives standard expressions for reproduction numbers (R_0s) under static environmental conditions with temperature-dependent entities, while assessing the local and global stability of equilibria associated with single species sub-models and co-dynamic model, offering detailed biological interpretations. The reproduction numbers are used to demonstrate mutual interaction effects between both species and evaluate the impact of infection on each other. The study also examines the impact of treatment inferred from the recovery rate, establishing temperature conditions for disease-free and disease prevalence. The theoretical quantitative framework provides analytical insights with user-friendly expressions of R_0s, aiding in guiding disease control strategies and investigating the contribution of each model parameter to disease spread. For example, it assists in determining an appropriate treatment strategy based on specific seasonal or monthly temperature conditions.

Parameterized with temperature variant and invariant data, our model numerical simulation shows that *S. mansoni* is more sensitive to temperature during transmission to *Biomphalaria* snails than *S. haematobium* to *Bulinus* snails. Contrary, *S. haematobium* exhibits higher sensitivity to temperature in transmission to the human compared to *S. mansoni*. Additionally, Moderate temperatures (20°C and 25°C) increase human infection levels, while higher temperatures (35°C) reduce incidence. Recovery rates of both single and co-infected individuals rise with temperature, favoring *S. haematobium* than *S. mansoni* and mixed infection, suggesting that temperature variations significantly impact the efficacy of schistosomiasis treatment protocols. In addition, co-infections often present overlapping symptoms and complications, complicating the process of accurately distinguishing and effectively treating each infection. The model offers a theoretical framework that simulates these interactions, suggesting that aligning treatment interventions with specific temperature ranges could improve their effectiveness.

Moreover, parameters influencing reproduction numbers underscore a positive influence of *S. haematobium* on *S. mansoni* dynamics. *Biomphalaria* snails are more susceptible than *Bulinus*, with varied temperature impacts on their populations, i.e. temperatures less than 25°C seem favorable while temperatures above 26ºC result in a significant decrease in their population. The variations in schistosomiasis transmissibility between humans and intermediate host snails are primarily associated with temperature-dependent parameters. These findings have significant public health implications, recommending tailored seasonal and timely treatment strategies.

Our findings are consistent with previous studies that demonstrated that transmission traits in the life cycle of the *Schistosoma* species exhibit distinct patterns under different temperature conditions [7, 17, 18, 34, 41]. In contrast, the experiment conducted by He and Ramaswamy [42] demonstrated that *S. mansoni* and *S. haematobium* larvae can pass through human skin indistinguishably, resulting in no differences in transmissions. However, this study did not consider temperature fluctuations, thus our results underscores the importance of considering temperature control over the temperature sensitive stages of *Schistosoma* life cylce to unravel the differences, and interactions between closely related single and mixed species infections. For instance, our model revealed the role of *S. haematobium* in mutually increasing susceptibility to *S. mansoni* co-

infections. This result is supported by the studies that highlight the impact of *S. haematobium* on the local genital tract and the global immune system [1, 12]. Furthermore, earlier studies, including Mbabazi et al. [43], have also established its association with other diseases such as HIV. The cumulative evidence suggests that the effects of *S. haematobium* are not confined to the local site of infection but have systemic consequences. This necessitates a comprehensive approach to the management of *Schistosoma* species, their potential mutual interactions and impacts on co-infections and other diseases such as HIV based on the environmental conditions.

Moreover, the results reveal distinct impacts of temperature on the dynamics of *S. haematobium-Bulinus* and *S. mansoni-Biomphalaria* infection. Generally, the latter system exhibits a lower sensitivity to temperature variations, indicating a lower risk of outbreak and fewer infection cases. These findings are consistent with field studies, including Cunin et al. [28], Garba et al. [29], and Nassar et al. [30], which consistently report a higher prevalence of *S. haematobium* compared to *S. mansoni* in areas where both species coexist. Specifically, our study supports prior observations that populations, including both individuals and intermediate hosts, exhibit higher infection levels with *S. haematobium* or *S. mansoni* at moderate temperatures (20°C and 25°C) compared to 35°C, where infections notably decrease[7, 17, 18, 34, 41]. The low infection levels indicate restricted schistosomiasis activities, higher mortality rates among intermediate hosts, and notably decreased transmissibility, particularly at 35°C. This consensus underscores the role of temperature in shaping the dynamics of *Schistosoma* species infections in diverse environments and populations. For example, temperature variation in different endemic areas can be a possible explanation for reported cases of low cure rates, and drug resistance, due to persistent transmission patterns and increased re-infection rates [15, 47]. Therefore, the impact of temperature extends beyond schistosomiasis, as it has been shown to shape disease dynamics and stability in various ecological systems [44, 45, 46, 47]. Therefore, temperature-dependent models are effective tools for predicting disease patterns in regions where the specified temperature ranges align with the local climate. This applicability is particularly notable in East Africa, where typical temperature ranges, [20, 35] °C coincide with the prevalence of *Biomphalaria* and *Bulinus* species, and both *S. mansoni* and *S. haematobium* infections are widespread [4, 22, 47]. Additionally, the range of demographic parameters Λ_h, Λ_1, τ, and υ_1 align with the rates observed in East Africa, as evident in Tabo et al. [47].

6. Limitations and outlook

Although our model remains robust and provides valuable insights, there are some limitations. Firstly, the parameter values employed in our model, reflecting the biological aspects and real-life scenarios of schistosomiasis transmission, were drawn from published literature. This introduces potential inconsistencies and variability within the data collected under diverse conditions, leading to uncertainties in our model results. Secondly, using estimated baseline values introduces potential biases, such as systematic errors and reduced generalizability. Thirdly, it is essential to acknowledge the current absence of real-life epidemiological data for the two infection systems to cross-verify and validate our model. To address this, a crucial step in the future involves applying the model in a schistosomiasis endemic region with established local climates and healthcare or treatment data. This application should encompass a comparison of predicted endemic states with available real-epidemiological data on *S. mansoni* and *S. haematobium* infections. Additionally, future research could further refine our understanding by incorporating human worm burden dynamics and integrating optimal control strategies. These endeavors aim to determine effective means of infection control and represent essential avenues for enhancing our comprehension of schistosomiasis.

7. Conclusions

In light of our findings in this study, recognizing the temperature-dependent impact on reproduction numbers underscores the need to integrate temperature into models for predicting and managing schistosomiasis dynamics. Public health and policymakers should implement targeted control strategies, considering seasonal variations in sensitive parameters like snail/human transmissibility and snail natural death rates. Targeting snail control during seasons with temperatures below 25°C to capitalize on increased susceptibility is a strategic approach. It is imperative to monitor and adapt treatment protocols, considering temperature-dependent recovery rates, for enhanced overall treatment effectiveness. For instance, interventions during seasons around 25-35°C, where higher recovery rates are observed, may yield better results. Empowering communities to implement preventive measures during specific temperature conditions can further bolster schistosomiasis control initiatives. Our mathematical model provides a sturdy framework for understanding the interplay between temperature and various forms of schistosomiasis transmission dynamics. Functioning as a quantitative framework, it offers a reasonable approximation with baseline parameter values, thereby enriching our comprehension of the impact of temperature, and the timing of interventions. Thus, our study strengthens the One Health approach by integrating human and animal (IH snail) health strategies with environmental factors and seasonal variations to optimise schistosomiasis control. The study also shows how the model can be applied in different regions with similar climates.

Availability of data and materials

This published article incorporates all the data generated or analyzed during the study.

Declarations

Ethics approval and consent to participate

Not applicable

Consent for publication

Not applicable.

Competing interests

The authors declare no competing interests.

Funding

ZT received a PhD scholarship (Grant No. 57507871) from the German Academic Exchange Service (DAAD). The funder had no involvement in the study design, data collection, analysis, decision to publish, or preparation of the manuscript.

Authors' contributions

ZT: Conceptualization, Methodology, Formal analysis, Visualization, Writing – original draft, Writing – review & editing. LB: Funding acquisition, Supervision, Writing – review & editing.

CA: Conceptualization, Funding acquisition, Supervision, Writing – review & editing. All authors reviewed and approved the final version of the manuscript.

Acknowledgements

The authors express their sincere gratitude to the German Academic Exchange Service (DAAD) for supporting ZT with a PhD scholarship.

References

1. World Health Organization. Schistosomiasis. 2023 [cited 2023 June 3]. Available from: https://www.who.int/news-room/fact-sheets/detail/schistosomiasis
2. Molehin AJ, Rojo JU, Siddiqui SZ, Gray SA, Carter D, Siddiqui AA et al. Development of a schistosomiasis vaccine. Expert Review Vaccines. 2016;15(5):619-27. https://doi.org/10.1586/14760584.2016.1131127
3. Steinmann P, Keiser J, Bos R, Tanner M, Utzinger J. Schistosomiasis and water resources development: systematic review, meta-analysis, and estimates of people at risk. Lancet Infect Dis. 2006;6(7):411-25. https://doi.org/10.1016/S1473-3099(06)70521-7
4. Gryseels B, Polman K, Clerinx J, Kestens L. Human schistosomiasis. Lancet. 2006:368(9541):106-18. https://doi.org/10.1016/S0140-6736(06)69440-3
5. Utzinger J, Raso G, Brooker S, De Savigny D, Tanner M, Ørnbjerg N, et al. Schistosomiasis and neglected tropical diseases: towards integrated and sustainable control and a word of caution. J Parasitol. 2009; 136(13):1859-74. https://doi.org/10.1017/S0031182009991600
6. Morgan JA, Dejong RJ, Snyder S D, Mkoji GM, Loker ES. *Schistosoma mansoni* and *Biomphalaria*: past history and future trends. J Parasitol. 2001; 123(7):211-28. https://doi.org/10.1017/S0031182001007703
7. Stothard D, Southgate JR, Southgate VR. Interactions between intermediate snail hosts of the genus *Bulinus* and schistosomes of the *Schistosoma haematobium* group. Journal of Parasitology. 2001;123(7):245-60. http://dx.doi.org/10.1017/S0031182001008046
8. Wang L, Utzinger J, Zhou XN. Schistosomiasis Control: Experiences and Lessons from China. Lancet 2008;372(9652):1793–1795. https://doi.org/10.1016/S0140-6736(08)61358-6
9. Colley DG, Bustinduy AL, Secor WE, King C H. Human Schistosomiasis. Lancet 2009;383 (9936):2253–2264. https://doi.org/10.1016/S0140-6736(13)61949-2
10. Elbaz T, Esmat G. Hepatic and intestinal schistosomiasis. J Adv Res. 2013;4(5):445-52.
11. Lapa M, Dias B, Jardim C, Fernandes CJ, Dourado PM, Figueiredo M, et al. Cardiopulmonary manifestations of hepatosplenic schistosomiasis. Circulation. 2009;119(11):1518-23. https://doi.org/10.1161/CIRCULATIONAHA.108.803221
12. Khalaf I, Shokeir A, M. Shalaby. Urologic complications of genitourinary schistosomiasis. World J Urol. 2012;30:31-8.https://doi.org/10.1007/s00345-011-0751-7
13. Barsoum RS, Esmat G, El-Baz T. Human schistosomiasis: clinical perspective. J Adv Res 2013;4(5):433-44. https://doi.org/10.1016/j.jare.2013.01.005
14. King CH. Parasites and poverty: the case of schistosomiasis. Acta Trop. 2010;13(2):95-104. https://doi.org/10.1016/j.actatropica.2009.11.012

15. Fallon PG. Immunopathology of schistosomiasis: a cautionary tale of mice and men. Immunol Today. 21(1) (2000) 29-35. https://doi.org/10.1016/S0167-5699(99)01551-0

16. Bull FC, Al-Ansari SS, Biddle S, Borodulin K, Buman MP, Cardon G, et al. World Health Organization 2020 guidelines on physical activity and sedentary behaviour. Br J Sports Med. 2020;4(24):1451-1462.

17. Mangal TD, Paterson S, A. Fenton. Predicting the impact of long-term temperature changes on the epidemiology and control of schistosomiasis: a mechanistic model. PLoS One. 2008;3(1):1438. https://doi.org/10.1371/journal.pone.0001438

18. Kalinda C, Chimbari MJ, Mukaratirwa S. Effect of temperature on the *Bulinus globosus*-*Schistosoma haematobium* system. Infect Dis Poverty. 2017;6(1):1-7. https://doi.org/10.1186/s40249-017-0260-z

19. Paull SH, Johnson PT. High temperature enhances host pathology in a snail–trematode system: possible consequences of climate change for the emergence of disease. Freshwater Biol. 2011;56(4):767-78. https://doi.org/10.1111/j.1365-2427.2010.02547.x

20. Abruzzi A, Fried B. Coinfection of S*chistosoma* (Trematoda) with bacteria, protozoa and helminths. Advances Parasitol. 2011;77:1-85. https://doi.org/10.1016/B978-0-12-391429-3.00005-8

21. Wilson S, Jones FM, Mwatha JK, Kimani G, Booth M, Kariuki HC, et al. Hepatosplenomegaly associated with chronic malaria exposure: evidence for a pro-inflammatory mechanism exacerbated by schistosomiasis. Parasite Immunol. 2009;31(2):64-71. https://doi.org/10.1111/j.1365-3024.2008.01078.x

22. Gouvras AN, Kariuki C, Koukounari A, Norton AJ, Lange CN, Ireri E, et al. The impact of single versus mixed *Schistosoma haematobium* and *Schistosoma mansoni* infections on morbidity profiles amongst school-children in Taveta, Kenya. Acta Trop. 28(2) (2013) 309-17. https://doi.org/10.1016/j.actatropica.2013.01.001

23. Lloyd-Smith JO, Poss M, Grenfell BT. HIV-1/parasite co-infection and the emergence of new parasite strains. J Parasitol. 2008;135(7):795-806. https://doi.org/10.1017/S0031182008000292

24. Bhunu CP, Tchuenche JM, Garira W, Magombedze G, Mushayabasa S. Modeling the effects of schistosomiasis on the transmission dynamics of HIV/AIDS. JBiol Syst. 2010;18(02):277-97. https://doi.org/10.1142/S0218339010003196

25. Bakare EA, Nwozo CR. Bifurcation and sensitivity analysis of malaria–schistosomiasis co-infection model. Int J Appl and Comput Math. 2017;3:971-1000. https://doi.org/10.1007/s40819-017-0394-5

26. Okosun KO, Smith R. On the Co-infection of Malaria and Schistosomiasis. In Mathematical and computational approaches in advancing modern science and engineering. Springer International Publishing. 2016; p. 289-298.

27. Okosun OK, Khan MA, Bonyah E, Okosun OO. Cholera-schistosomiasis coinfection dynamics. Optim Control Appl Meth. 2019;40(4):703-27. https://doi.org/10.1002/oca.2507

28. P. Cunin, L. A. T. Tchuem Tchuenté, B. Poste, K. Djibrilla, P. M. Martin. Interactions between Schistosoma haematobium and Schistosoma mansoni in humans in north Cameroon. Trop Med Int Health. 8(12) (2003) 1110-7. https://doi.org/10.1046/j.1360-2276.2003.01139.x

29. Garba A, Barkiré N, Djibo A, Lamine MS, Sofo B, Gouvras AN, et al. Schistosomiasis in infants and preschool-aged children: infection in a single *Schistosoma haematobium* and a mixed *S. haematobium-S. mansoni* foci of Niger. Acta Trop. 115(3):212-9. https://doi.org/10.1016/j.actatropica.2010.03.005

30. Nassar AS, Adetoro TA, Adebimpe WA, Muhibi MA. Presumptive diagnosis of *Schistosoma haematobium* and Schistosoma mansoni using microscopy as gold standard in a Riverrine community of Southwestern Nigeria. Afr J Clin Exp Microbiol. 2013;14(3):180-3. https://doi.org/10.4314/ajcem.v14i3.11

31. Nyabadza F, Bonyah E. On the transmission dynamics of Buruli ulcer in Ghana: Insights through a mathematical model. BMC Res Notes. 2015;8:1-5.https://doi.org/10.1186/s13104-015-1619-5

32. Chiyaka ET, Magombedze G, Mutimbu L. Modelling within host parasite dynamics of schistosomiasis. Computa MathMethods Med. 2010;11(3):255-80. https://doi.org/10.1080/17486701003614336

33. Feng Z, Li CC, Milner FA. Schistosomiasis models with two migrating human groups. Math Comput Model. 2005;41(11-12):1213-30. https://doi.org/10.1016/j.mcm.2004.10.023

34. Tabo Z, Kalinda C, Breuer L, Albrecht C. Adapting Strategies for Effective Schistosomiasis Prevention: A Mathematical Modeling Approach. Mathematics. 2023;11(12):2609. https://doi.org/10.3390/math11122609

35. Diekmann O, Heesterbeek JAP, Metz JA. On the definition and computation of the basic reproduction ratio R0 in models for infectious diseases in heterogeneous populations. J Math Biol. 1990;28:365-382.

36. Sanchez MA, Blower SM. Uncertainty and sensitivity analysis of the basic reproductive rate: tuberculosis as an example. Am J Epidemiol. 145(12) (1997) 1127-37. https://doi.org/10.1093/oxfordjournals.aje.a009076

37. Core Team RR: A Language and Environment for Statistical Computing. Version 4.0.3. Vienna: R Foundation for Statistical Computing. 2020. Available from: http://www.R-project.org

38. Van den Driessche P, Watmough J. Reproduction numbers and sub-threshold endemic equilibria for compartmental models of disease transmission. Math Biosci. 2002; 180(1-2):9-48. https://doi.org/10.1016/S0025-5564(02)00108-6

39. Grabiner DJ. Descartes' rule of signs: Another construction. An Math Mon. 1999; 106(9):854-6. https://doi.org/10.1080/00029890.1999.12005131

40. Castillo-Garsow, Castillo-Chavez C. A tour of the basic reproductive number and the next generation of researchers. An Introduction to Undergraduate Research in Computational and Mathematical Biology: From Birdsongs to Viscosities. 2020; 87-124. https://doi.org/10.1007/978-3-030-33645-5

41. Blankespoor HD, Babiker SM, Blankespoor CL. Influence of temperature on the development of *Schistosoma haematobium* in *Bulinus truncatus*. J MedAppl Malacol. 1989; 1:123-31.

42. He YX, Chen L, Ramaswamy K. *Schistosoma mansoni*, *S. haematobium*, and *S. japonicum*: early events associated with penetration and migration of schistosomula through human skin. Exp Parasitol. 2002; 102(2):99-108. https://doi.org/10.1016/S0014-4894(03)00024-9

673 **43.** Mbabazi PS, Andan O, Fitzgerald DW, Chitsulo L, Engels D, Downs JA. Examining the
674 relationship between urogenital schistosomiasis and HIV infection. PLoS Negl Trop Dis.
675 2011; 5(12):e1396. https://doi.org/10.1371/journal.pntd.0001396
676 **44.** Wu X, Lu Y, Zhou S, Chen L, Xu B. Impact of climate change on human infectious
677 diseases: Empirical evidence and human adaptation. Environ Int. 2016; 86:14-23.
678 **45.** Williams PC, Bartlett AW, Howard-Jones, McMullan B, Khatami A, Britton PN, et al.
679 Impact of climate change and biodiversity collapse on the global emergence and spread of
680 infectious diseases. J Paediatr Child Health. 2021; 57(11):1811-8.
681 https://doi.org/10.1111/jpc.15681
682 **46.** Xie G, Wang Z, Zhang Z, Li J. Effects of temperature and relative humidity on the
683 development and survival of the aquatic stages of *Schistosoma japonicum*. Parasites
684 Vectors. 8(1) (2015) 1-8.
685 **47.** Tabo Z, Kalinda C, Breuer L, Albrecht C. Exploring the interplay between climate change
686 and schistosomiasis transmission dynamics. Inf Dis Model. 2024; 9(1):154-176.
687 https://doi.org/10.1016/j.idm.2023.12.003
688 **48.** Utzinger J, N'goran EK, N'dri A, Lengeler C, Tanner M. Efficacy of praziquantel against
689 *Schistosoma mansoni* with particular consideration for intensity of infection. Trop Med Int
690 Health. 2000; 5:771–8
691 **49.** Castillo-Chavez C, Song B. Dynamical models of tuberculosis and their applications. Math
692 Biosci Eng. 2004; 1(2):361-404.

693

694 ## Appendix A

695 **Table A1:** Temperature-dependent parameters from Mangal et al. [17]

parameter	Definition	20ºC	25ºC	30ºC	35ºC
β_i	Transmissibility of Schistosomiasis to humans	0.028	0.059	0.092	0.122
β_2	Transmissibility of Schistosomiasis to snails	0.000127	0.000091	0.0014	0.0012
γ_2	Natural death rate of snails	0.004	0.003	0.008	0.0182
α_2	Schistosomiasis-induced death in snails	0.002	0.0145	0.0295	0.05

696

697 **Table A2:** Temperature-dependent parameters from Kalinda et al. [18]

parameter	Definition	15ºC	22ºC	25.8ºC	31ºC	36ºC
β_u	Transmissibility of Schistosomiasis to humans	0.00638	0.0353	0.06433	0.09753	0.12825
γ_1	Natural death rate of snails	0.00049	0.00434	0.00763	0.01635	0.0318
α_1	Schistosomiasis-induced death in snails	0.00122	0.004505	0.011989	0.022717	0.036391

698

699 ## Appendix B

700 ## Analysis of the stability of equilibria

701 ### 1. SH sub-model

702 The following equations represent the SH sub model

$$H' = \Lambda_h + \varepsilon R_h - \beta_u I_1 H - \upsilon_1 H$$

$$I_h' = \beta_u I_1 H - (\omega + \delta_u + \upsilon_1) I_h$$

$$R_h' = \omega I_h - (\varepsilon + \upsilon_1) R_h \qquad \text{(B.1)}$$

$$S_1' = \Lambda_1 - \beta_1 I_h S_1 - \gamma_1 S_1$$

$$I_1' = \beta_1 I_h S_1 - (\gamma_1 + \alpha_1) I_1$$

1.1 Local stability of the SH sub-model

Theorem 2: *The SH sub-model in* Eq. (B.1)*, at disease free* E_{0h}*, is locally asymptotically stable if* $R_{0h} < 1$*, otherwise unstable for* $R_{0h} > 1$.

Proof: The SH sub-model Eq. (B.1) has the following Jacobian matrix at E_{0h}

$$J(E_{0h}) = \begin{pmatrix} -\upsilon_1 & 0 & \varepsilon & 0 & \frac{-\beta_u \Lambda_h}{\upsilon_1} \\ 0 & -(\omega + \delta_u + \upsilon_1) & 0 & 0 & \frac{\beta_u \Lambda_h}{\upsilon_1} \\ 0 & \omega & -(\varepsilon + \upsilon_1) & 0 & 0 \\ 0 & \frac{-\beta_1 \Lambda_1}{\gamma_1} & 0 & -\gamma_1 & 0 \\ 0 & \frac{\beta_1 \Lambda_1}{\gamma_1} & 0 & 0 & -(\gamma_1 + \alpha_1) \end{pmatrix} \qquad \text{(B.2)}$$

The eigenvalues of the Jacobian matrix in Eq. (B.2) are given by the characteristic equation below,

$$(\lambda + \upsilon_1)(\lambda + \gamma_1)(\lambda + \varepsilon + \upsilon_1)(\lambda^2 + p\lambda + q) = 0, \qquad \text{(B.3)}$$

where, $p = (\omega + \delta_u + \upsilon_1) + (\gamma_1 + \alpha_1)$ and $q = (\omega + \delta_u + \upsilon_1)(\gamma_1 + \alpha_1)(1 - R_{0h})$.

It can be seen from Eq. (B.3) that $-\upsilon_1$, $-\gamma_1$, and $-(\varepsilon + \upsilon_1)$ are negative eigenvalues of $J(E_{0h})$, while the other two eigenvalues are defined by the quadratic equation and are negative provided $R_{0h} < 1$. The SH sub-model Eq. (B.1) is locally asymptotically stable for $R_{0h} < 1$ because all of its eigenvalues at E_{0h} are negative.

1.2 Existence of endemic equilibrium for the SH sub-model

Lemma 1. The SH sub-model Eq. (B.1) possesses a unique endemic equilibrium (E_{1h}) *if* $R_{0h} > 1$.

Lemma 1 can be supported by the understanding that the SH sub-model system attains a distinct endemic equilibrium (E_{1h}) only when $R_{0h} > 1$. This condition implies that the potential for sustained transmission of *Schistosoma haematobium* infections within the population is determined by whether the reproductive rate of the parasite surpasses its control factors. Therefore, when $R_{0h} > 1$, E_{1h} emerges as the dominant outcome, signifying the potential establishment and persistence of *Schistosoma haematobium* infections in the population.

1.3 Global stability of the SH sub-model

The global stability for the SH sub-model can be computed using the center manifold theory [48] to determine the local asymptotic stability or nature of the bifurcation of the endemic equilibrium.

Theorem 3. *The endemic equilibrium E_{1h} of SH sub-model Eq. (B.1) is locally asymptotically stable if $R_0 > 1$ and the bifurcation parameter $\beta_u = \beta_u^* > \frac{\upsilon_1\gamma_1(\gamma_1+\alpha_1)(\omega+\delta_u+\upsilon_1)}{\beta_1\Lambda_1\Lambda_h}$.*

Proof: We transform the SH sub-model Eq. (B.1), where $H = x_1$, $I_h = x_2$, $R_h = x_3$, $S_1 = x_4$, and $I_1 = x_5$ with the vector notation $X = (x_i)^T, i = 1,2,3,4,5$ and $\frac{dX}{\mathrm{dt}} = \boldsymbol{F} =: (f_1, f_2, f_3, f_4, f_5)^T$. Thus, the following model system is obtained

$$\begin{aligned}
x_1' =: f_1 &= \Lambda_h + \varepsilon x_3 - \beta_u x_1 x_5 - \upsilon_1 x_1 \\
x_2' =: f_2 &= \beta_u x_1 x_5 - (\omega + \delta_u + \upsilon_1) x_2 \\
x_3' =: f_3 &= \omega x_2 - (\varepsilon + \upsilon_1) x_3 \\
x_4' =: f_4 &= \Lambda_1 - \beta_1 x_2 x_4 - \gamma_1 x_4 \\
x_5' =: f_5 &= \beta_1 x_2 x_4 - (\gamma_1 + \alpha_1) x_5
\end{aligned} \tag{B.4}$$

The linearized SH sub-model Eq. (B.4) evaluated at disease-free equilibrium $E_{0h} = \left(x_1 = \frac{\Lambda_h}{\upsilon_1}, x_2 = 0, x_3 = 0, x_4 = \frac{S_1}{\gamma_1}, x_5 = 0\right)$ with the bifurcation parameter $\beta_u = \beta_u^* = \frac{\upsilon_1\gamma_1(\gamma_1+\alpha_1)(\omega+\delta_u+\upsilon_1)}{\beta_1\Lambda_1\Lambda_h}$, has a simple eigenvalue associated with a right eigenvector $\boldsymbol{u} = (u_1, u_2, u_3, u_4, u_5)^T$ and a left eigenvector $\boldsymbol{w} = (w_1, w_2, w_3, w_4, w_5)$ satisfying $\boldsymbol{u}.\boldsymbol{w} = \mathbf{1}$, where

$$\begin{aligned}
&\boldsymbol{u} \\
&= \left(u_1 = \frac{\varepsilon\omega\upsilon_1\gamma_1(\gamma_1+\alpha_1) - \beta_1\beta_u\Lambda_1\Lambda_h(\varepsilon+\upsilon_1)}{\gamma_1(\gamma_1+\alpha_1)(\varepsilon+\upsilon_1)u_1^2}u_2, \quad u_2 > 0, \quad u_3 = \frac{\omega}{(\varepsilon+\upsilon_1)}u_2, \quad u_4 = \frac{-\beta_1\Lambda_1}{\gamma_1^2}u_2, \quad u_5 = \frac{\beta_1\Lambda_1}{\gamma_1(\gamma_1+\alpha_1)}u_2\right)^T \\
&\boldsymbol{w} = \left(w_1 = 0 \quad w_2 > 0 \quad w_3 = 0 \quad w_4 = 0 \quad w_5 = \frac{\beta_u\Lambda_h}{\upsilon_1(\gamma_1+\alpha_1)}w_2\right)
\end{aligned}$$

Thus, based on $\boldsymbol{w}$, it can be seen that the second-order partial derivatives, f_k for $k = 1, 3, 4$ associated with left eigenvalues will varnish at the disease-free equilibrium, as a result,

$$\begin{aligned}
a &= w_2u_1u_5\frac{\partial^2 f_2(0,0)}{\partial x_1\partial x_5} + w_5u_2u_4\frac{\partial^2 f_5(0,0)}{\partial x_2\partial x_4} = \left(\frac{\omega\varepsilon\gamma_1\beta_1(\gamma_1+\alpha_1) - \beta_u\Lambda_h(\varepsilon+\upsilon_1)(\gamma_1\upsilon_1+\alpha_1\upsilon_1+\Lambda_1\beta_1^2)}{(\varepsilon+\upsilon_1)(\gamma_1+\alpha_1)^2\upsilon_1^2\gamma_1^2}\right)\beta_1\Lambda_1w_2u_2^2 \\
b &= w_2u_1\frac{\partial^2 f_2(0,0)}{\partial x_1\partial\beta_u^*} + w_2u_5\frac{\partial^2 f_2(0,0)}{\partial x_5\partial\beta_u^*} = \frac{\beta_1\Lambda_1\Lambda_h}{\gamma_1\upsilon_1(\gamma_1+\alpha_1)}w_2u_2
\end{aligned}$$

It is evident that $b > 0$, and the local dynamics around the disease-free equilibrium point E_{0h} for $\beta_u = \beta_u^*$ depend on the sign of the coefficient a. Consequently, if $\omega\varepsilon\gamma_1\beta_1(\gamma_1+\alpha_1) > \beta_u\Lambda_h(\varepsilon+\upsilon_1)(\gamma_1\upsilon_1+\alpha_1\upsilon_1+\Lambda_1\beta_1^2)$, a backward bifurcation occurs. This leads to the absence of global

stability for the disease-free equilibrium and the presence of an endemic equilibrium. Conversely, if the condition $\omega\varepsilon\gamma_1\beta_1(\gamma_1+\alpha_1) < \beta_u\Lambda_h(\varepsilon+\upsilon_1)(\gamma_1\upsilon_1+\alpha_1\upsilon_1+\Lambda_1\beta_1^2)$ holds, a forward bifurcation arises at $R_{0h}=1$, and the disease-free equilibrium becomes globally stable. In this scenario, the disease-free equilibrium is the only local attractor, and an endemic equilibrium does not occur. Furthermore, analyzing the terms $\omega\varepsilon\gamma_1\beta_1(\gamma_1+\alpha_1)$ and $\beta_u\Lambda_h(\varepsilon+\upsilon_1)(\gamma_1\upsilon_1+\alpha_1\upsilon_1+\Lambda_1\beta_1^2)$ reveals the significance of individual parameters in influencing the occurrence of forward or backward bifurcations.

2. SM sub model

The following equations represent the SM sub-model

$$\begin{aligned} H' &= \Lambda_h + \alpha R_m - \beta_i I_2 H - \upsilon_1 H \\ I_m' &= \beta_i I_2 H - (\gamma+\delta_i+\upsilon_1) I_m \\ R_m' &= \gamma I_m - (\alpha+\upsilon_1) R_m \\ S_2' &= \Lambda_2 - \beta_2 I_m S_2 - \gamma_2 S_2 \\ I_2' &= \beta_2 I_m S_2 - (\gamma_2+\alpha_2) I_2 \end{aligned} \qquad \text{(B.5)}$$

The same procedures used to examine the SH sub-model in Eq. (B.1) were also used to analyze the SM sub-model in Eq. (B.5).

2.1 Local stability of the SM sub-model

Theorem 4. *The SM sub-model Eq. (B.5), at E_{0m}, is locally asymptotically stable if $R_{0m}<1$, otherwise unstable for $R_{0m}>1$.*

Proof: The SH sub-model has the following Jacobian matrix at E_{0m}

$$J(E_{0m}) = \begin{pmatrix} -\upsilon_1 & 0 & \alpha & 0 & \frac{-\beta_i\Lambda_h}{\upsilon_1} \\ 0 & -(\gamma+\delta_i+\upsilon_1) & 0 & 0 & \frac{\beta_i\Lambda_h}{\upsilon_1} \\ 0 & \gamma & -(\alpha+\upsilon_1) & 0 & 0 \\ 0 & \frac{-\beta_2\Lambda_2}{\gamma_2} & 0 & -\gamma_2 & 0 \\ 0 & \frac{\beta_2\Lambda_2}{\gamma_2} & 0 & 0 & -(\gamma_2+\alpha_2) \end{pmatrix} \qquad \text{(B.6)}$$

Clearly, in Jacobian matrix Eq. (B.6), $-\upsilon_1$, $-\gamma_2$, and $-(\alpha+\upsilon_1)$ are negative eigenvalues of $J(E_{0m})$. The resultant quadratic equation $\left(\lambda^2+\left[(\gamma+\delta_i+\upsilon_1)+(\gamma_2+\alpha_2)\right]\lambda+(\gamma+\delta_i+\upsilon_1)(\gamma_2+\alpha_2)(1-R_{0m})\right)=0$, has two negative eigenvalues provided $R_{0h}<1$. Thus, SM sub-model Eq. (B.5) is locally stable as long as all eigenvalues at E_{0m} are negative

2.2 Existence of endemic equilibrium for the SM sub-model

Lemma 2. *If $R_{0m} > 1$, the SM sub-model Eq. (B.5) has an endemic equilibrium (E_{1m}).*

The computation of the endemic equilibrium point $E_{1m} = (H'^*, I_m'^*, R_m'^*, S_2'^*; I_2'^*)$ results,

$$H'^* = \frac{(\gamma_2+\alpha_2)((\alpha+\upsilon_1)\Lambda_2+\alpha\gamma I_m)(\beta_2 I_m+\gamma_2)}{(\alpha+\upsilon_1)(\gamma_2+\alpha_2)(\beta_2 I_m+\gamma_2)}, R_m'^* = \frac{\omega}{(\alpha+\upsilon_1)} I_m, S_2'^* = \frac{\Lambda_2}{(\beta_2 I_m+\gamma_2)} I_m, I_2'^* = \frac{\beta_2\Lambda_2 I_m}{(\gamma_2+\alpha_2)(\beta_2 I_m+\gamma_2)} I_m$$

The endemic equilibrium of the SM sub-model Eq. (B.5) is satisfied by the resultant polynomial provided in equation Eq. (B.7),

$$\lambda^3 + m_2\lambda^2 + m_1\lambda + m_0 = 0 \qquad \text{(B.7)}$$

where $m_0 = -\frac{\gamma_2\beta_i\beta_2\Lambda_2\Lambda_h}{\beta_2(\gamma_2+\alpha_2)(\gamma+\delta_i+\upsilon_1)}$, $m_1 = \frac{(\gamma_2+\alpha_2)(\gamma+\delta_i+\upsilon_1)(\gamma_2-\beta_2\Lambda_h)-\gamma_2\beta_i\beta_2\Lambda_2}{\beta_2(\gamma_2+\alpha_2)(\gamma+\delta_i+\upsilon_1)}$, $m_2 = \frac{(\gamma_2+\alpha_2)(\gamma+\delta_i+\upsilon_1)(\gamma_2-\beta_2\Lambda_h)-(\gamma_2+\alpha_2)\alpha\gamma\gamma_2\beta_i\beta_2\Lambda_2}{\beta_2\gamma_2(\gamma_2+\alpha_2)(\gamma+\delta_i+\upsilon_1)}$. There is no doubt that $m_0 < 0$, and in line with Descartes' rule of signs [39], if either or both of $m_i > 0, i = 1,2$ results in at least one positive root for equation Eq. (B.7), and thus endemic equilibrium occurs.

2.3 Global stability of the SM sub-model

Theorem 5. *The endemic equilibrium E_{1m} of SM sub-model Eq. (B.5) is locally asymptotically stable if $R_0 > 1$ and the bifurcation parameter $\beta_i = \beta_i^* > \frac{\upsilon_1\gamma_2(\gamma_2+\alpha_2)(\gamma+\delta_i+\upsilon_1)}{\beta_2\Lambda_1\Lambda_h}$.*

Proof: We transform the SM sub-model Eq. (B.5) according to Castillo and Songs [48], where $H = y_1, I_m = y_2, R_m = y_3, S_2 = y_4$, and $I_2 = y_5$ with the vector notation $\boldsymbol{Y} = (y_i)^T, i = 1,2,3,4,5$ and $\frac{dy}{dt} = \boldsymbol{G} =: (g_1, g_2, g_3, g_4, g_5)^T$. Thus, the new SM sub-model system Eq. () is obtained

$$\begin{aligned}
y_1' &=: g_1 = \Lambda_h + \alpha y_3 - \beta_i y_1 y_5 - \upsilon_1 y_1 \\
y_2' &=: g_2 = \beta_i y_1 y_5 - (\gamma + \delta_i + \upsilon_1) y_2 \\
y_3' &=: g_3 = \gamma y_2 - (\alpha + \upsilon_1) y_3 \qquad \text{(B.8)} \\
y_4' &=: g_4 = \Lambda_2 - \beta_2 y_2 y_4 - \gamma_2 y_4 \\
y_5' &=: g_5 = \beta_2 y_2 y_4 - (\gamma_2 + \alpha_2) y_5
\end{aligned}$$

The linearized Jacobian matrix of the SM sub-model in Eq. (B.8) at E_{0m} and $\beta_i = \beta_i^* = \frac{\upsilon_1\gamma_2(\gamma_2+\alpha_2)(\gamma+\delta_i+\upsilon_1)}{\beta_2\Lambda_2\Lambda_h}$ has a simple eigenvalue associated with a right ($\boldsymbol{\upsilon}$) and a left ($\boldsymbol{\eta}$) eigenvector satisfying $\boldsymbol{\upsilon}.\boldsymbol{\eta} = \mathbf{1}$, where

$$\boldsymbol{v} = \left(v_1 = \frac{\alpha v_1 \gamma_{\gamma_2}(\gamma_2+\alpha_2) - \beta_2 \beta_i \Lambda_2 \Lambda_h (\alpha+v_1)}{\gamma_2(\gamma_2+\alpha_2)(\alpha+v_1)u_1^2} v_2, \quad v_2 > 0, \quad v_3 = \frac{\alpha}{(\alpha+v_1)} v_2, \quad v_4 = \frac{-\beta_2 \Lambda_2}{\gamma_2^2} v_2, \quad v_5 = \frac{\beta_2 \Lambda_2}{\gamma_2(\gamma_2+\alpha_2)} v_2\right)^T$$

$$\boldsymbol{\eta} = \left(\eta_1 = 0 \quad \eta_2 > 0 \quad \eta_3 = 0 \quad \eta_4 = 0 \quad \eta_5 = \frac{\beta_i \Lambda_h}{v_1(\gamma_2+\alpha_2)} \eta_2\right)$$

The coefficients a and b as defined in Castillo and Songs [48], are given as

$$a = \eta_2 v_1 v_5 \frac{\partial^2 f_2(0,0)}{\partial x_1 \partial x_5} + \eta_5 v_2 v_4 \frac{\partial^2 f_5(0,0)}{\partial x_2 \partial x_4} = \left(\frac{\alpha v_1 \gamma_2 \beta_2 (\gamma_1+\alpha_1) - \beta_i \Lambda_h (\alpha+v_1)(\gamma_2 v_1 + \alpha_2 v_1 + \Lambda_2 \beta_2^2)}{(\alpha+v_1)(\gamma_2+\alpha_2)^2 v_1^2 \gamma_2^2}\right) \beta_2 \Lambda_2 \eta_2 v_2^2$$

$$b = \eta_2 v_1 \frac{\partial^2 f_2(0,0)}{\partial x_1 \partial \beta_u^*} + \eta_2 v_5 \frac{\partial^2 f_2(0,0)}{\partial x_5 \partial \beta_u^*} = \frac{\beta_2 \Lambda_2 \Lambda_h}{\gamma_2 v_1 (\gamma_2+\alpha_2)} \eta_2 v_2$$

Consequently, b is positive, and the local stability dynamics are determined by the sign of coefficient a. Thus, backward bifurcation occurs if and only if $a > 0$, given that $\alpha v_1 \gamma_2 \beta_2 (\gamma_1 + \alpha_1) > \beta_i \Lambda_h (\alpha + v_1)(\gamma_2 v_1 + \alpha_2 v_1 + \Lambda_2 \beta_2^2)$, On the other hand, a forward bifurcation takes place whenever $a < 0$.

3. Co-dynamics model system

3.1 Local stability of the co-dynamics model

Theorem 6. *The SHM co-infection model Eq. (1-11) at E_{0hm}, is locally asymptotically stable if $R_{0hm} < 1$, otherwise unstable for $R_{0hm} > 1$*

Proof: We evaluate the Jacobian matrix $J(E_{0hm})$ at E_{0hm} given in equation Eq. (B.9)

$$\begin{pmatrix}
-v_1 & 0 & 0 & 0 & \alpha & \varepsilon & \theta & 0 & \frac{-\beta_u \Lambda_h}{v_1} & 0 & \frac{-\beta_i \Lambda_h}{v_1} \\
0 & -\rho_1 & 0 & 0 & 0 & 0 & 0 & 0 & 0 & 0 & \frac{\beta_i \Lambda_h}{v_1} \\
0 & 0 & -\rho_2 & 0 & 0 & 0 & 0 & 0 & \frac{\beta_u \Lambda_h}{v_1} & 0 & 0 \\
0 & 0 & 0 & -\rho_3 & 0 & 0 & 0 & 0 & 0 & 0 & 0 \\
0 & \gamma & 0 & \tau_1(1-\delta) & -(\alpha+v_1) & 0 & 0 & 0 & 0 & 0 & 0 \\
0 & 0 & \omega & \rho_4 & 0 & -(\varepsilon+v_1) & 0 & 0 & 0 & 0 & 0 \\
0 & 0 & 0 & \delta & 0 & 0 & -(\theta+v_1) & 0 & 0 & 0 & 0 \\
0 & 0 & \frac{-\beta_1 \Lambda_1}{\gamma_1} & \frac{-\beta_1 \Lambda_1}{\gamma_1} & 0 & 0 & 0 & -\gamma_1 & 0 & 0 & 0 \\
0 & 0 & \frac{\beta_1 \Lambda_1}{\gamma_1} & \frac{\beta_1 \Lambda_1}{\gamma_1} & 0 & 0 & 0 & 0 & -(\gamma_1+\alpha_1) & 0 & 0 \\
0 & \frac{-\beta_2 \Lambda_1}{\gamma_2} & 0 & \frac{-\beta_2 \Lambda_1}{\gamma_2} & 0 & 0 & 0 & 0 & 0 & -\gamma_2 & 0 \\
0 & \frac{\beta_2 \Lambda_1}{\gamma_2} & 0 & \frac{\beta_2 \Lambda_1}{\gamma_2} & 0 & 0 & 0 & 0 & 0 & 0 & -(\gamma_2+\alpha_2)
\end{pmatrix} \quad \text{(B.9)}$$

where $\rho_1 = (\gamma + \delta_i + v_1)$, $\rho_2 = (\omega + \delta_u + v_1)$, $\rho_3 = (\delta + \delta_i + \delta_u + v_1)$, $\rho_4 = (1-\tau_1)(1-\delta)$. The eigenvalues of the SHM co-infection model system that have negative real parts are $-v_1$, $-(\omega + \delta_u + v_1)$, $-(\alpha + v_1)$, $-(\varepsilon + v_1)$, $-(\theta + v_1)$, $-\gamma_1$, $-(\gamma_1 + \alpha_1)$, and $-\gamma_2$. The Jacobian in Eq. (B.9) can be solved to obtain the remaining three eigenvalues, given by the polynomial in equation Eq. (B.10).

$$\lambda^3 + a_2\lambda^2 + a_1\lambda + a_0 = 0 \quad \text{(B.10)}$$

where $a_0 = (\gamma + \delta_i + \upsilon_1)(\delta + \delta_i + \delta_u + \upsilon_1)(\gamma_2 + \alpha_2) - \beta_i\beta_2(\delta + \delta_i + \delta_u + \upsilon_1)\Lambda_1\Lambda_h$

$a_1 = (\gamma + \delta_i + \upsilon_1)(\delta + \delta_i + \delta_u + \upsilon_1) + (\delta + \delta_i + \delta_u + \upsilon_1)(\gamma_2 + \alpha_2) + (\gamma_2 + \alpha_2)(\gamma + \delta_i + \upsilon_1) - \beta_i\beta_2\Lambda_1\Lambda_h$

$$a_2 = (\gamma + \delta_i + \upsilon_1) + (\delta + \delta_i + \delta_u + \upsilon_1) + (\gamma_2 + \alpha_2)$$

Routh-Hurwitz stability criterion states that equatioin Eq. (B.10) has negative roots only when $a_0 > 0$, $a_1 > 0$, $a_2 > 0$, and $a_2a_1 > a_0$. Thus, the *S.haematobium-mansoni* co-infection model is locally asymptotically stable.

3.2 Global stability of the co-infection model

To determine whether endemic equilibrium is asymptotic at the local level, we use the centre manifold theory in Castillo and Song [48]. Let $H = z_1$, $I_m = z_2$, $I_h = z_3$, $I_{hm} = z_4$, $R_m = z_5$, $R_h = z_6$, $R_{hm} = z_7$, $S_1 = z_8$, $I_1 = z_9$, $S_2 = z_{10}$, and $I_2 = z_{11}$ and with the vector notation $Z = (z_i)^T, i = 1,2,3,4,5$ and $\frac{dZ}{\mathrm{dt}} = \boldsymbol{\psi} =: (\psi_i)^T, i = 1, 2, \ldots, 11$. Thus, the resultant transformed *S. haematobium-mansoni* co-infection in model (*Eq25*) exhibits the same disease-free equilibrium point (E_{0hm}) as the original sytem in equations Eq. (1-11).

$$\begin{aligned}
z_1' &= \psi_1 := \Lambda_h + \varepsilon z_6 + \alpha z_5 + \theta z_7 - (\beta_i z_{11} + \beta_u z_9)z_1 - \upsilon_1 z_1 \\
z_2' &= \psi_2 := \beta_i z_{11} z_1 - \beta_u z_9 z_2 - (\gamma + \delta_i + \upsilon_1)z_2 \\
z_3' &= \psi_3 := \beta_u z_9 z_1 - \beta_i z_{11} z_3 - (\omega + \delta_u + \upsilon_1)z_3 \\
z_4' &= \psi_4 := \beta_u z_9 z_2 + \beta_i z_{11} z_3 - (\delta + \delta_i + \delta_u + \upsilon_1)z_4 \\
z_5' &= \psi_5 := \gamma z_2 + \tau_1(1 - \delta)z_4 - (\alpha + \upsilon_1)z_5 \\
z_6' &= \psi_6 := \omega z_3 + (1 - \tau_1)(1 - \delta)z_4 - (\varepsilon + \upsilon_1)z_6 \\
z_7' &= \psi_7 := \delta z_4 - (\theta + \upsilon_1)z_7 \\
z_8' &= \psi_8 := \Lambda_1 - \beta_1(z_3 + z_4)z_8 - \gamma_1 z_8 \\
z_9' &= \psi_9 := \beta_1(z_3 + z_4)z_8 - (\gamma_1 + \alpha_1)z_9 \\
z_{10}' &= \psi_{10} := \Lambda_2 - \beta_2(z_2 + z_4)z_{10} - \gamma_2 z_{10} \\
z_{11}' &= \psi_{11} := \beta_2(z_2 + z_4)z_{10} - (\gamma_2 + \alpha_2)z_{11}
\end{aligned} \tag{B.11}$$

Therefore, in the linearized Jacobian matrix of the SHM sub-model, Eq. (B.8) at E_{0hm} and $\beta_i = \beta_i^*$ as a bifurcation parameter, a straightforward eigenvalue is associated with both the right eigenvector ($\boldsymbol{u}$) and the left eigenvector ($\boldsymbol{v}$), with the condition $\boldsymbol{u}.\boldsymbol{v} = \mathbf{1}$. Thus eigenvectors $\boldsymbol{u}$ and $\boldsymbol{v}$ are given as

$$\boldsymbol{u} = \begin{pmatrix} u_1 \\ u_2 \\ u_3 \\ u_4 \\ u_5 \\ u_6 \\ u_7 \\ u_8 \\ u_9 \\ u_{10} \\ u_{11} \end{pmatrix} = \begin{pmatrix} r_1u_2 + r_2u_3 \\ u_2 > 0 \\ u_3 > 0 \\ 0 \\ \left(\frac{\gamma}{\alpha+\upsilon_1}\right)u_2 \\ \left(\frac{\omega}{\alpha+\upsilon_1}\right)u_3 \\ 0 \\ \left(\frac{-\beta_u\beta_1\Lambda_1}{\gamma_1}\right)u_3 \\ \left(\frac{\beta_u\beta_1\Lambda_1}{\gamma_1+\alpha_1}\right)u_3 \\ \left(\frac{\beta_i\beta_2\Lambda_1}{\gamma_2}\right)u_2 \\ \left(\frac{\beta_u\beta_1\Lambda_1}{(\gamma_2+\alpha_2)}\right)u_2 \end{pmatrix}, \quad \boldsymbol{v} = \begin{pmatrix} v_1 \\ v_2 \\ v_3 \\ v_4 \\ v_5 \\ v_6 \\ v_7 \\ v_8 \\ v_9 \\ v_{10} \\ v_{11} \end{pmatrix} = \begin{pmatrix} 0 \\ v_2 > 0 \\ v_3 > 0 \\ r_3v_2 \\ 0 \\ 0 \\ 0 \\ 0 \\ \left(\frac{\beta_i\Lambda_h}{\gamma_2}\right)v_3 \\ 0 \\ \left(\left(\frac{\beta_u\Lambda_h}{\gamma_1+\alpha_1}\right)v_3\right) \end{pmatrix}$$

where $r_1 = \left(\frac{\alpha\gamma}{\alpha+\upsilon_1} - \frac{\beta_i\beta_2\Lambda_1\Lambda_h}{(\gamma_2+\alpha_2)}\right)$, $r_2 = \left(\frac{\varepsilon\omega}{\varepsilon+\upsilon_1} - \frac{\beta_u\beta_1\Lambda_1\Lambda_h}{(\gamma_1+\alpha_1)}\right)$ and $r_3 = \frac{(\gamma_2+\alpha_2)(\beta_u\beta_1\Lambda_1\Lambda_h v_3+(\gamma_1+\alpha_1)\beta_i\beta_2\Lambda_1\Lambda_h)v_2}{(\gamma_1+\alpha_1)(\gamma_2+\alpha_2)(\delta+\delta_i+\delta_u+\upsilon_1)}$. Hence, upon examining $\boldsymbol{v}$, it becomes evident that the second-order partial derivatives, denoted as ψ_k for $k = 1, 5, 6, 7, 8, 10$, linked to the left eigenvalues, will vanish. Consequently, only the partial derivatives associated with $k = 2, 3, 4, 9$ and 11 at the disease-free equilibrium are taken into consideration. This leads to the determination of the coefficients a and b as follows:

$$a = v_2u_2u_9\frac{\partial^2\psi_2(0,0)}{\partial z_2\partial z_9} + v_2u_3u_{11}\frac{\partial^2\psi_2(0,0)}{\partial z_3\partial z_{11}} + v_3u_3u_{11}\frac{\partial^2\psi_3(0,0)}{\partial z_3\partial z_{11}} + v_4u_2u_9\frac{\partial^2\psi_4(0,0)}{\partial z_2\partial z_9} + v_9u_3u_8\frac{\partial^2\psi_9(0,0)}{\partial z_3\partial z_8} + v_{11}u_2u_{10}\frac{\partial^2\psi_{11}(0,0)}{\partial z_2\partial z_{10}}$$

$$= \left(\frac{\beta_u\beta_1\beta_2\Lambda_1}{\gamma_2+\alpha_2} + \frac{(r_3-1)\beta_1\beta_u^2\Lambda_1}{\gamma_1+\alpha_1}\right)v_2u_2u_3 + \frac{\beta_1^2\beta_2^2\Lambda_1\Lambda_h}{\gamma_2^2}v_2u_2^2 + \frac{\beta_u\beta_2\Lambda_1[\gamma_1\gamma_2\beta_2v_2u_2^2 - (\gamma_2+\alpha_2)\beta_i\Lambda_2v_3u_3^2]}{\gamma_1\gamma_2(\gamma_1+\alpha_1)}$$

$$b = v_9u_3\frac{\partial^2\psi_9(0,0)}{\partial z_3\partial\beta_i^*} + v_9u_4\frac{\partial^2\psi_9(0,0)}{\partial z_4\partial\beta_i^*} = \frac{\beta_1\Lambda_1\Lambda_h}{\gamma_1\gamma_2}v_3^2$$

The computation of the coefficient reveals that despite $b > 0$, it is not evident that a is also positive. In such instances, the disease-free equilibrium does not exhibit asymptotic stability, and there is a possibility of an endemic equilibrium if $r_3 > 1$ and $\gamma_1\gamma_2\beta_2v_2u_2^2 > (\gamma_2+\alpha_2)\beta_i\Lambda_2v_3u_3^2$. However, if the aforementioned condition holds true, resulting in a positive value for a, the SHM co-infection model experiences a backward bifurcation, given that both a and b are positive.

Der Lebenslauf wurde aus der elektronischen Version der Arbeit entfernt.

The curriculum vitae was removed from the electronic version of the paper.

Publications/ submitted papers

Tabo Zadoki*, Breuer, L., & Albrecht, C. (2024, **under revision**). Modelling temperature-dependent schistosomiasis dynamics for single and co-infections with *S. mansoni* and *S. haematobium*. (To be published in PLOS ONE)

Tabo Zadoki*, Luboobi, L., Kraft, P., Breuer, L., & Albrecht, C. (**2024**). Control of schistosomiasis by the selective competitive and predatory intervention of intermediate hosts: A mathematical modeling approach *Mathematical Biosciences* 376 (2024): 109263. https://doi.org/10.1016/j.mbs.2024.109263

Tabo Zadoki*, Breuer, L., Fabia, C., Samuel, G., & Albrecht, C. (**2024**). A machine learning approach for modeling the occurrence of the major intermediate hosts for schistosomiasis in East Africa. *Scientific Reports*, *14*(1), 4274. https://doi.org/10.1038/s41598-024-54699-1

Tabo, Zadoki*, Kalinda, C., Breuer, L., & Albrecht, C. (**2024**). Exploring the interplay between climate change and schistosomiasis transmission dynamics. *Infectious Disease Modelling*, *9*(1), 158-176. https://doi.org/10.1016/j.idm.2023.12.003

Tabo, Zadoki*, Kalinda, C., Breuer, L., & Albrecht, C. (**2023**). Adapting Strategies for Effective Schistosomiasis Prevention: A Mathematical Modeling Approach. *Mathematics*, *11*(12), 2609. https://www.mdpi.com/2227-7390/11/12/2609

Tabo, Zadoki *, Neubauer, T. A., Tumwebaze, I., Stelbrink, B., Breuer, L., Hammoud, C., & Albrecht, C. (**2022**). Factors Controlling the Distribution of Intermediate Host Snails of Schistosoma in Crater Lakes in Uganda: A Machine Learning Approach. *Frontiers in Environmental Science*, 341. https://doi.org/10.3389/fenvs.2022.871735

Tabo Zadoki*, Livingstone S. Luboobi, & Joseph Ssebuliba (**2016**). Mathematical modelling of the in-host Dynamics of Malaria and the Effects of Treatment. Published in the Journal of Mathematics and Computer Science Vol.17 (2017), 1- 12. http://dx.doi.org/10.22436/jmcs.017.01.01

Conferences/workshops/Seminars

Presentations Feb. 2024	Applicability of integrative mathematical and statistical modeling combining intrinsic and extrinsic parameters - towards eradicating schistosomiasis. Global schistosomiasis Alliance, GSA snail vector group (online)
2014-2015	Mathematical modelling of immune regulation of type 1 diabetes, seminar series Dept. of Math., Makerere University.
	Mathematical modelling of within host dynamics of malaria and the effects of Treatment, seminar series. Dept. of Math., Makerere University
Conferences April. 2015	Makerere University International Research and Innovations Dissemination Conference titled ``Community Transformation through Research, Innovation and knowledge Translation'' held at Hotel Africana-Uganda, organised by Makerere University and Sweden
Workshops Nov. 2014	Mathematics and life Relevance" held at the Department of Mathematics Makerere University, organised by Makerere University and Finland
Oct. 2014	Basic Sciences For Sustainable Development at Makerere University organised by Swedish International Development Agency SIDA Science day
Seminar Nov. 2013	Mathematical Modelling workshop at Makerere University organised by Makerere University and Finland

References

Associate Prof. Dr. Christian Albrecht
Dep. of Animal Ecology and Systematics
Justus Liebig University Giessen
H.-Buff-Ring 26-32 (IFZ)
D-35392 Giessen, Germany
Tel.: ++49 641 9935722
Fax: ++49 641 9935709
E-Mail:christian.albrecht@allzool.bio.uni-giessen.de

Prof. Dr. Lutz Breuer
Department of Landscape Ecology and Resource Management
Justus Liebig University Giessen
H.-Buff-Ring 26-32 (IFZ)
D-35392 Giessen, Germany
Tel.: ++49 641 99 37380
Fax: ++49 641 99 37389
E-Mail: lutz.breuer@umwelt.uni-giessen.de

Prof. Livingstone S. Luboobi
Department of Mathematics Makerere University
Tel: +256 759 170077, +254 733 292990
luboobi@gmail.com
/livingstone.luboobi@mak.ac.ug

Acknowledgement

First, I express my gratitude to the gracious and merciful God, whose steadfast support guided me with wisdom through moments of uncertainty, contributing to the success of this PhD journey. May this achievement reflect His glory, impacting lives and advancing knowledge for the greater good of humanity.

My deepest appreciation goes to Apl. Prof. Dr. Christian Albrecht and Prof. Dr. Lutz Bueur for their exceptional supervision, guidance, unwavering support, scholarship funds acquisition, and invaluable mentorship. Their expertise, insightful feedback, and encouragement have shaped the trajectory of my research and academic development.

I am profoundly thankful for their dedication, patience, and commitment to nurturing my intellectual curiosity. Special thanks to the Deutscher Akademischer Austauschdienst (DAAD) for generous funding that facilitated advanced studies and empowered significant contributions to my research. The opportunities provided by DAAD played a pivotal role in shaping my academic and personal growth, and I appreciate their commitment to fostering excellence in education and international cooperation.

I am grateful to the faculty Dean Prof. Dr. Thomas Wilke for his commitment to fostering an enriching academic environment that has contributed to my growth and development as a researcher. My sincere gratitude extends to the members of the biodiversity lab and field sampling team for diligently collecting and providing invaluable snail data, forming the basis of my research and subsequent publications. I am especially fortunate to have worked alongside Dr. Thomas Neubauer, and I am grateful for his lasting impact on my academic journey. Thanks goes to Prof. Luboobi Livingstone for his invaluable contribution to shaping the mathematical aspects and providing insightful ideas enriched the research, enhancing its quality.

I acknowledge my collaborators for their dedication, expertise, and invaluable contributions to our research endeavors. Heartfelt thanks to my esteemed course mates, including my beloved wife, Dr. Immaculate Tumwebaze, Claire Dusabe, and Marcellin Rwibwutso, whose camaraderie, encouragement, and collective pursuit of knowledge enriched my doctoral journey. Special appreciation goes to Ludwig Uhland Schule and Kita Ludwigstrasse Giessen Kindergarten for their exceptional care and support provided to my children during my doctoral journey.

I extend my heartfelt gratitude to Associate Professor Albrecht and his entire family for their exceptional support that goes beyond academia. Special thanks to Oma Petra Albrecht for her generosity.

Finally, I extend heartfelt gratitude to my family, particularly my wife, Dr. Immaculate Tumwebaze, our children, mum Grace Nahyuha Ddamulira, Dad Emmanuel Ddamulira, all my brothers, and sisters as well as all relatives, friends, and well-wishers for being there for me every day.

*No chance at all if you think you can pull it off yourself. Every chance in the world if you trust God to do it……****Mathew 19:26****……*